

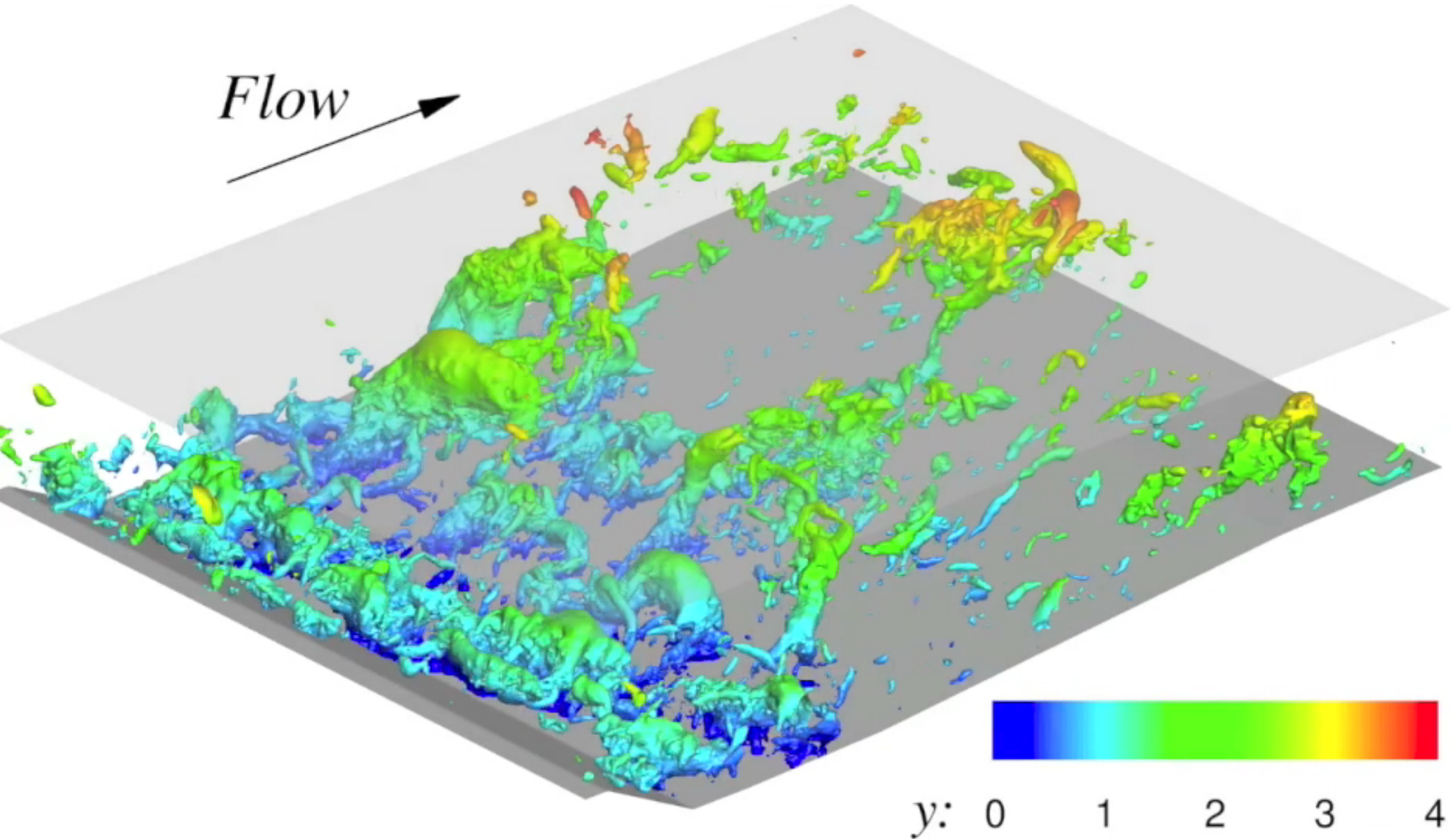


- Motivation
- Governing equations for LES
- Boundary conditions
- Subfilter-scale modelling
- Validation of an LES
- **Applications**
 - *Flow over dunes*
 - *Wall jets*
 - *Rough-wall boundary layers*
 - *Impinging jets*
- Hybrid RANS/LES methods
- Challenges
- Conclusions



APPLICATIONS

FLOW OVER RIVER DUNES (M. Omidyeganeh)





- Interaction of a flow field with a mobile sand bed results in bed deformation.
- The shape depends on:
 - *Flow properties (Re , Fr , etc.)*
 - *Sand type*
 - *Amount of sand available*
- For unidirectional mean flow, high Reynolds numbers (rivers)
⇒ *Transverse dunes*





- Interaction of a flow field with a mobile sand bed results in bed deformation.
- The shape depends on:
 - *Flow properties (Re , Fr , etc.)*
 - *Sand type*
 - *Amount of sand available*
- For unidirectional mean flow, high Reynolds numbers (rivers)
⇒ *Transverse dunes*
- Limited sediment supply (desert)
⇒ *Barchan dunes*





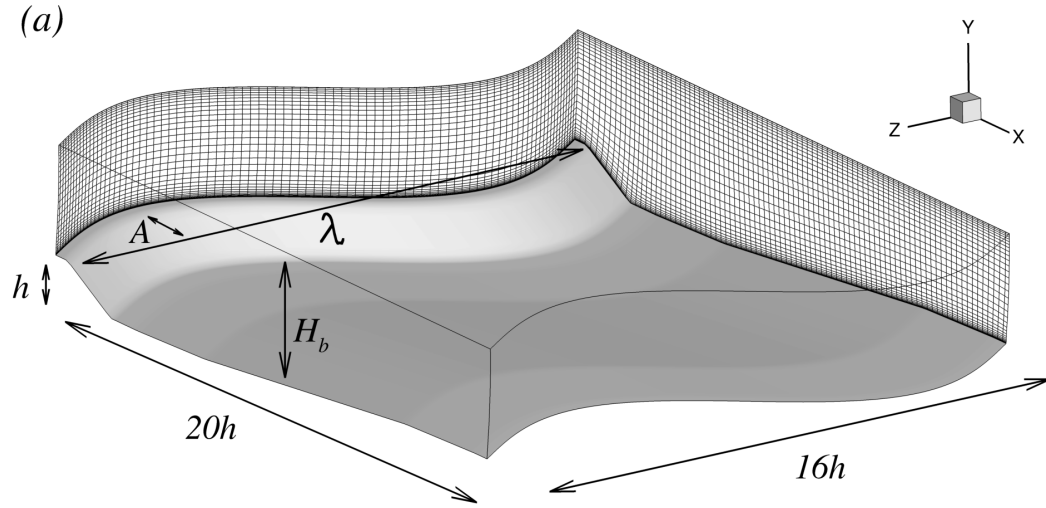
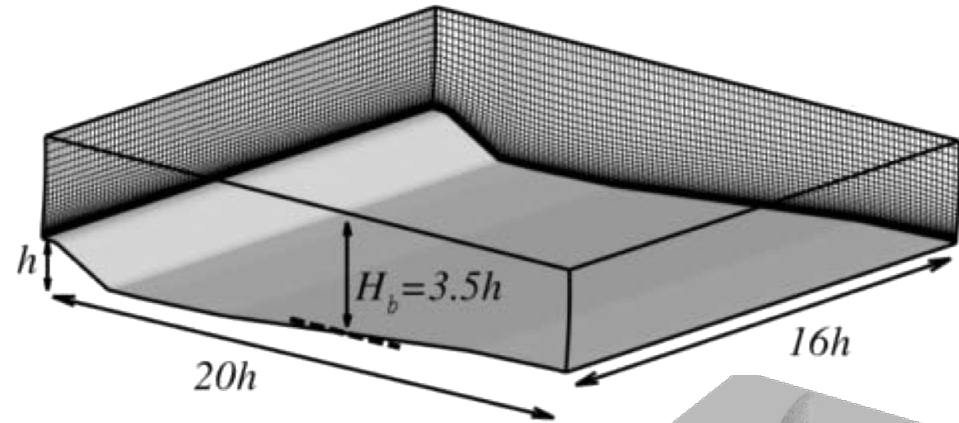
- In dunes, turbulence affects bed morphology and sediment transport.
- Field and laboratory experiments can highlight many of the important turbulent phenomena.
 - *Mean flow*
 - *Instantaneous flow structure*
- Experiments have limitations:
 - *Control of boundary conditions*
 - *Access to full field*
 - *Near-wall measurements*
- Improved numerical models are required to complement the experiments.

- Curvilinear code
 - *2nd-order accurate in time and space.*
 - *Central differences on all terms*
 - *Lagrangian Dynamic subfilter-scale model*
- The model has been extensively validated in engineering and geophysical flows.
- Grids between 6×10^6 and 41×10^6 points.
 - *Up to 16,000 CPU-hours per simulation*

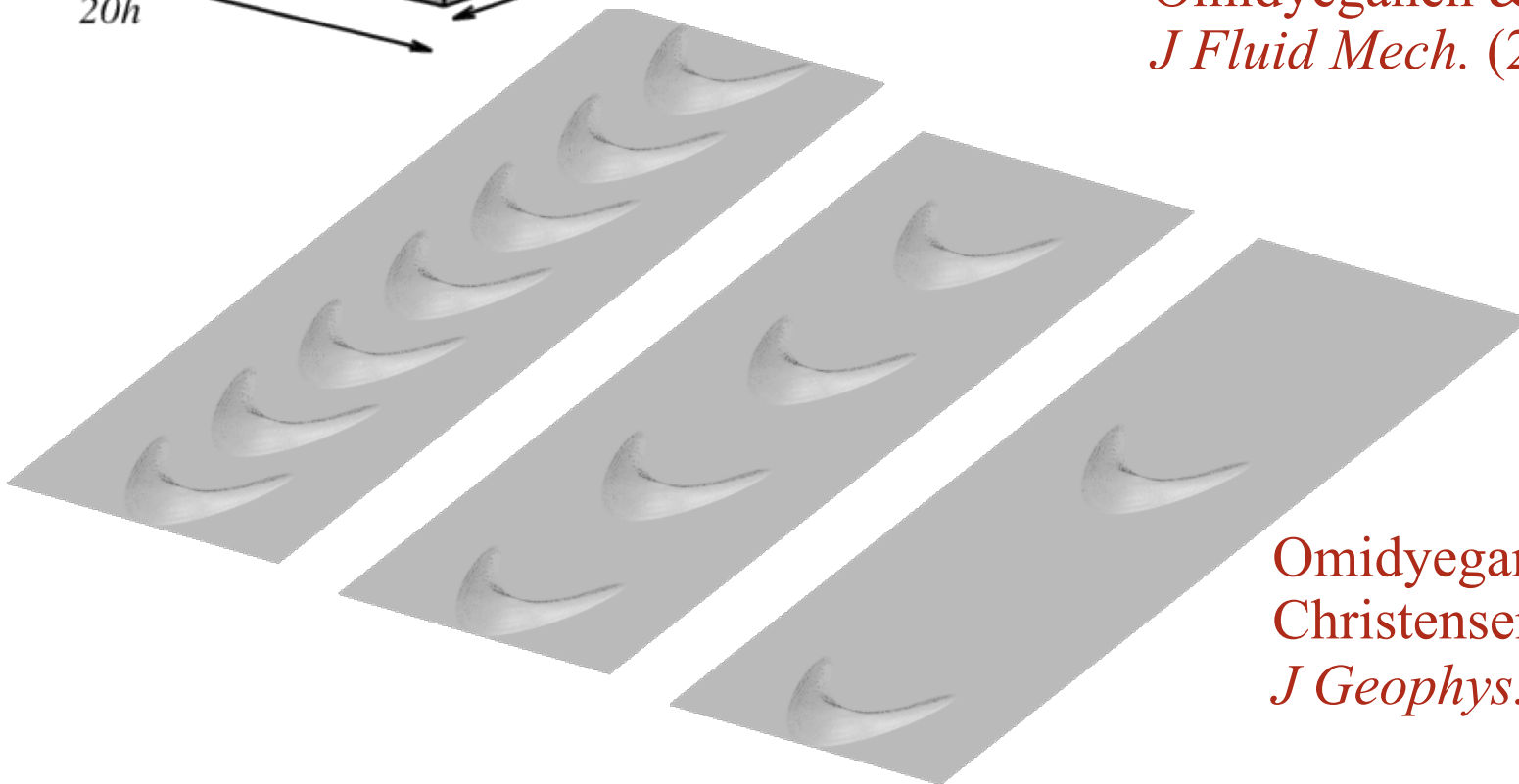


LES OF FLOWS OVER DUNES

Omidyeganeh & Piomelli
J of Turbulence (2010)



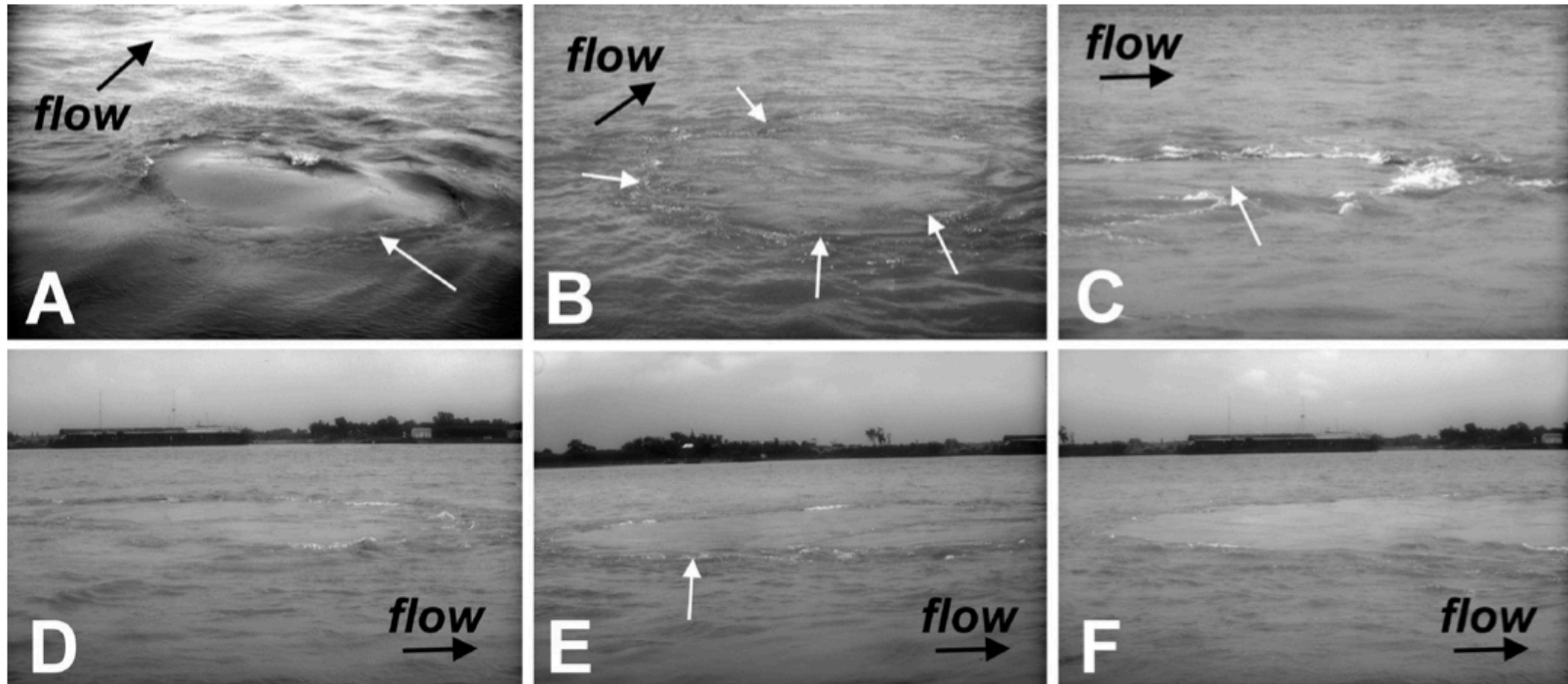
Omidyeganeh & Piomelli
J Fluid Mech. (2013a, 2013b)



Omidyeganeh, Piomelli,
Christensen & Best
J Geophys. Res. (2013)



- “Boils” are eruptions at the water surface associated with large turbulent structures.



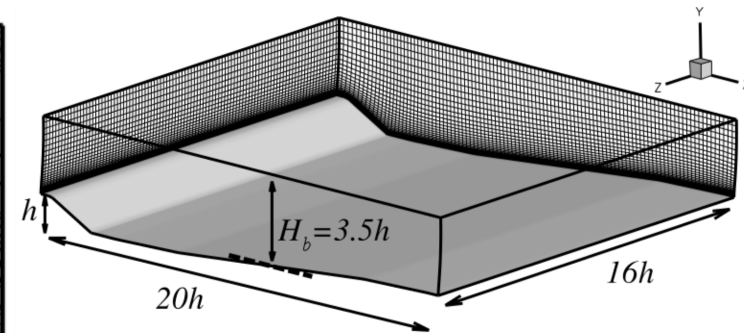
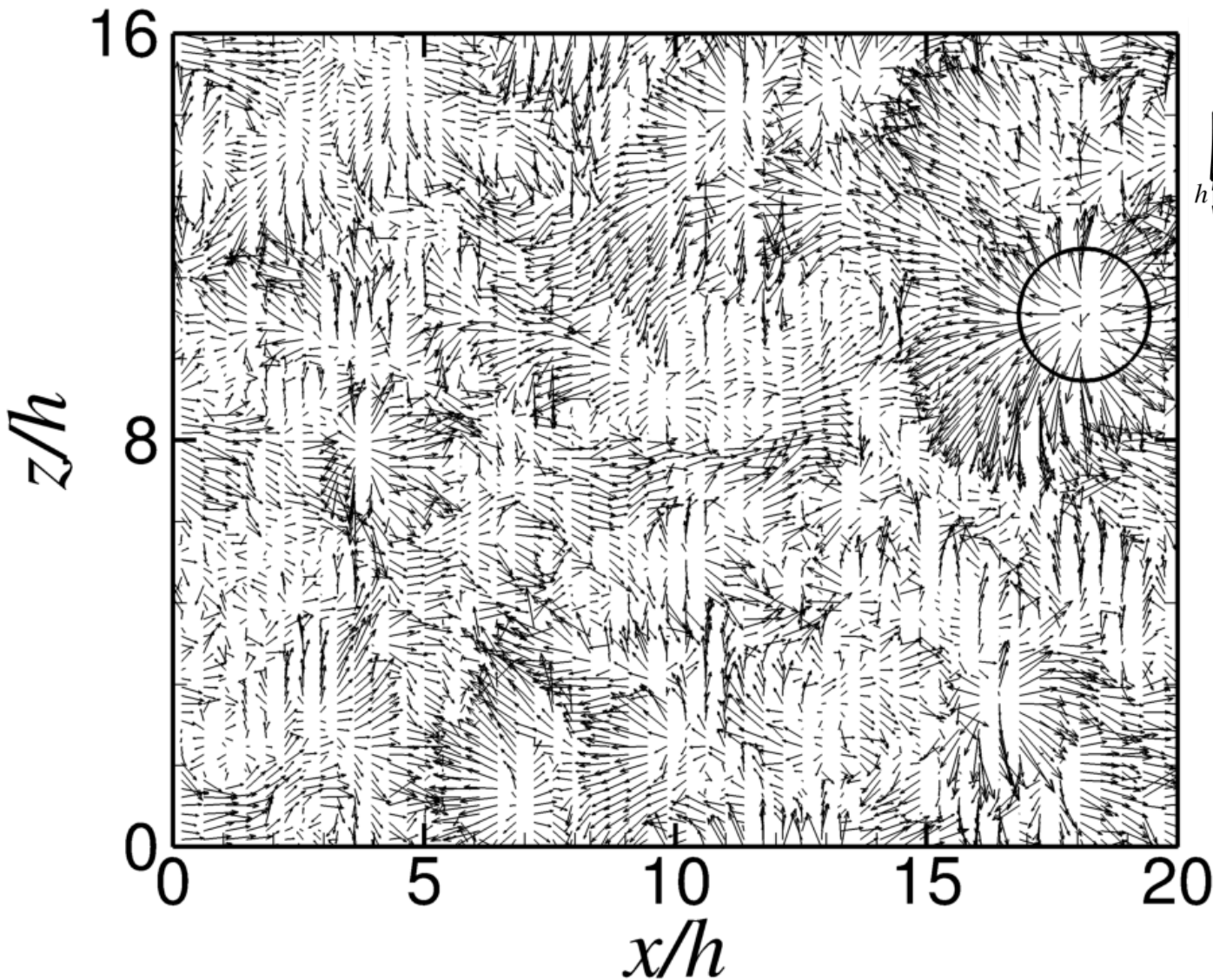
Photographs of vortex–free-surface interactions
in the Jamuna River, Bangladesh.
From Best (2005)



- “Boils” are eruptions at the water surface associated with large turbulent structures.
- Occur infrequently but generate significant Reynolds stress
- Are responsible for transport of fluid (sediment, nutrients....) from the bottom to the surface.
- Three conjectures on their generation:
 - *Oscillations of the reattachment line*
 - *Turbulent eddies from the stoss side*
 - *Eddies in the separated shear layer*
- Full-field, time dependent information is needed.



- Boils can be identified in the numerical simulations

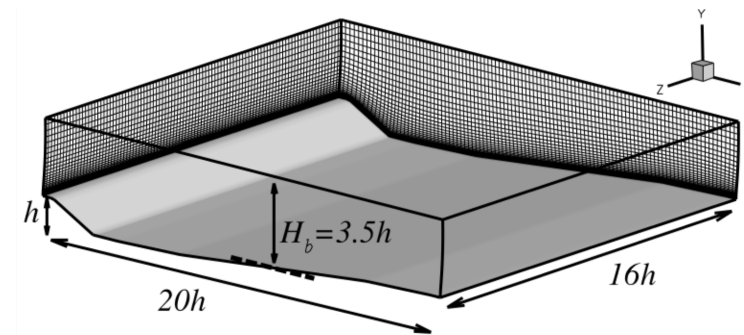
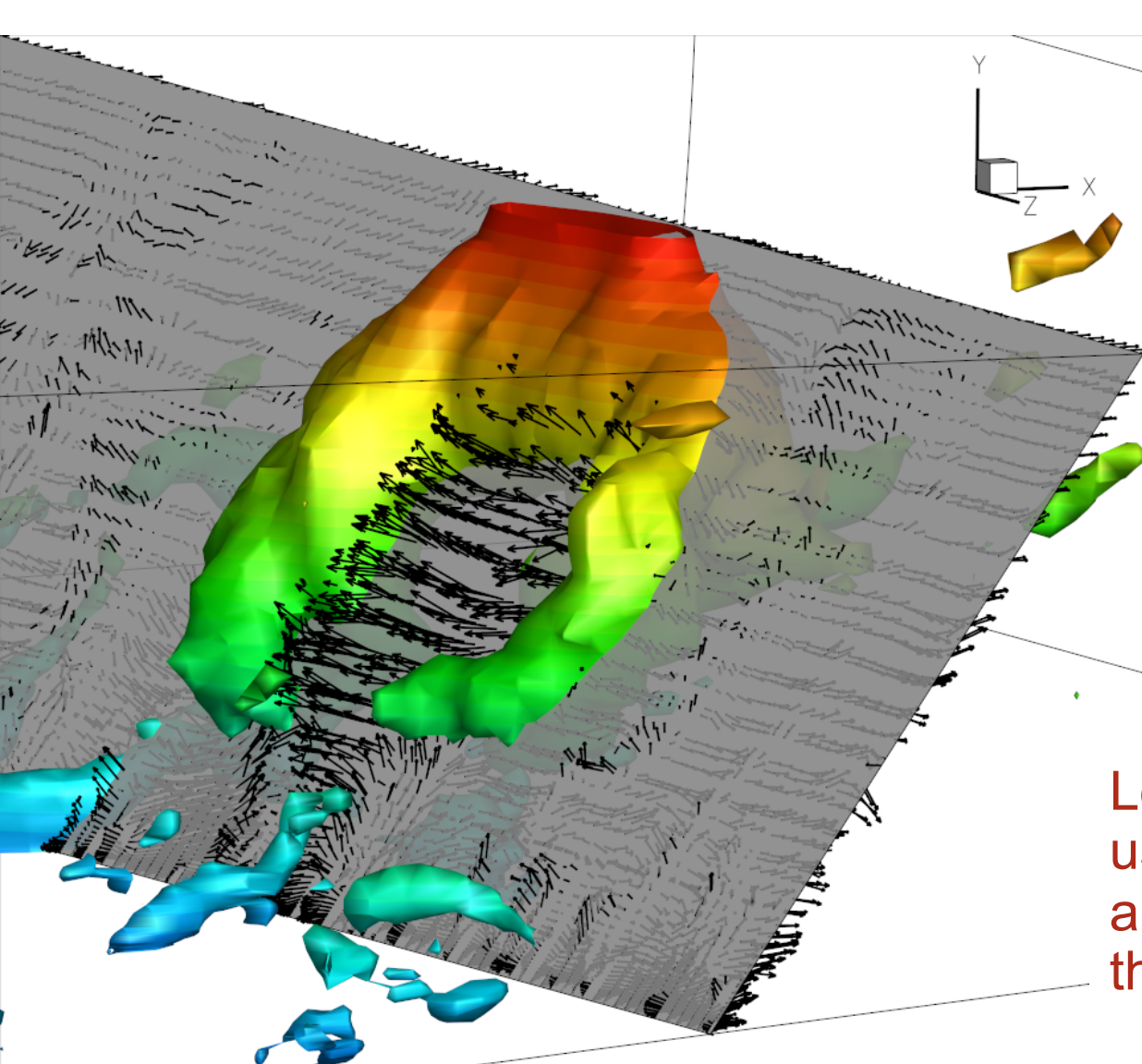


Velocity vectors at
the water surface. 2D
dunes



BOIL IDENTIFICATION

- Boils can be identified in the numerical simulations and related too the vortical structures.

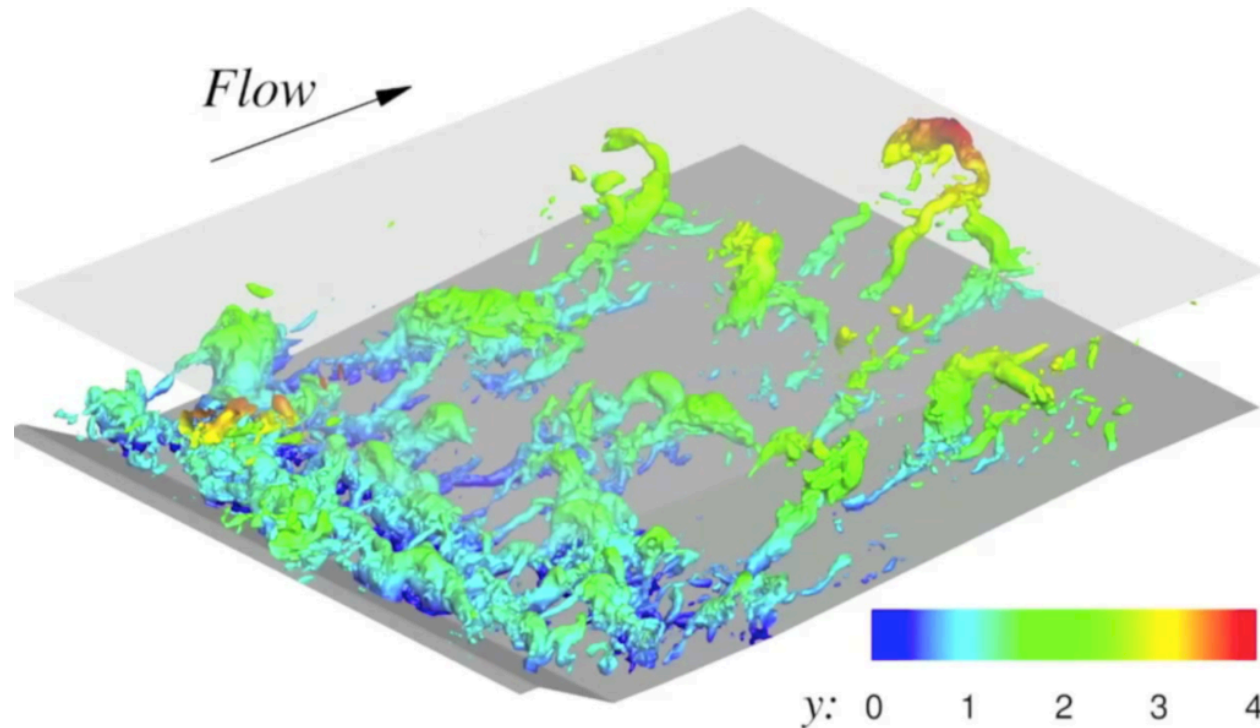


Visualization of a horseshoe vortex touching the water surface. 2D dunes.

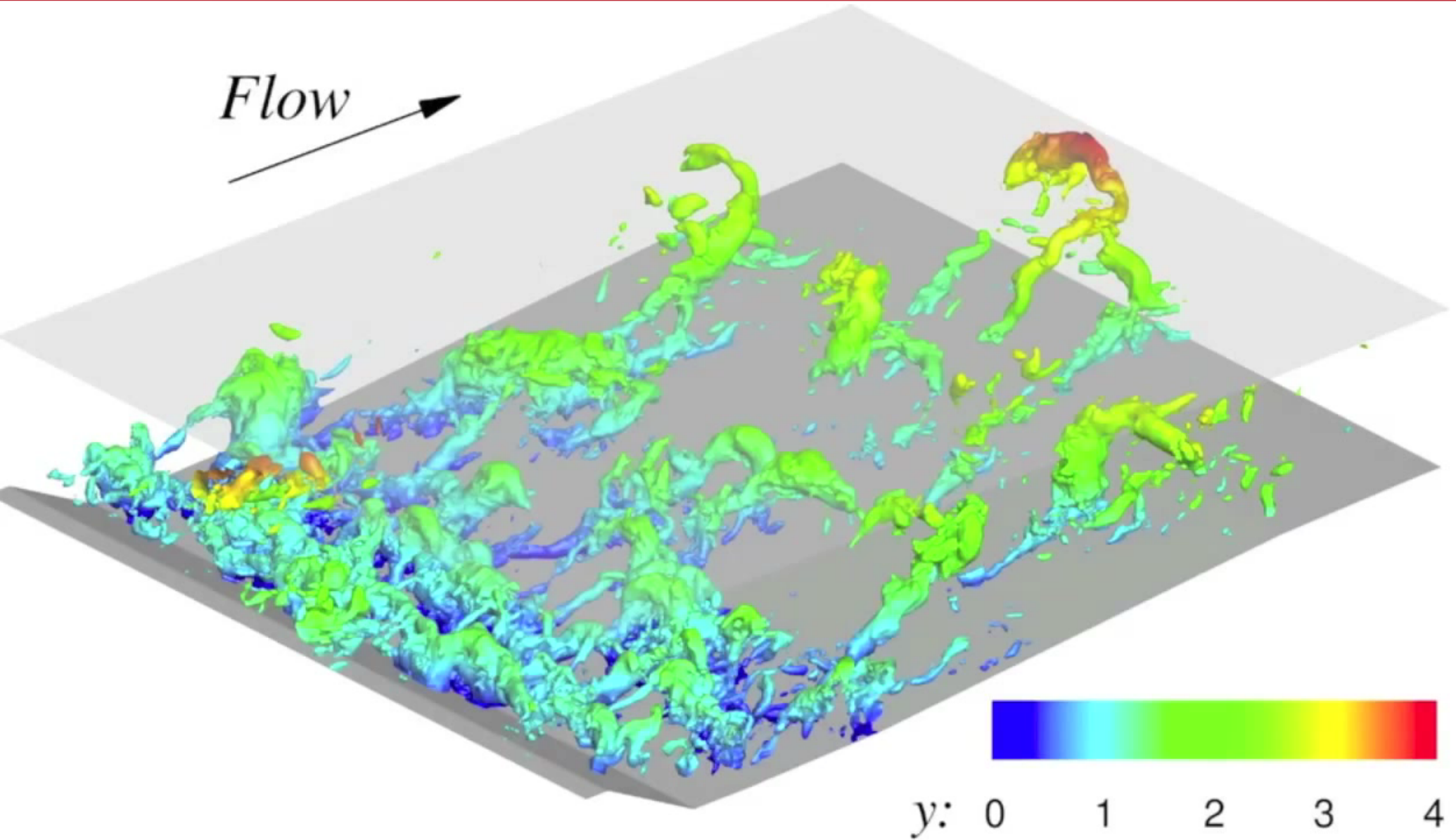
Low-pressure isosurfaces are used to visualize the vortex, and are coloured by the distance to the free surface (0→4).

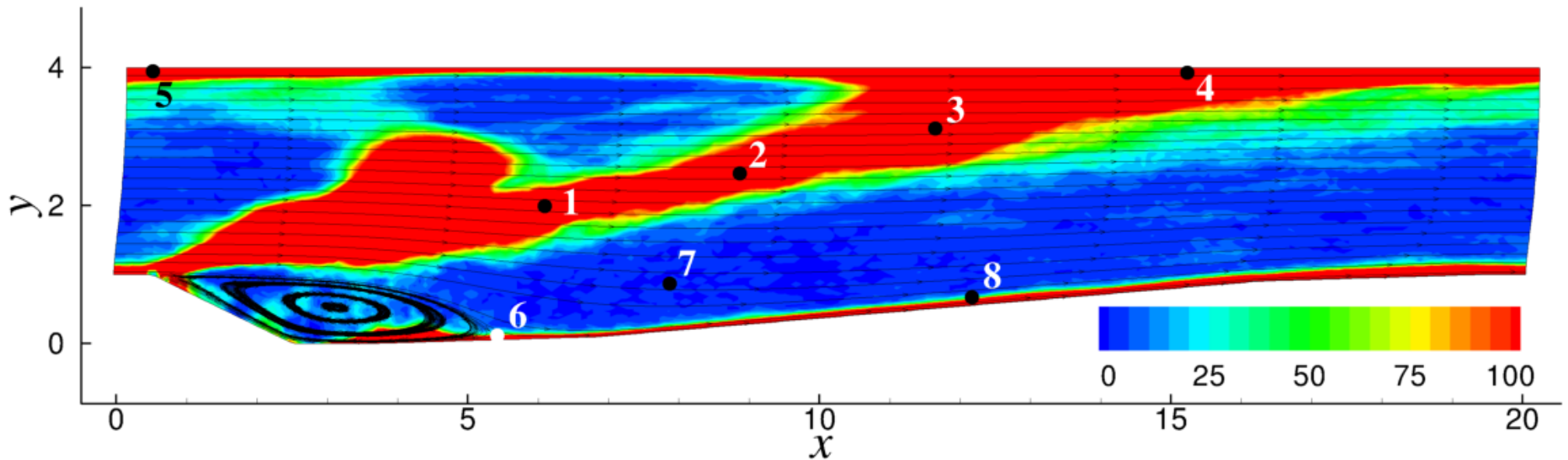


- Boils can be identified in the numerical simulations and related too the vortical structures.
- Once the structures are identified, we can consider the full field.



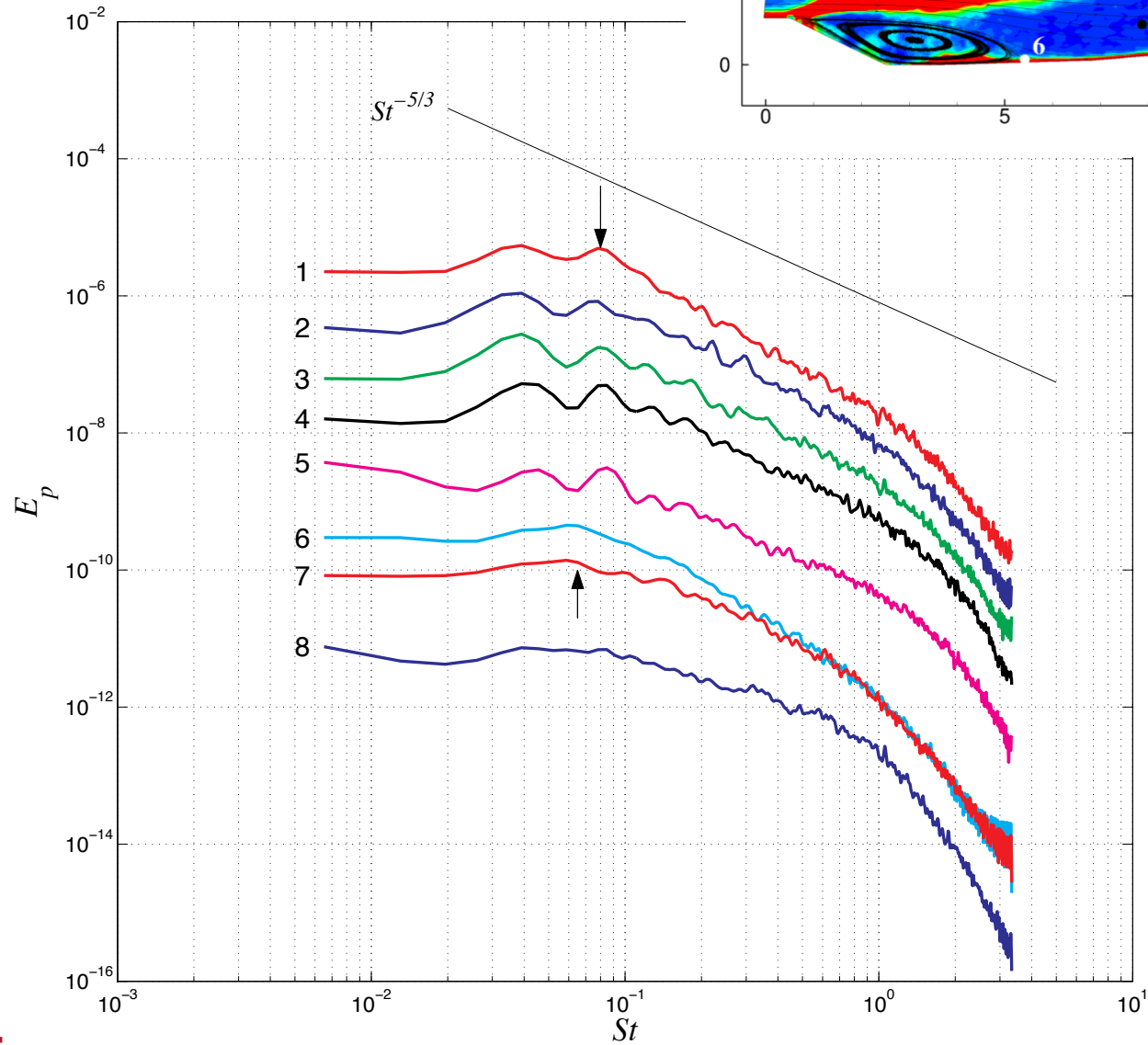
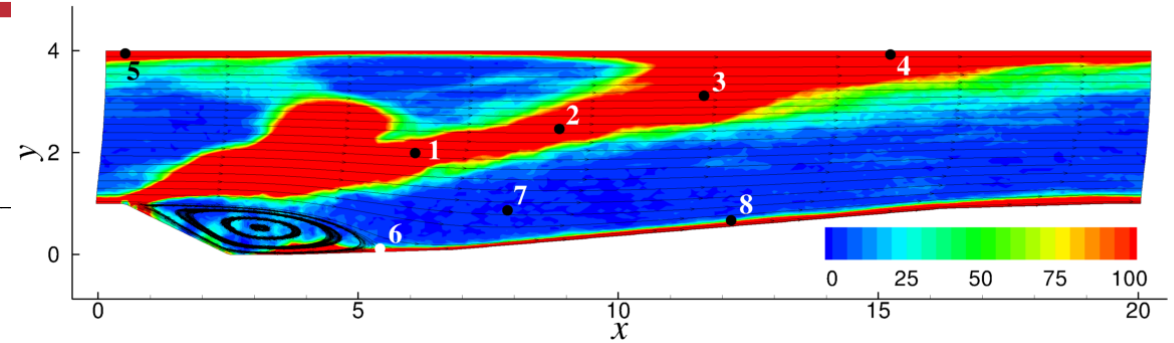
Low-pressure isosurfaces are used to visualize the vortex, and are coloured by the distance to the free surface (0→4).





Frequency of horseshoe vortex appearance

QUANTITATIVE ANALYSIS



Power spectra of
pressure

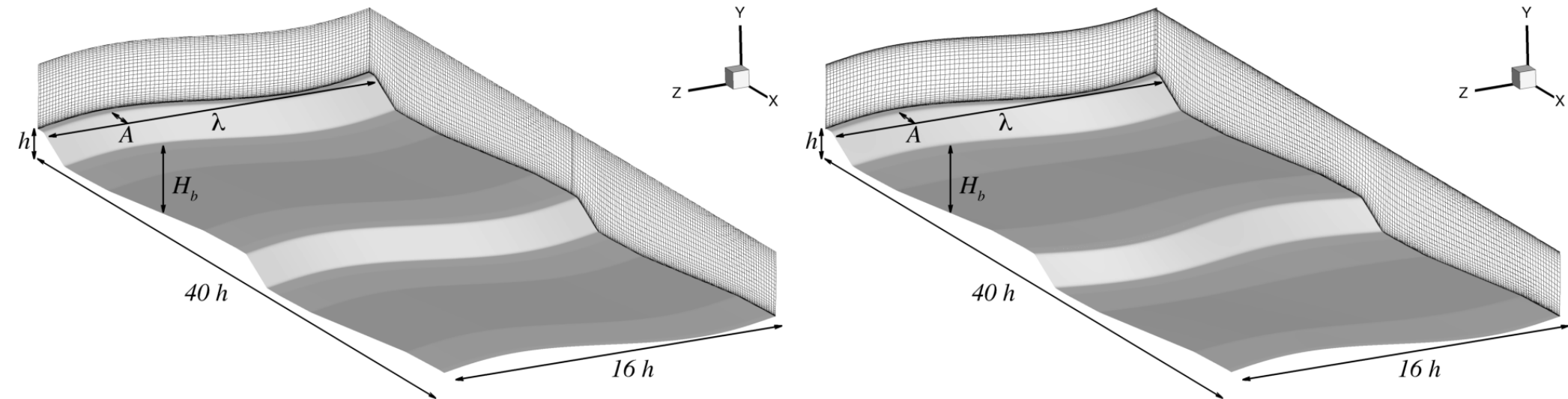


3D DUNES: MOTIVATION

- Real world: Dunes are three-dimensional.
- Effects of three-dimensionality on flow resistance, sediment transport, and turbulence production are not well known.
- Experiments on three-dimensional dunes lack precise measurements of skin friction and form drag, as well as spatially-resolved turbulence stresses.



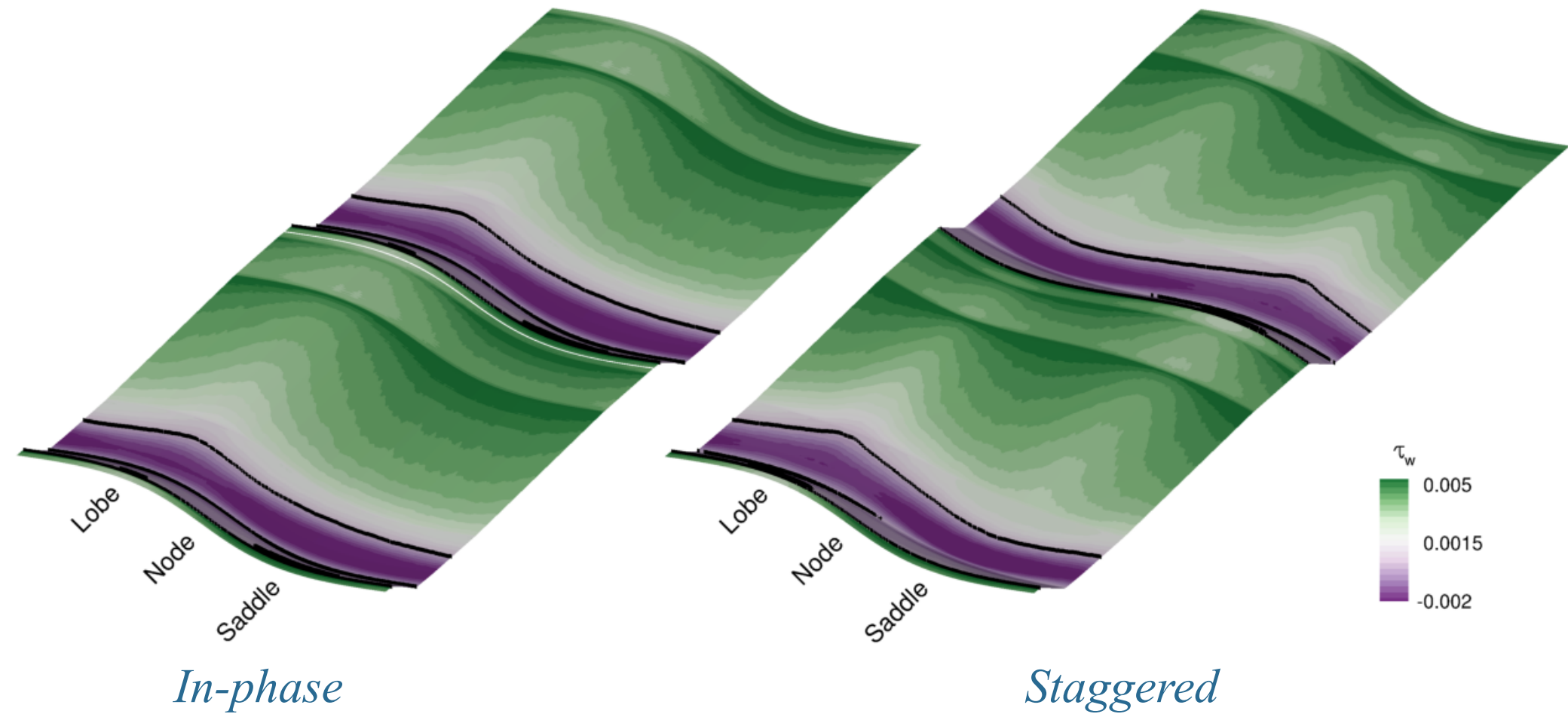
- Reynolds number: $Re = \frac{U_b H_b}{\nu} = 18,900$
- Two configurations: in-phase and staggered



Cases	A/h	λ/h	$N_x \times N_y \times N_z$	Δs^+	Δn^+	Δz^+
<i>In-phase</i>	1.0	16.0	512 × 96 × 256	22.0	0.7	18.1
<i>Staggered</i>	1.0	16.0	640 × 128 × 320	17.6	0.7	14.0



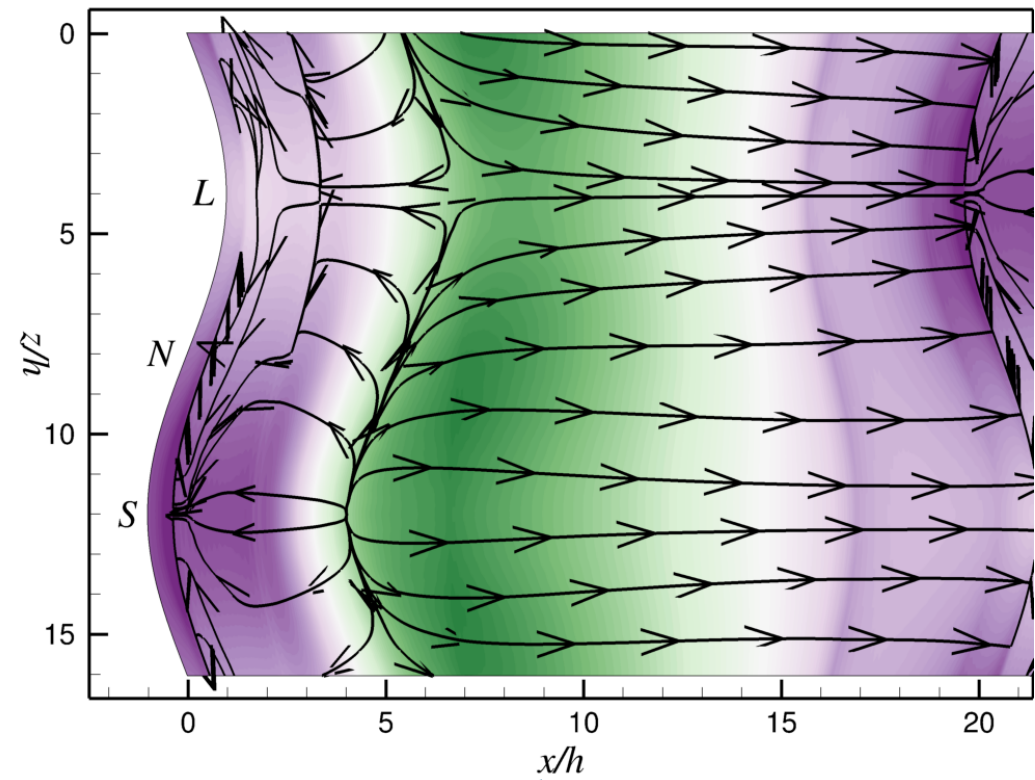
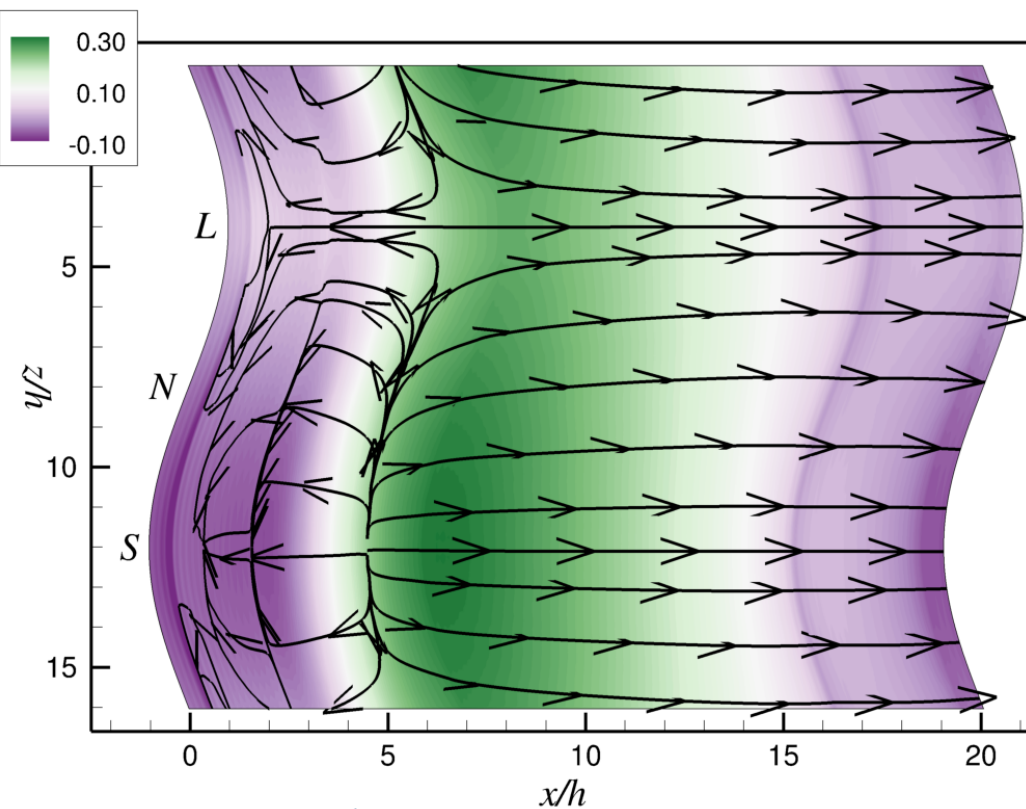
Wall stress τ_w





- Lateral pressure gradient (from node to lobe) induces spanwise flow

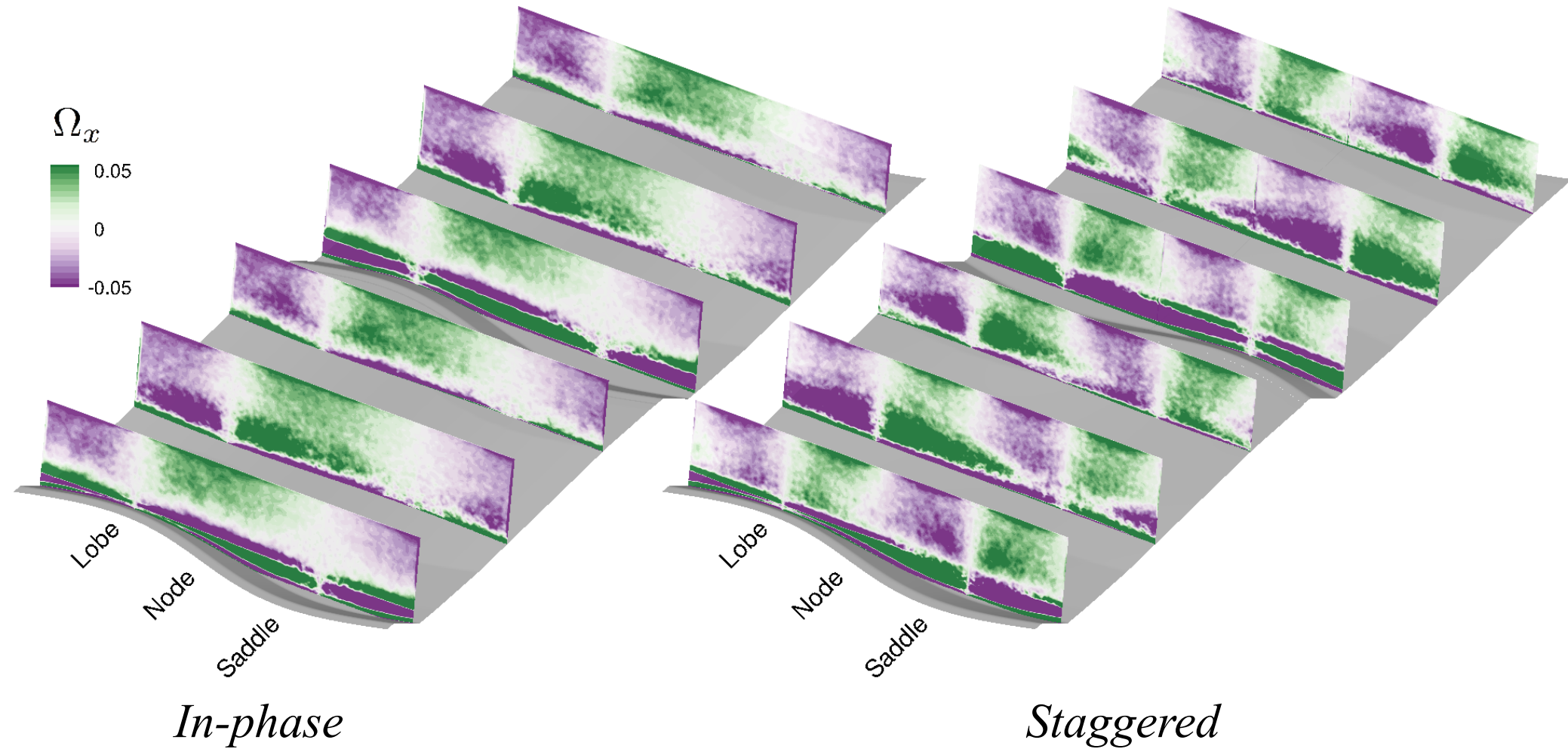
Mean wall pressure and wall streamlines



4.19 *In-phase*

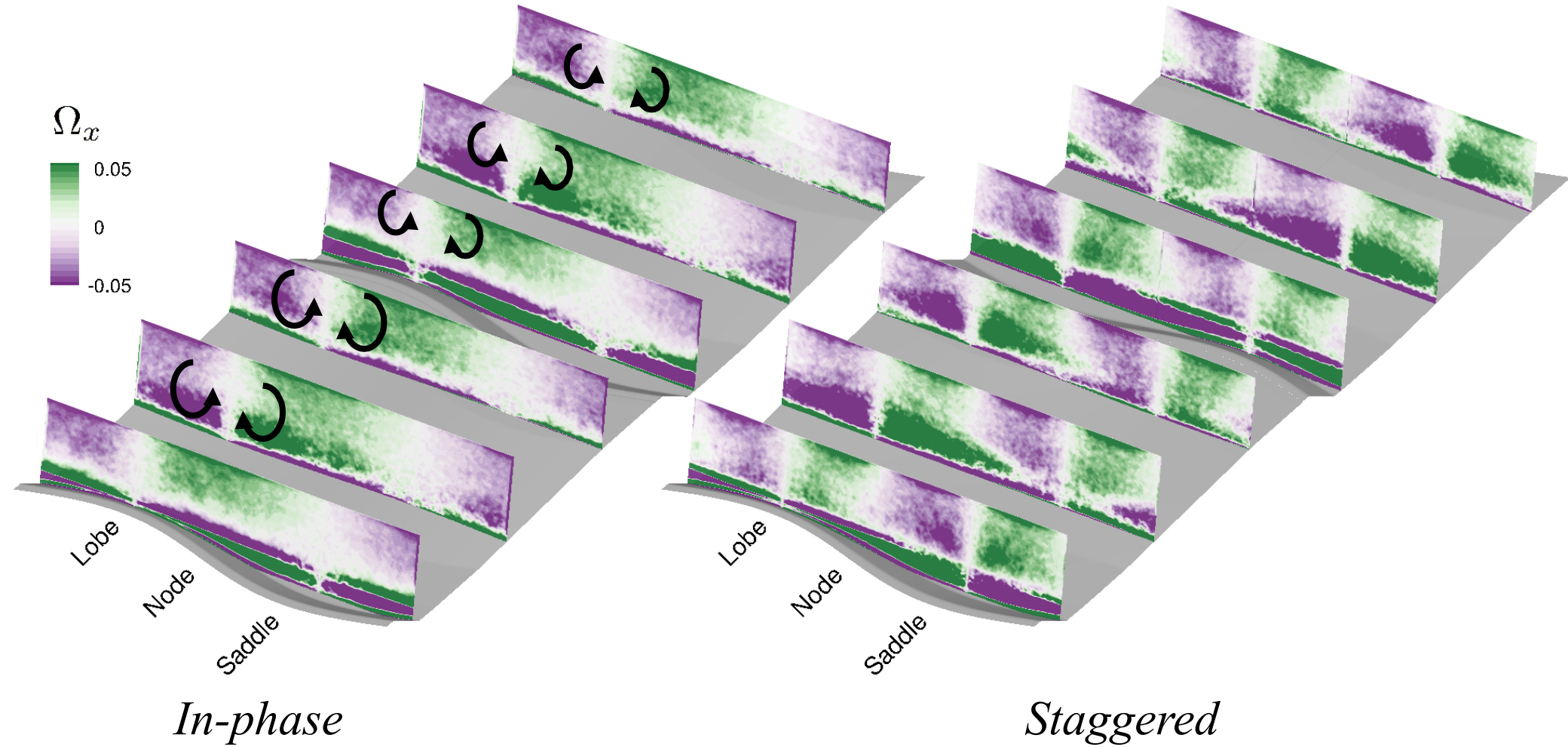
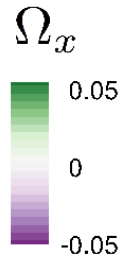
Staggered

Mean streamwise vorticity Ω_v



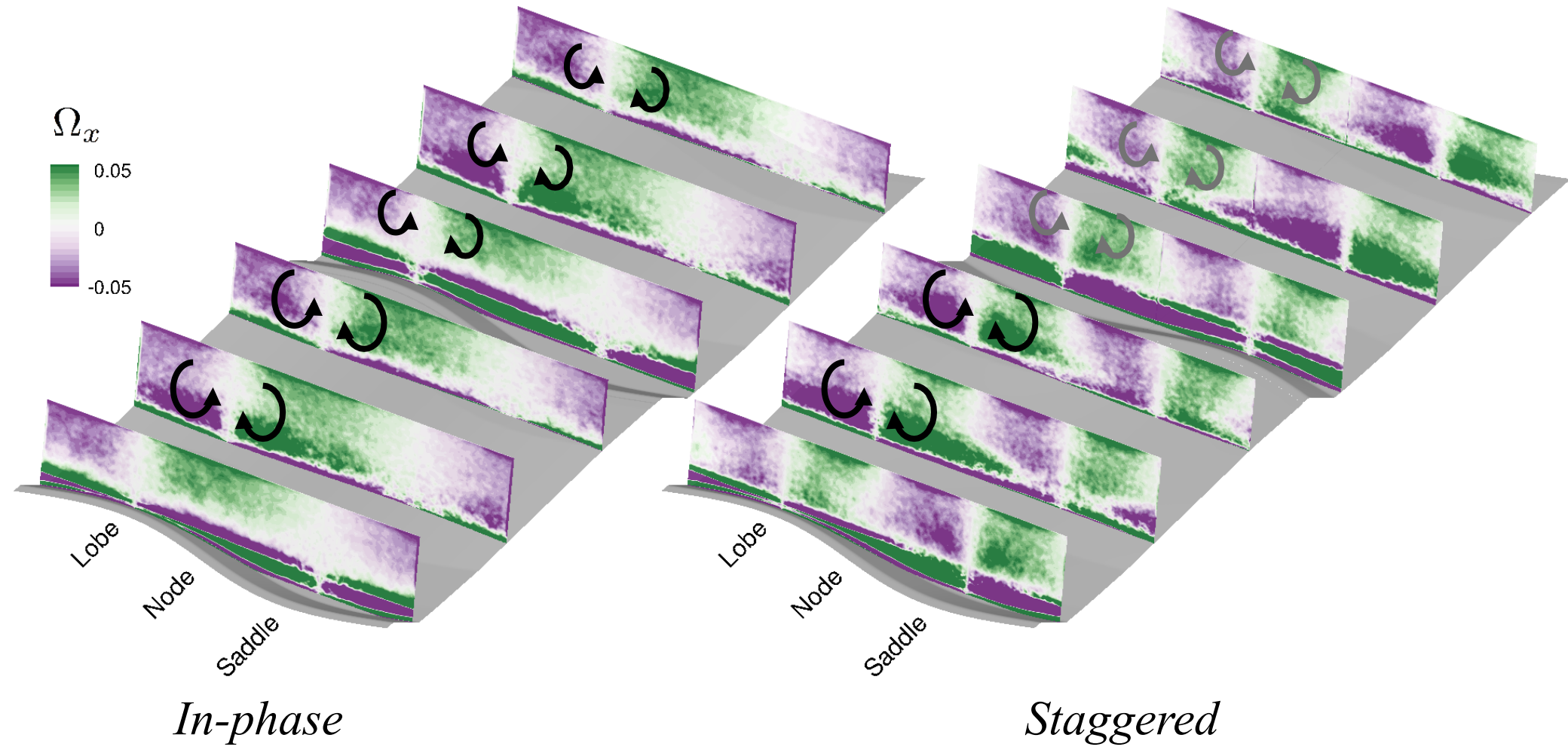


Mean streamwise vorticity Ω_x





Mean streamwise vorticity Ω_x

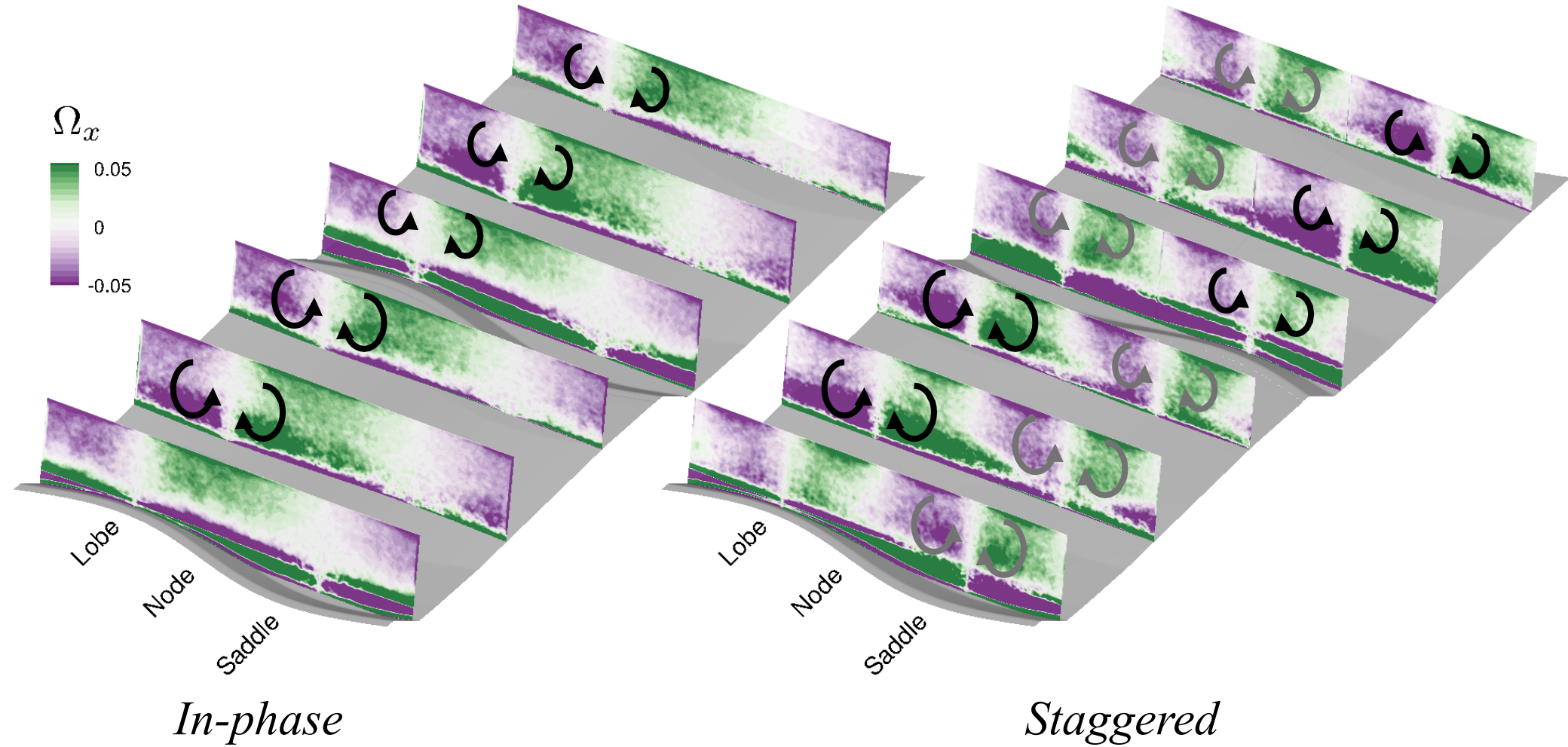


In-phase

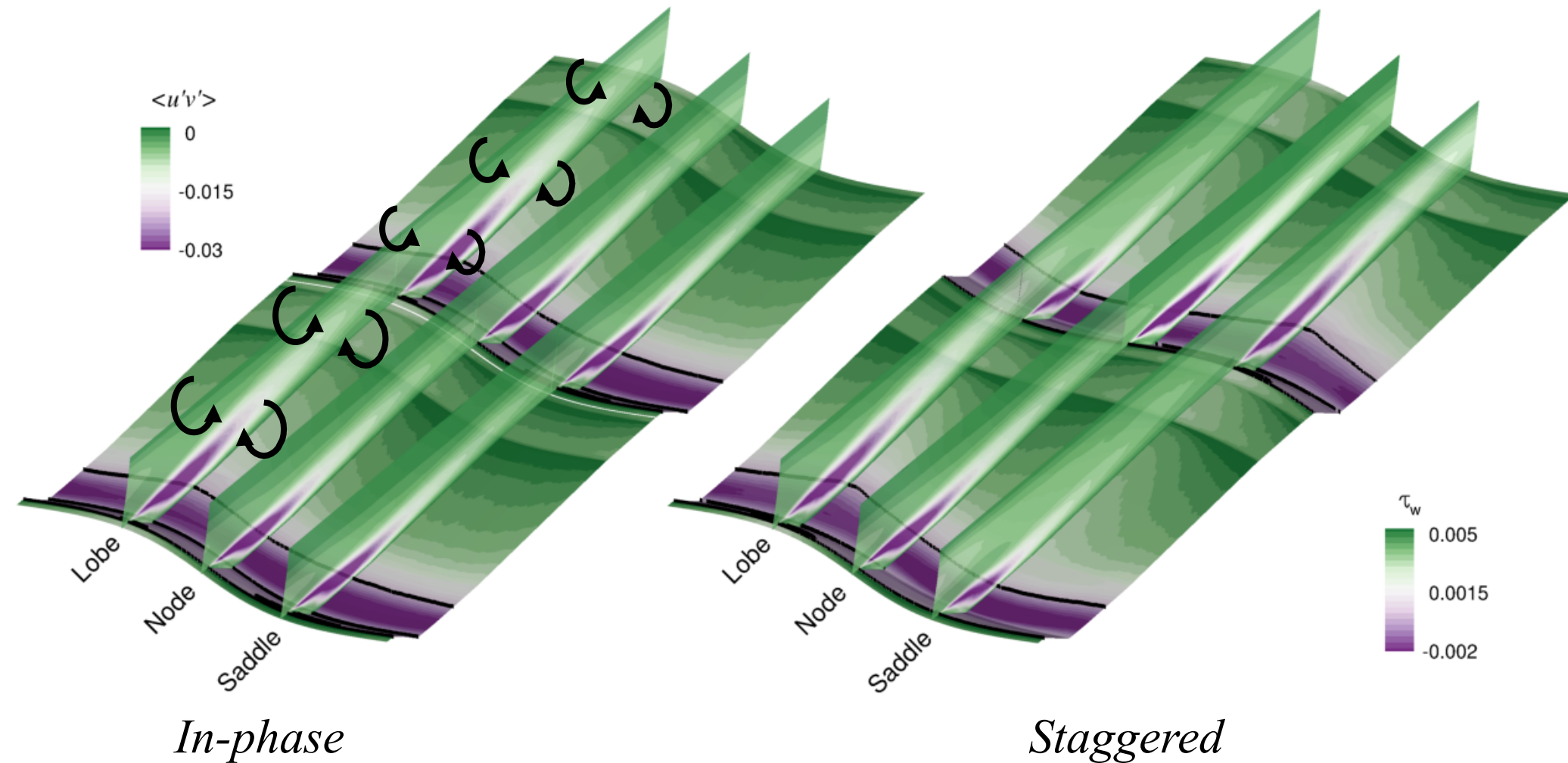
Staggered



Mean streamwise vorticity Ω_x

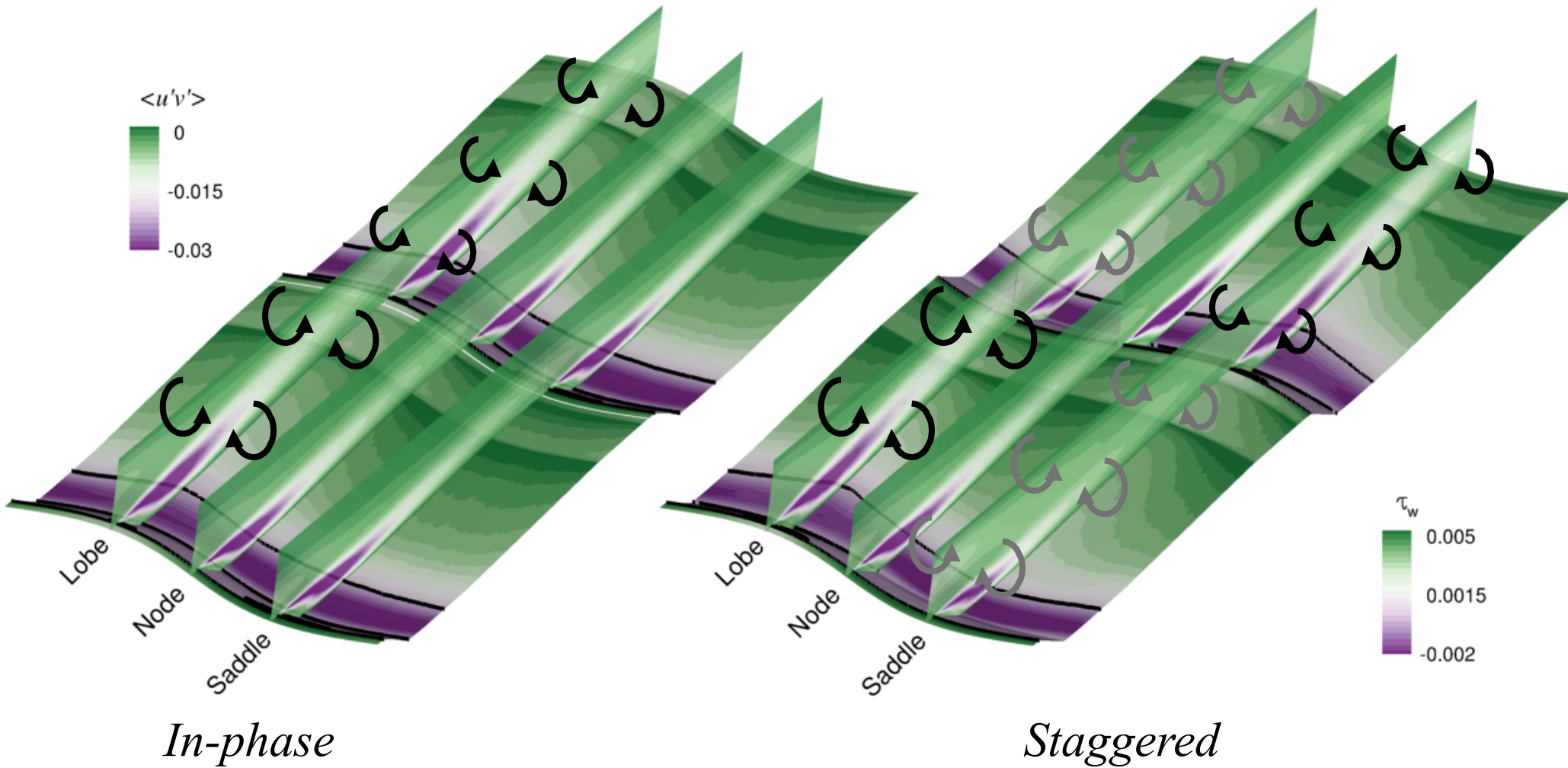


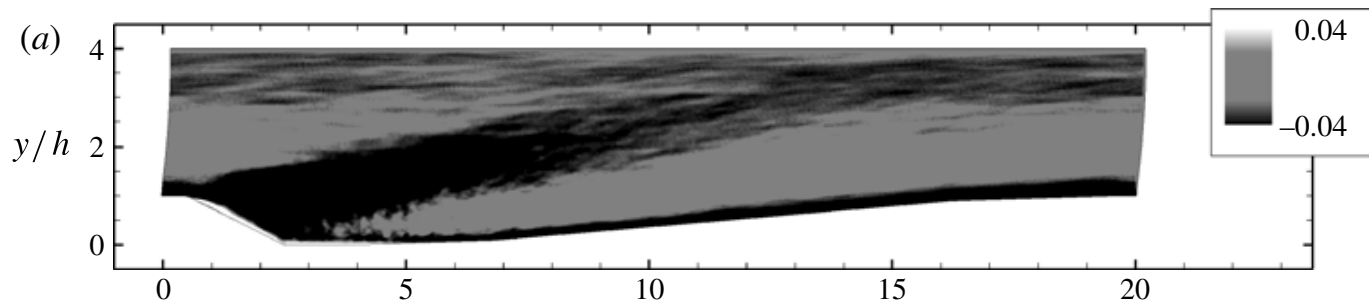
Reynolds shear stress $\langle u'v' \rangle$ and wall stress τ_w



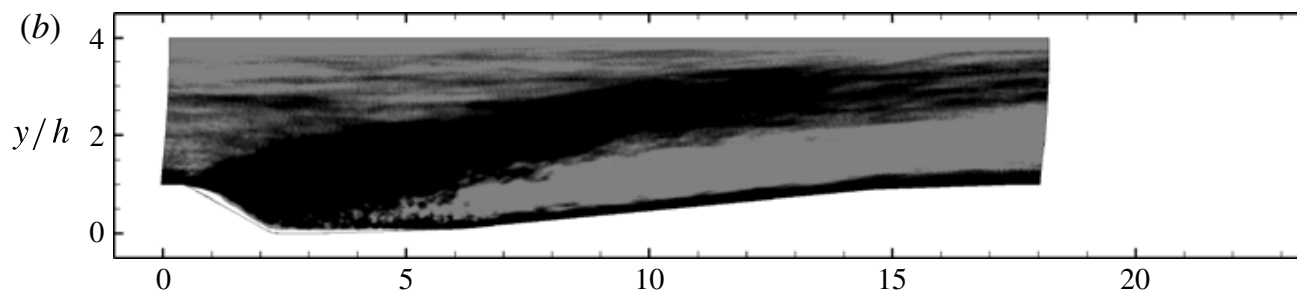


Reynolds shear stress $\langle u'v' \rangle$ and wall stress τ_w

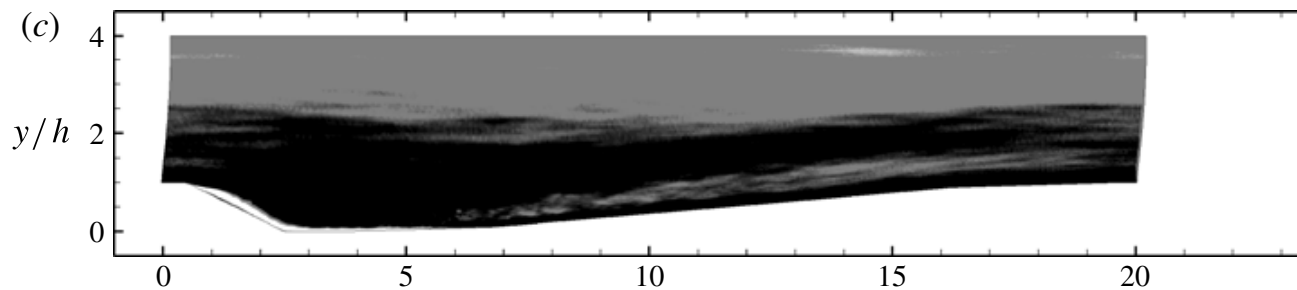




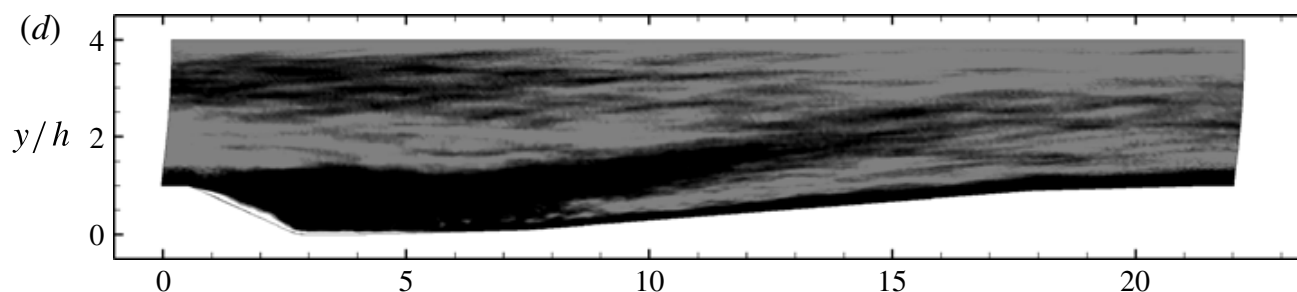
Lobe, in-phase



Lobe, staggered



Saddle, in-phase



Saddle, staggered

$(x - x_s)/h$ Frequency of horseshoe vortex appearance

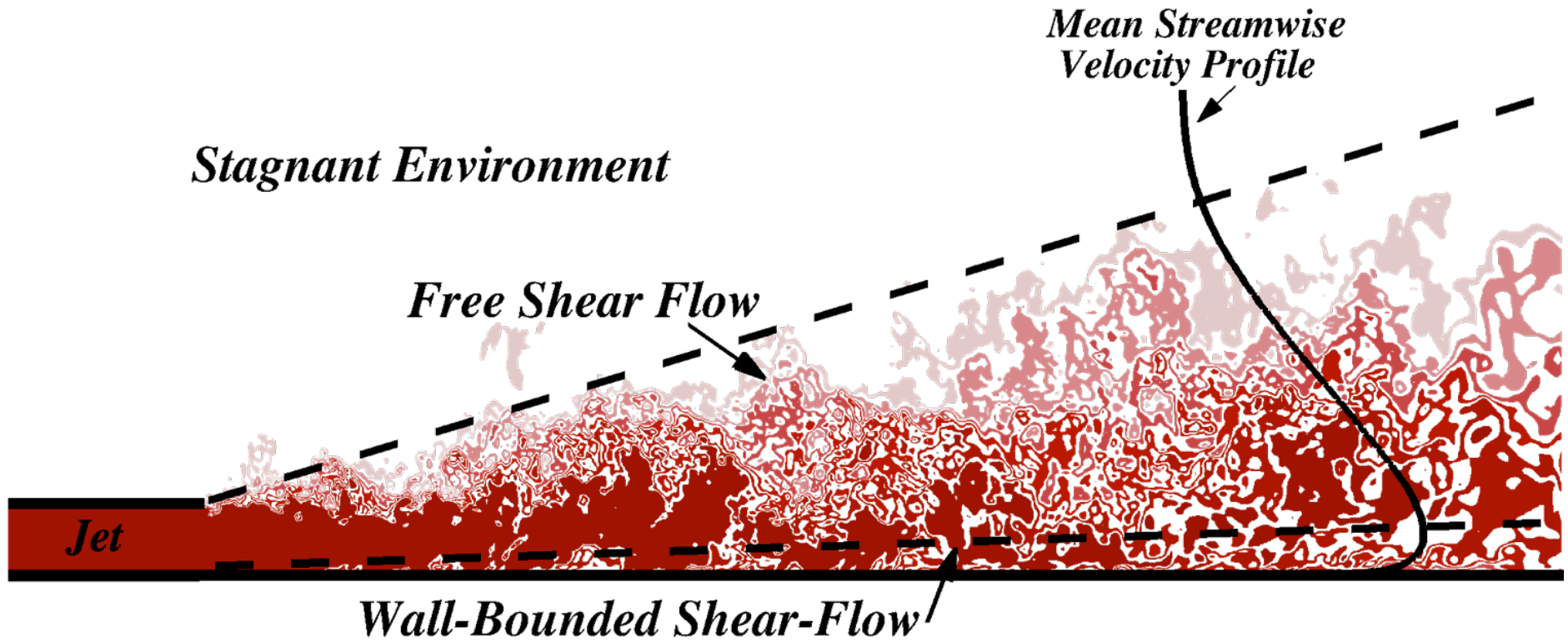


- The three-dimensional bed form induces mean secondary flow in the streamwise direction.
 - *Low-momentum fluid close to the bed moves from the saddle plane toward the lobe plane, generating a vortex pair.*
 - *The secondary flow affects the whole flow depth.*
 - *In the staggered configuration, there are two vortex pairs, one formed at the lobe and one advected over the saddle from the previous dune.*
- The spatial distribution of the separated-shear layer alters the flow across the channel.
 - *The upwash of slow fluid enhances the flow deceleration and acceleration in the lobe plane.*
 - *Advection displaces the shear layer and the horseshoe vortices upwards.*



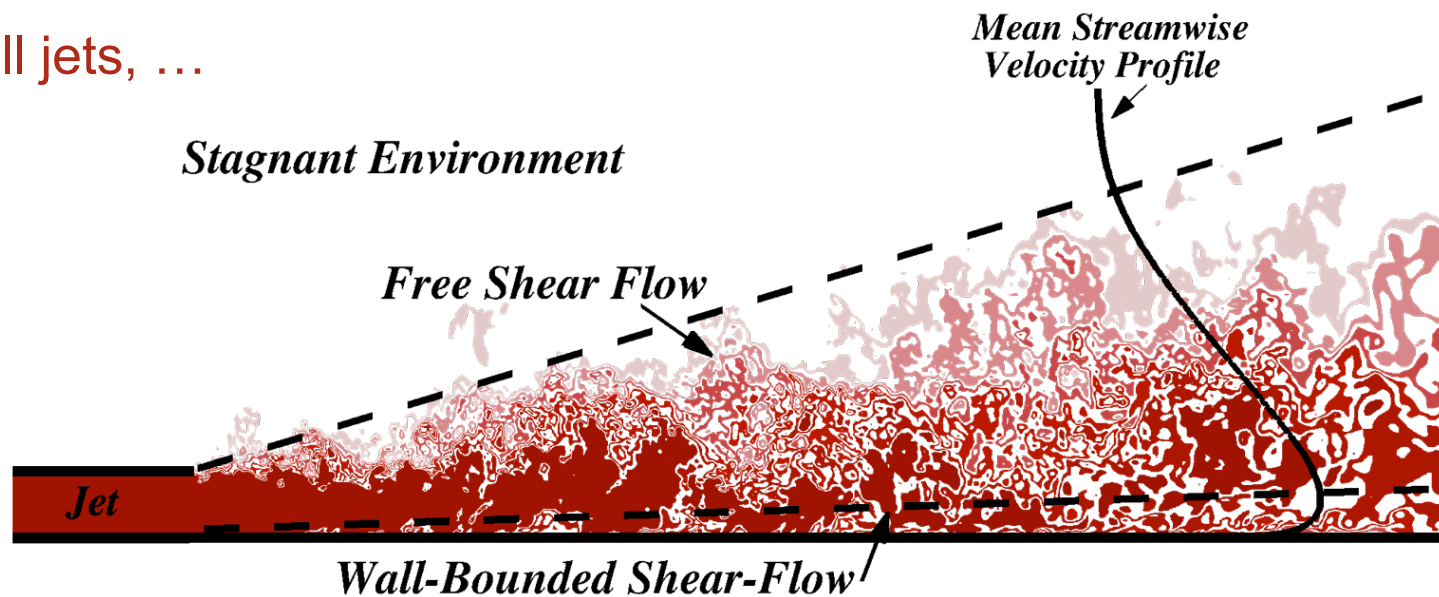
APPLICATIONS: WALL JETS

RAYHANEH BANYASSADY



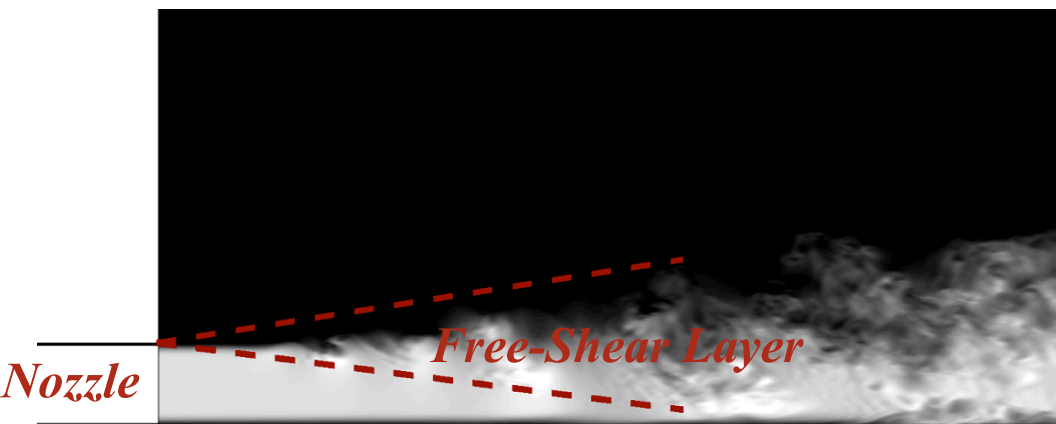


- Canonical turbulent shear-flows
 - *Wall-bounded shear flows*
 - Channel flows, pipes , boundary layers, ...
 - *Free-shear flows*
 - Jets, wakes, ...
- Hybrid turbulent shear-flows
 - *A combination of two or more of the canonical shear flows*
 - Wall jets, ...



- Two classes of wall-jets considered in this research
 - *Plane (two-dimensional) wall-jets*
 - *Radial wall-jets*

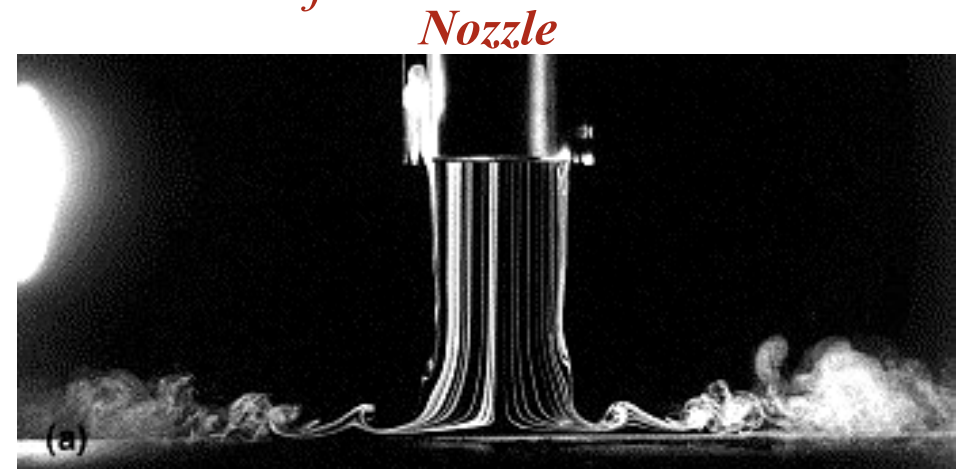
Plane wall-jet:



*Fully-developed
wall-jet region*

Source: Current study

Radial wall-jet:

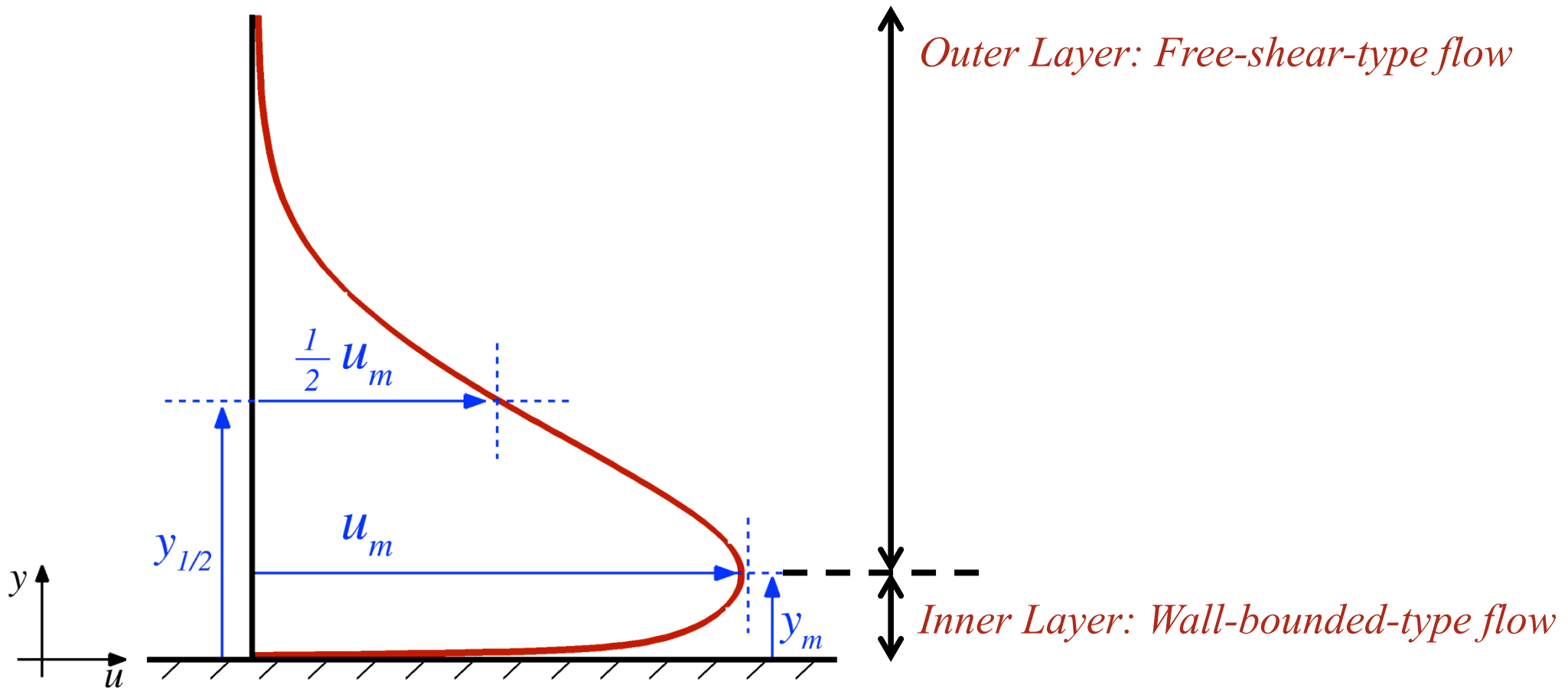


*Impingement
region* *Fully-developed
wall-jet region*

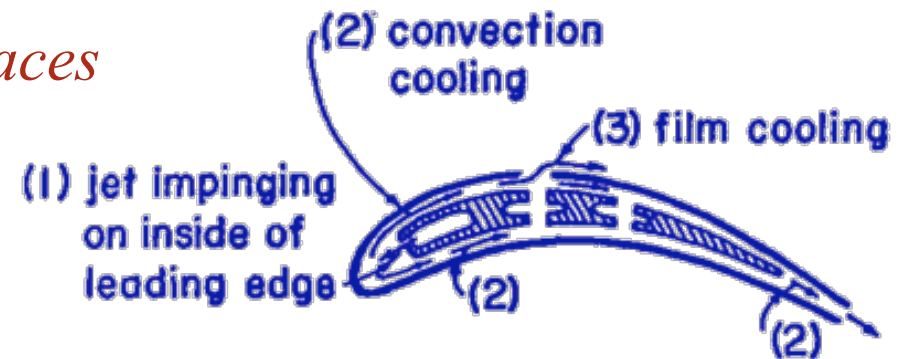
Source: Cornaro et al., Exp. Therm. Fluid Sci., 1999



- Typical fully-developed mean streamwise velocity profile



- Wall-jets have diverse applications in the fields of
 - *Downwash of vertical take-off and landing aircrafts and helicopters*
 - *Heating, cooling, and drying of surfaces*
 - *Separation control over airfoils*
 - *Air-conditioning in the buildings*
 - *Water flow under sluice gates*
 - *Downburst of a tornado*



Source: J.L. Kerrebrock, *Aircraft Engine and Gas Turbines (2nd Edition)*, MIT Press, 1992.

- The study of wall-jets will be useful in understanding
 - *More complex flows with two or more interacting shear layers*
 - *All sorts of asymmetric turbulent shear-flow*

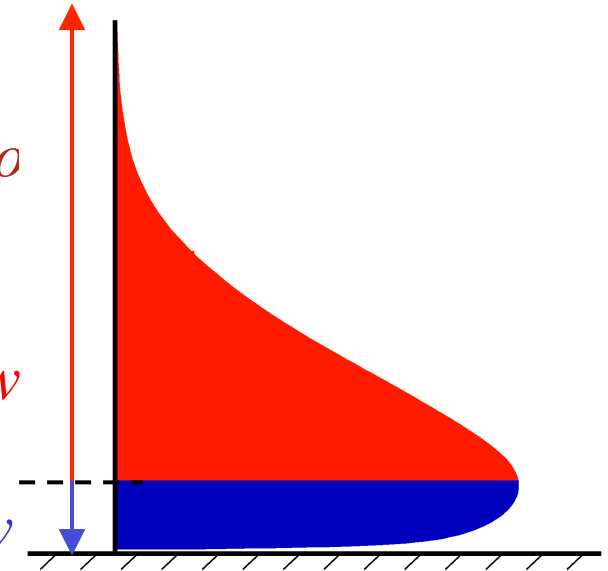


- Two non-interacting shear layers

- *Glauert (1956), Abrahamsson et al. (1994), Ro*

Outer Layer: Free-shear-type flow

Inner Layer: Wall-bounded-type flow

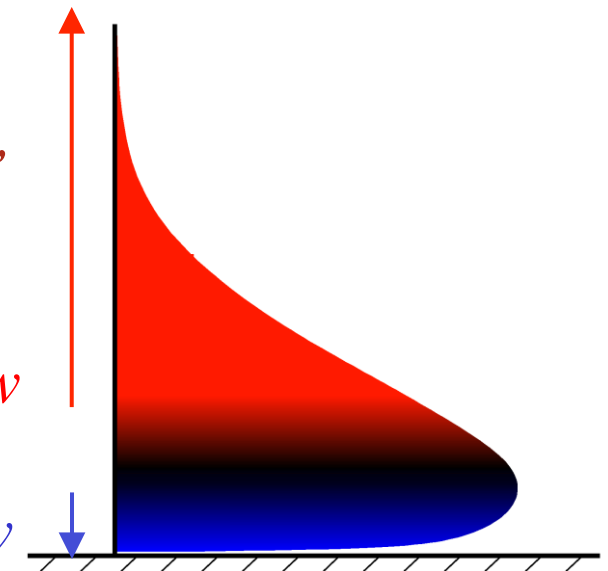


- Two interacting layers or three layers

- *George et al. (1997), Barenblatt et al. (2005), (2004-2007), ...*

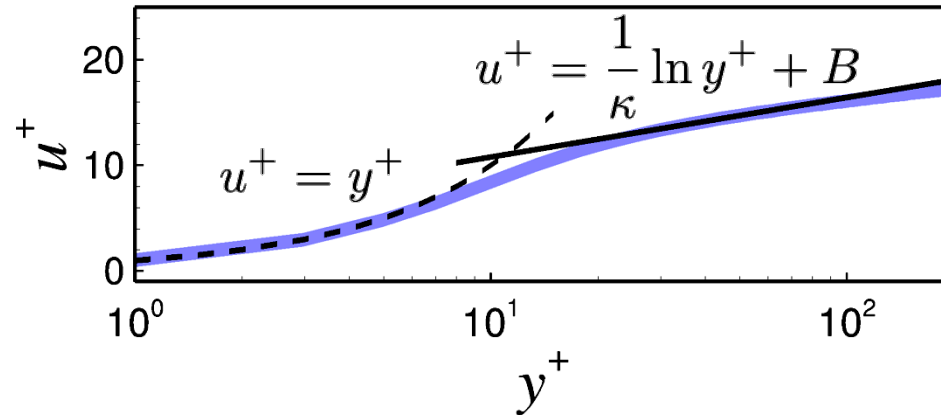
Outer Layer: Free-shear-type flow

Inner Layer: Wall-bounded-type flow





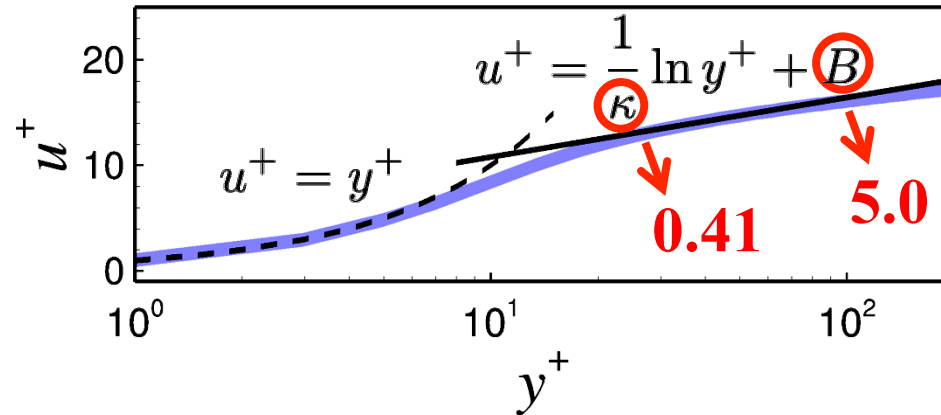
- Logarithmic law of the wall



Reference	Wall-jet type	κ	B
Bradshaw and Gee, 1962	Plane	0.49	6.8
Patel, 1962	Plane	0.49 to 0.60	6.8
Wyganski <i>et al.</i> , 1992	Plane	0.42	5.5 to 9.5
Ozdemir and Whitelaw, 1992	Radial	0.41	$1.292 u_m/u_\tau - 6.2$
Abrahamsson <i>et al.</i> , 1994	Plane	0.41	5.0
Eriksson <i>et al.</i> , 1998	Plane	0.41	5.0
Tachie <i>et al.</i> , 2002	Plane	0.41	5.0
Dejoan and Leschziner, 2005	Plane	0.41	5.0
Smith, 2008	Plane	0.55	8.7
Uddin <i>et al.</i> , 2013	Radial	0.41	$1.122 u_m/u_\tau - 10.53$



- Logarithmic law of the wall

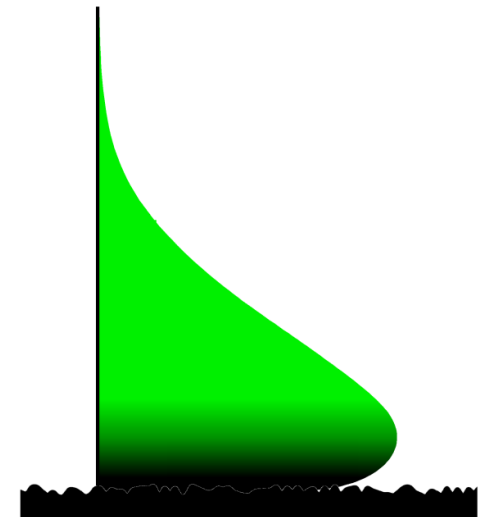
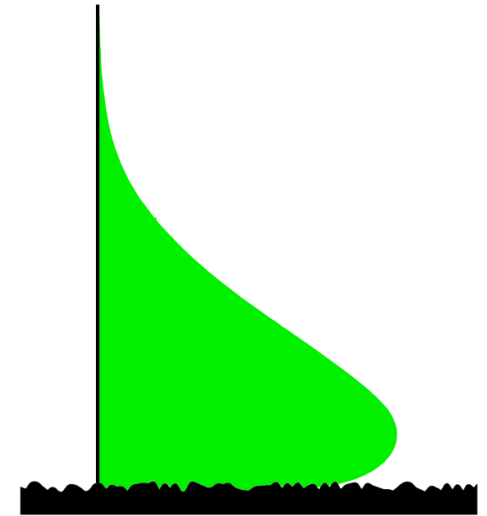


Reference	Wall-jet type	κ	B
Bradshaw and Gee, 1962	Plane	0.49	6.8
Patel, 1962	Plane	0.49 to 0.60	6.8
Wyganski <i>et al.</i> , 1992	Plane	0.42	5.5 to 9.5
Ozdemir and Whitelaw, 1992	Radial	0.41	$1.292 u_m/u_\tau - 6.2$
Abrahamsson <i>et al.</i> , 1994	Plane	0.41	5.0
Eriksson <i>et al.</i> , 1998	Plane	0.41	5.0
Tachie <i>et al.</i> , 2002	Plane	0.41	5.0
Dejoan and Leschziner, 2005	Plane	0.41	5.0
Smith, 2008	Plane	0.55	8.7
Uddin <i>et al.</i> , 2013	Radial	0.41	$1.122 u_m/u_\tau - 10.53$

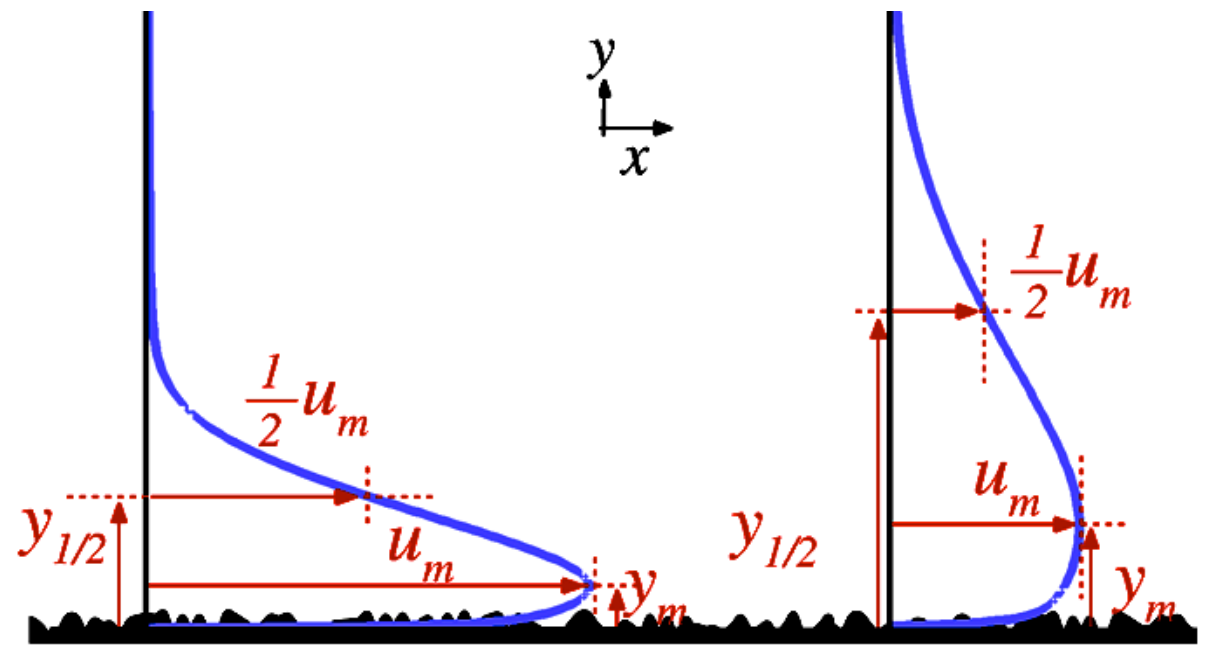


- Analysis of first order statistics
 - *Rajaratnam (1976), Hogg et al. (1997), ...*

- Analysis of the effects of roughness on different features of wall-jets
 - *Tachie et al. (2002-2004), Smith (2008), Rajaratnam and Mazurek (2005), Rostamy et al. (2011), ...*



- Rates of evolution of wall-jets



	u_m	y_m	$y_{1/2}$	$-du_m/dx$	dy_m/dx	$dy_{1/2}/dx$
Rajaratnam <i>et al.</i> (1981)	↓	-	-	-	↑	c
Tachie <i>et al.</i> (2004)	↓	↑	c	↑	↑	c
Smith (2008)	c	↑ or $\approx c$	c	c	-	c
Rostamy <i>et al.</i> (2011)	↓	↑	↑	↑	-	c

↑, increased; ↓, decreased; c, constant; -, not reported



- The objective of this research is to
 - *Investigate some of the unknown aspects of plane and radial wall-jets*
 - The interaction of inner and outer layers
 - The extend to which the effects of roughness spreads away from the wall
 - The similarities and differences between plane and radial wall-jet
 - *Employ the results to answer some of the open questions in the literature*
 - Universality of the log-law constant
 - Effects of roughness on the rates of evolution of wall-jets



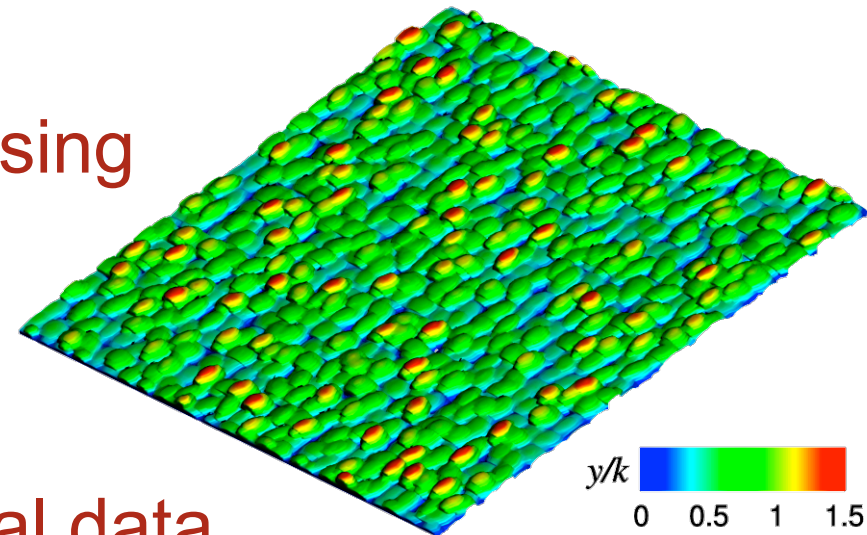
- Filtered continuity and Navier-Stokes equations

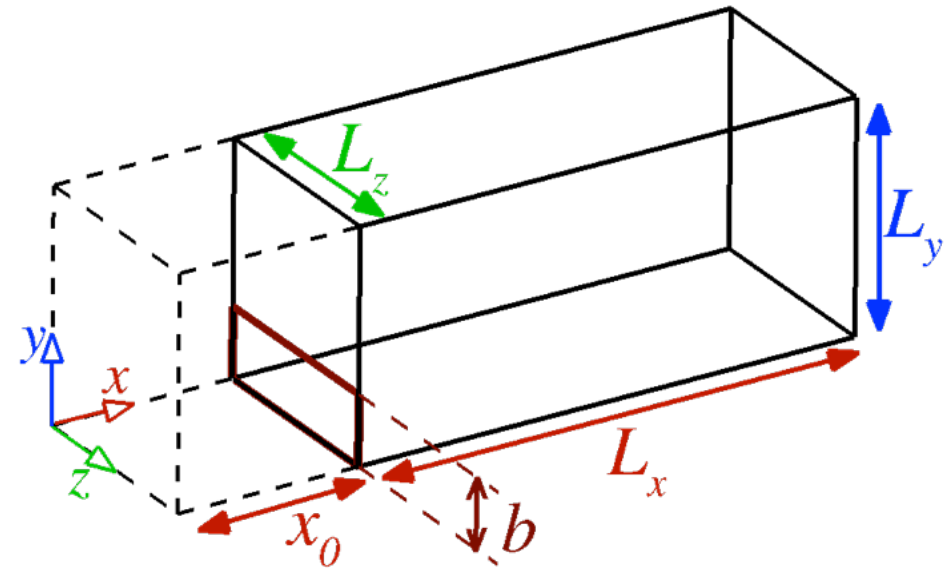
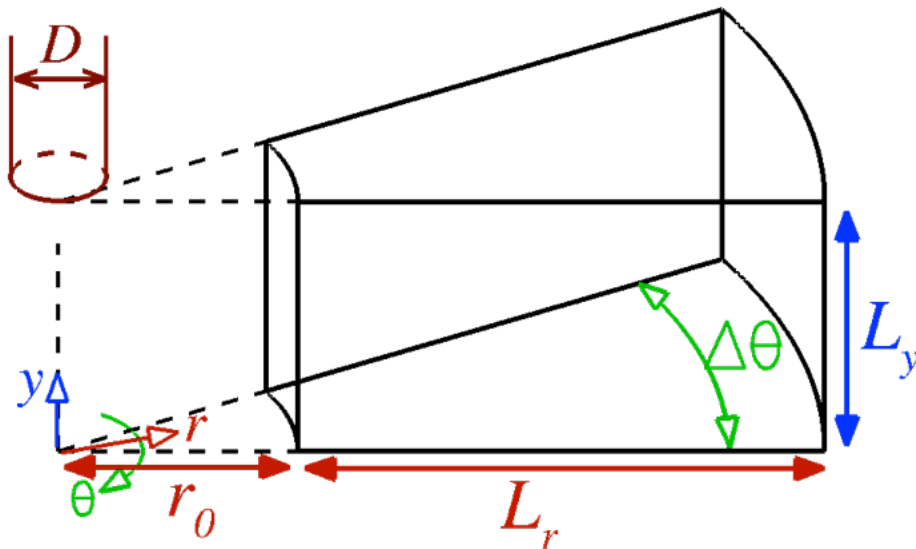
$$\nabla \cdot \bar{\mathbf{u}} = 0 \quad \frac{D\bar{\mathbf{u}}}{Dt} = -\nabla \bar{P} + 2\nabla \cdot (\nu_{tot} \bar{\mathbf{S}}) \quad \nu_{tot} = \frac{1}{Re} + \nu_t$$

- Eddy-viscosity assumption

$$\nu_t = C \bar{\Delta}^2 |\bar{\mathbf{S}}|$$

- Lagrangian dynamic eddy-viscosity model
- 2nd –order accurate in space and time, staggered finite difference code
- Random roughness is modeled using
 - *Virtual sandpaper model (Scotti 2006)*
 - *Immersed boundary method (IBM) based on volume of fluid (VOF) approach*
- Validated against the experimental data

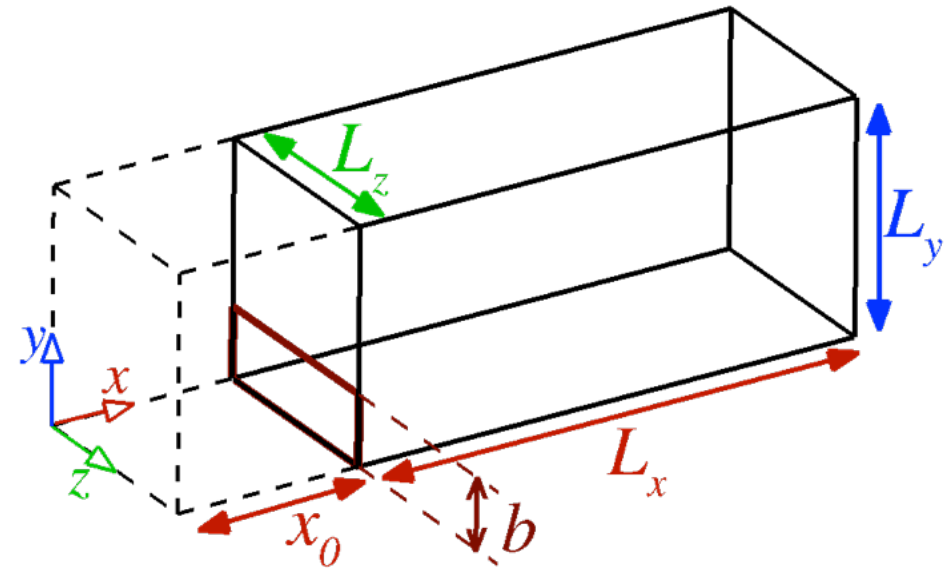
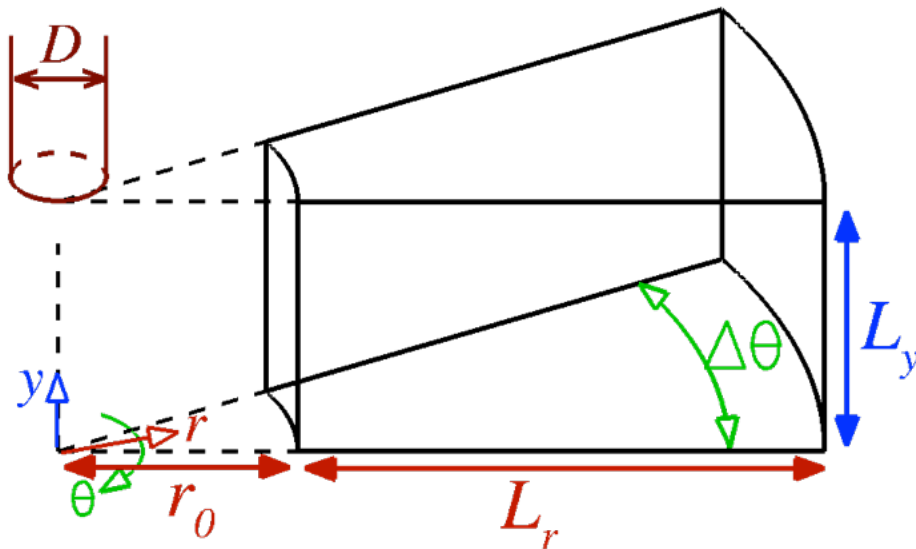




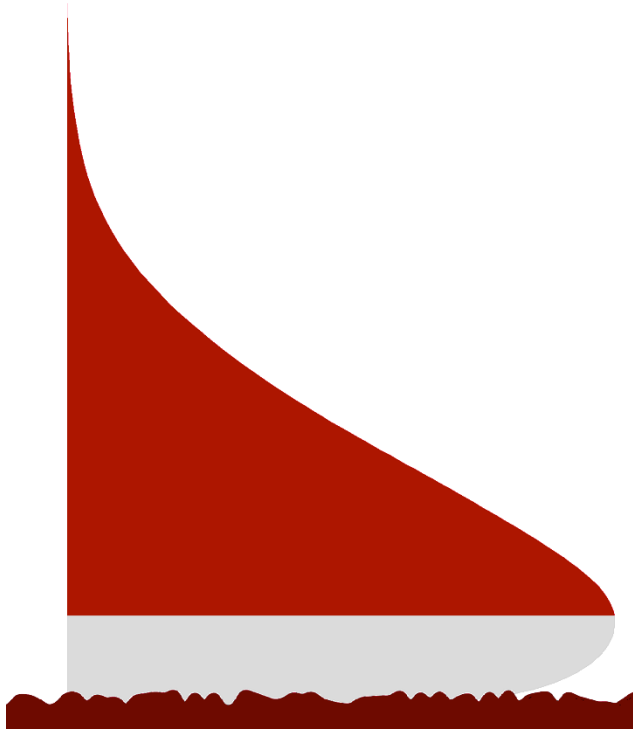
	x_0 or r_0	L_x or L_r	L_y	L_z or $\Delta\theta$	Re	Roughness	k_s^+
Plane-S2	0	$40b$	$20b$	$10b$	$u_b b/\nu = 7,500$	-	-
Plane-R	0	$40b$	$20b$	$10b$	$u_b b/\nu = 7,500$	$10b$ to $35b$	80 to 100
Radial-S	$1D$	$29D$	$6D$	$\pi/3$	$v_b D/\nu = 40,00$	-	-
Radial-R	$1D$	$29D$	$6D$	$\pi/3$	$v_b D/\nu = 40,00$	$6D$ to $26D$	20 to 40
Plane-S-I	$1D$	$29D$	$10D$	$10D$	$v_b D/\nu = 40,00$	-	-
Plane-S-L	$1D$	$29D$	$10D$	$10D$	$v_b D/\nu = 7,500$	-	-
Plane-S-H	0	$30b$	$10b$	$5.5b$	$u_b b/\nu = 40,000$	-	-



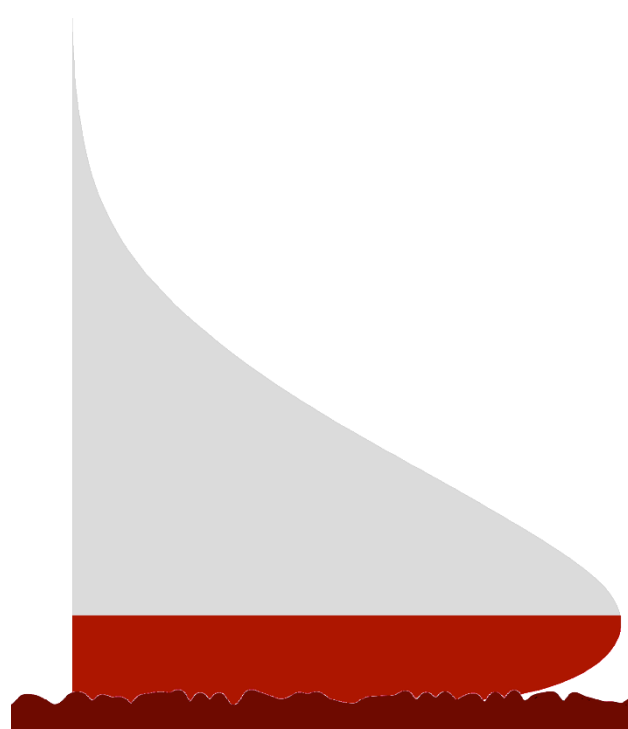
SETUP INNER/OUTER LAYER INTERACTION



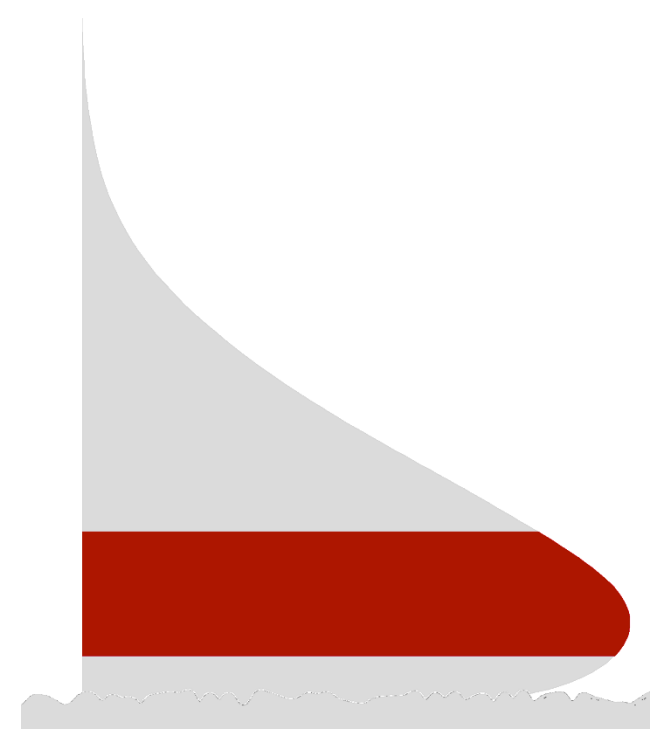
	x_0 or r_0	L_x or L_r	L_y	L_z or $\Delta\theta$	Re	<i>Roughness</i>	k_s^+
<i>Plane-S2</i>	0	$40b$	$20b$	$10b$	$u_b b/\nu = 7,500$	-	-
<i>Plane-R</i>	0	$40b$	$20b$	$10b$	$u_b b/\nu = 7,500$	$10b$ to $35b$	80 to 100
<i>Radial-S</i>	$1D$	$29D$	$6D$	$\pi/3$	$v_b D/\nu = 40,000$	-	-
<i>Radial-R</i>	$1D$	$29D$	$6D$	$\pi/3$	$v_b D/\nu = 40,000$	$6D$ to $26D$	20 to 40
<i>Plane-S-I</i>	$1D$	$29D$	$10D$	$10D$	$v_b D/\nu = 40,000$	-	-
<i>Plane-S-L</i>	$1D$	$29D$	$10D$	$10D$	$v_b D/\nu = 7,500$	-	-
<i>Plane-S-H</i>	0	$30b$	$10b$	$5.5b$	$u_b b/\nu = 40,000$	-	-



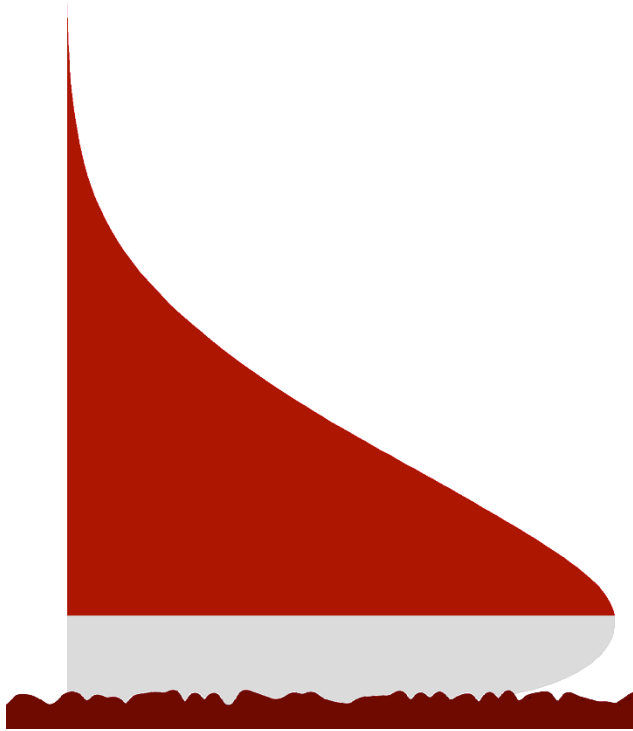
*roughness
outer layer*



*roughness
inner layer*



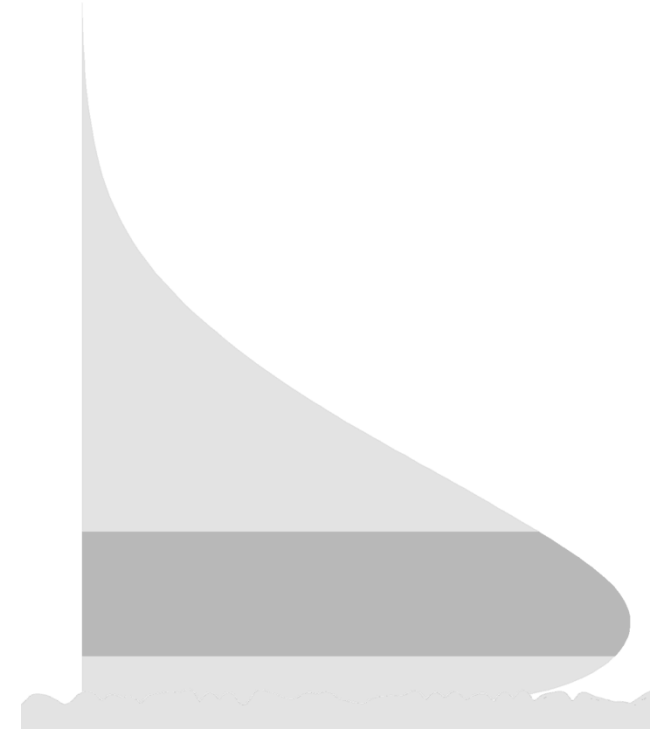
*Interaction inner
outer layers*



*roughness
outer layer*

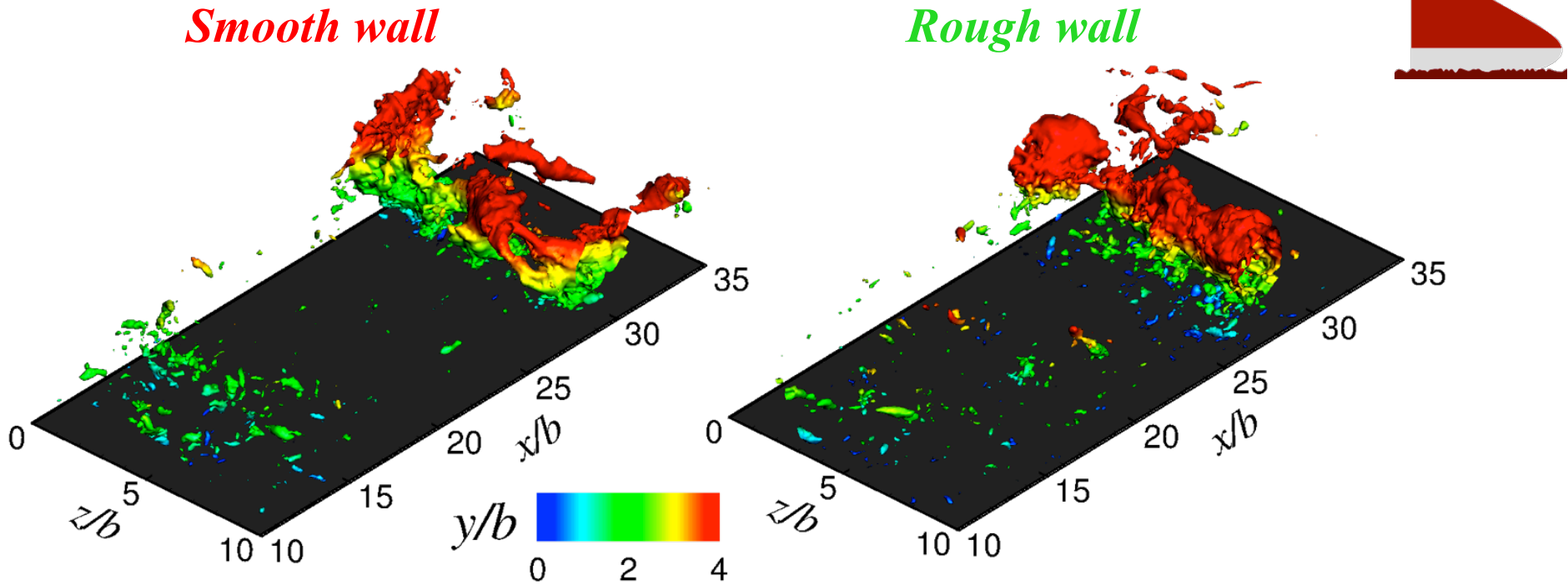


*Effects of roughness
on the inner layer*



*Interaction of inner
and outer layers*

- Visualization of the instantaneous flow field



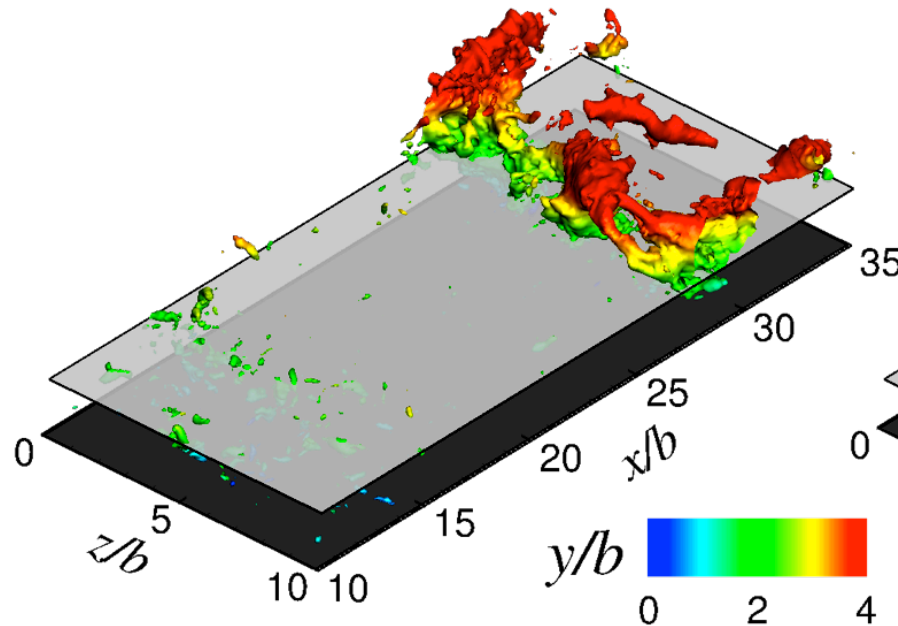


RESULTS

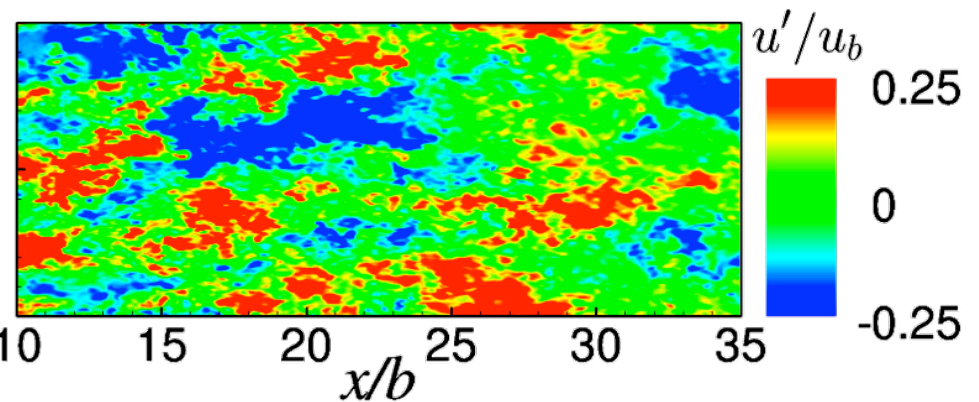
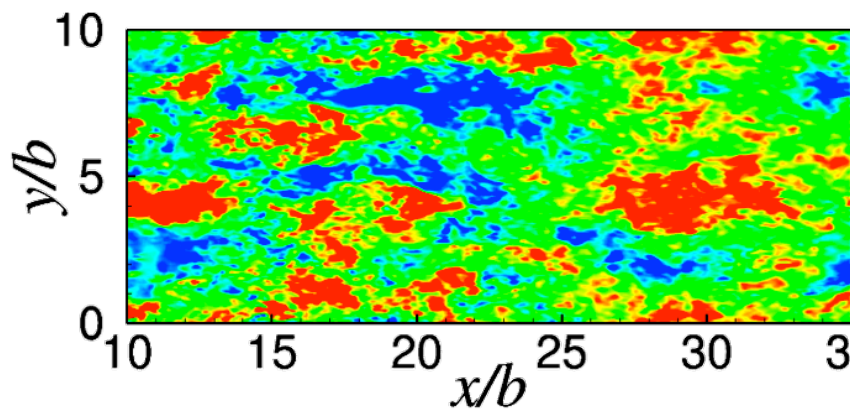
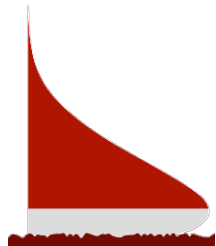
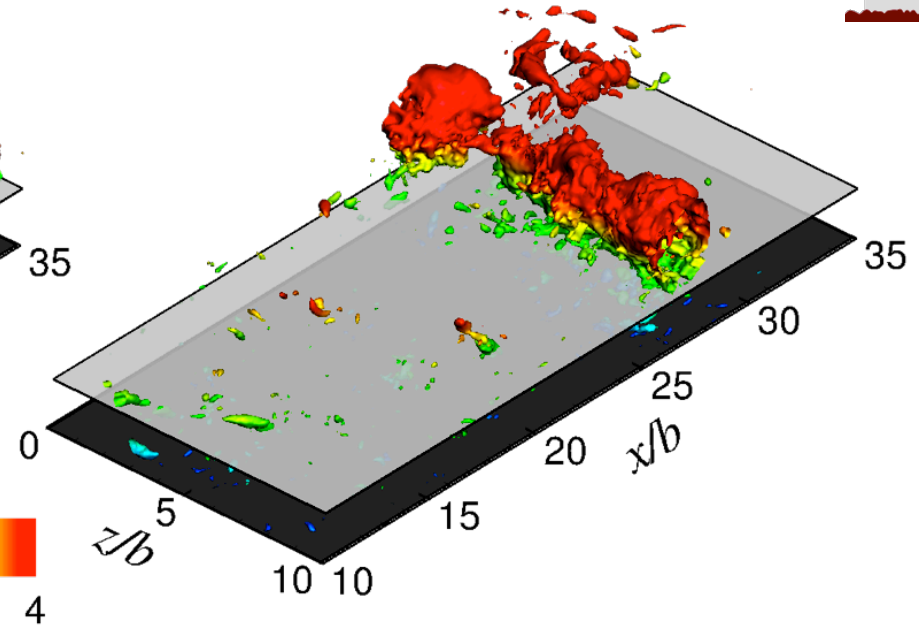
EFFECT OF ROUGHNESS ON THE OUTER LAYER

- Visualization of the instantaneous flow field

Smooth wall

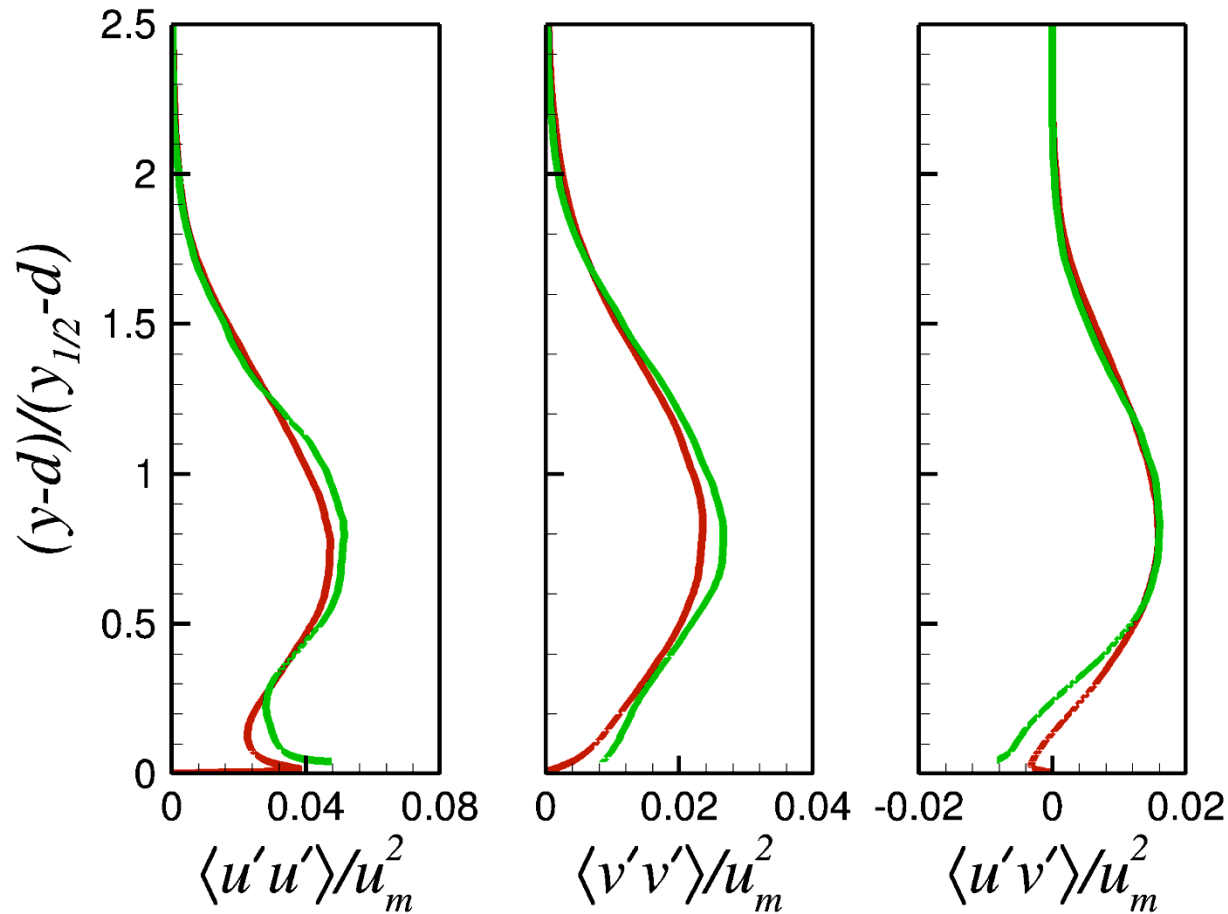
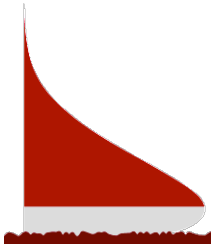


Rough wall





- Profiles of mean Reynolds stresses at $x = 20b$



— Smooth wall

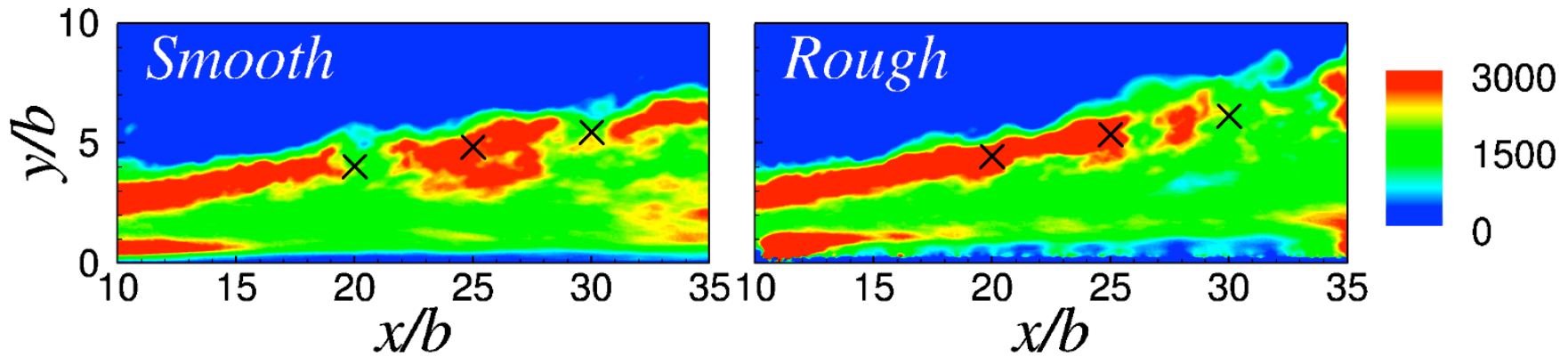
— Rough wall



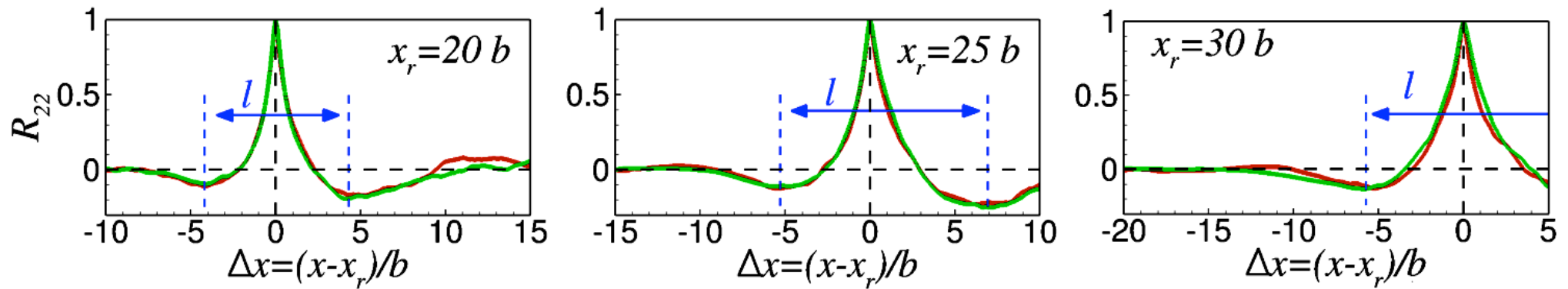
EFFECT OF ROUGHNESS ON THE OUTER LAYER

RESULTS

- Contours of number of occurrence of $p' < -5p_{rms}$ events

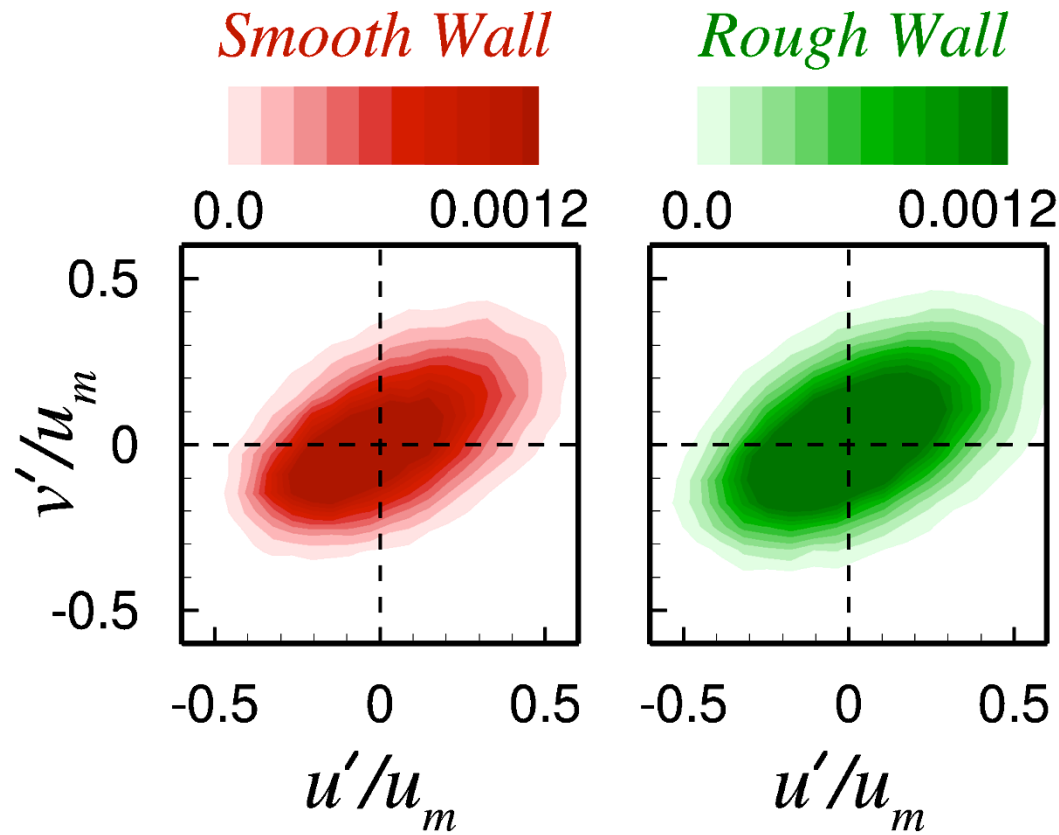
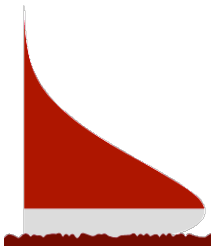


- Two-point autocorrelation: $R_{22}(x_r, y_r, x) = \frac{\langle v'(x_r, y_r) \cdot v'(x, y_r) \rangle}{\langle v'(x_r, y_r) \cdot v'(x_r, y_r) \rangle}$

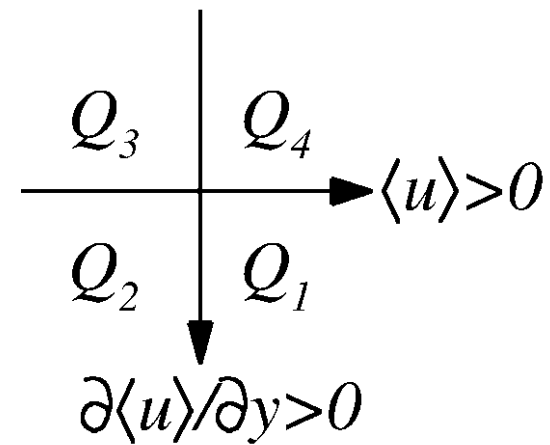


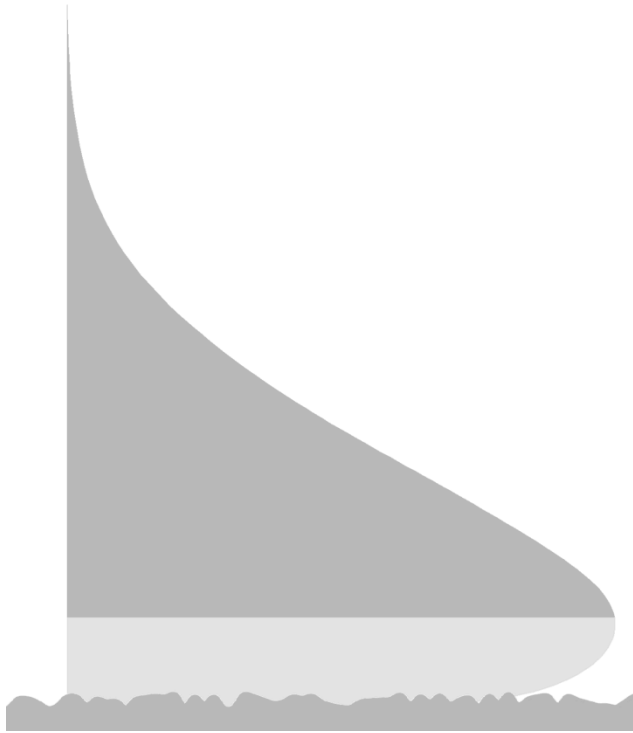
— Smooth wall — Rough wall

- Joint Probability Density Function

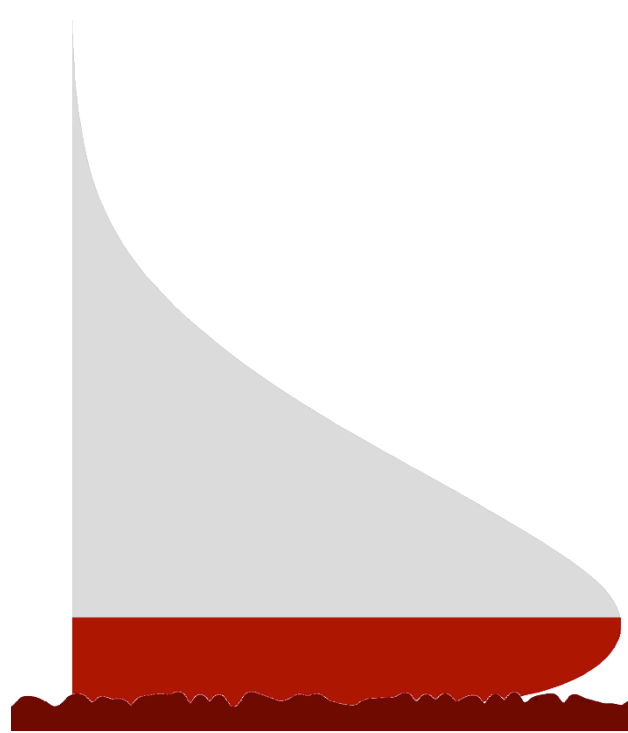


$$y = y_{1/2} \text{ and } x/b = 30$$

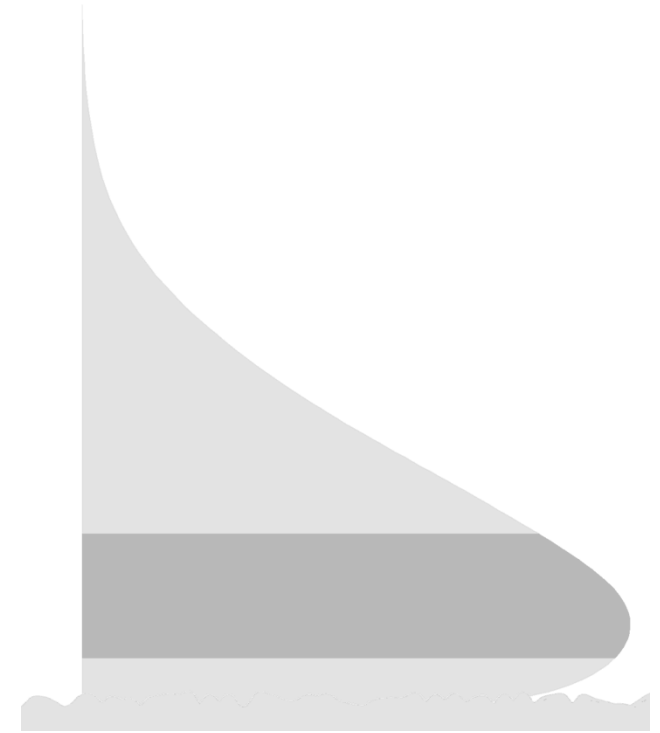




*Effects of roughness
on the outer layer*

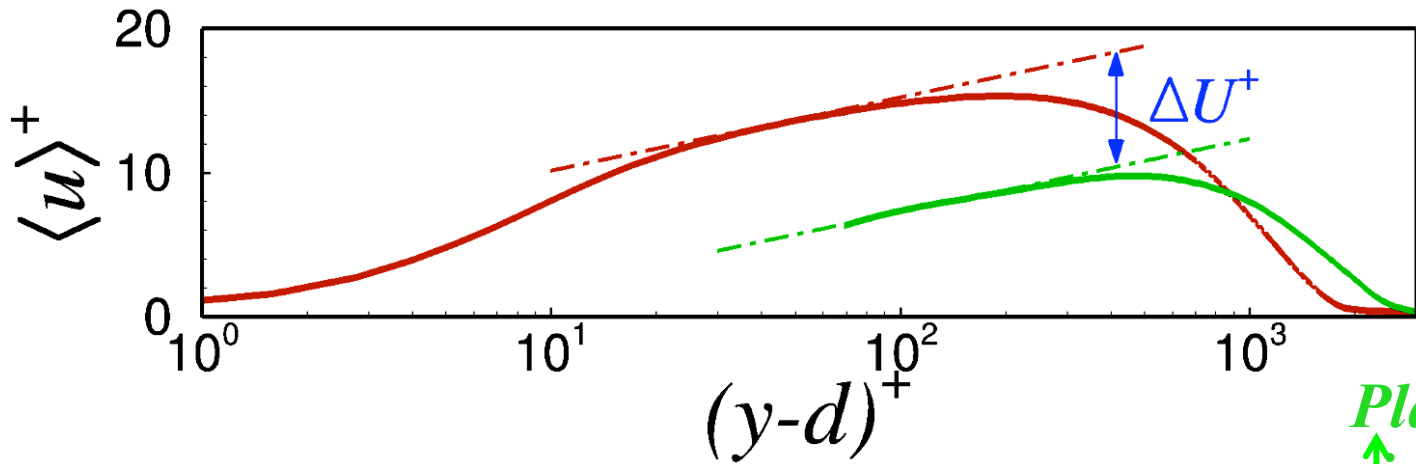
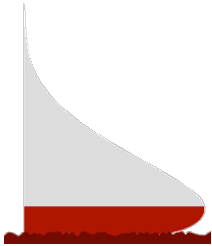


***roughness
inner layer***

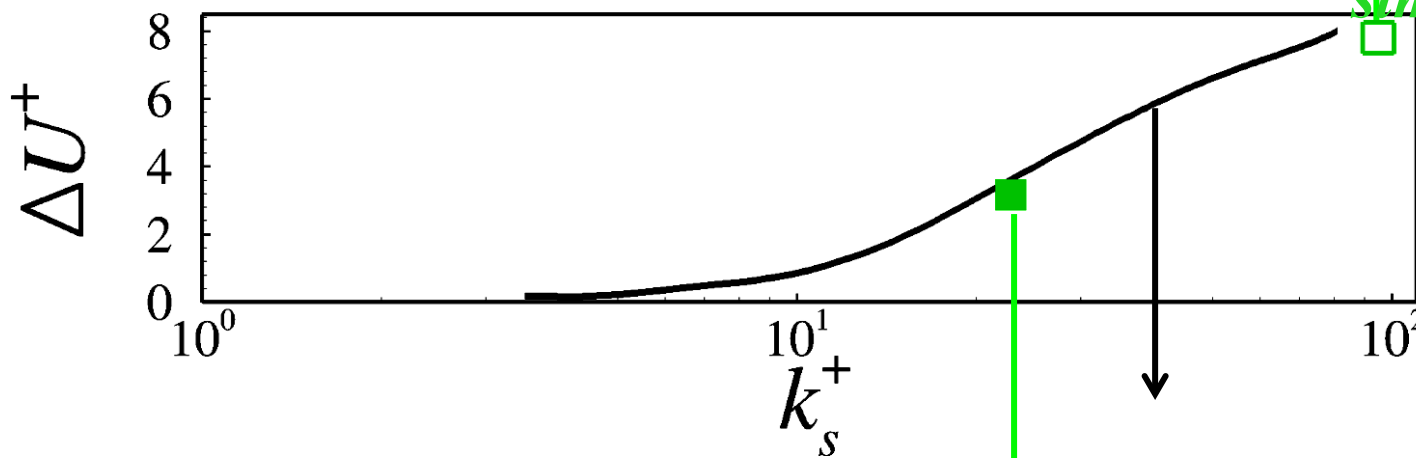


*Interaction of inner
and outer layers*

- Roughness function



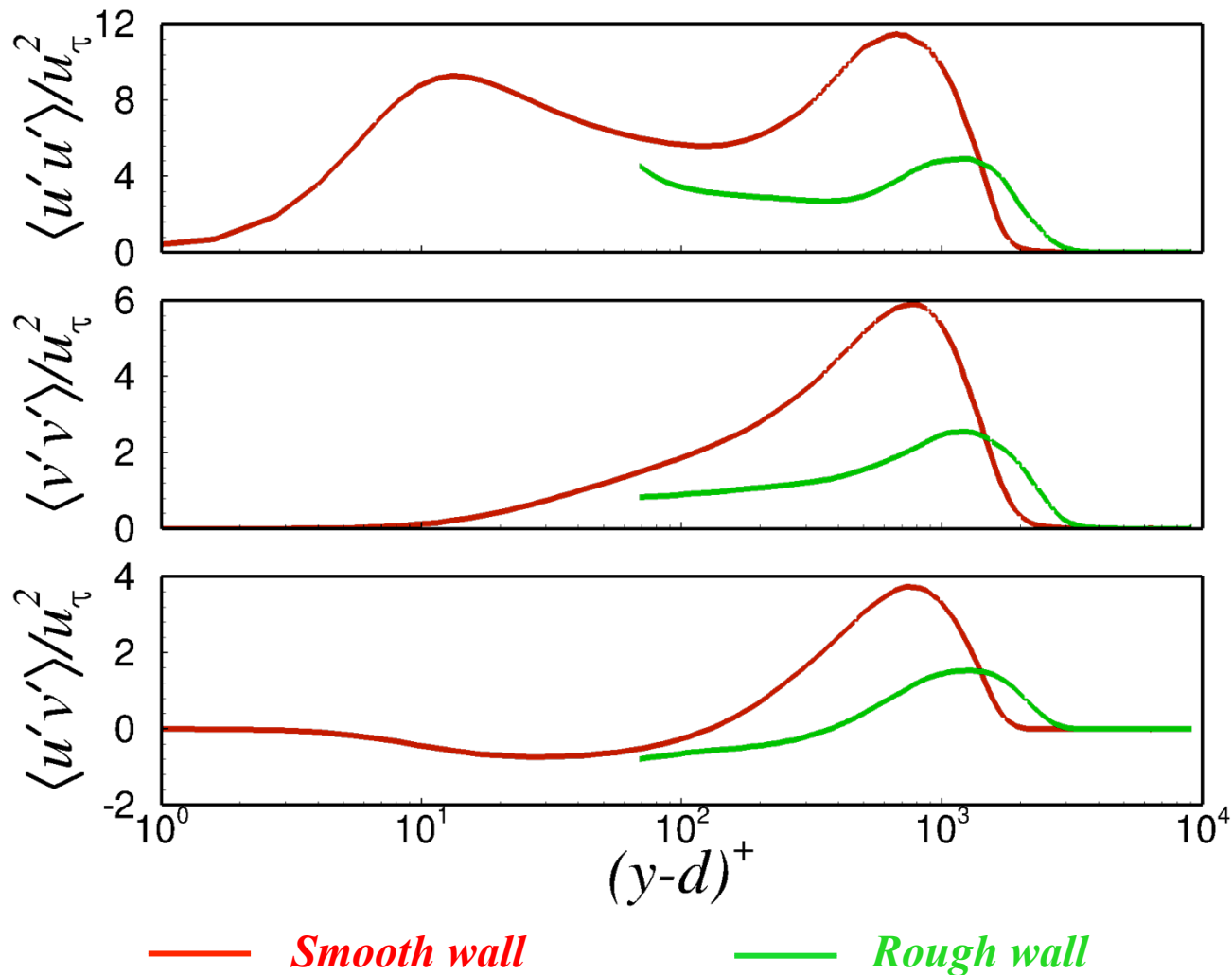
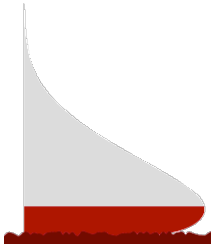
— Smooth wall
— Rough wall



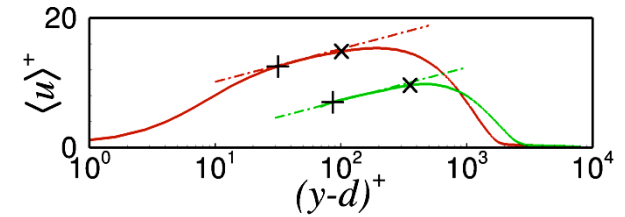
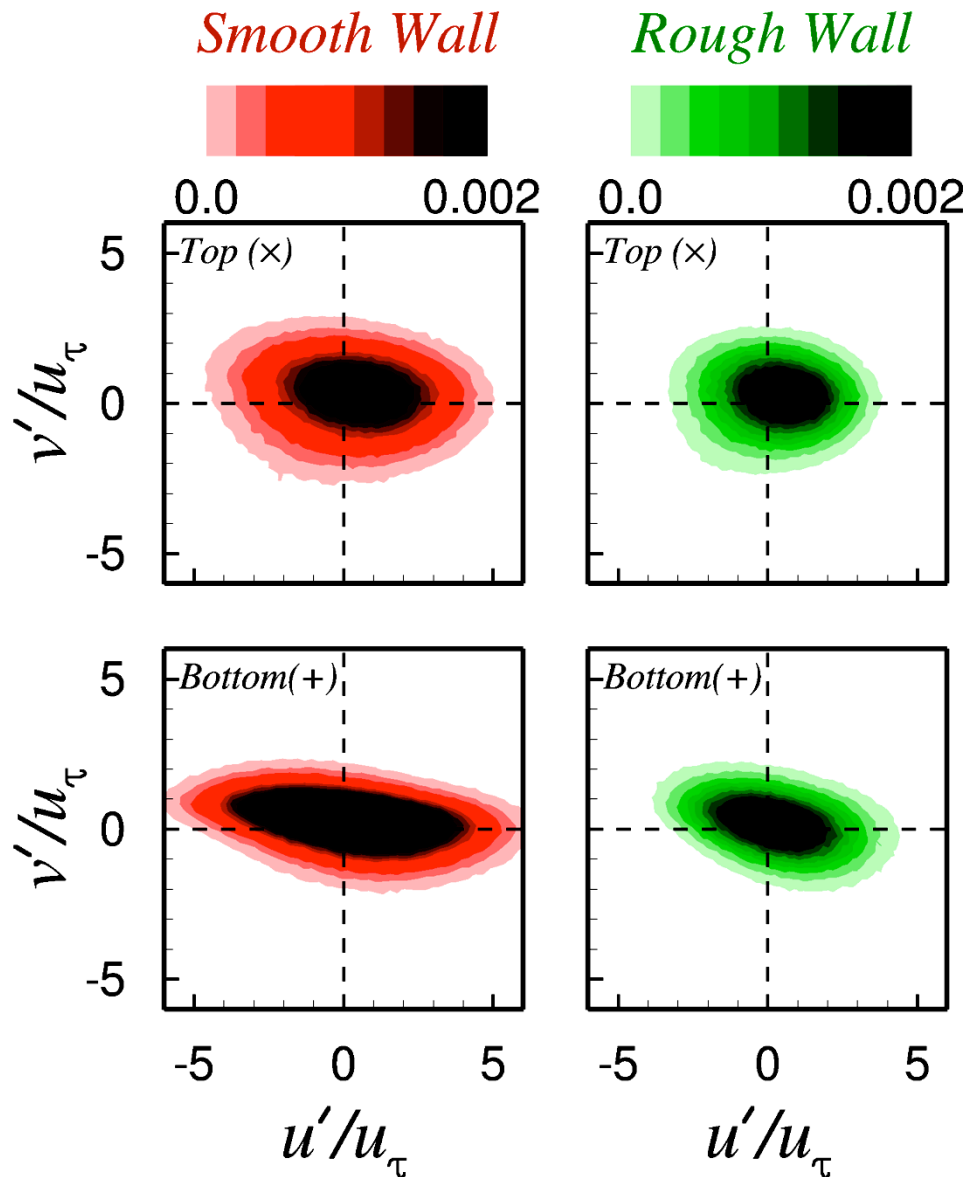
Plane wall jet simulation

Radial wall-jet simulation

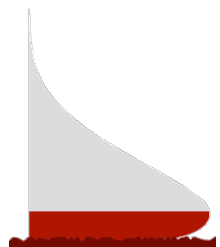
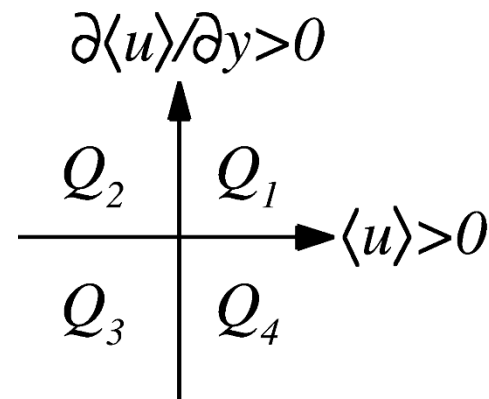
- Profiles of mean Reynolds stresses at $x = 20b$



- Joint Probability Density Function, $P(u', v')$

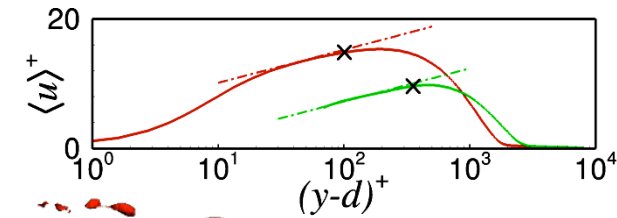


— Smooth wall
— Rough wall



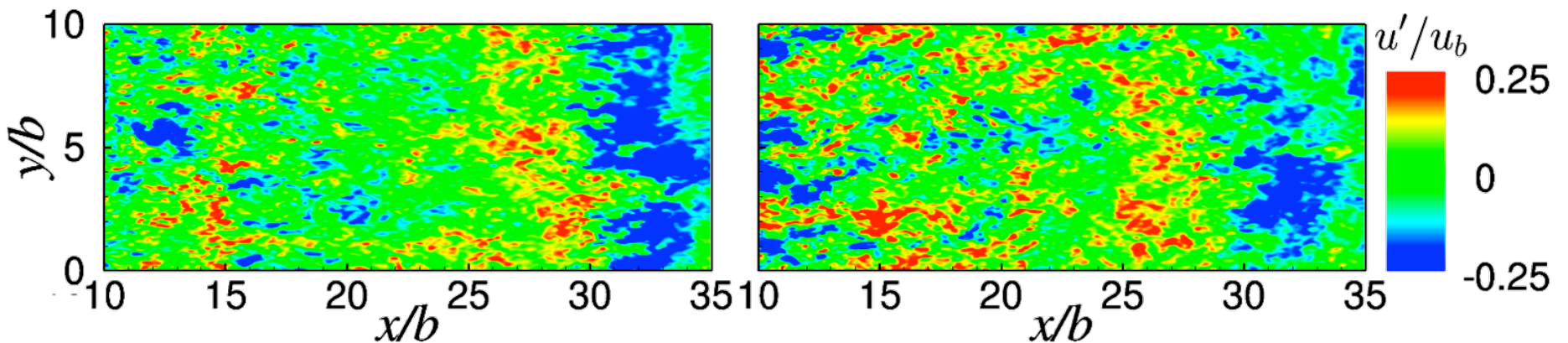
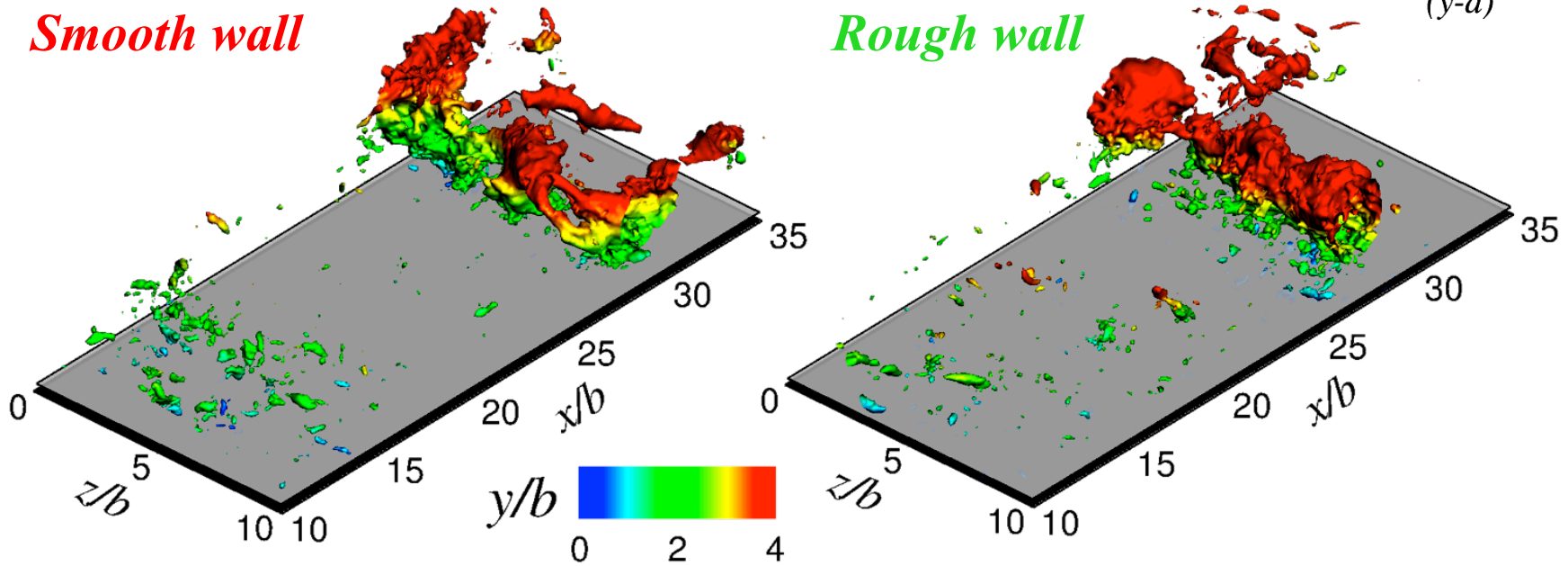


- Contours of radial velocity fluctuations



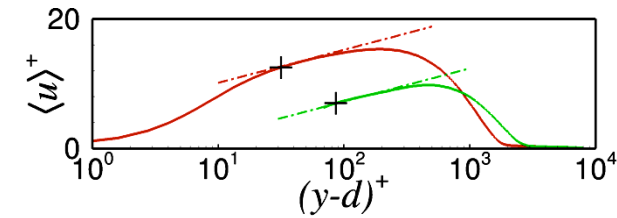
Smooth wall

Rough wall

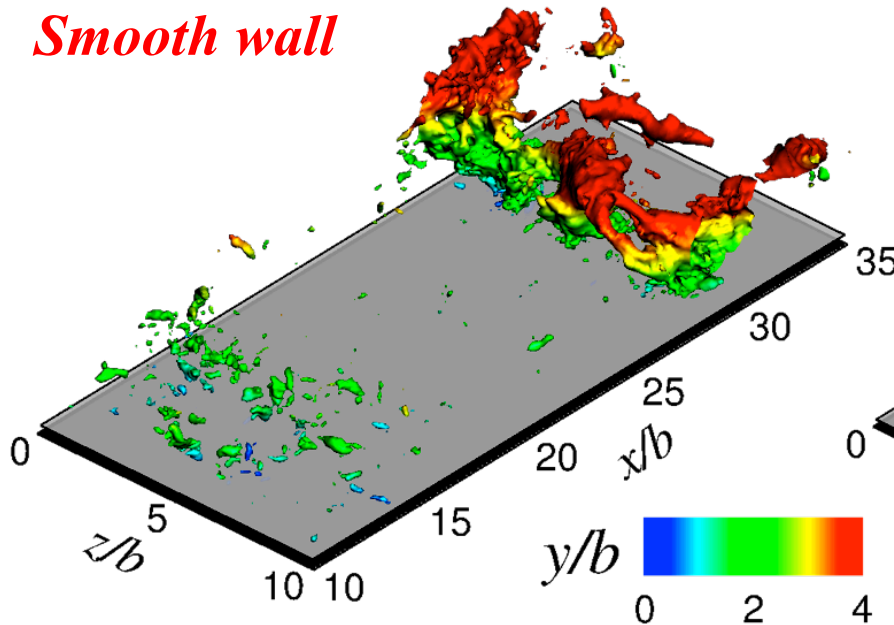




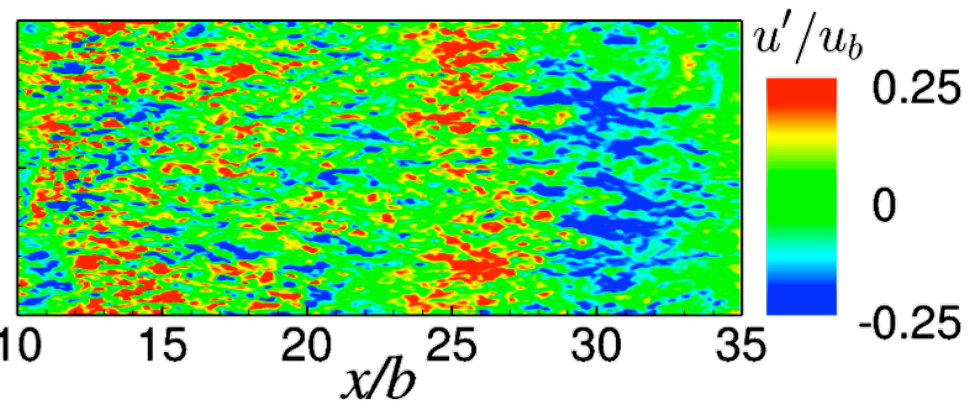
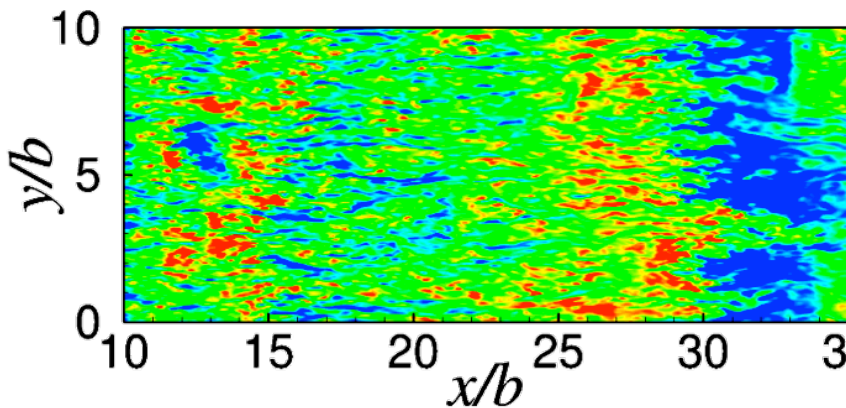
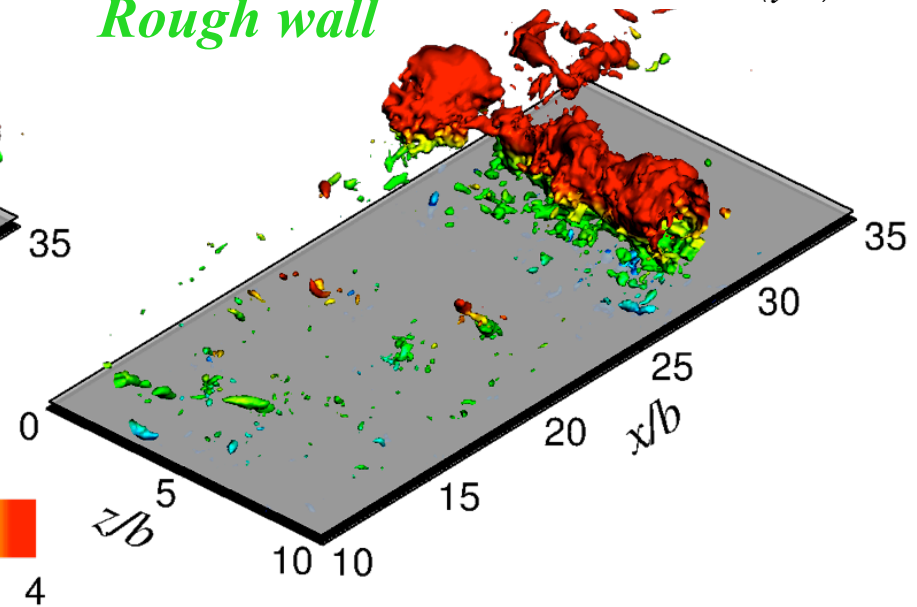
- Contours of radial velocity fluctuations



Smooth wall



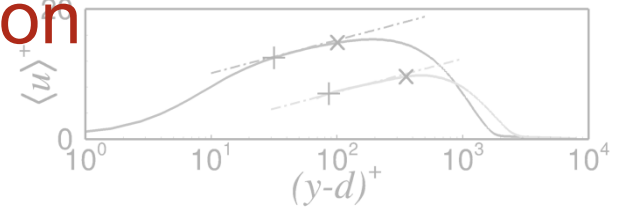
Rough wall



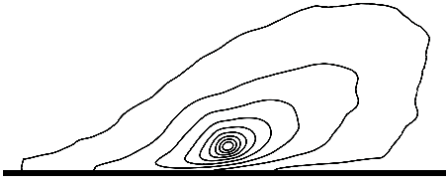


- Two-dimensional two-point autocorrelation

$$R_{11}(x_{ref}, y_{ref}, x, y) = \frac{\langle u'(x_{ref}, y_{ref}) \cdot u'(x, y) \rangle}{\langle u'(x_{ref}, y_{ref}) \cdot u'(x_{ref}, y_{ref}) \rangle}$$

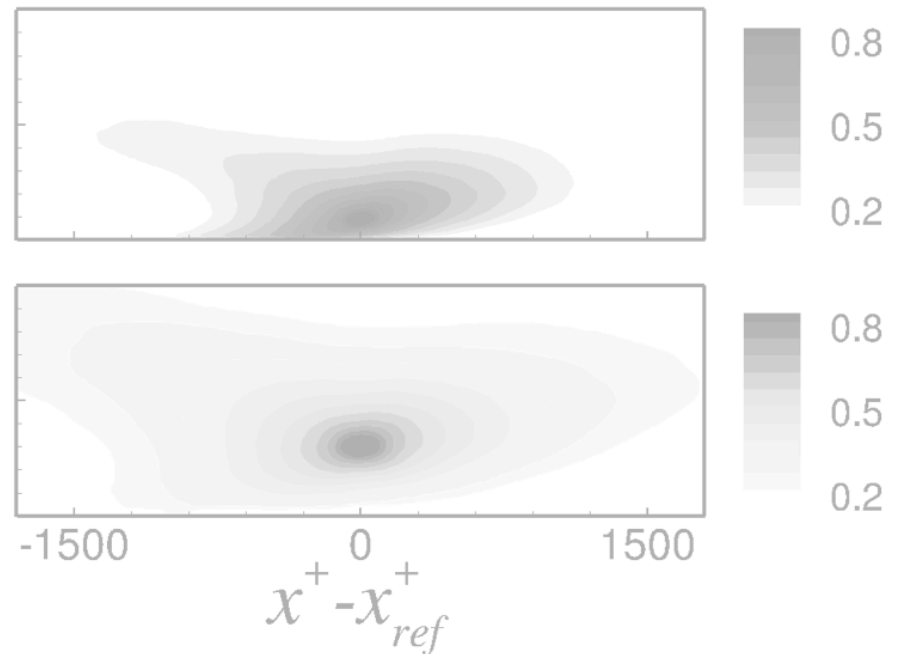
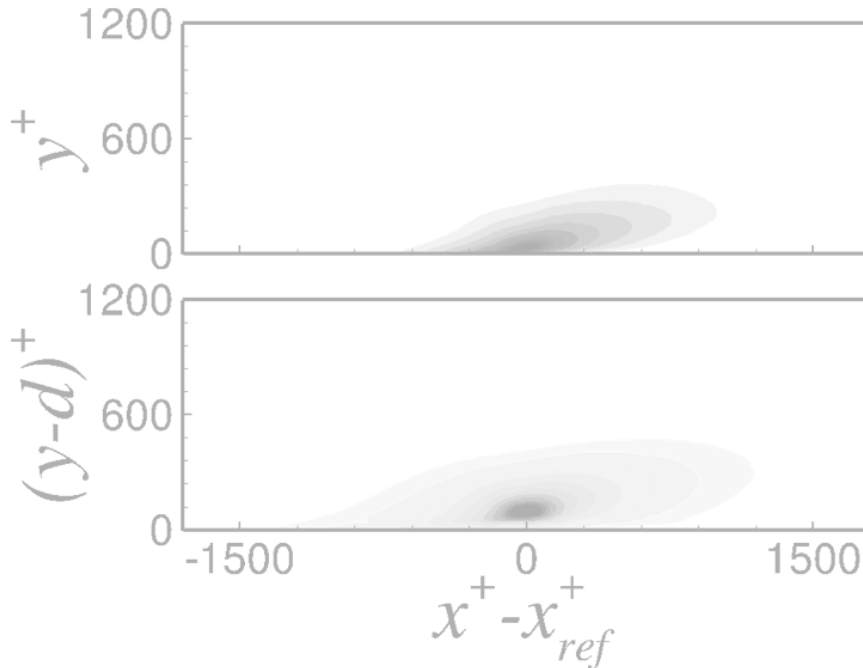


— Smooth wall
 - - - Rough wall



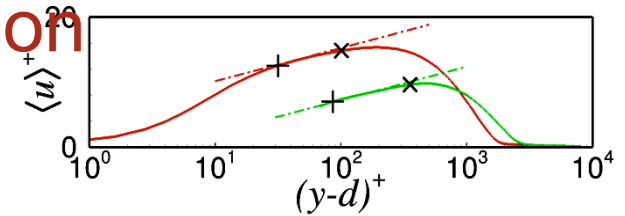
y_{ref} : Bottom of the logarithmic region (+)

y_{ref} : Top of the logarithmic region (x)

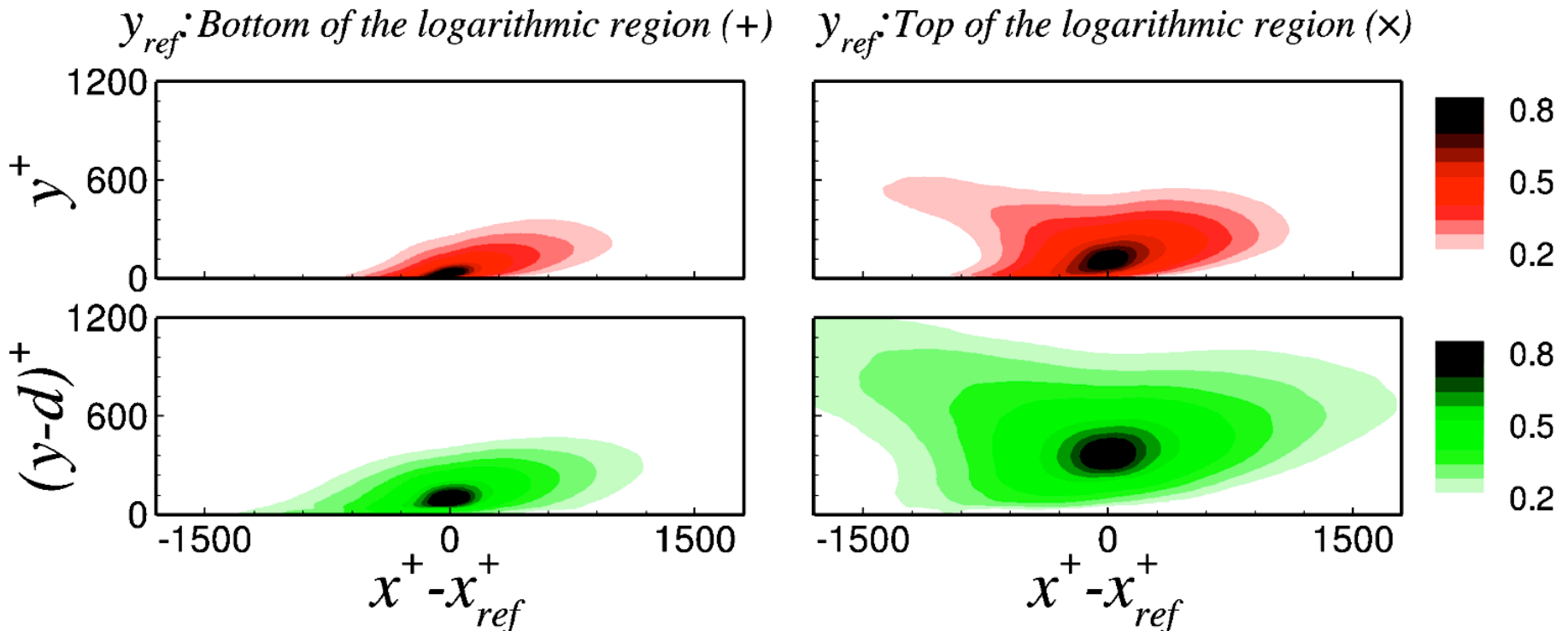
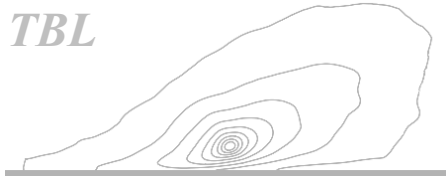


- Two-dimensional two-point autocorrelation

$$R_{11}(x_{ref}, y_{ref}, x, y) = \frac{\langle u'(x_{ref}, y_{ref}) \cdot u'(x, y) \rangle}{\langle u'(x_{ref}, y_{ref}) \cdot u'(x_{ref}, y_{ref}) \rangle}$$

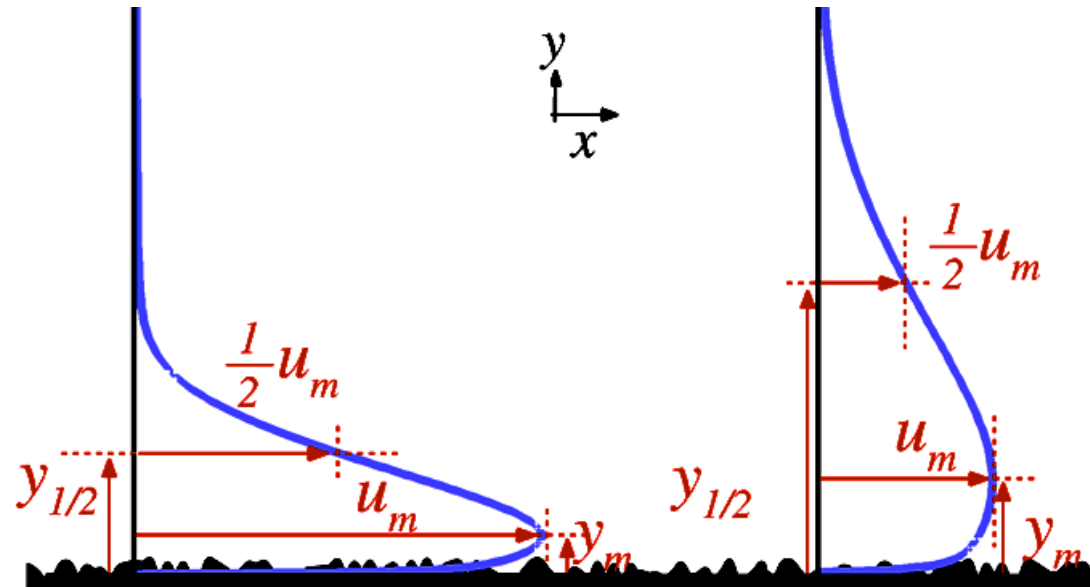


— Smooth wall
— Rough wall



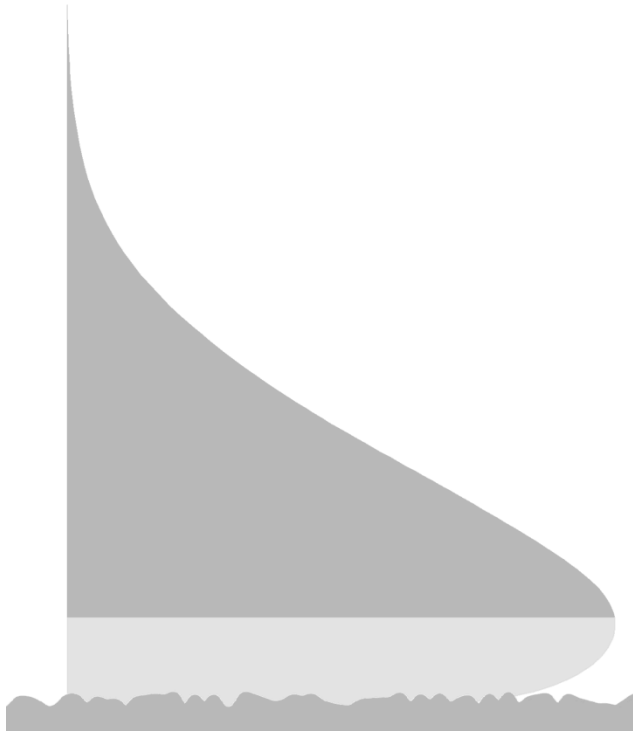


- Roughness effects are mostly confined to the inner layer of the flow



	u_m	y_m	$y_{1/2}$	$-du_m/dx$	dy_m/dx	$dy_{1/2}/dx$
Rajaratnam et al. (1981)	↓	-	-	-	↑	c
Tachie et al. (2004)	↓	↑	c	↑	↑	c
Smith (2008)	c	↑ or $\approx c$	c	c	-	c
Rostamy et al. (2011)	↓	↑	↑	↑	-	c
Current study	↓	↑	↑	↑	↑	$\approx c$

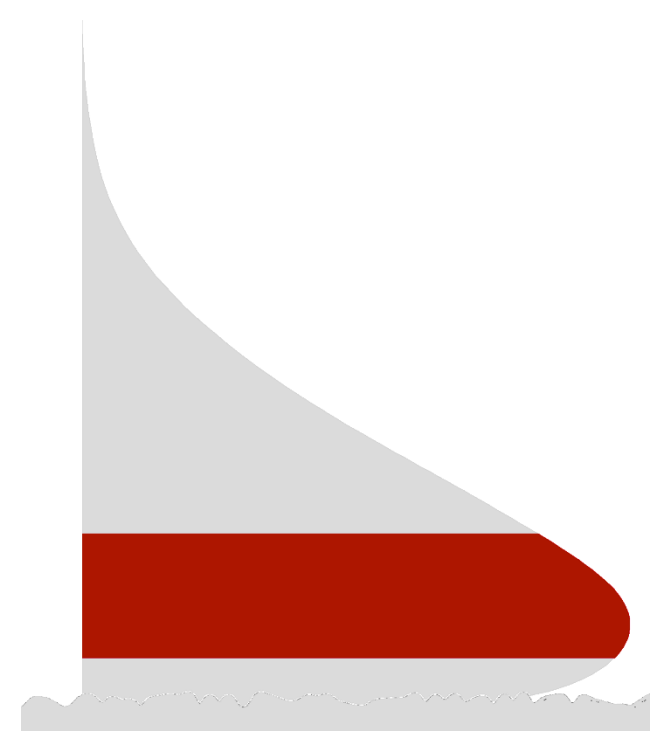
↑, increased; ↓, decreased; c, constant; -, not reported



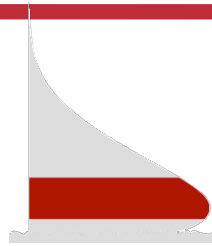
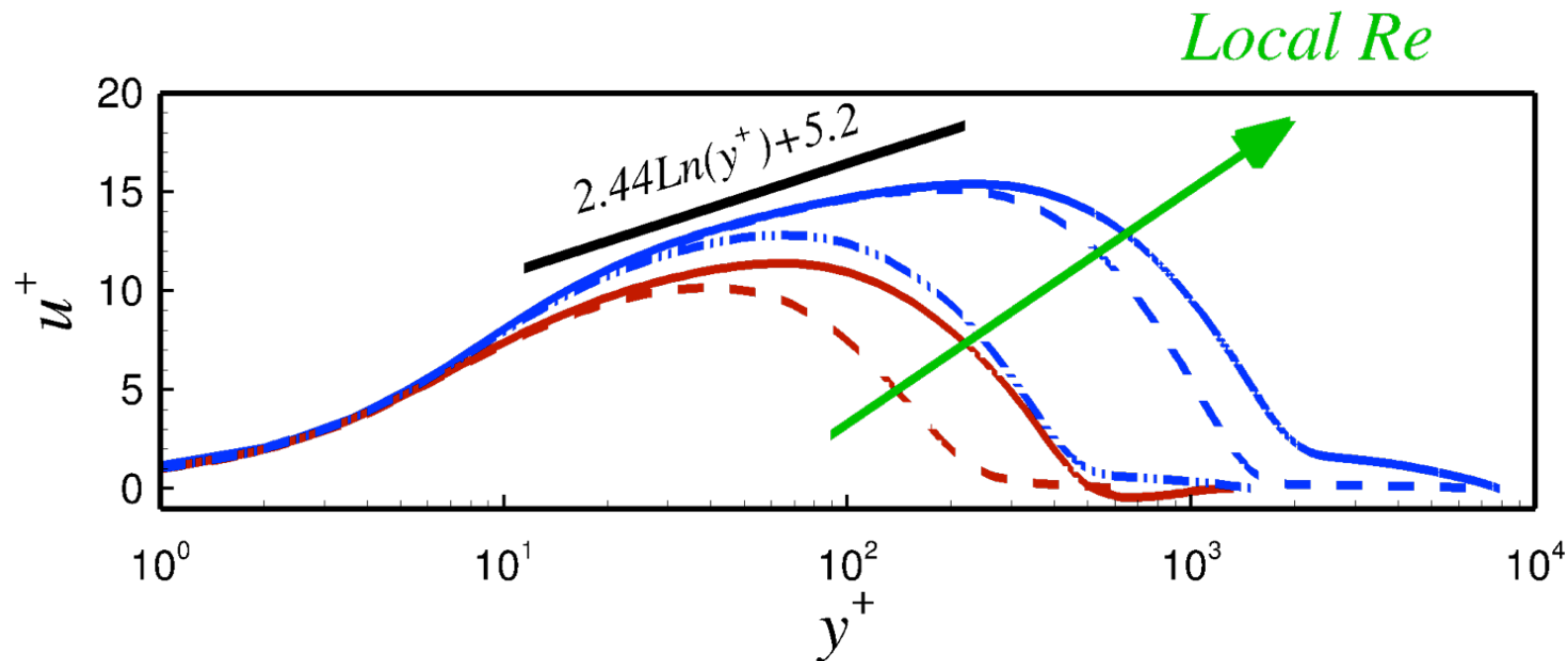
*Effects of roughness
on the outer layer*



*Effects of roughness
on the inner layer*



*Interaction inner
outer layers*

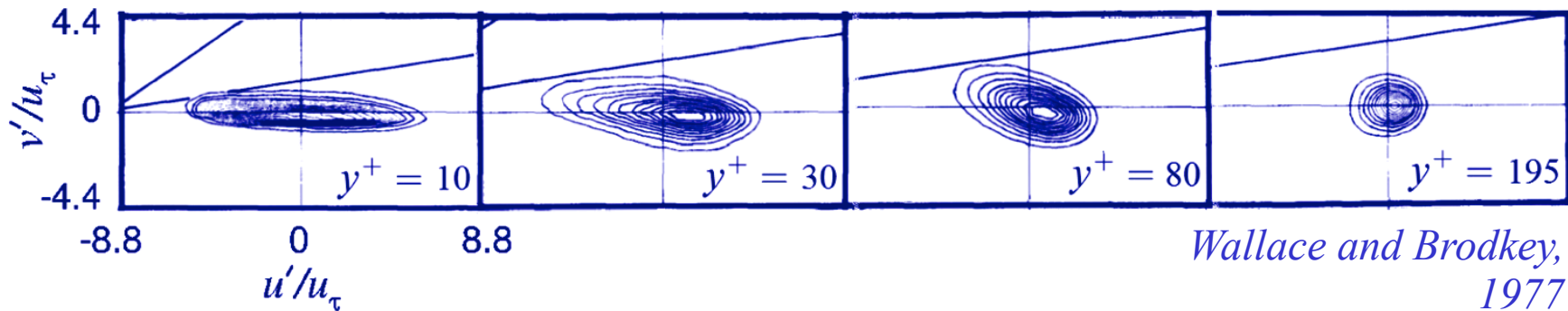
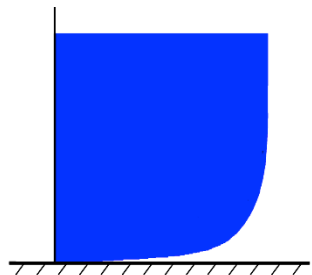


$$Re_m = u_m y_m / \nu, \quad y_{1/2}^+ = u_\tau y_{1/2} / \nu, \quad Re^+ = u_\tau y_m / \nu$$

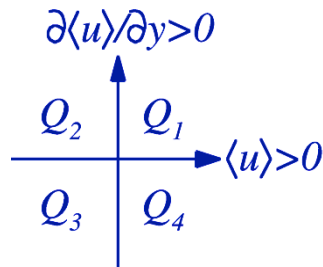
- , Law of the wall
- , $Re_m \approx 400$, Radial wall-jet
- , $Re_m \approx 700$, Radial wall-jet
- , $Re_m \approx 850$, Plane wall-jet
- , $Re_m \approx 2,900$, Plane wall-jet
- , $Re_m \approx 3,600$, Plane wall-jet



- JPDF of streamwise and wall-normal velocity fluctuations

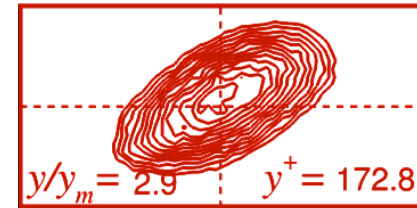
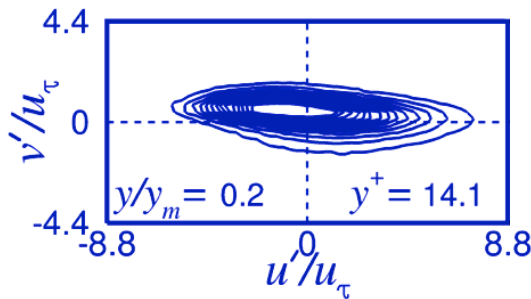
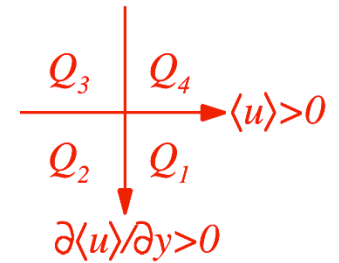
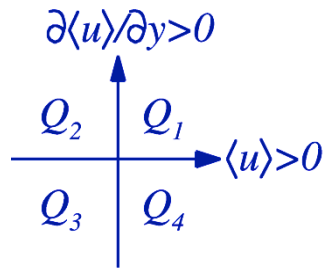
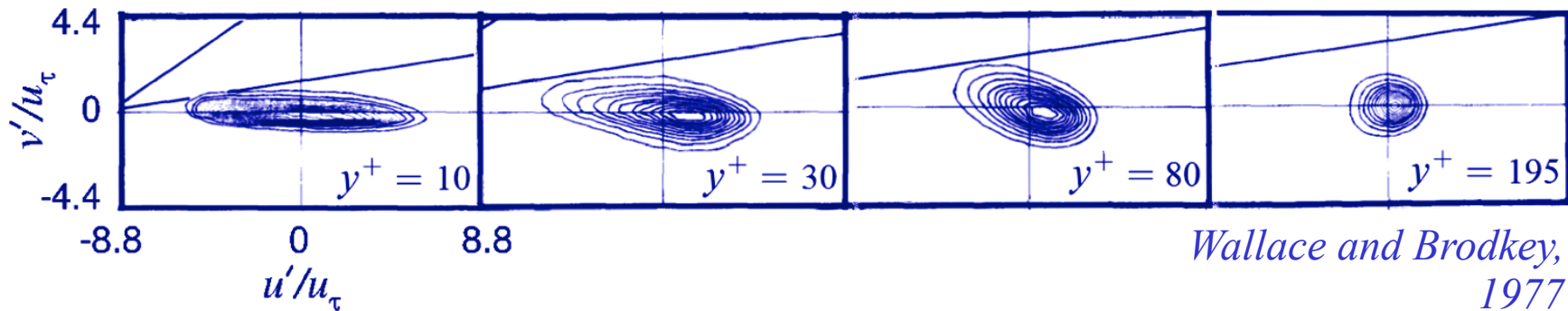
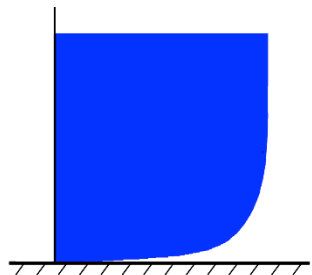


Wallace and Brodkey, 1977



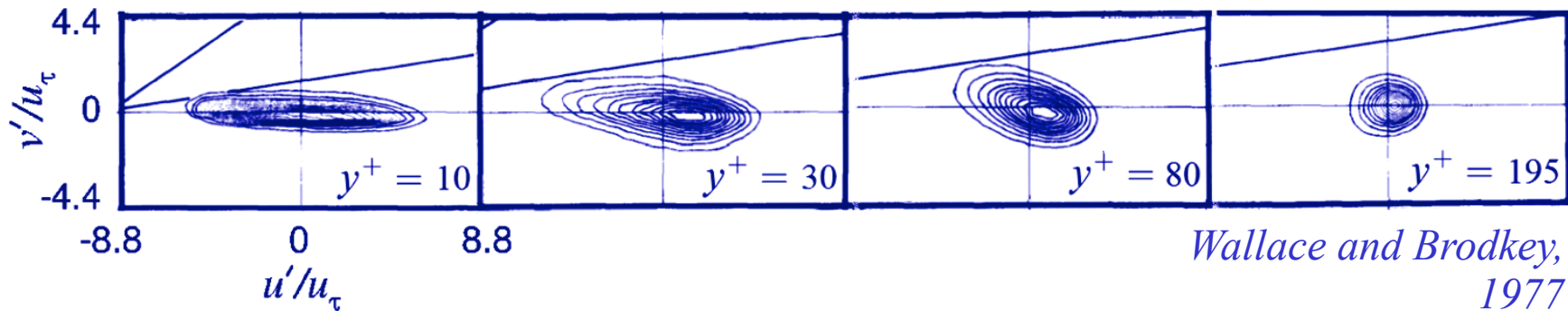
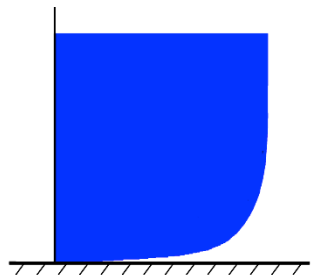


- JPDF of streamwise and wall-normal velocity fluctuations

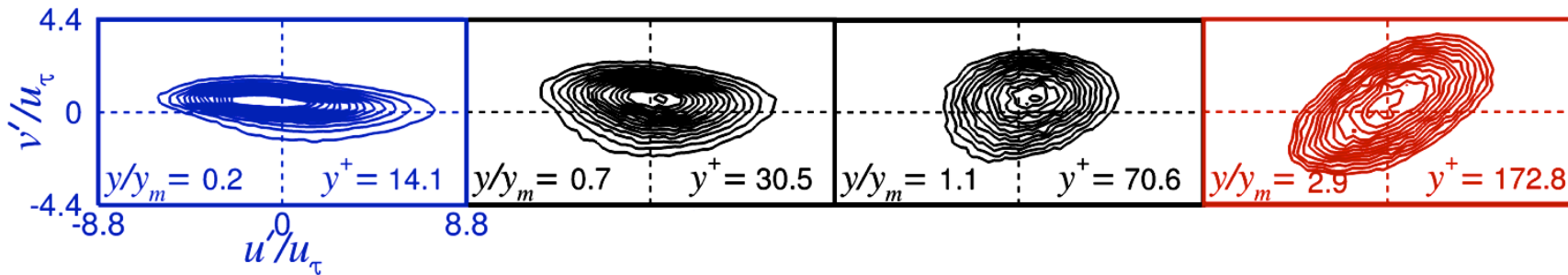
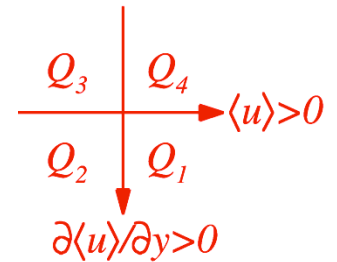
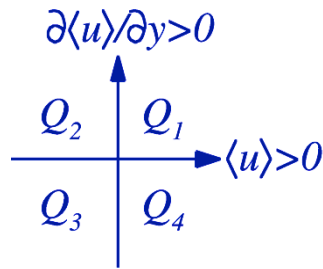




- JPDF of streamwise and wall-normal velocity fluctuations



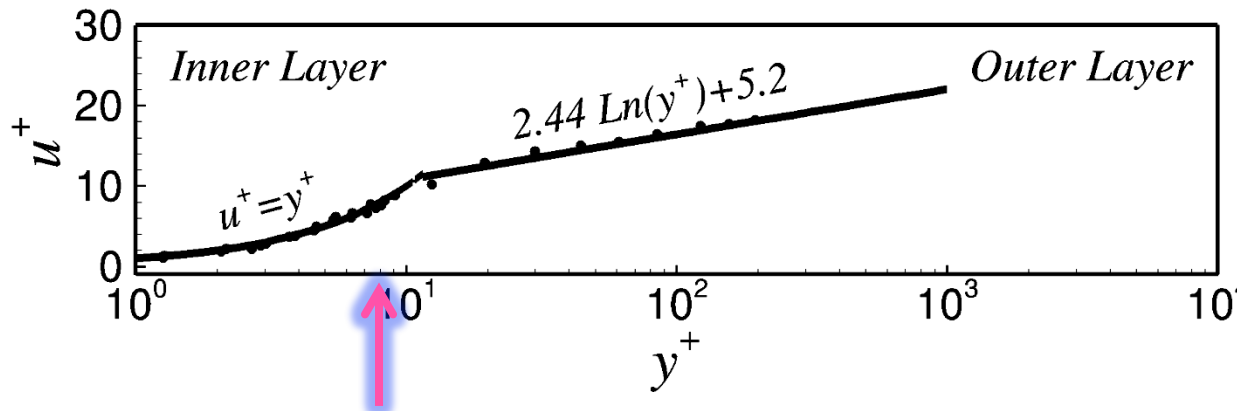
Wallace and Brodkey, 1977



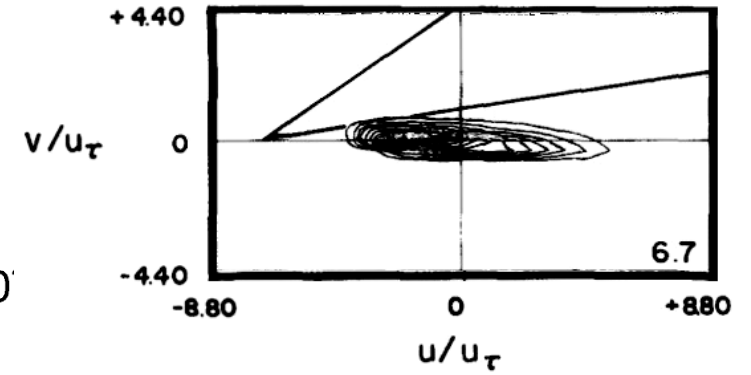


RESULTS

INNER/OUTER LAYER INTERACTION

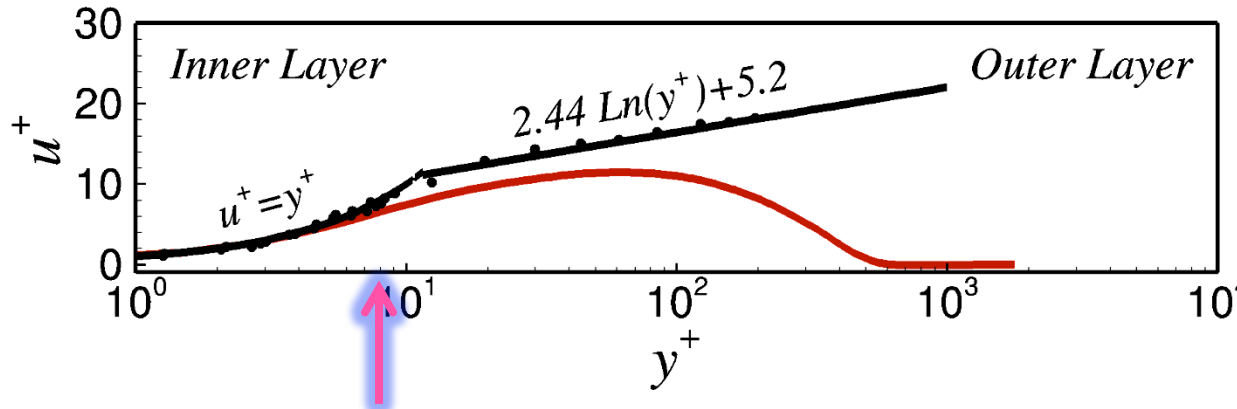


- Wallace et al., 1972



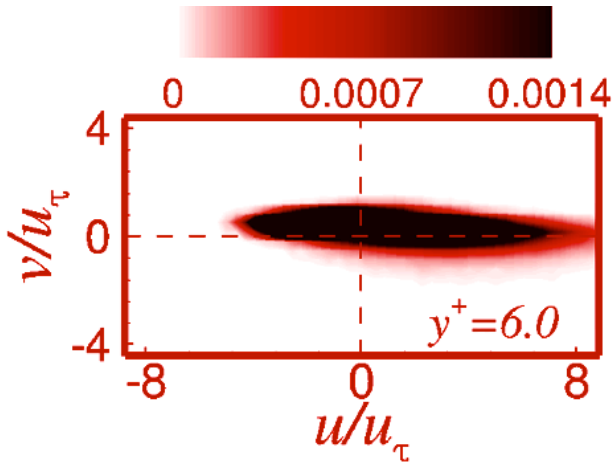
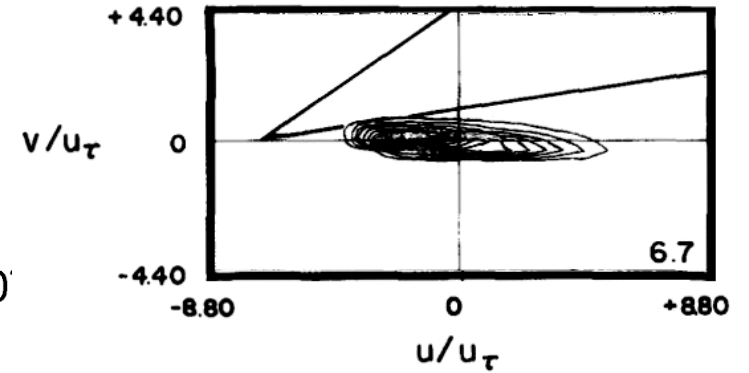


RESULTS INNER/OUTER LAYER INTERACTION



• Wallace et al., 1972

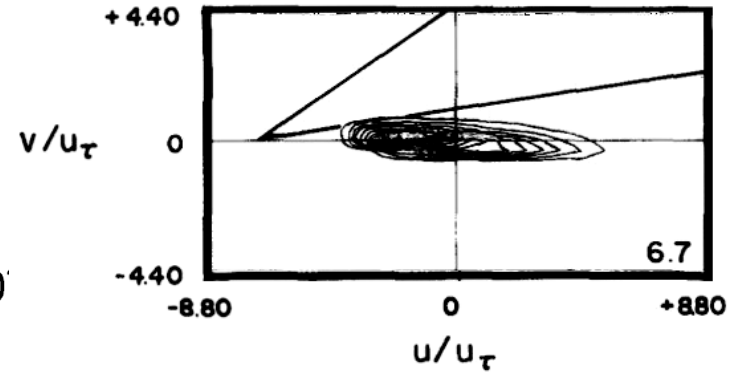
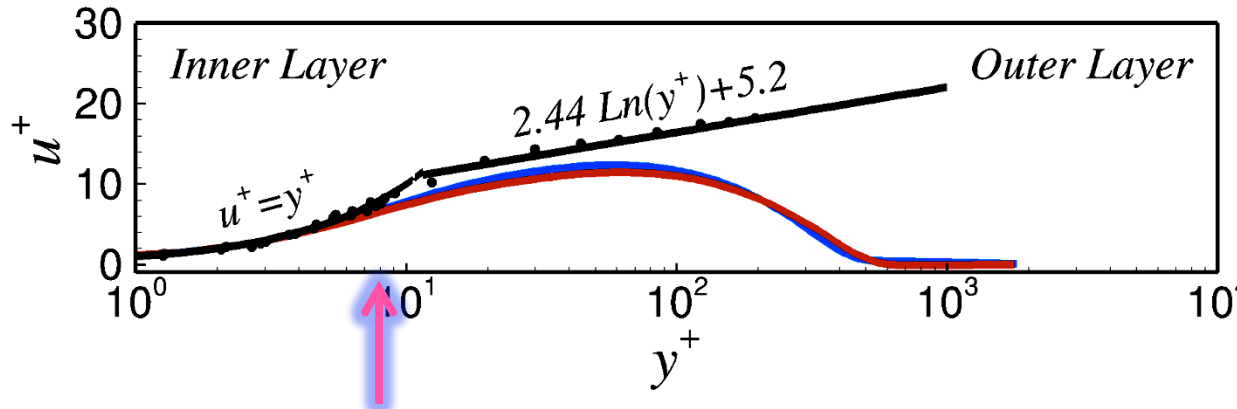
— Radial wall-jet simulation, $Re_m \approx 700$



4.6 Radial wall-jet, $Re_m \approx 700$



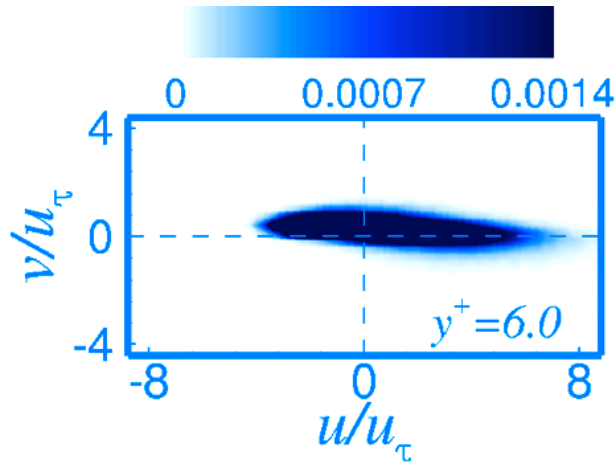
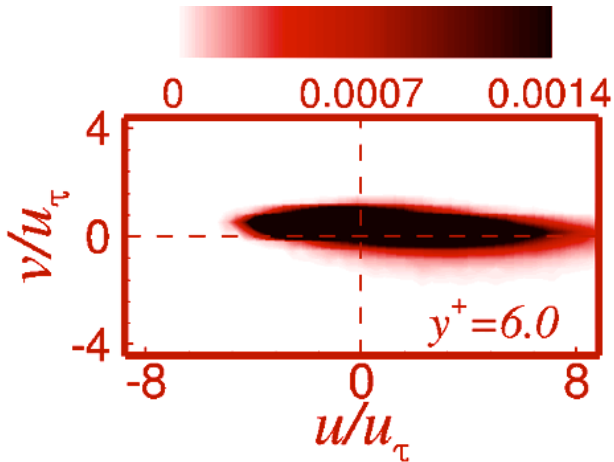
RESULTS INNER/OUTER LAYER INTERACTION



• Wallace et al., 1972

— Radial wall-jet simulation, $Re_m \approx 700$

— Plane wall-jet simulation, $Re_m \approx 700$

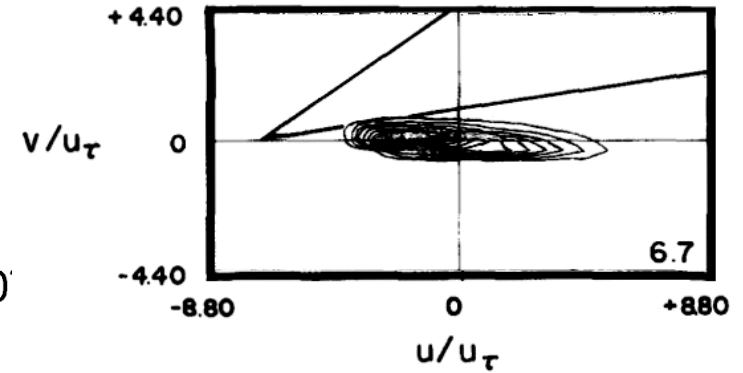
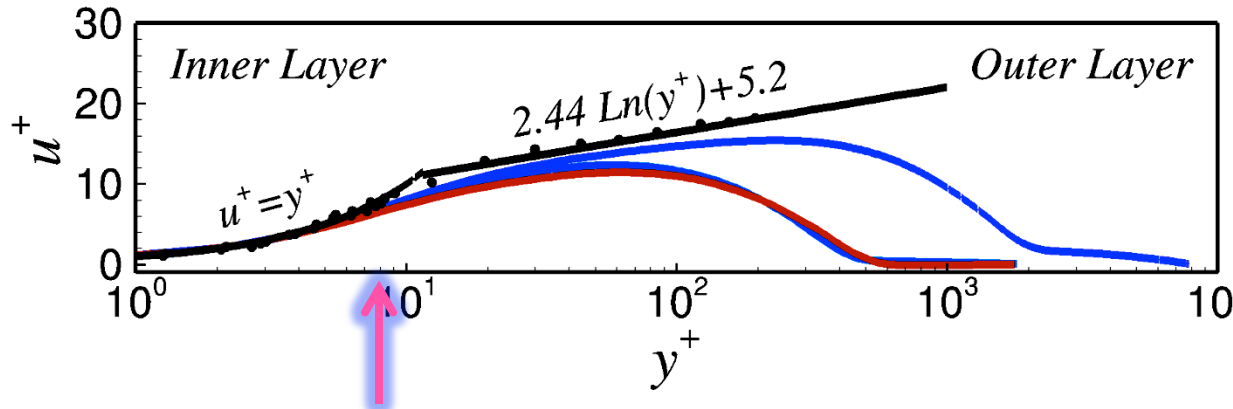


4.6 Radial wall-jet, $Re_m \approx 700$

Plane wall-jet, $Re_m \approx 700$



RESULTS INNER/OUTER LAYER INTERACTION

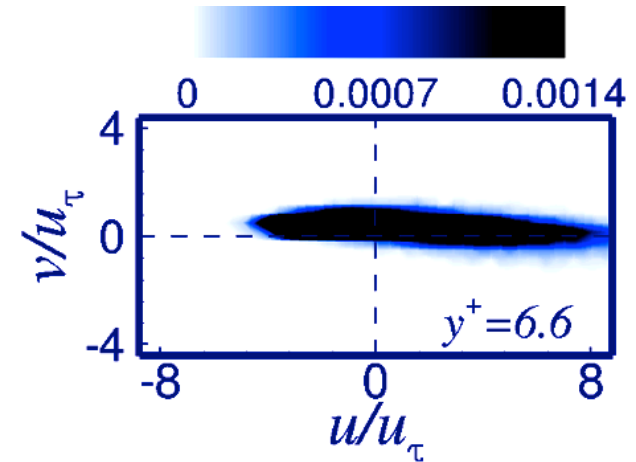
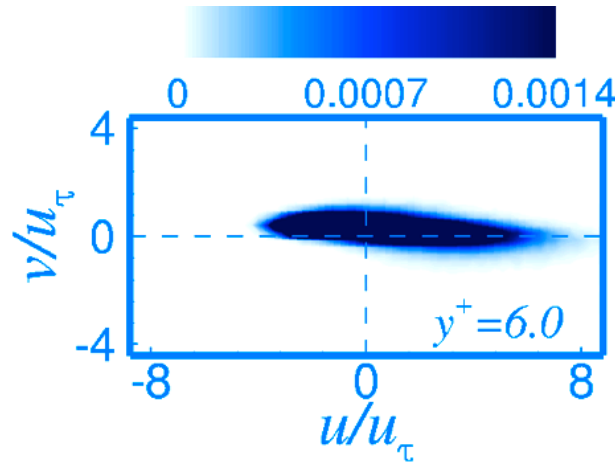
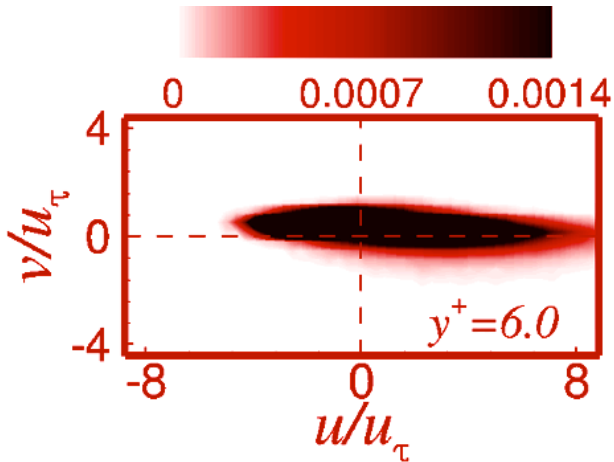


- Wallace et al., 1972

— Radial wall-jet simulation, $Re_m \approx 700$

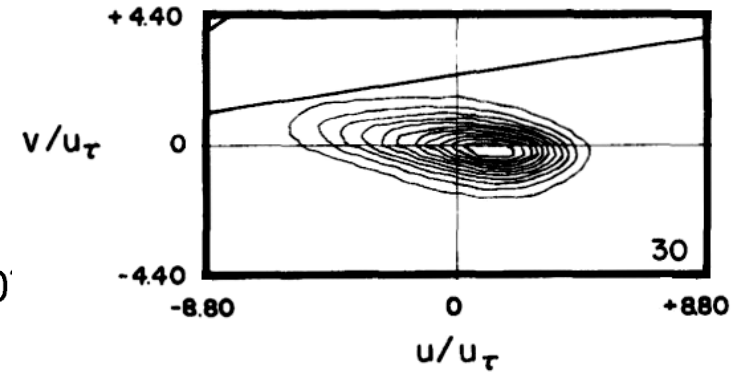
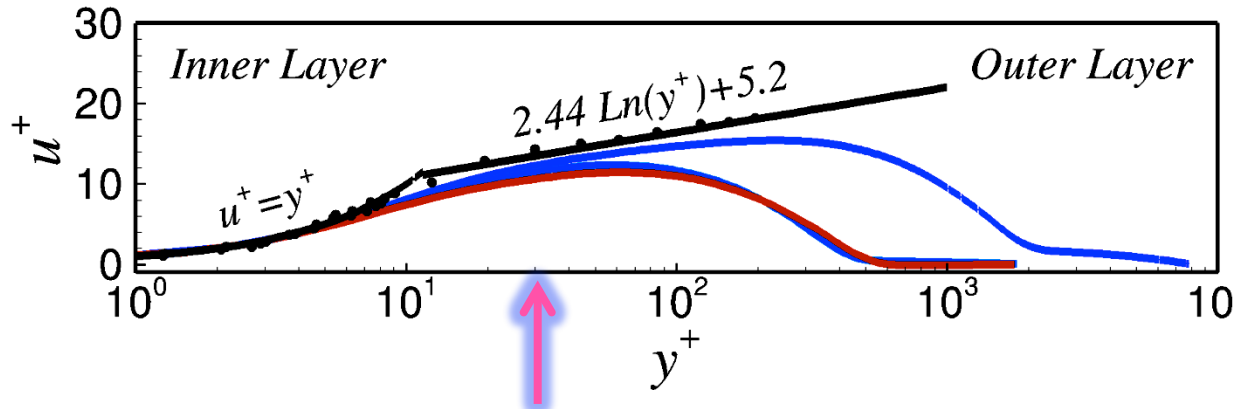
— Plane wall-jet simulation, $Re_m \approx 700$

— Plane wall-jet simulation, $Re_m \approx 3600$





RESULTS INNER/OUTER LAYER INTERACTION

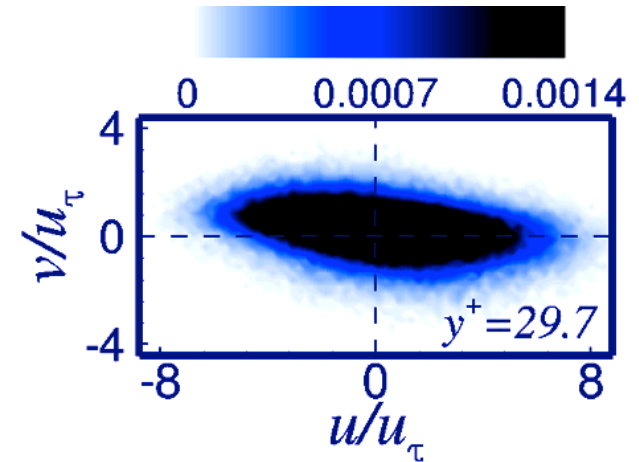
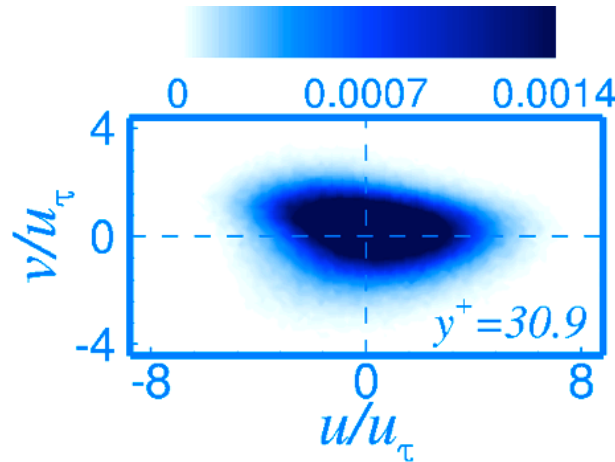
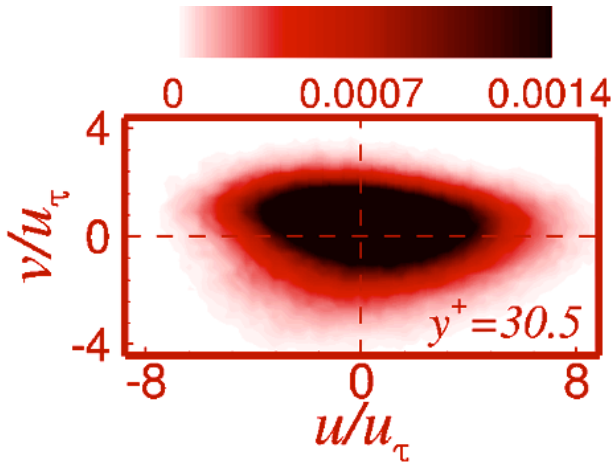


• Wallace et al., 1972

— Radial wall-jet simulation, $Re_m \approx 700$

— Plane wall-jet simulation, $Re_m \approx 700$

— Plane wall-jet simulation, $Re_m \approx 3600$



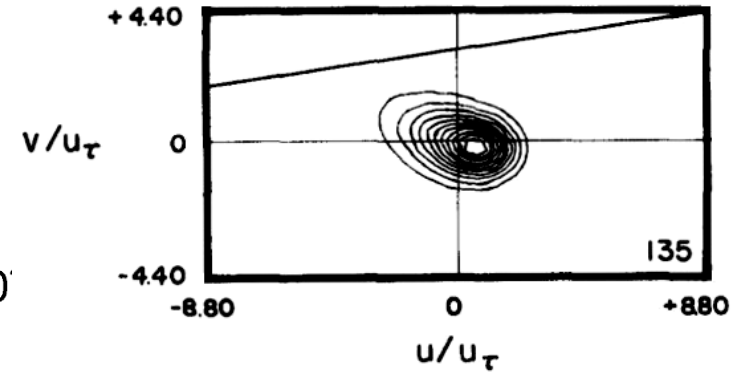
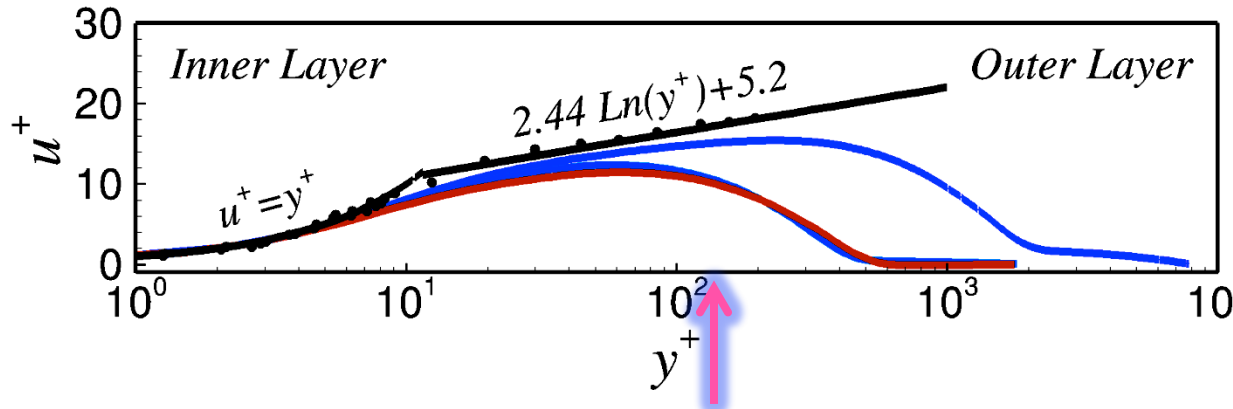
4.6 Radial wall-jet, $Re_m \approx 700$

Plane wall-jet, $Re_m \approx 700$

Plane wall-jet, $Re_m \approx 3600$



RESULTS INNER/OUTER LAYER INTERACTION

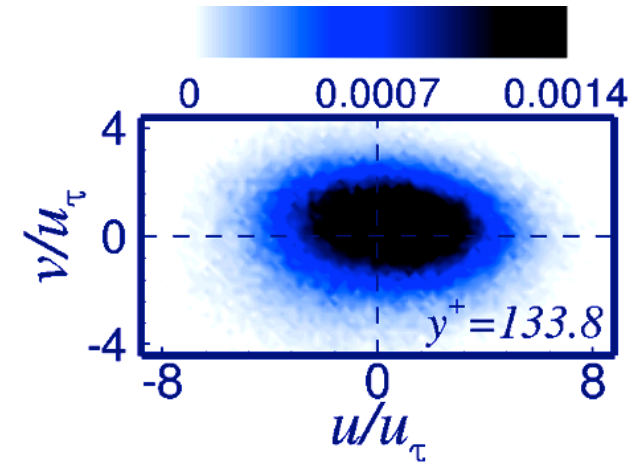
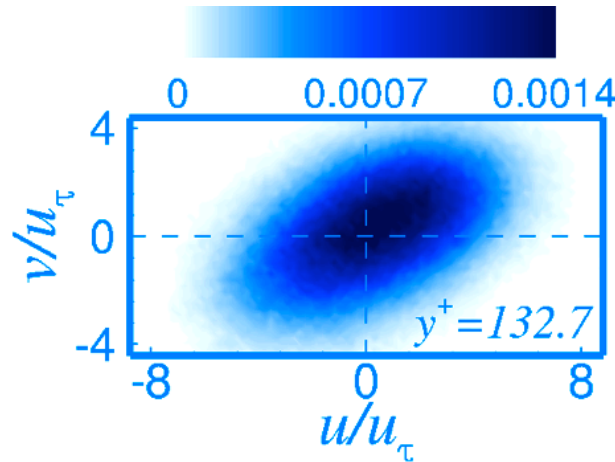
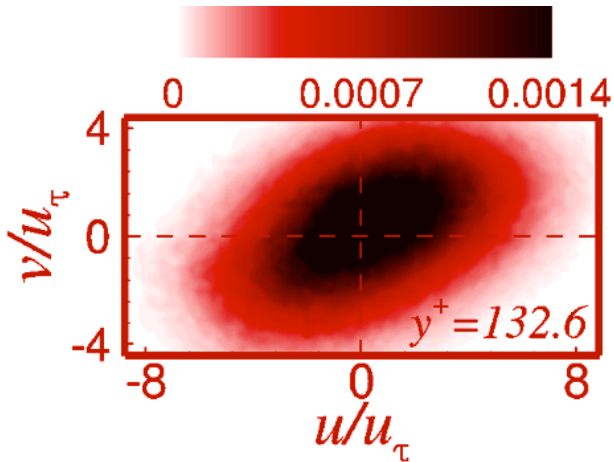


• Wallace et al., 1972

— Radial wall-jet simulation, $Re_m \approx 700$

— Plane wall-jet simulation, $Re_m \approx 700$

— Plane wall-jet simulation, $Re_m \approx 3600$



4.6 Radial wall-jet, $Re_m \approx 700$

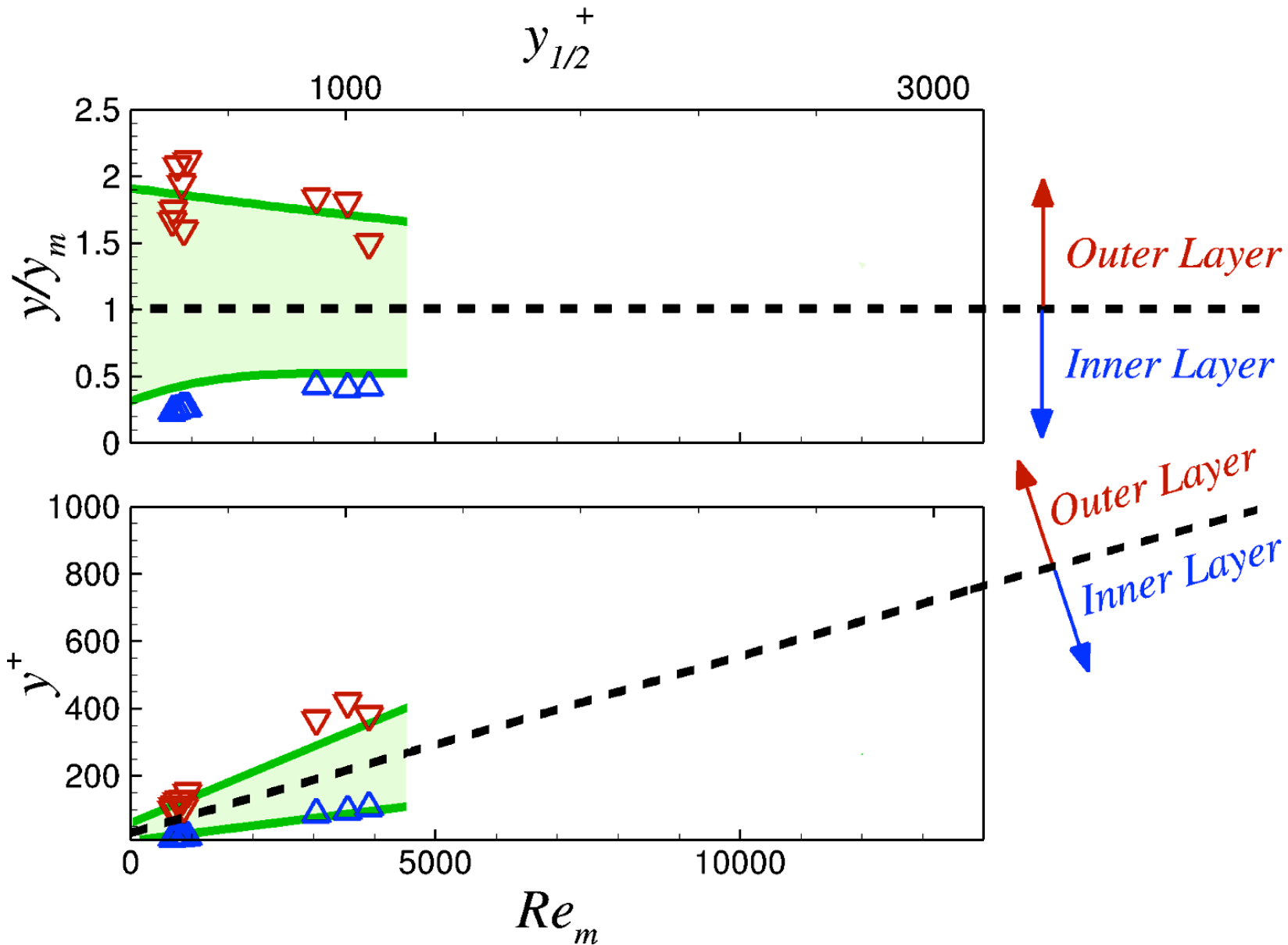
Plane wall-jet, $Re_m \approx 700$

Plane wall-jet, $Re_m \approx 3600$



RESULTS

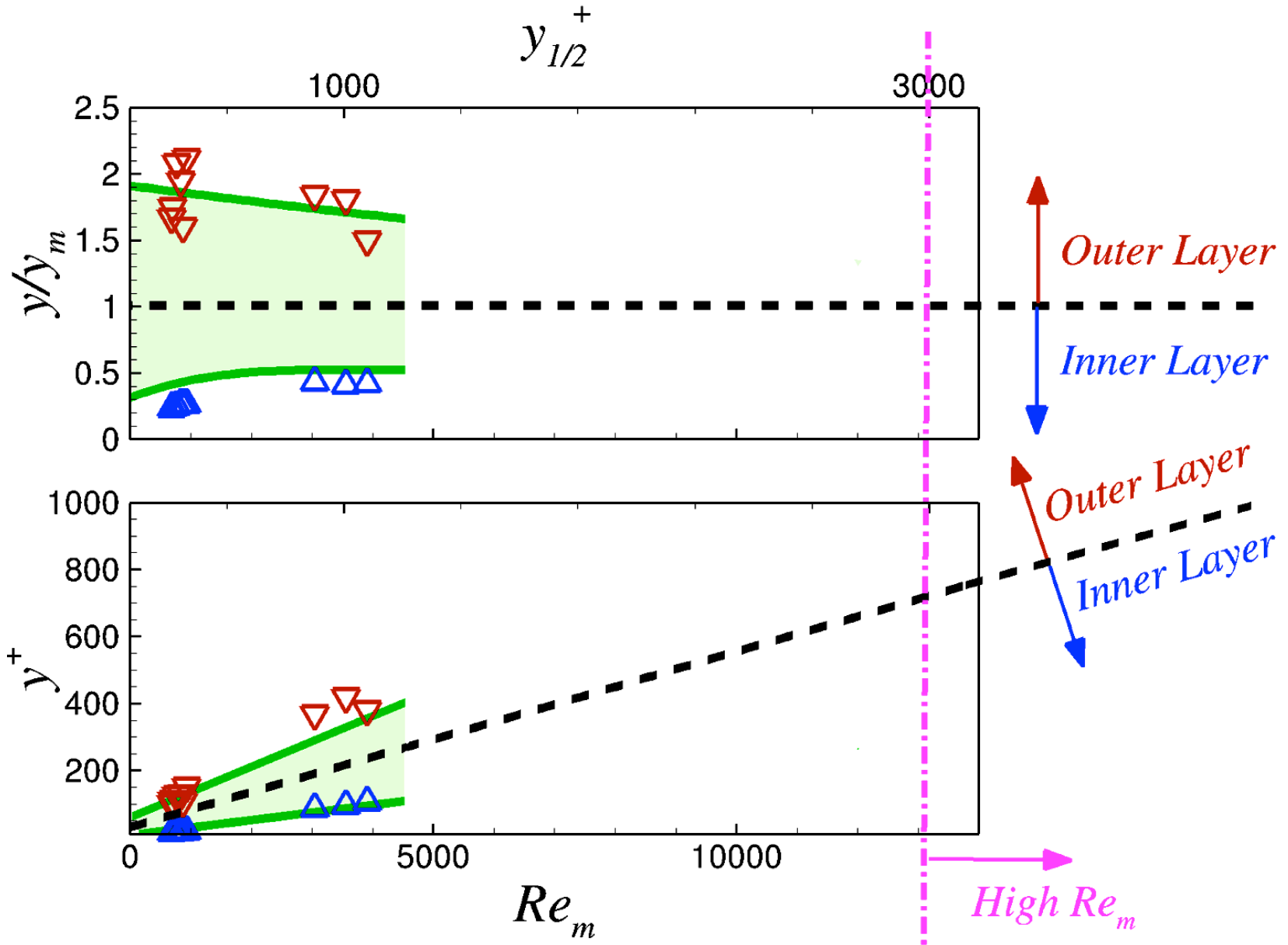
INNER/OUTER LAYER INTERACTION





RESULTS

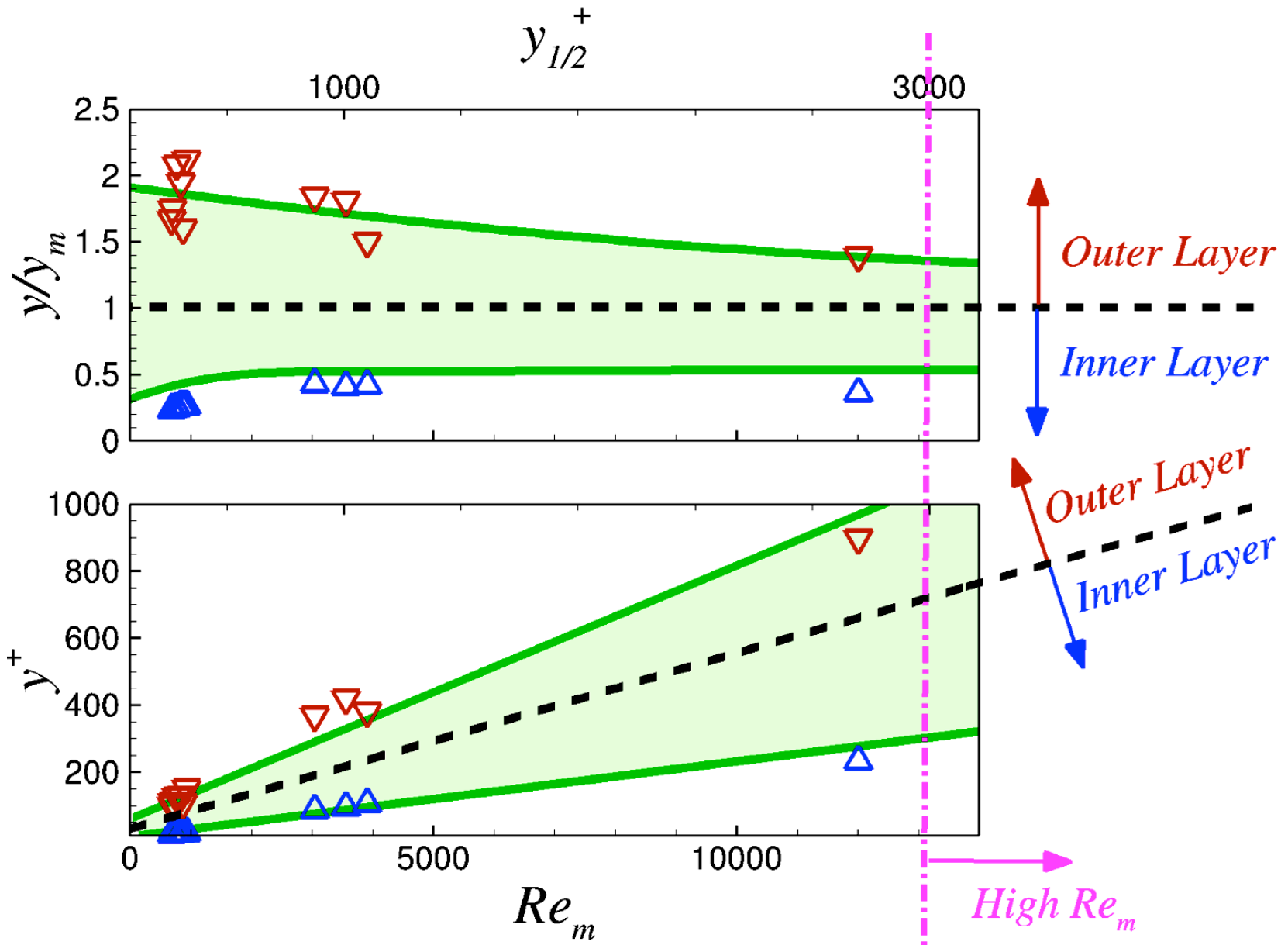
INNER/OUTER LAYER INTERACTION

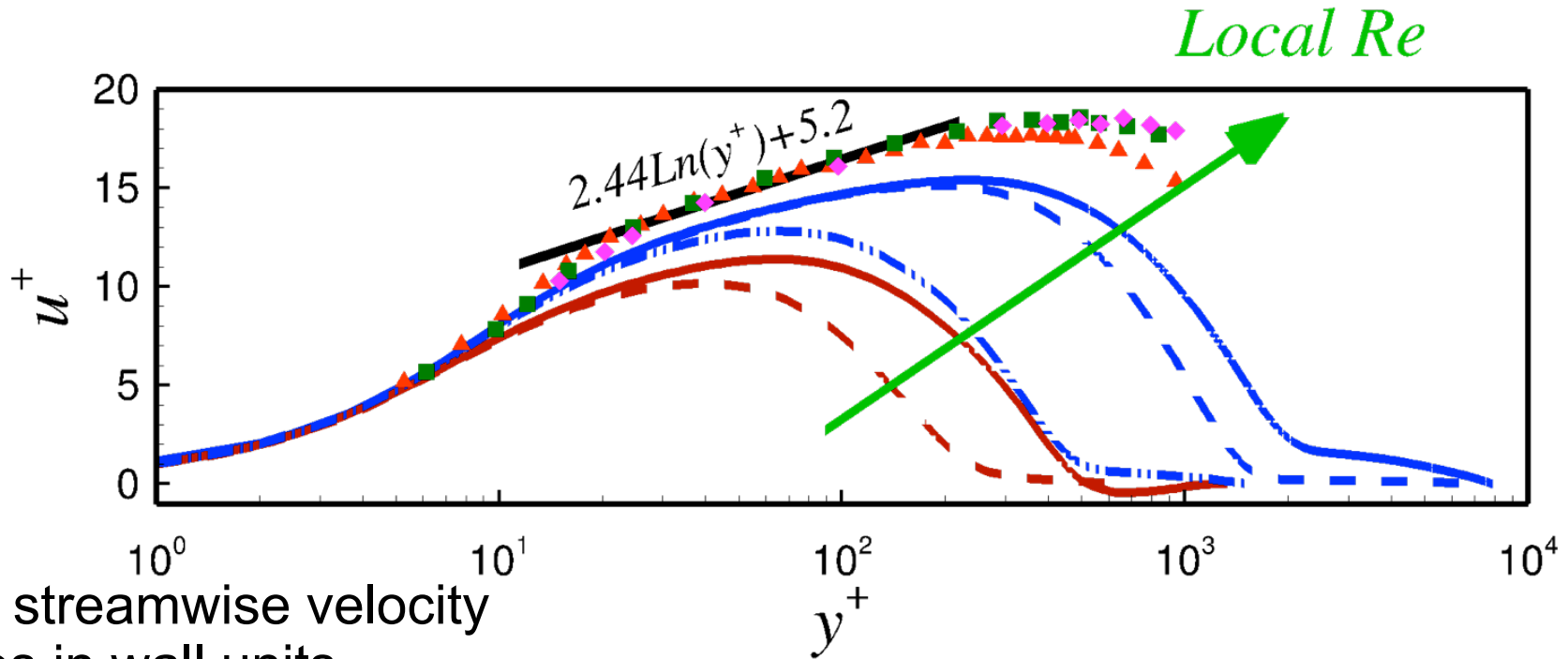




RESULTS

INNER/OUTER LAYER INTERACTION

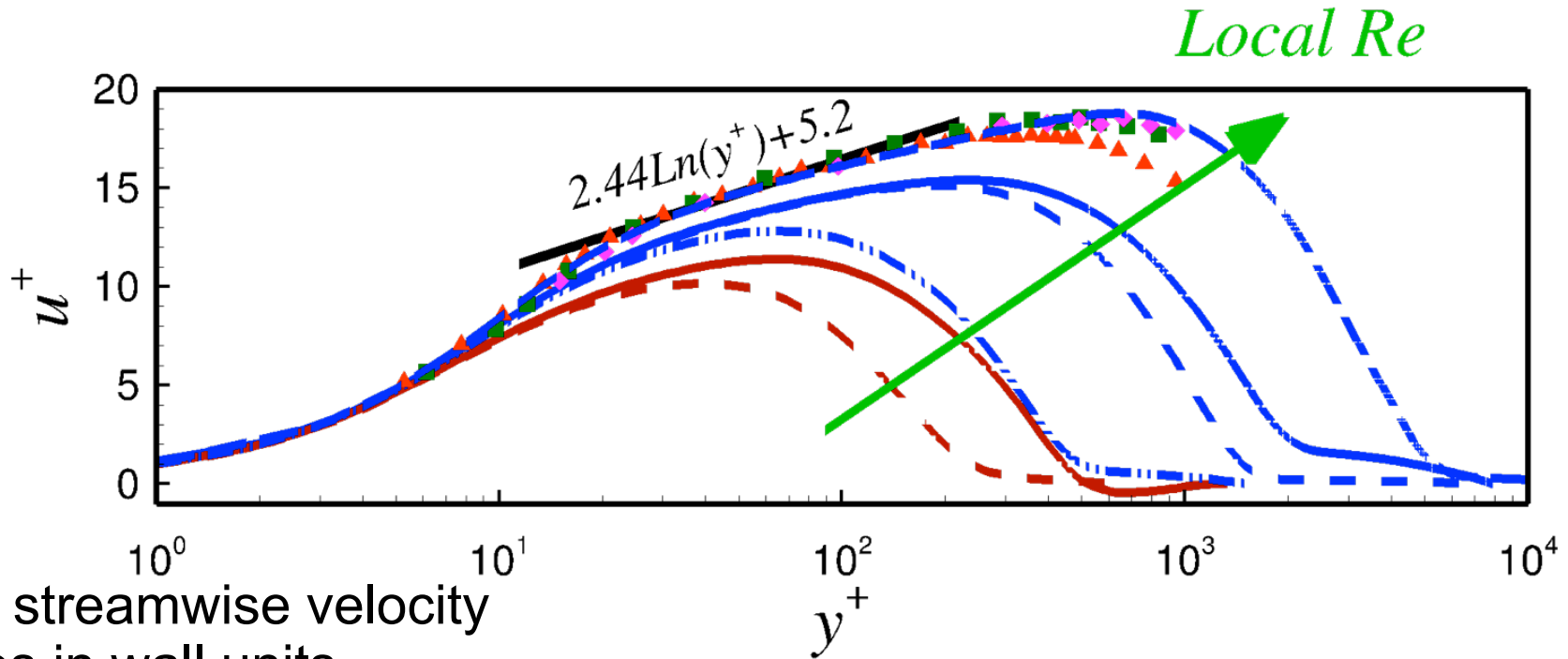




Mean streamwise velocity profiles in wall units

$$Re_m = u_m y_m / \nu, \quad y_{1/2}^+ = u_\tau y_{1/2} / \nu, \quad Re^+ = u_\tau y_m / \nu$$

- , Law of the wall
- , $Re_m \approx 400$, Radial wall-jet
- - , $Re_m \approx 700$, Radial wall-jet
- · - · , $Re_m \approx 850$, Plane wall-jet
- - - , $Re_m \approx 2,900$, Plane wall-jet
- , $Re_m \approx 3,600$, Plane wall-jet
- ▲, $Re_m \approx 5,200$ (Eriksson *et al.*, 1998)
- , $Re_m \approx 8,600$ (Bradshaw and Gee, 1960)
- ◆, $Re_m \approx 12,200$ (Abrahamsson *et al.* 1994)



Mean streamwise velocity profiles in wall units

$$Re_m = u_m y_m / \nu, \quad y_{1/2}^+ = u_\tau y_{1/2} / \nu, \quad Re^+ = u_\tau y_m / \nu$$

- , Law of the wall
- (red) , $Re_m \approx 400$, Radial wall-jet
- - (red) , $Re_m \approx 700$, Radial wall-jet
- · - · (blue) , $Re_m \approx 850$, Plane wall-jet
- - - (blue) , $Re_m \approx 2,900$, Plane wall-jet
- (blue) , $Re_m \approx 3,600$, Plane wall-jet
- ▲ (red) , $Re_m \approx 5,200$ (Eriksson *et al.*, 1998)
- (green) , $Re_m \approx 8,600$ (Bradshaw and Gee, 1960)
- ◆ (magenta) , $Re_m \approx 12,200$ (Abrahamsson *et al.* 1994)
- - - (blue) , $Re_m \approx 12,100$

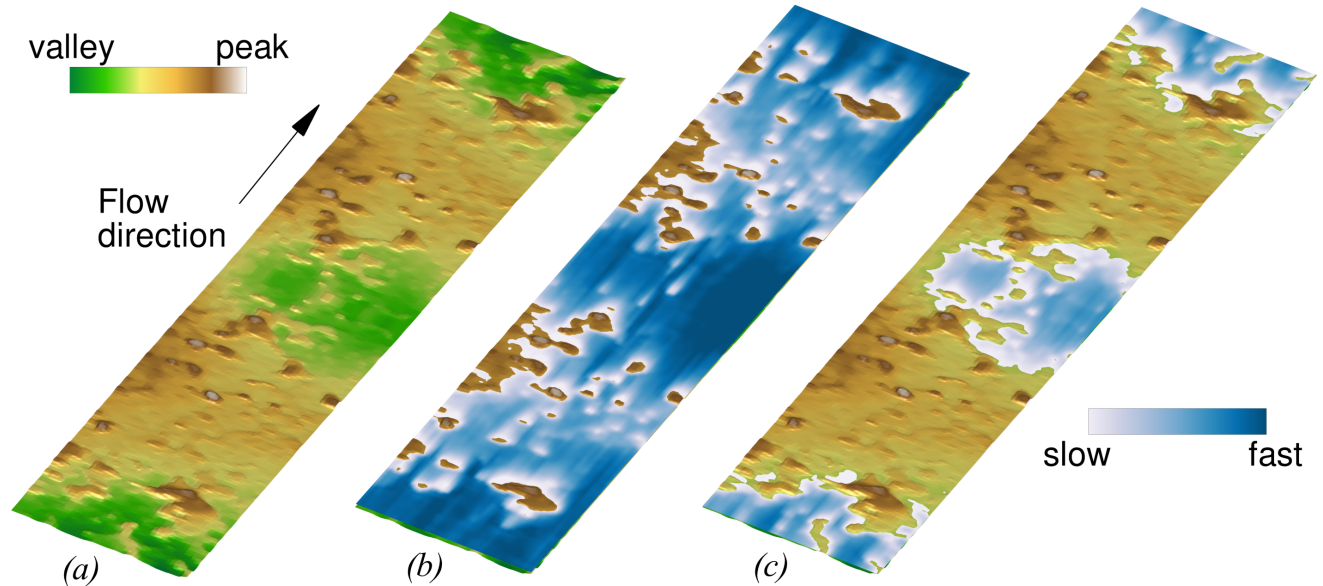
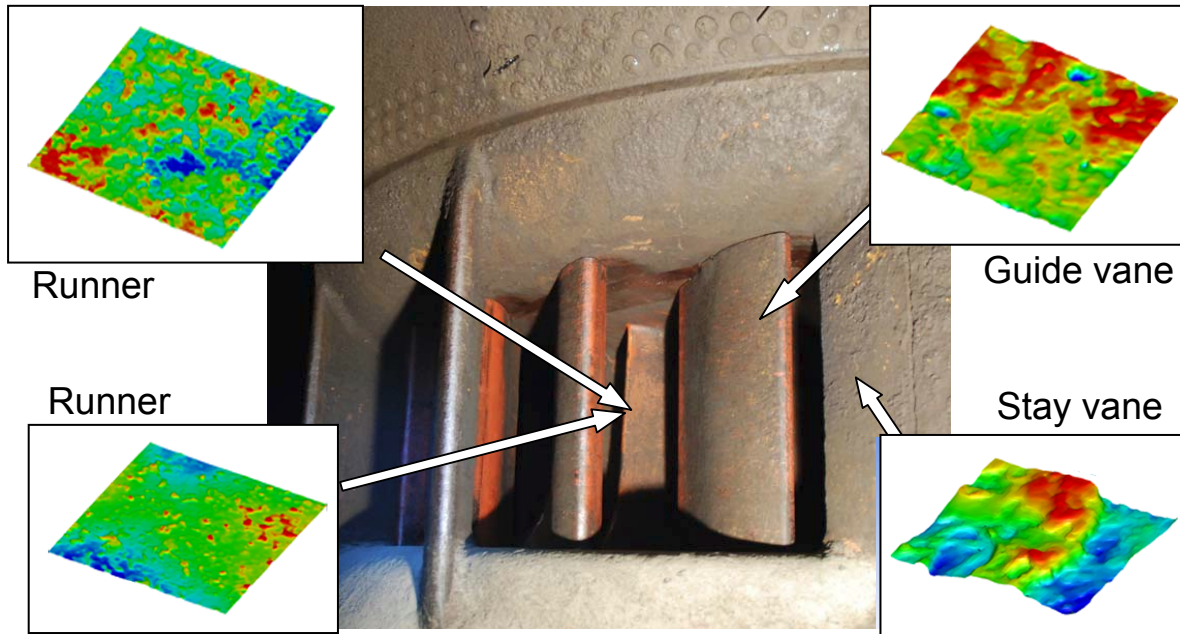


- **Conclusions**

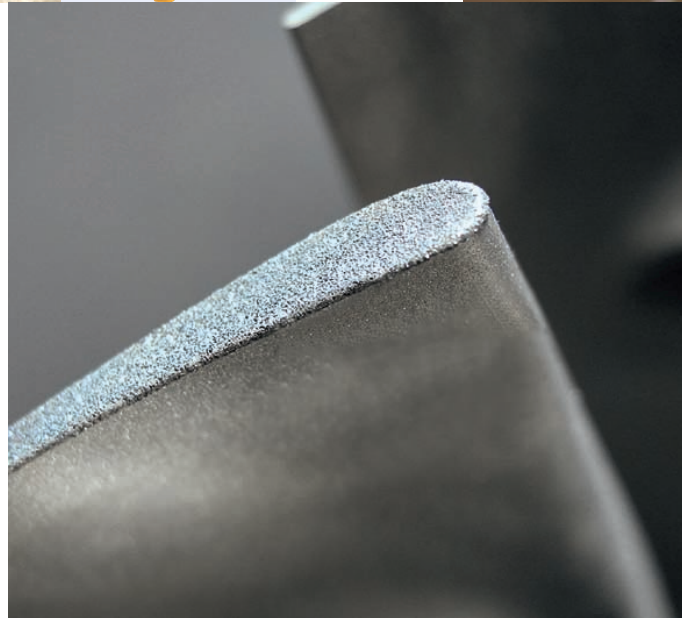
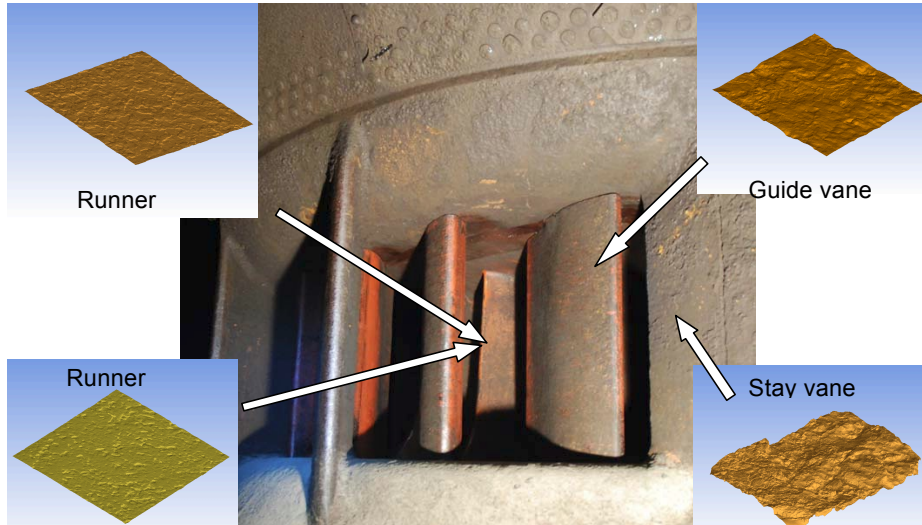
- *The outer layer is not sensitive to roughness*
- *The effects of roughness are confined to the inner layer*
- *The interaction of inner and outer layers depends on the local Reynolds number*
- *Plane and radial wall-jets behave the same at the same local Reynolds numbers*

- **Future work**

- *Analysis of wall-jet at very high local Reynolds numbers*
- *Systematic investigation of roughness height*
- *Assessment of turbulence closure models for prediction of wall jets using LES and DNS databases.*

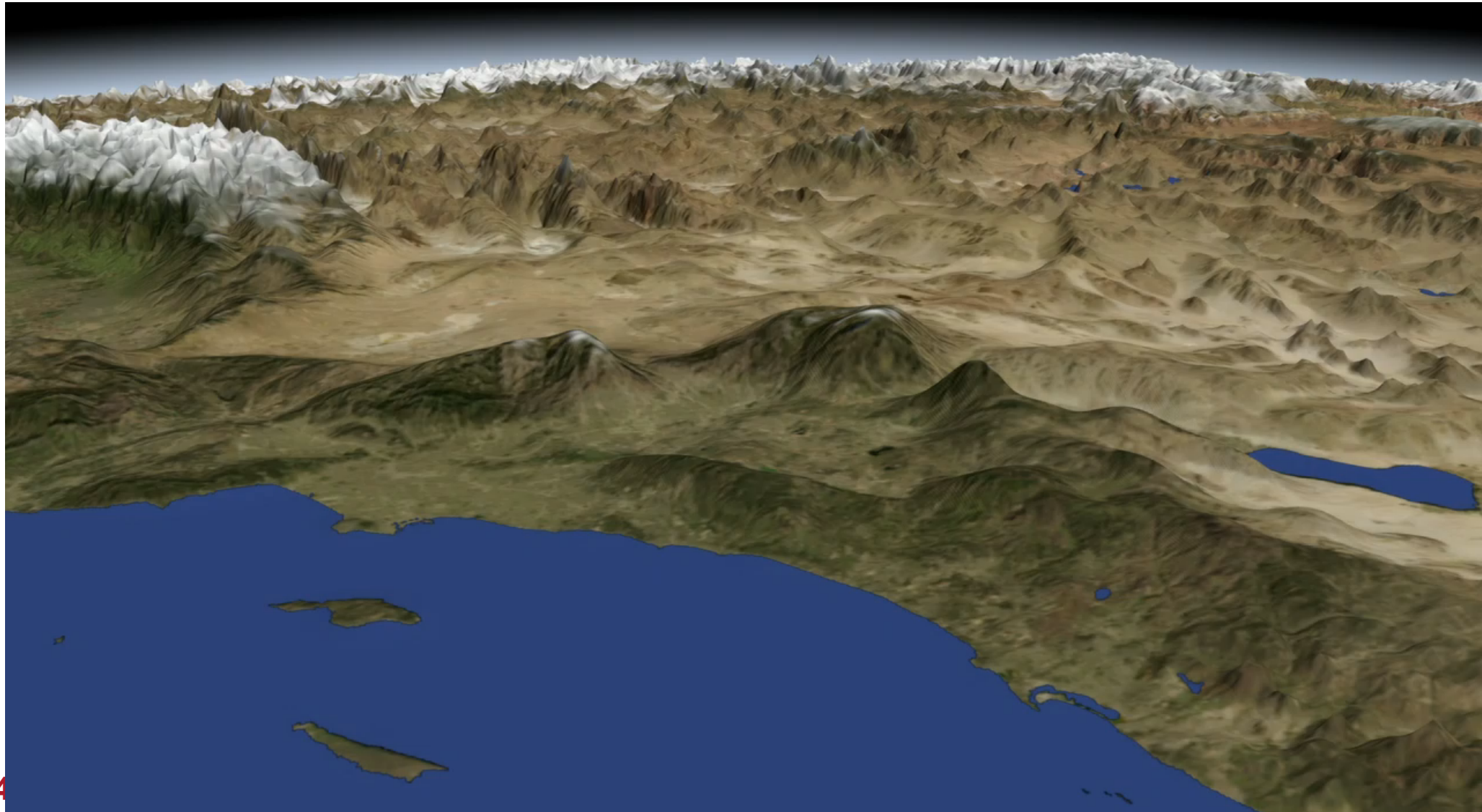


- Roughness occurs in many applications in engineering



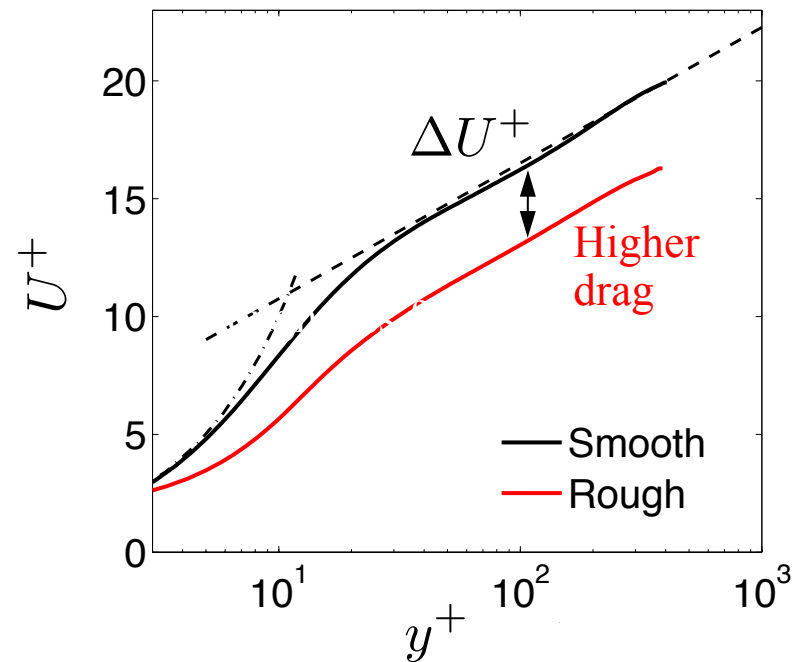
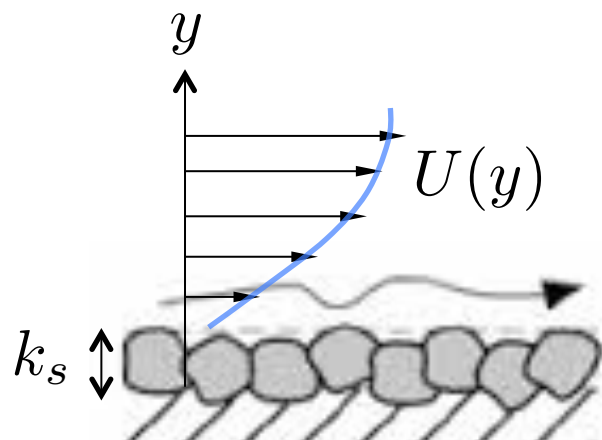


- Roughness occurs in many applications in engineering and the natural sciences.



- Nikuradse (1933), Colebrook (1939); Raupach et al. (1991); Jiménez (2004);...

□ *Increased drag*



k_s : “equivalent sand-grain (SG) height”

$k_s^+ = k_s u_\tau / \nu$: “roughness Reynolds number”

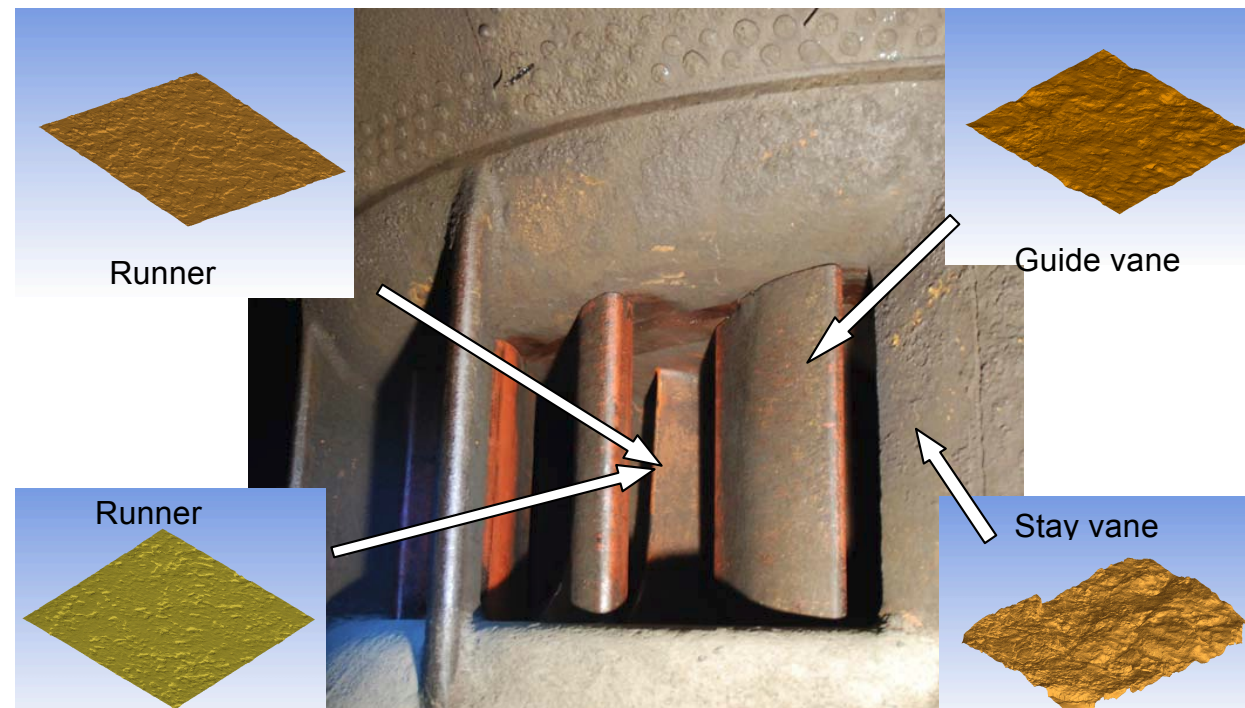


- Nikuradse (1933), Colebrook (1939); Raupach et al. (1991); Jiménez (2004);...
 - *Increased drag*
 - *Increased wall-normal fluctuations*
 - *Decreased Reynolds stress anisotropy*
 - *Dependence on roughness detail is confined to a “Roughness layer”*

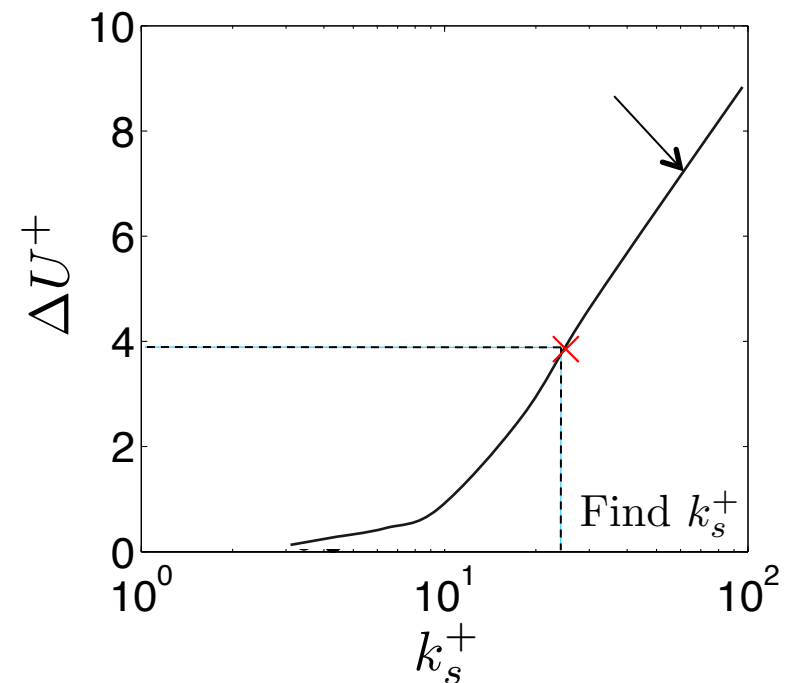
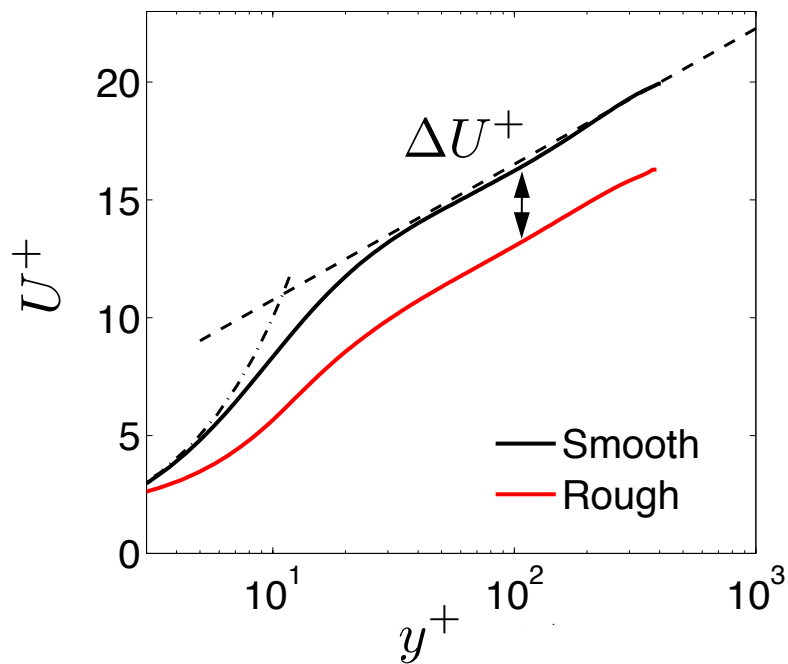
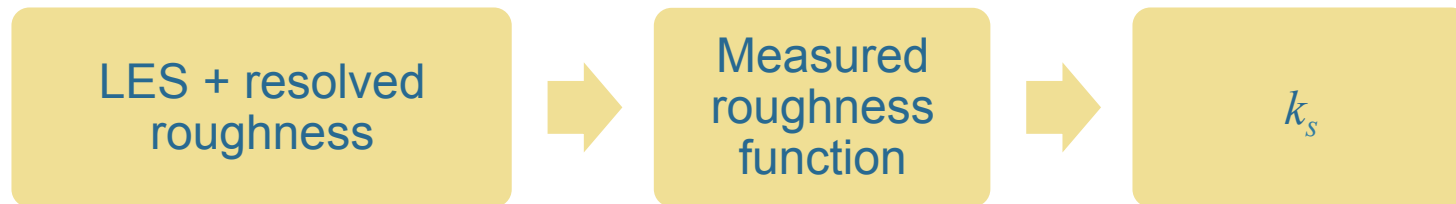


- Solution of the filtered NS equations
 - *Either Cartesian or curvilinear code*
- Roughness is modelled using an Immersed-Boundary Method (IBM)
 - *Force added to RHS of NS equations to enforce no-slip condition off grid points*
 - *Grid must be finer than the typical roughness length scales λ_x , \bar{k} , λ_z :*
$$\Delta x < \lambda_x/6; \quad \Delta y < \bar{k}/10; \quad \Delta z < \lambda_z/6$$

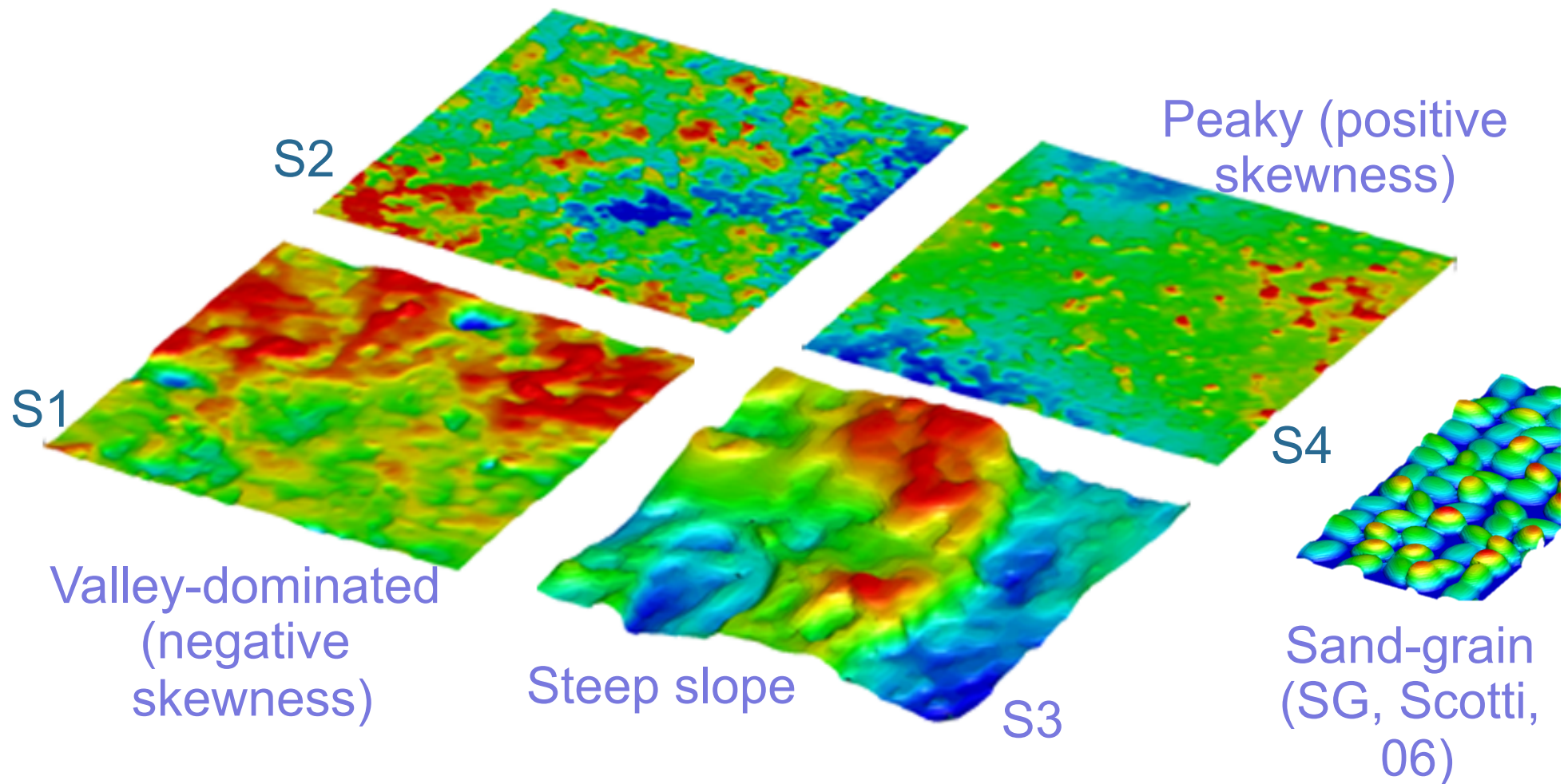
- Turbulence models for the RANS equations have been modified to include roughness
 - *Main parameter to describe the roughness in roughness extensions is k_s*
- Most realistic surfaces do not look like sandgrain roughness
- Need to determine the relationship between k and k_s for arbitrary surfaces.



- Determine k_s for arbitrary surfaces



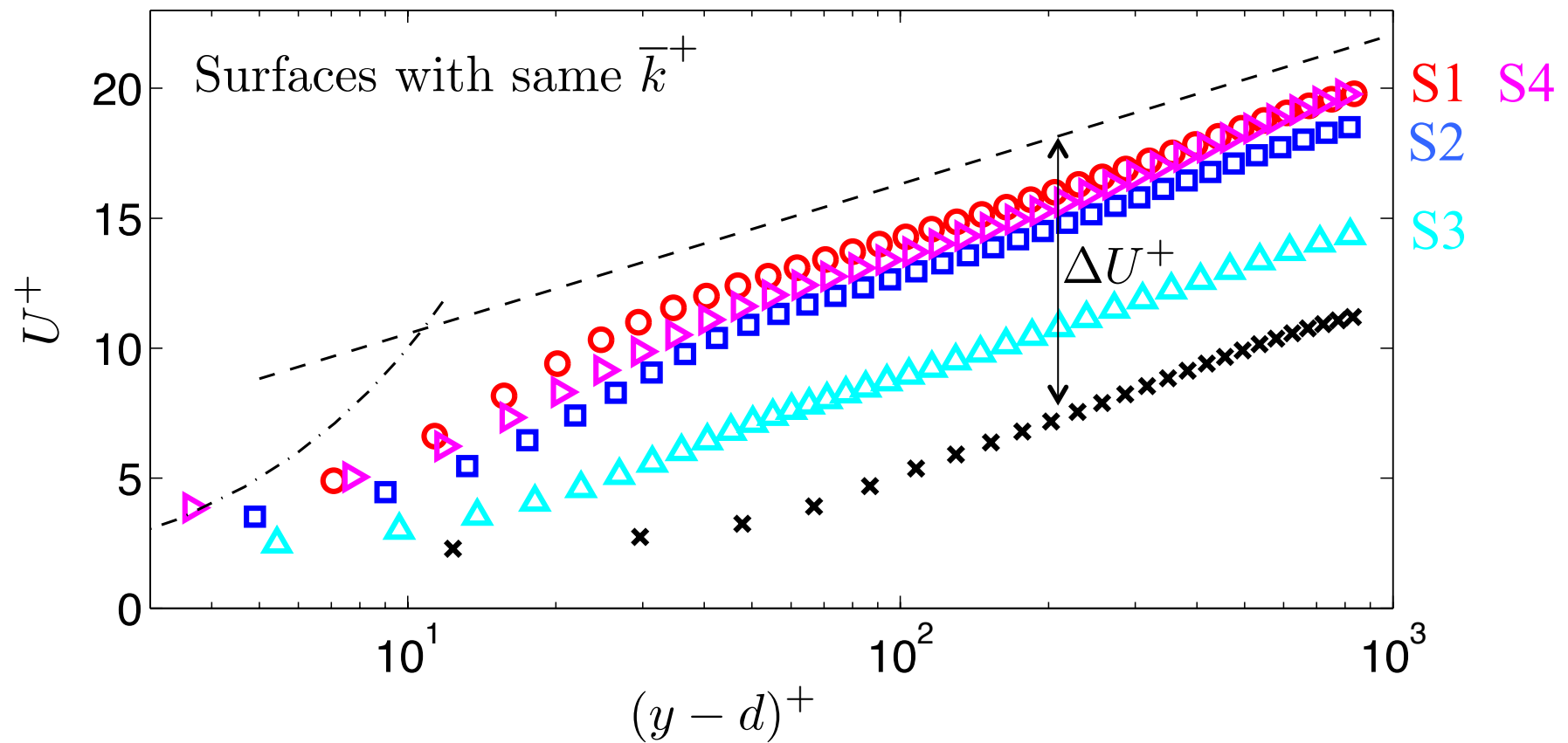
- Determine k_s for arbitrary surfaces





SURFACE CHARACTERIZATION

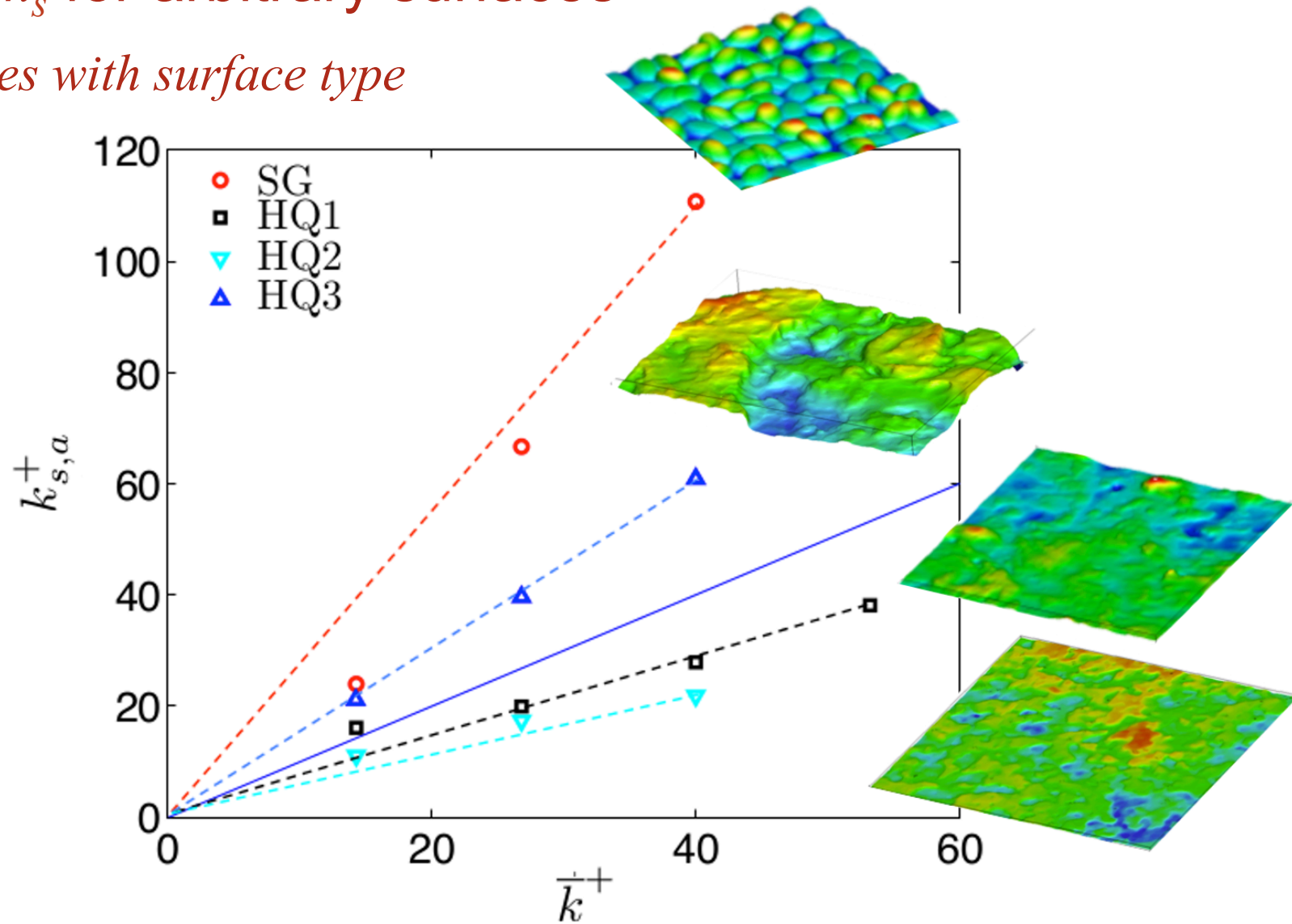
- Determine k_s for arbitrary surfaces
 - ΔU^+ varies with surface type





SURFACE CHARACTERIZATION

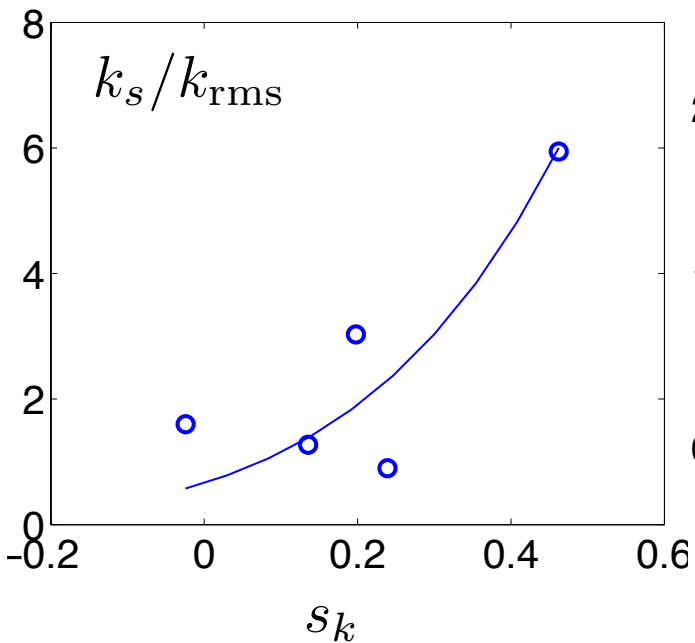
- Determine k_s for arbitrary surfaces
 - k_s/\bar{k} varies with surface type



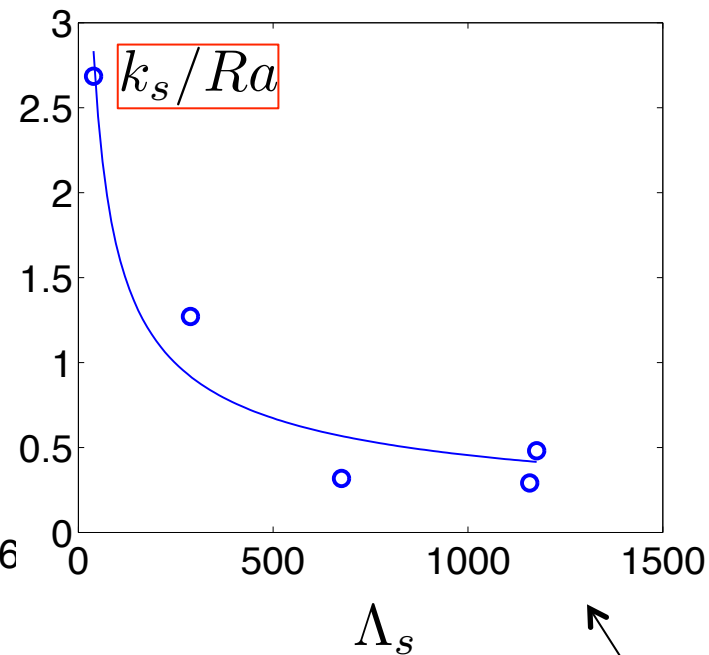
- Evaluation of k_s -correlations

- 5 surfaces \rightarrow 5 data points
- Evaluate existing correlation to obtain the sandgrain roughness

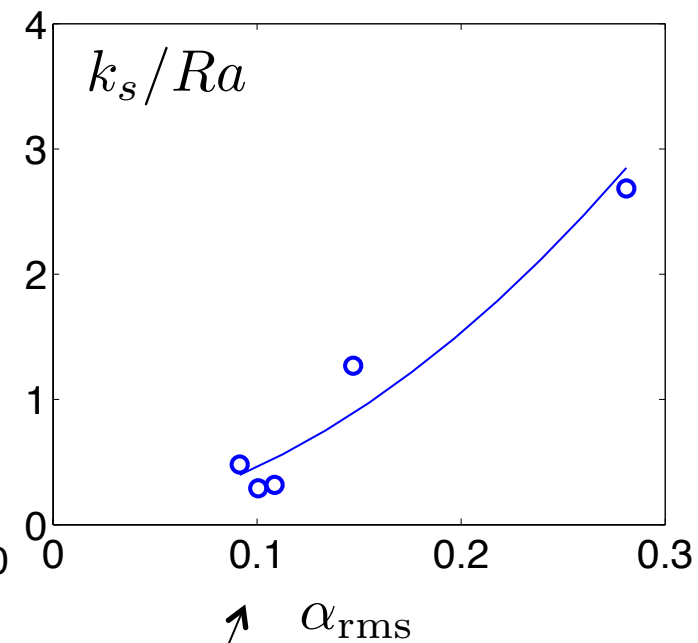
$$k_s = f(\text{RMS, skewness})$$



$$k_s = f(Ra, \text{slope})$$



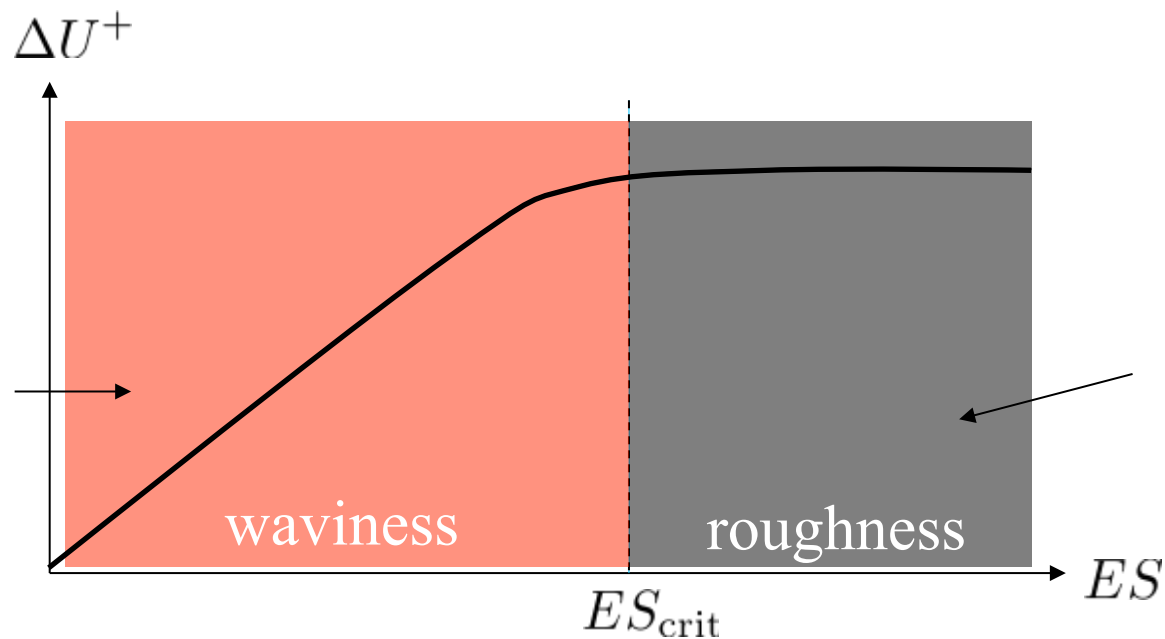
$$k_s = f(Ra, \text{slope \& shape})$$



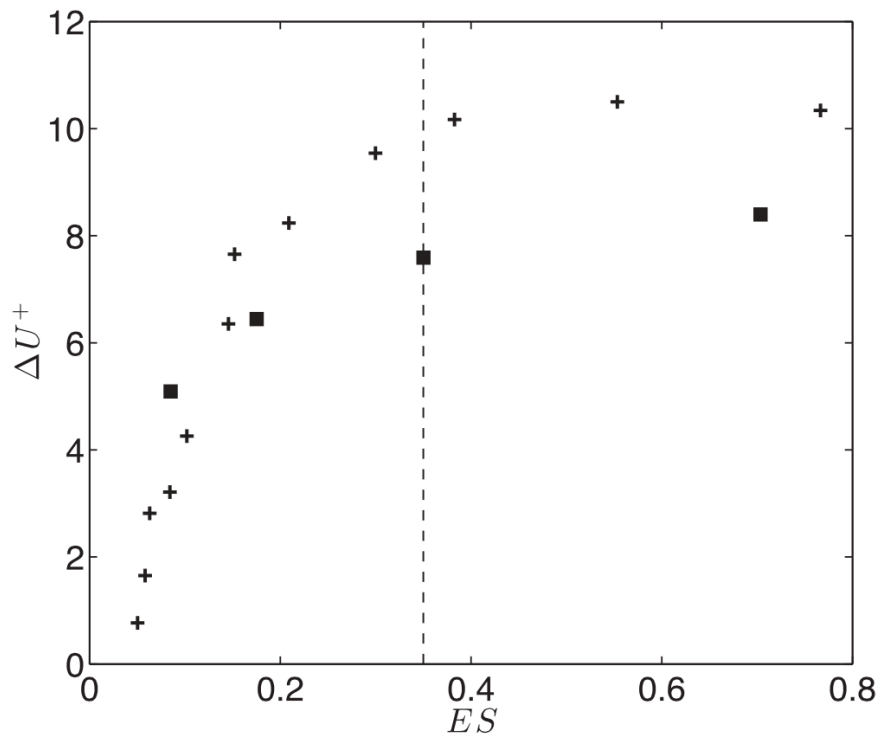
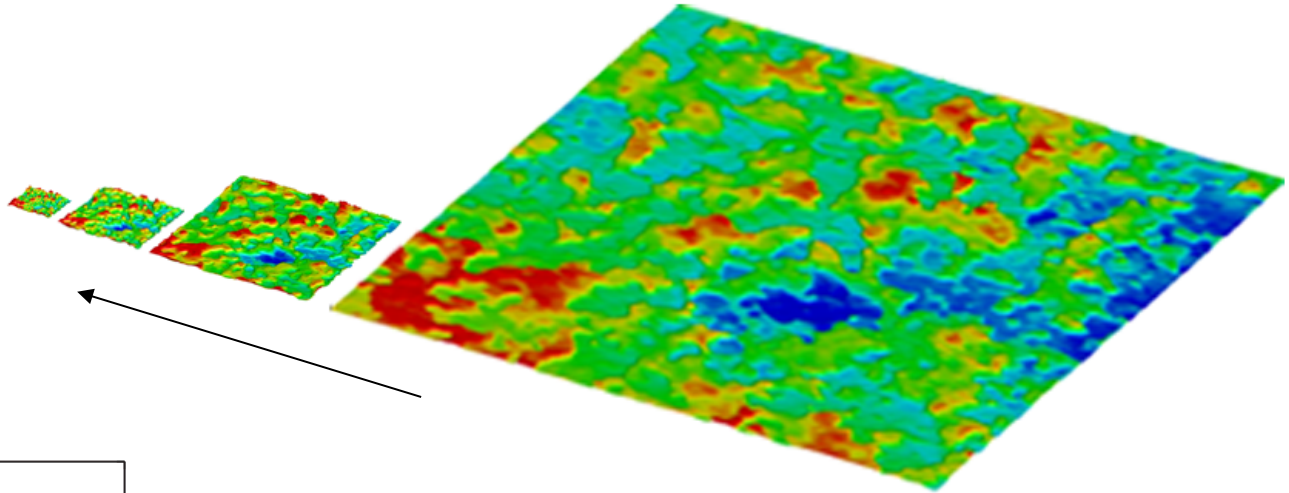
- Evaluations of k_s -correlations

- Effective slope $ES = \frac{1}{L} \int_0^L \left| \frac{dk}{dx} \right| dx$

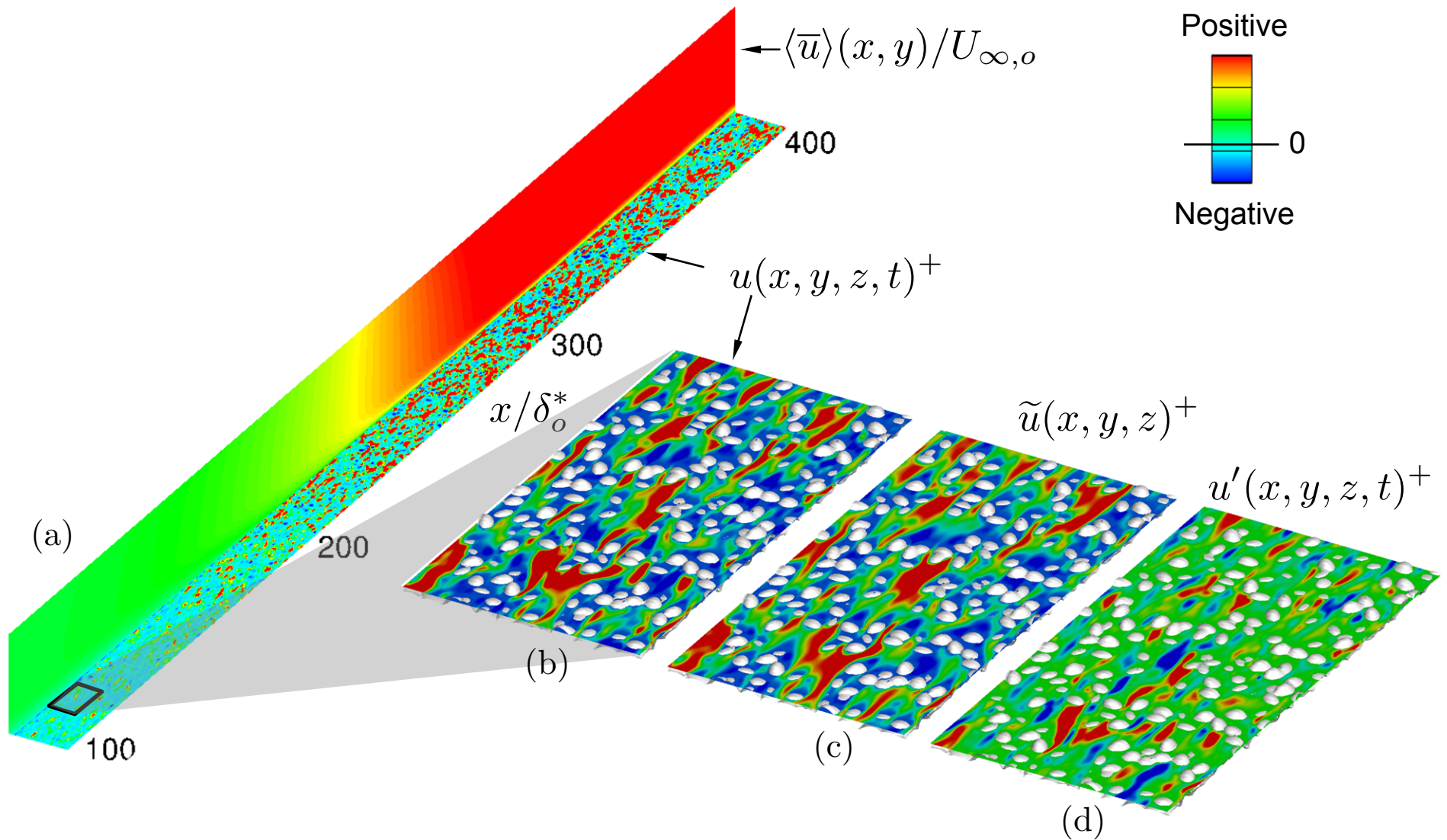
- “Slope is an important parameter only when ES is less than a critical value: 0.35, in ‘waviness regime’.”



- Stretch one type of surface to change the slope without changing the other surface



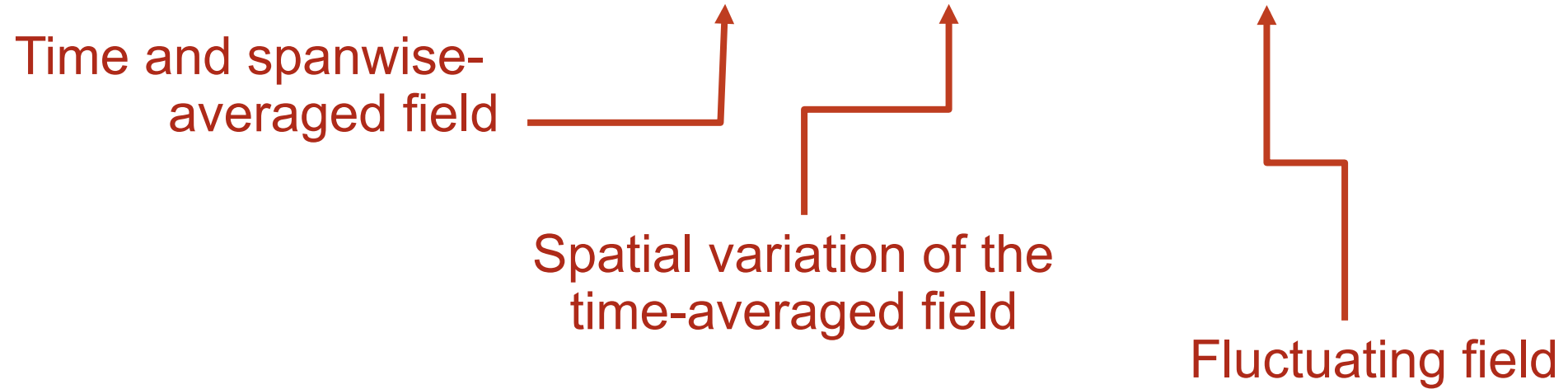
- The critical value of the ES depends on surface characteristics
- The surfaces considered are all in the “waviness” regime





DOUBLE AVERAGING

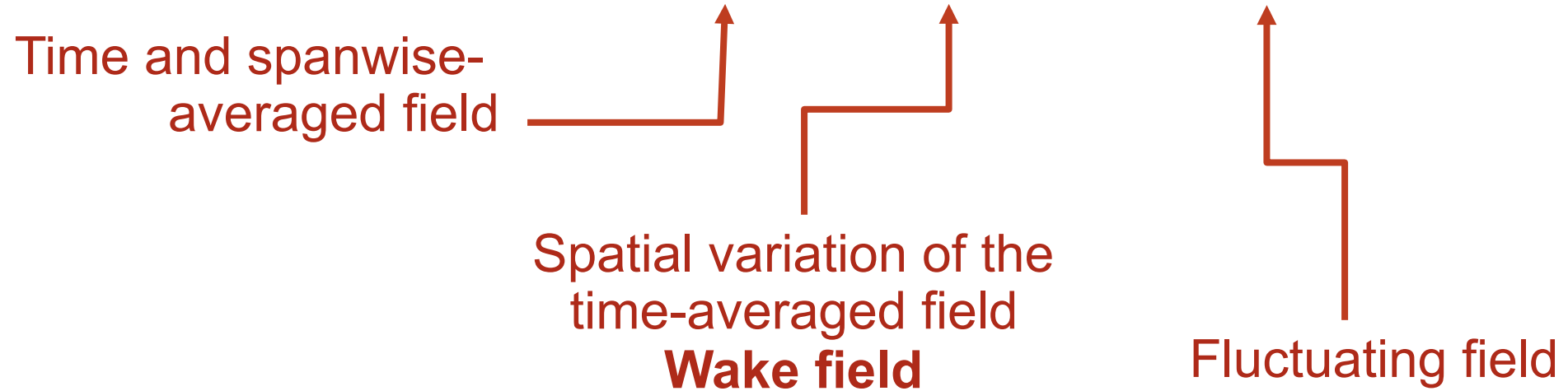
$$\theta(x, y, z, t) = \langle \bar{\theta} \rangle(x, y) + \tilde{\theta}(x, y, z) + \theta'(x, y, z, t).$$





DOUBLE AVERAGING

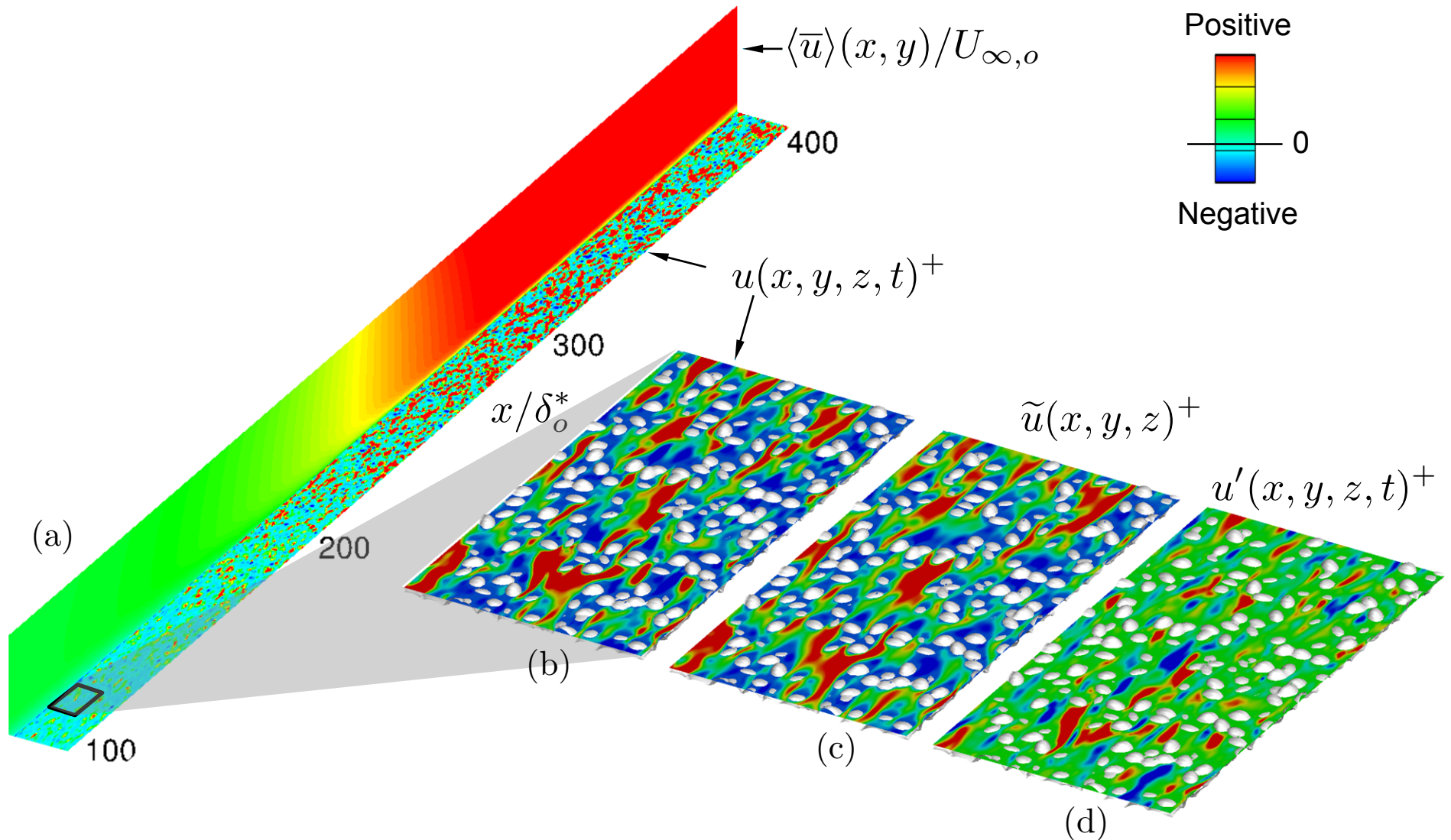
$$\theta(x, y, z, t) = \langle \bar{\theta} \rangle(x, y) + \tilde{\theta}(x, y, z) + \theta'(x, y, z, t).$$





DOUBLE AVERAGING

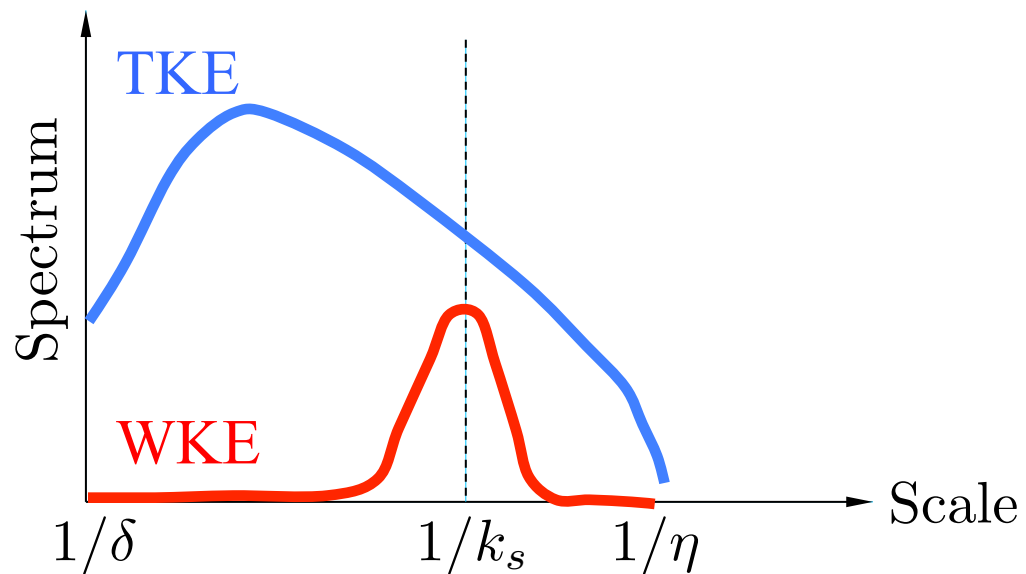
$$\theta(x, y, z, t) = \langle \bar{\theta} \rangle(x, y) + \tilde{\theta}(x, y, z) + \theta'(x, y, z, t).$$



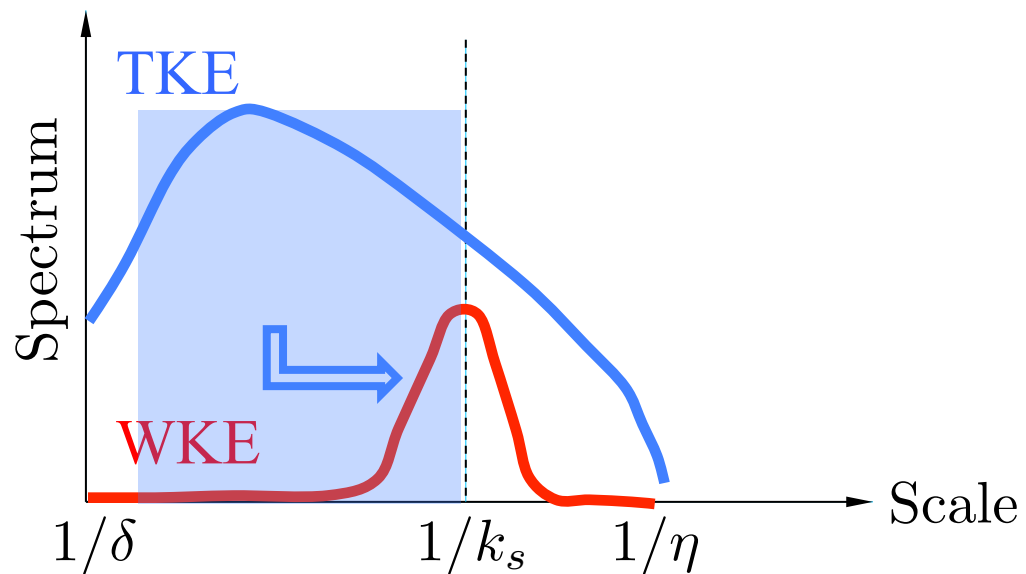
- Motivation

- *Wake fluctuation must play a role in differentiating between roughness types.*
- *v' , w' : important for near-wall instability & momentum transfer*
- *Roughness \rightarrow wake field \rightarrow change in Reynolds-stress budgets*

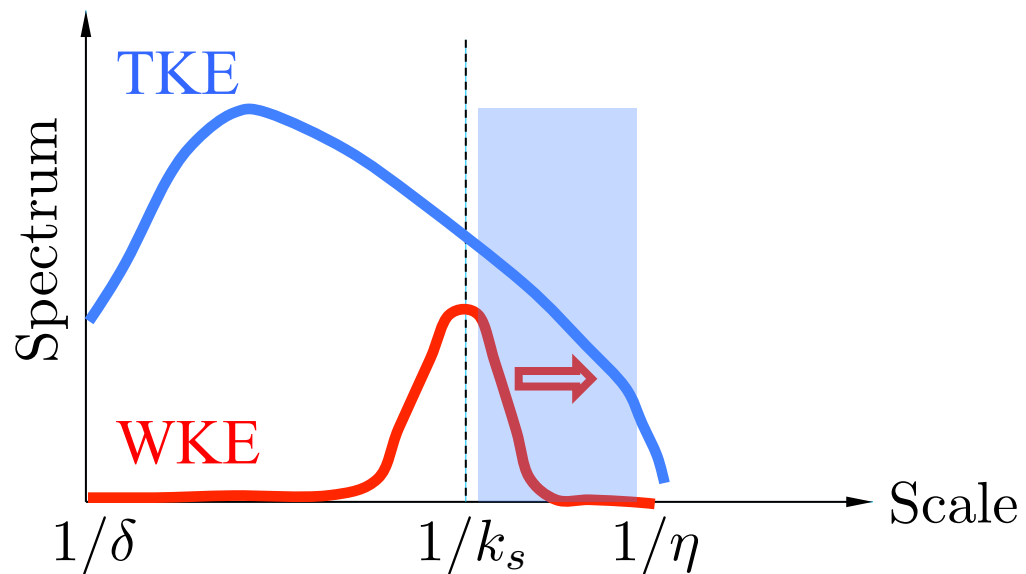
- Wake-turbulence interaction
 - *Two-way*



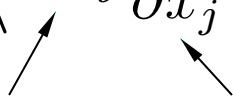
- Wake-turbulence interaction
 - *Two-way*



- Wake-turbulence interaction
 - *Two-way*



- Wake-turbulence interaction
 - *Two-way*
 - *Wake production, P_w*
 - Net conversion (Finnigan 00)
 - Shear term with opposite signs in budgets of WKE & TKE

$$P_w = - \left\langle \widetilde{u'_i u'_j} \frac{\partial \widetilde{u}_i}{\partial x_j} \right\rangle_s$$




WAKE-TURBULENCE INTERACTION

- Results

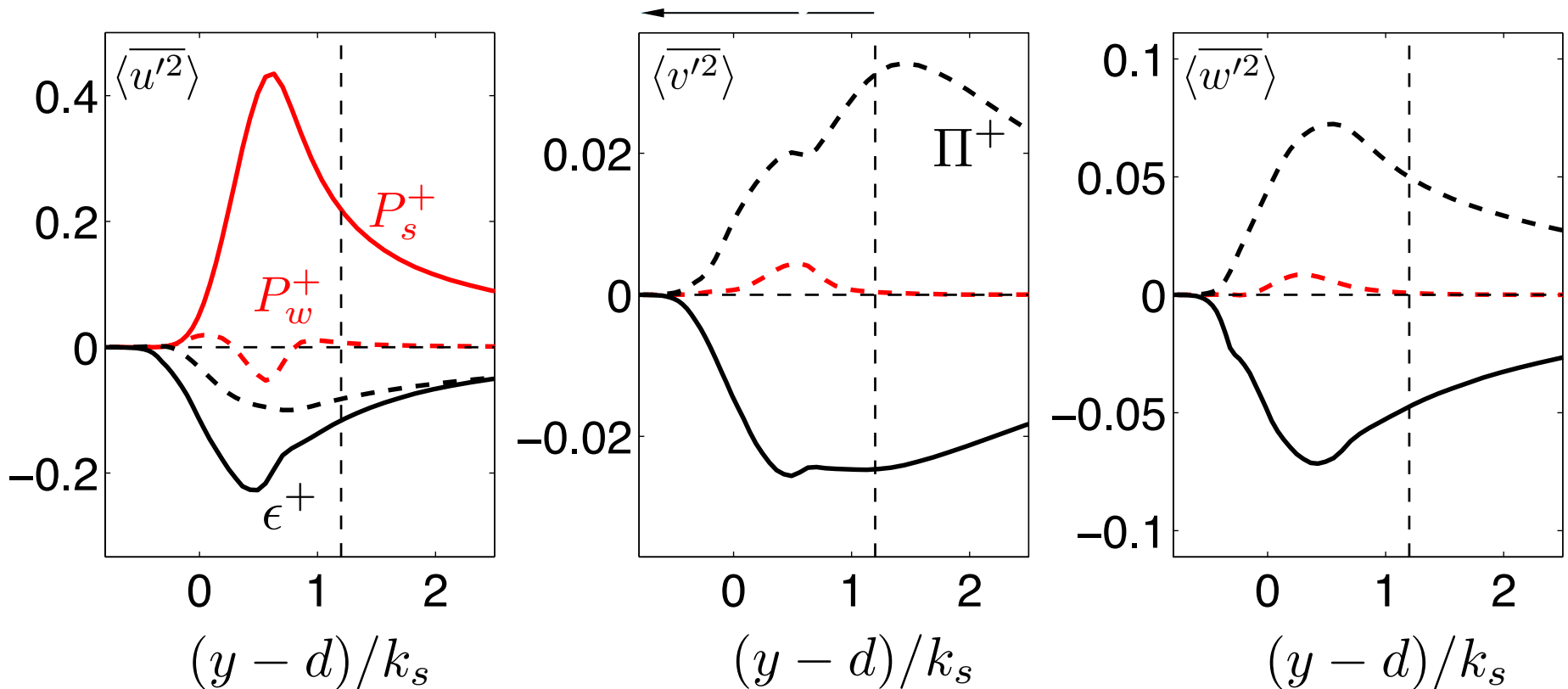
- P_w in ZPG boundary layer
- Reynolds-stress budgets

P_s : shear production

P_w : wake production

ϵ : dissipation

Π : pressure work





WAKE-TURBULENCE INTERACTION

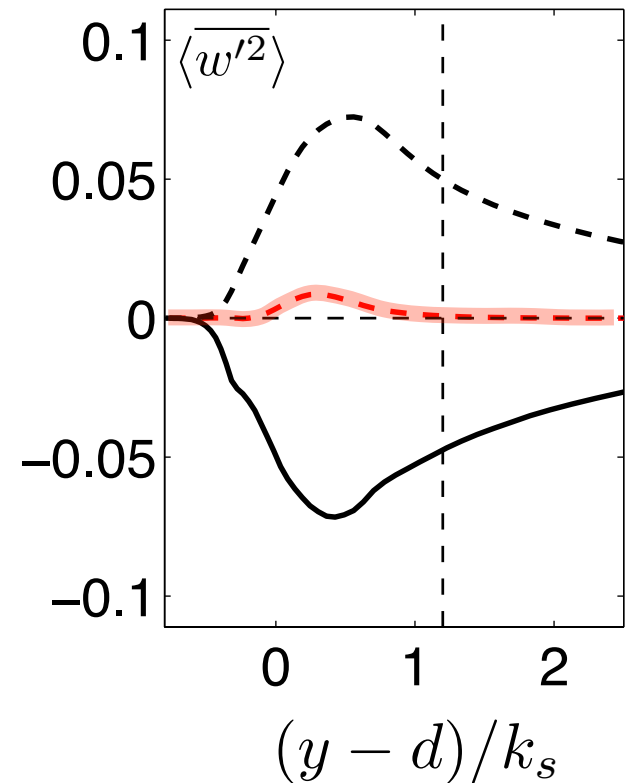
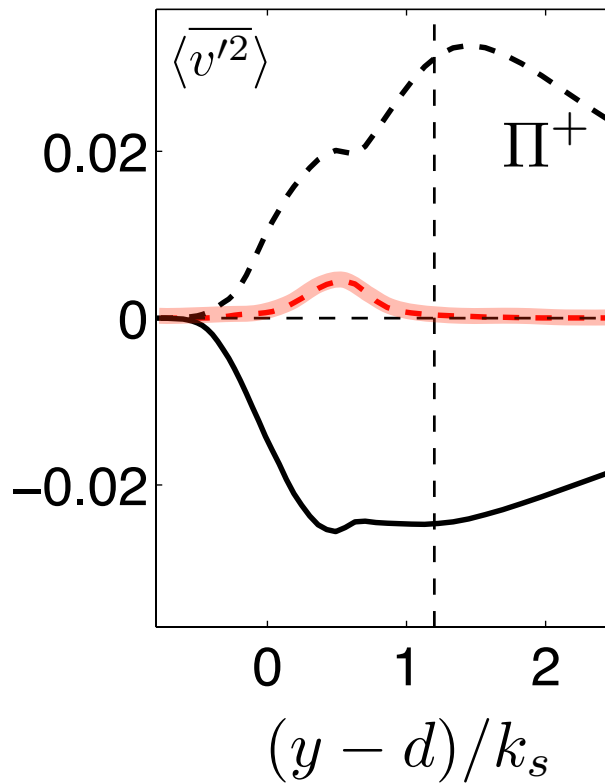
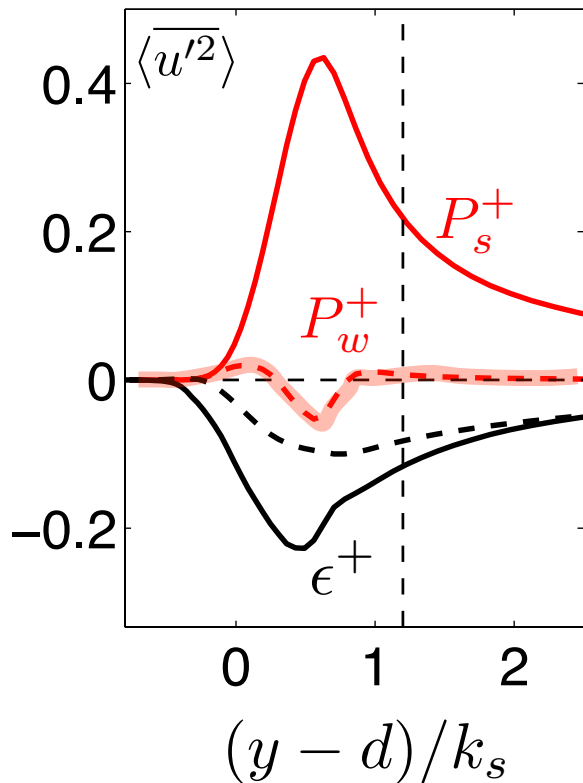
• Results

□ P_w in ZPG boundary layer

- Reynolds-stress budgets
- $P_w \rightarrow$ higher v' , w' , p'
- TKE redistribution \Rightarrow less anisotropy

$$P_w < 0$$

$$P_w > 0$$





Queen's
UNIVERSITY

APPLICATIONS

SEPARATION IN ROUGH-WALL BLS

Junlin Yuan, Pouya Mottaghian



- Canonical boundary layers
 - *Zero pressure gradient*
 - *Smooth wall*
- Realistic boundary layers
 - *Acceleration - Favourable pressure gradient (FPG)*
 - *Deceleration - Adverse pressure gradient (APG)*
 - *Curvature*
 - *3D mean-flow*



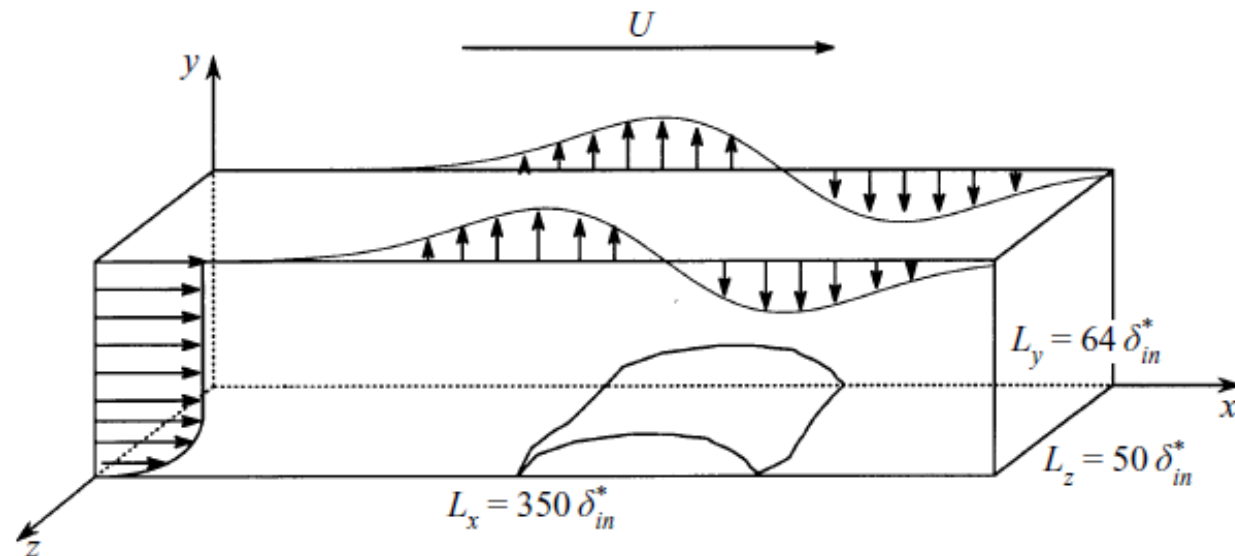
- Flat-plate boundary layer with APG

- *Laminar:*

- Spalart & Strelets (2000),

- *Turbulent*

- Perry and co-workers (1966+), Na & Moin (1998), Skote & Henningson (2002), ...

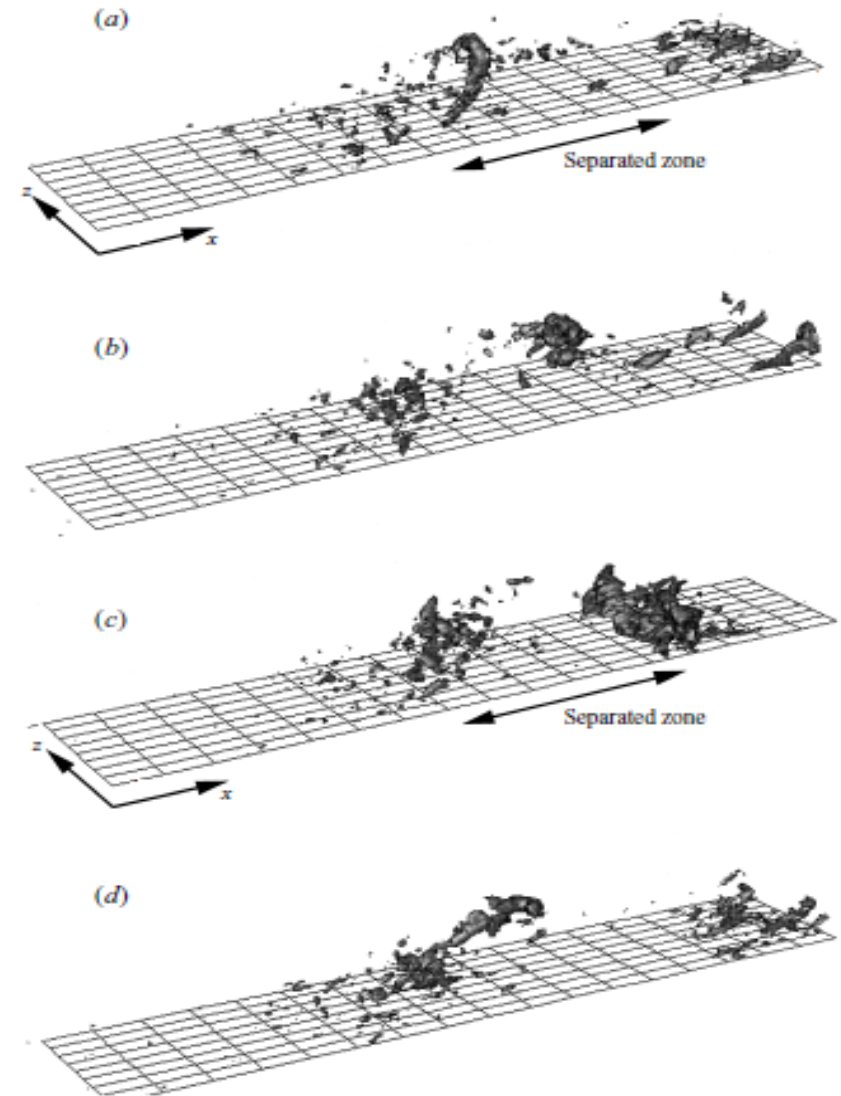




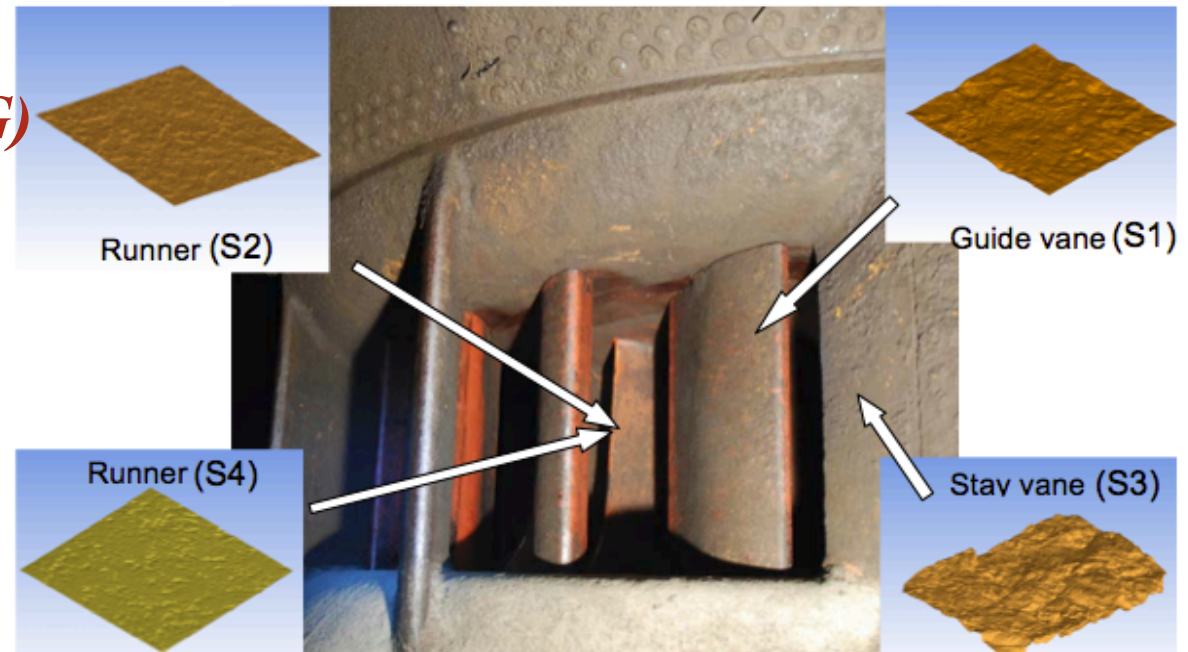
- Flat-plate boundary layer with APG

- *Observations:*

- Mean shear layer detachment
 - Unsteady separation bubble
 - Turbulent structures travel around the bubble.
 - Intensity increases inside shear layer.
 - Turbulence increases in intensity & homogeneity at reattachment.



- Canonical boundary layers
 - *Zero pressure gradient*
 - *Smooth wall*
- Realistic boundary layers
 - *Acceleration - Favourable pressure gradient (FPG)*
 - *Deceleration – Adverse pressure gradient (APG)*
 - *Curvature*
 - *3D mean-flow*
 - *Surface roughness*





- Rough-wall boundary layers with APG
 - *Song and Eaton (2002), Cao and Tamura (2005), Durbin et al. (2001), ...*
 - *Geometry studied*
 - Flow around ramp
 - Flow over hill
 - *Earlier separation & larger separation bubble (vs. smooth case)*
 - Larger momentum deficit
 - *Limitations*
 - More complex geometry \Rightarrow additional effects
 - Skin friction calculation
 - Flow structures
 - Accessibility of the roughness sublayer



- How do roughness (inner layer effect) and deceleration (outer layer effect) interact?

What we know

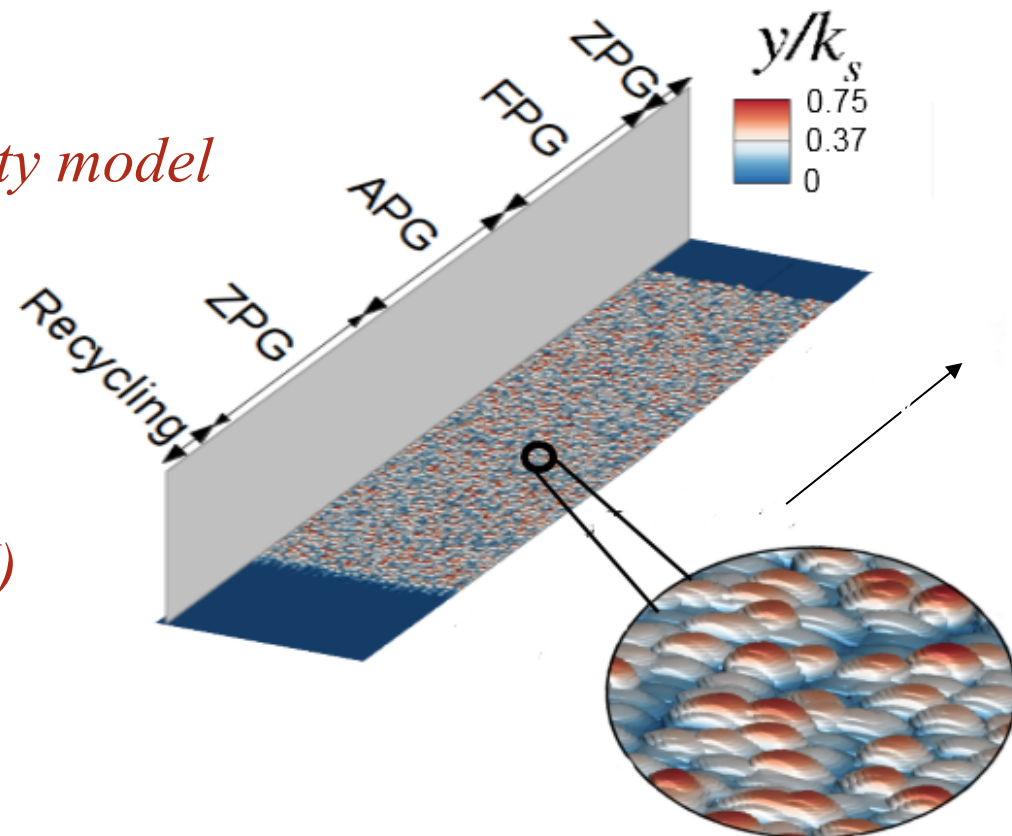
- Roughness promotes turbulence & mixing in the ZPG region
- Roughness increases drag
- APG (before separation) promotes turbulence & mixing



Questions

- Why earlier separation in rough case?
- Does separation communicate the roughness effects away from the wall?

- Continuity and Navier-Stokes equations
- 2nd-order accurate in space and time, staggered finite difference code
- Crank-Nicolson + Adams-Bashforth time advancement
- Large-eddy simulation
 - *Lagrangian dynamic eddy-viscosity model*
- Resolved roughness
 - *Virtual sandpaper model*
 - Scotti (2006)
 - *Immersed boundary method (IBM)*
 - Volume of fluid approach

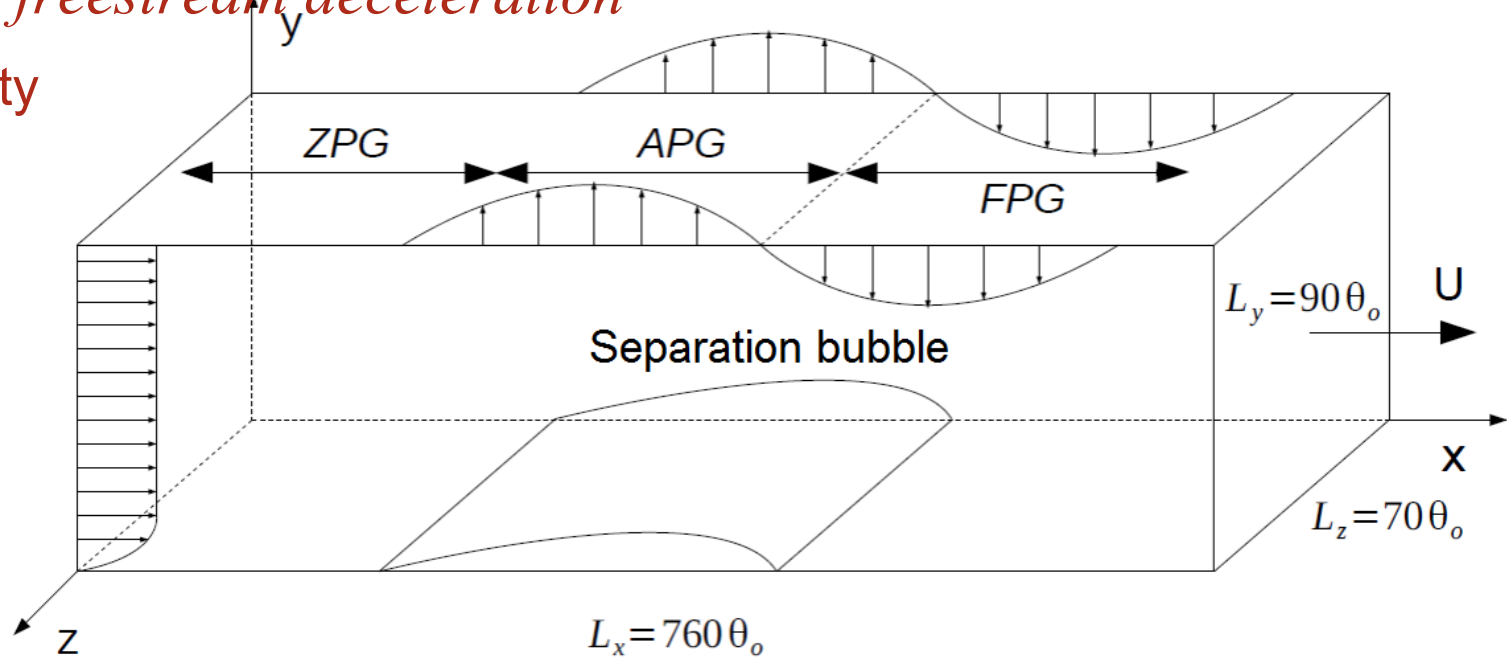




PROBLEM FORMULATION

- Boundary conditions

- *Spanwise: periodic boundary condition*
- *Inlet: Recycling/Rescaling method of Lund et al. (1998)*
- *Outlet: Convective outflow boundary condition*
- *Top: imposed freestream deceleration*
 - Zero vorticity



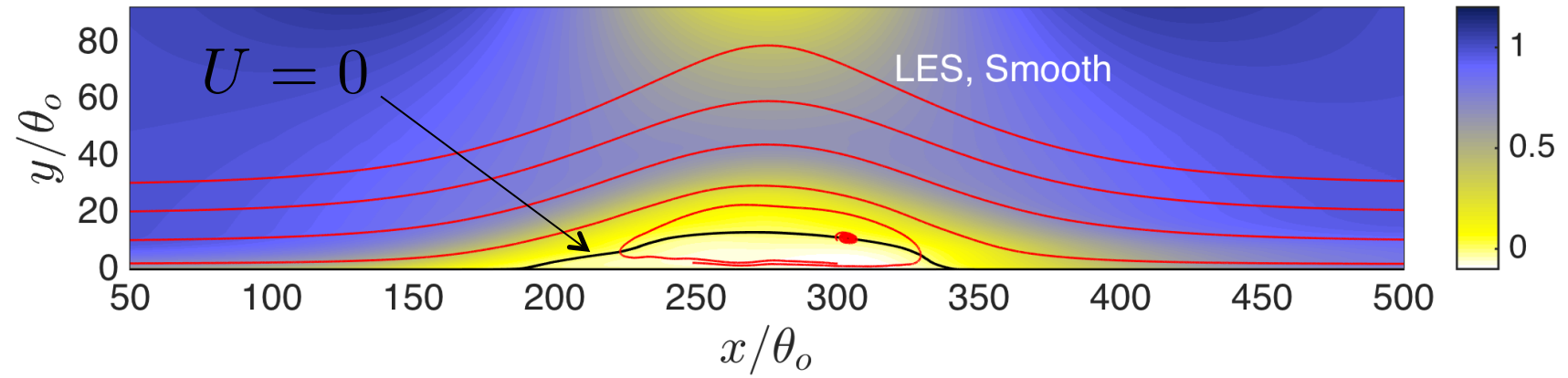


- Cases

- *Reference scales:* $u_{\infty,0}, \theta_0$

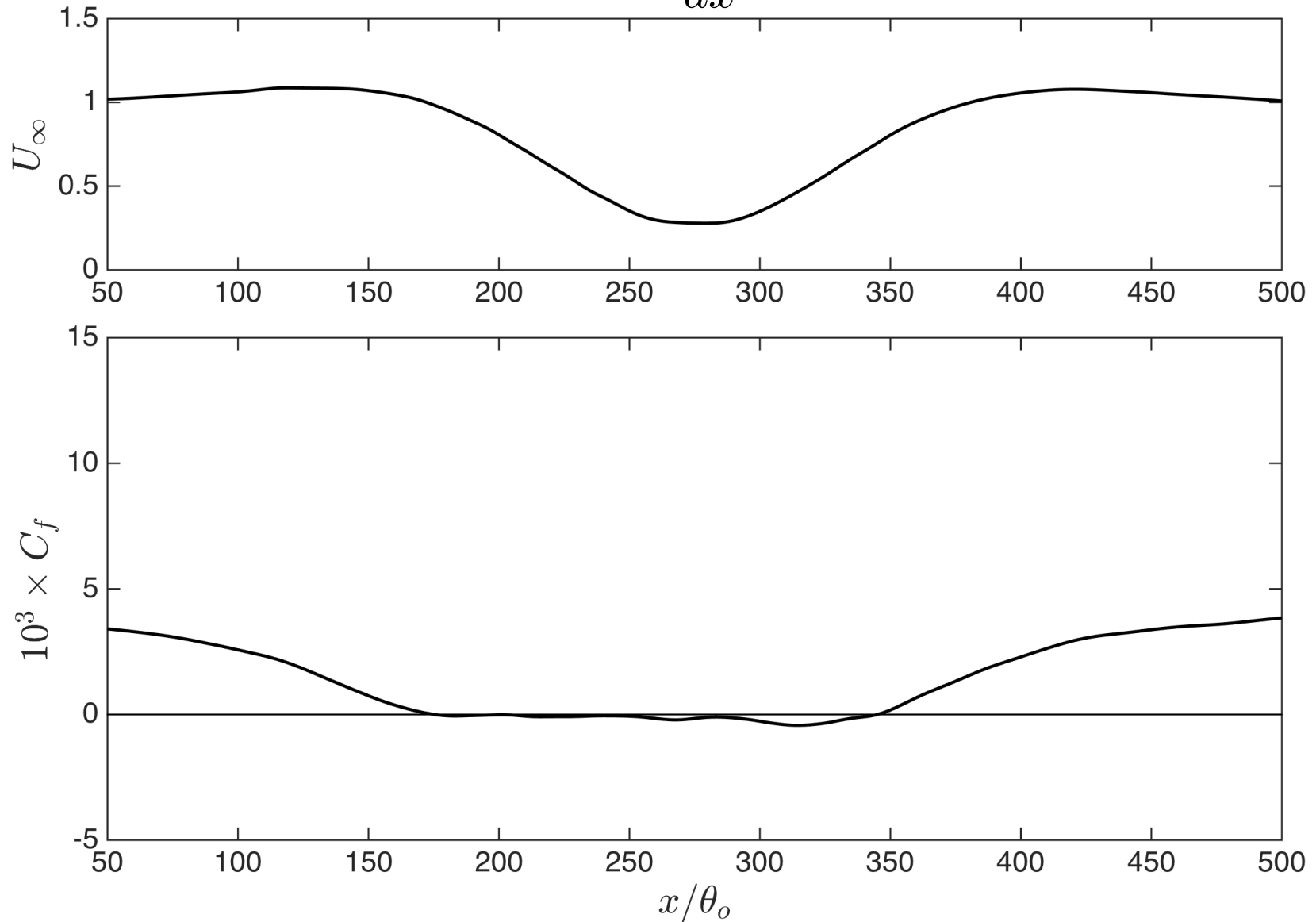
Case	$Re_{\theta,0}$	k/θ_0	Grid	Domain size	Δx_{max}^+	Δy_{min}^+	Δz_{max}^+
Smooth	300	0	640×192×128	$460\theta_0 \times 65\theta_0 \times 50\theta_0$	20	0.6	11
Smooth	2300	0	2560×384×384	$760\theta_0 \times 90\theta_0 \times 70\theta_0$	30	1	19
Rough	2300	0.47	2048×384×384	$760\theta_0 \times 90\theta_0 \times 70\theta_0$	50	1.5	26
Rough	2300	0.95	2560×432×384	$760\theta_0 \times 90\theta_0 \times 70\theta_0$	44	0.8	28

- *Between 750 and 1500 grid volumes per roughness element.*

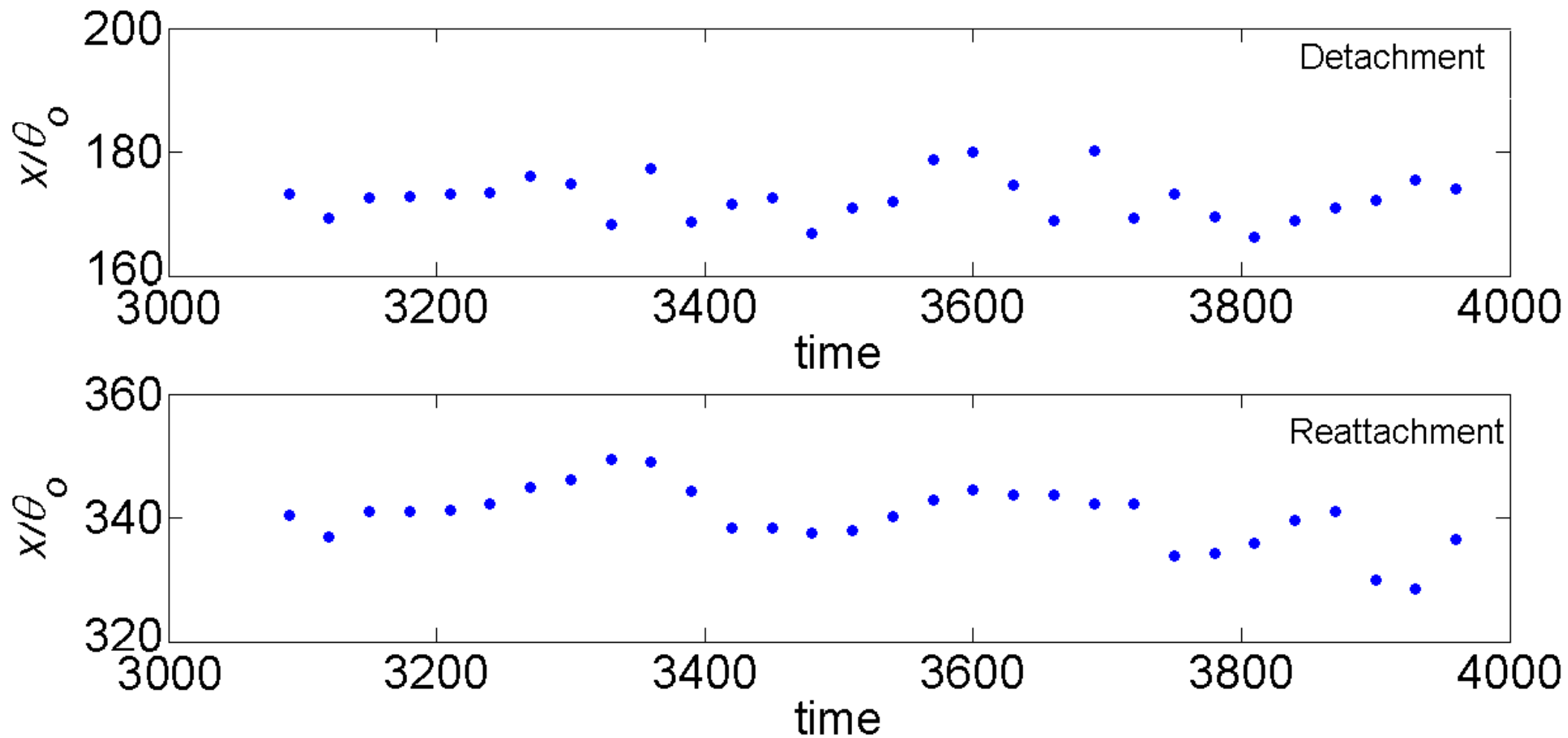




- Standard definition: $\tau_w = 0, \frac{d\tau_w}{dx} < 0$

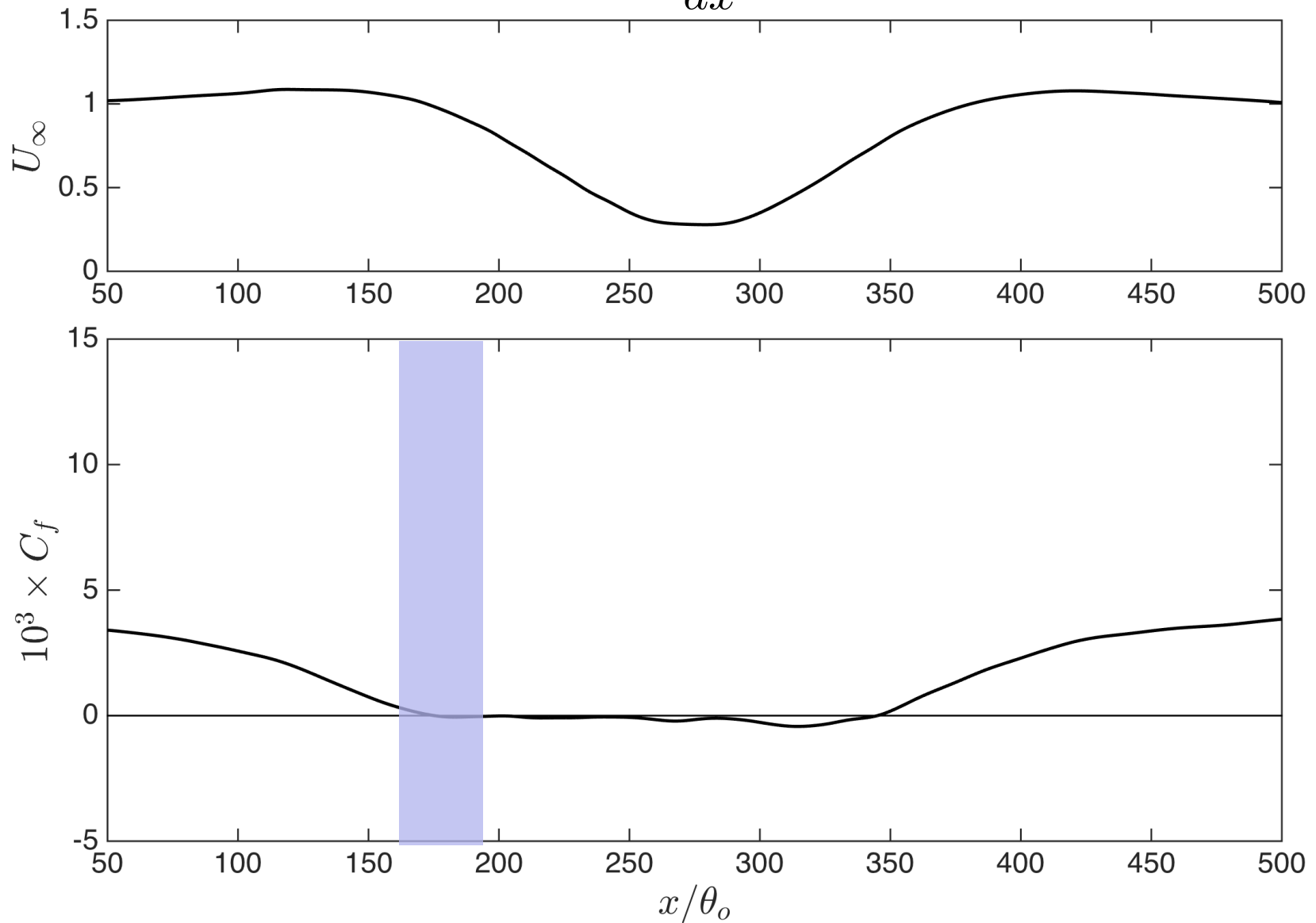


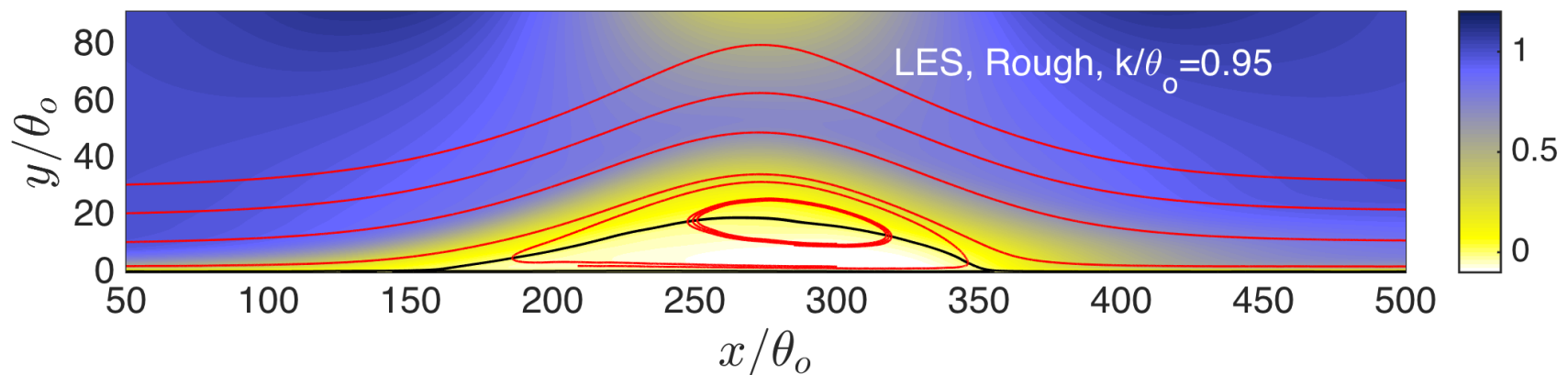
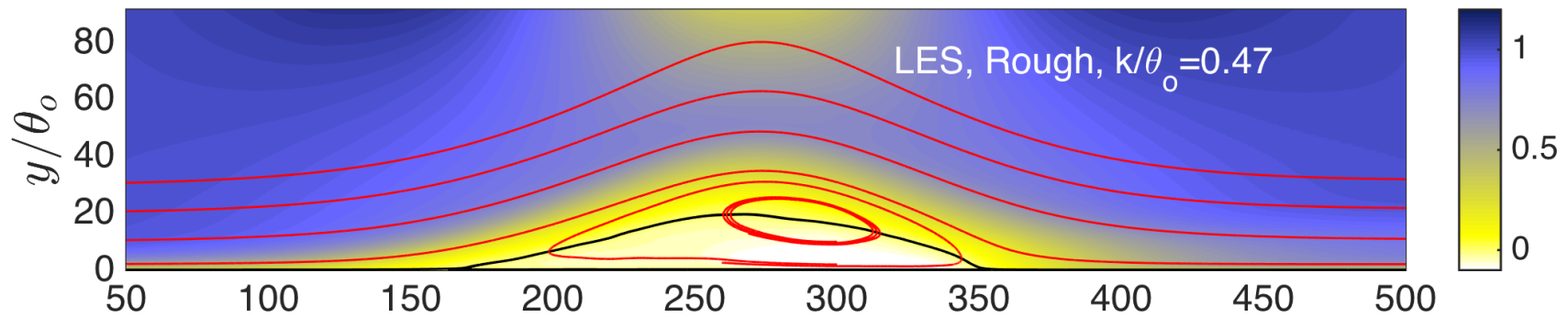
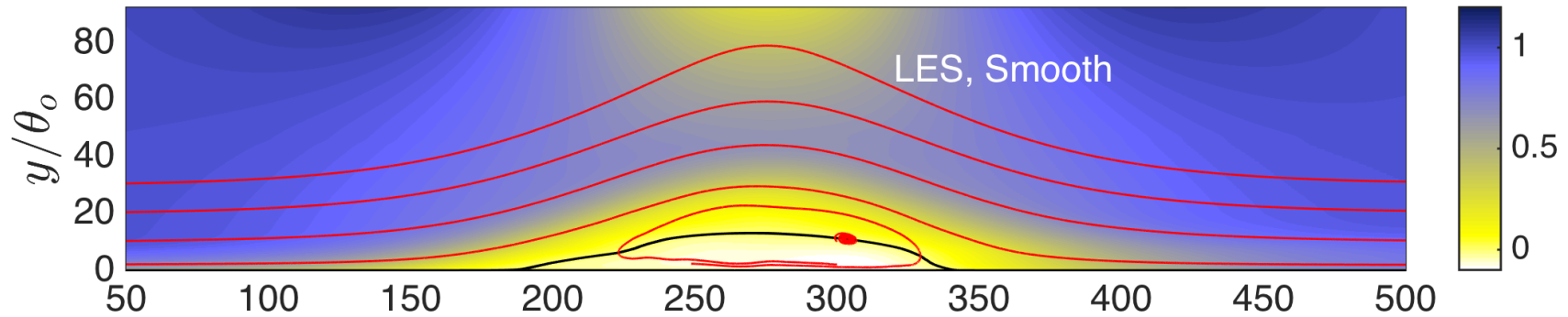
- The separation point is unsteady





- Standard definition: $\tau_w = 0, \frac{d\tau_w}{dx} < 0$



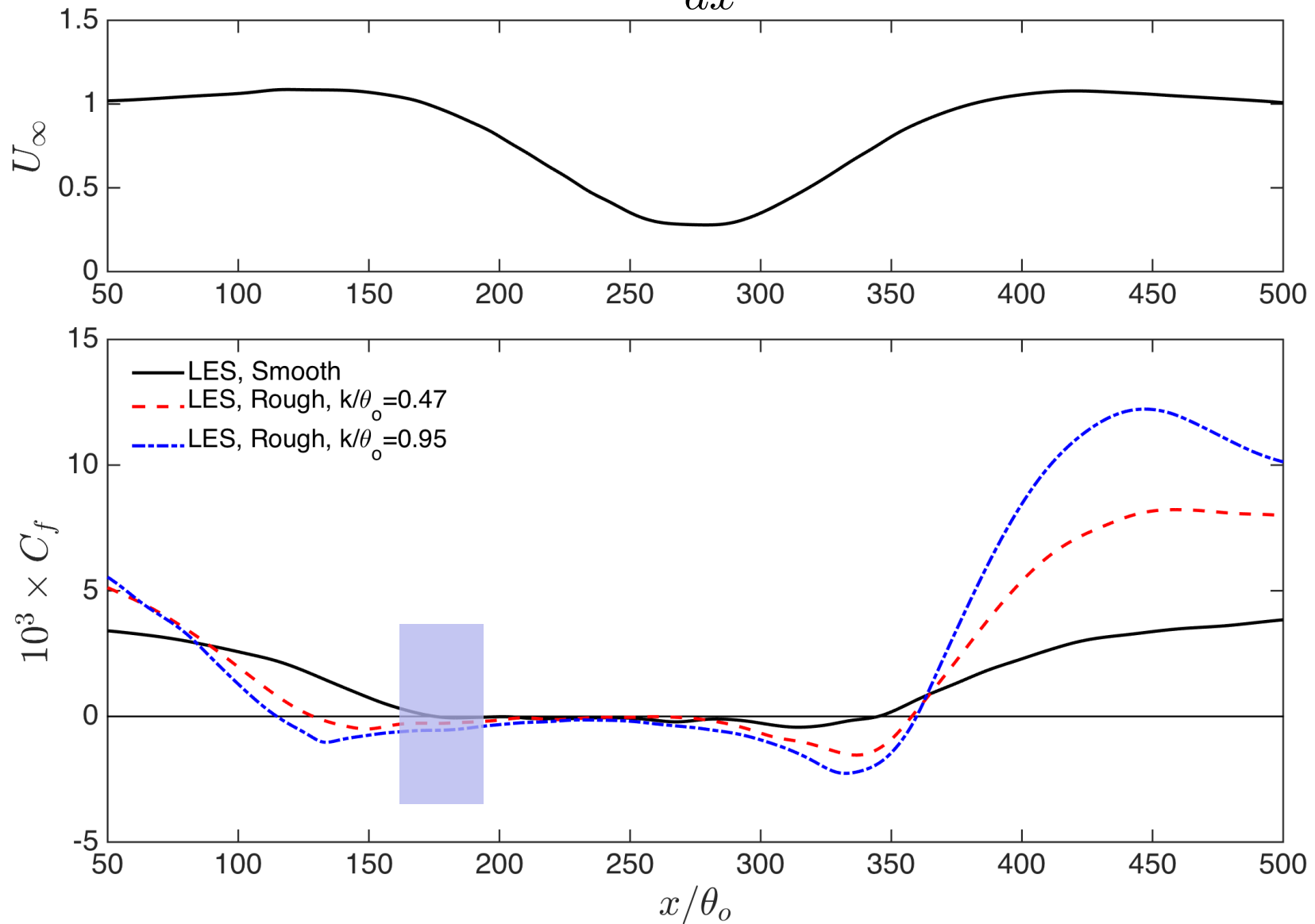




- Standard definition: $\tau_w = 0, \frac{d\tau_w}{dx} < 0$
 - τ_w includes viscous and form drag (from the wake of the roughness elements)
 - In the fully rough regime, form drag dominates



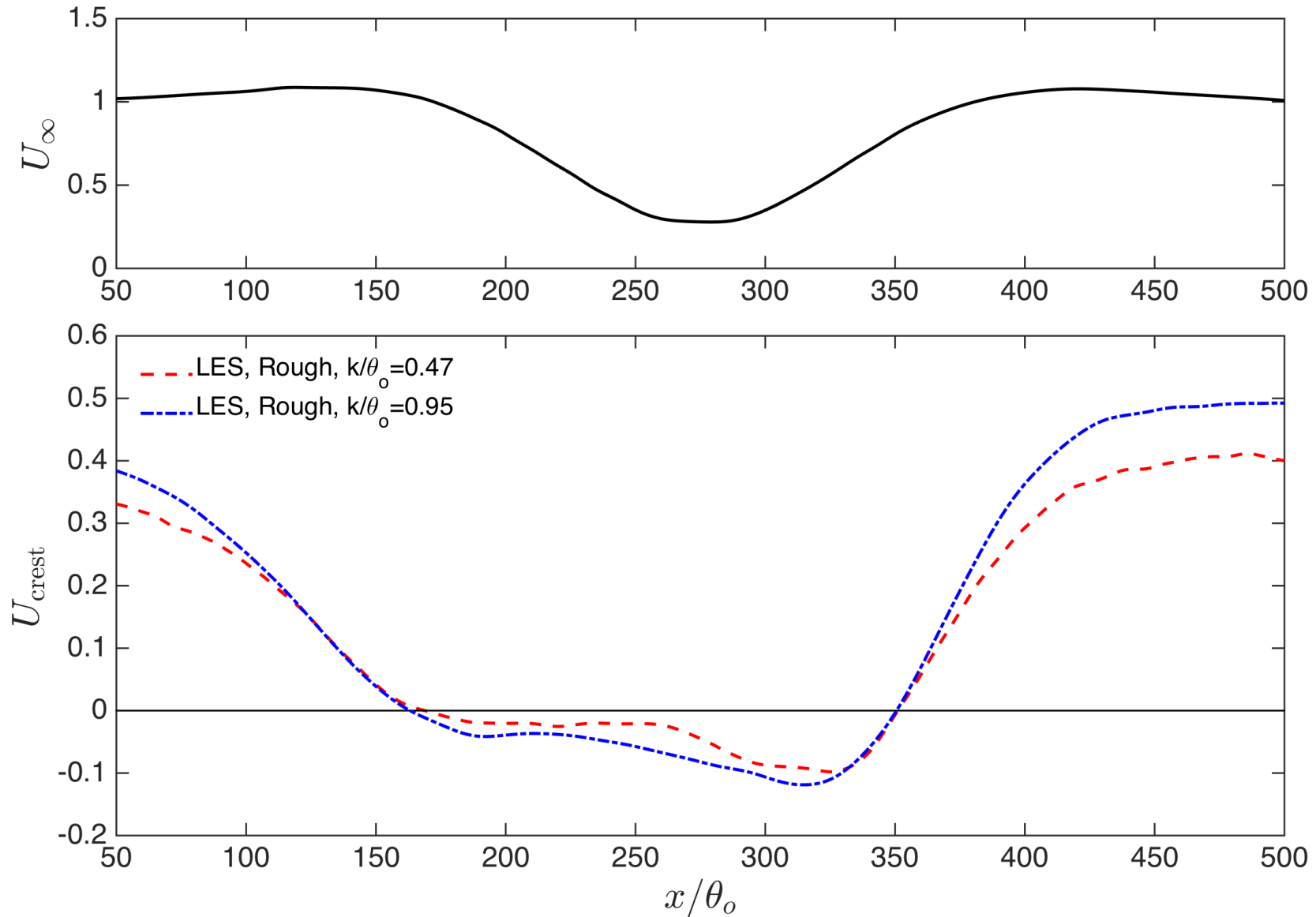
- Standard definition: $\tau_w = 0, \frac{d\tau_w}{dx} < 0$





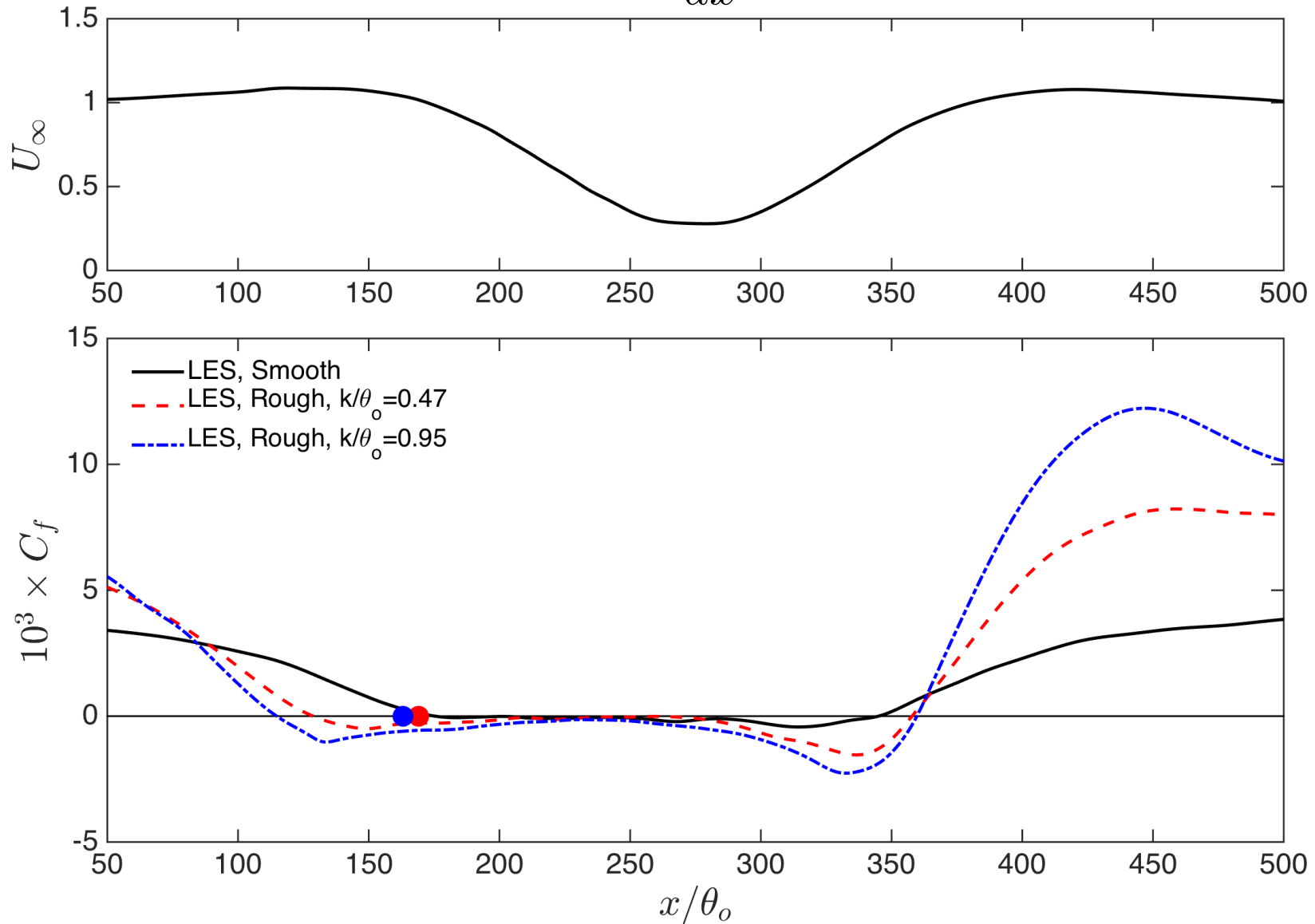
- Skin-friction coefficient crosses zero earlier for the rough cases
- Does this represent separation?
- How is separation determined in experiments?

... From the velocity above the crest

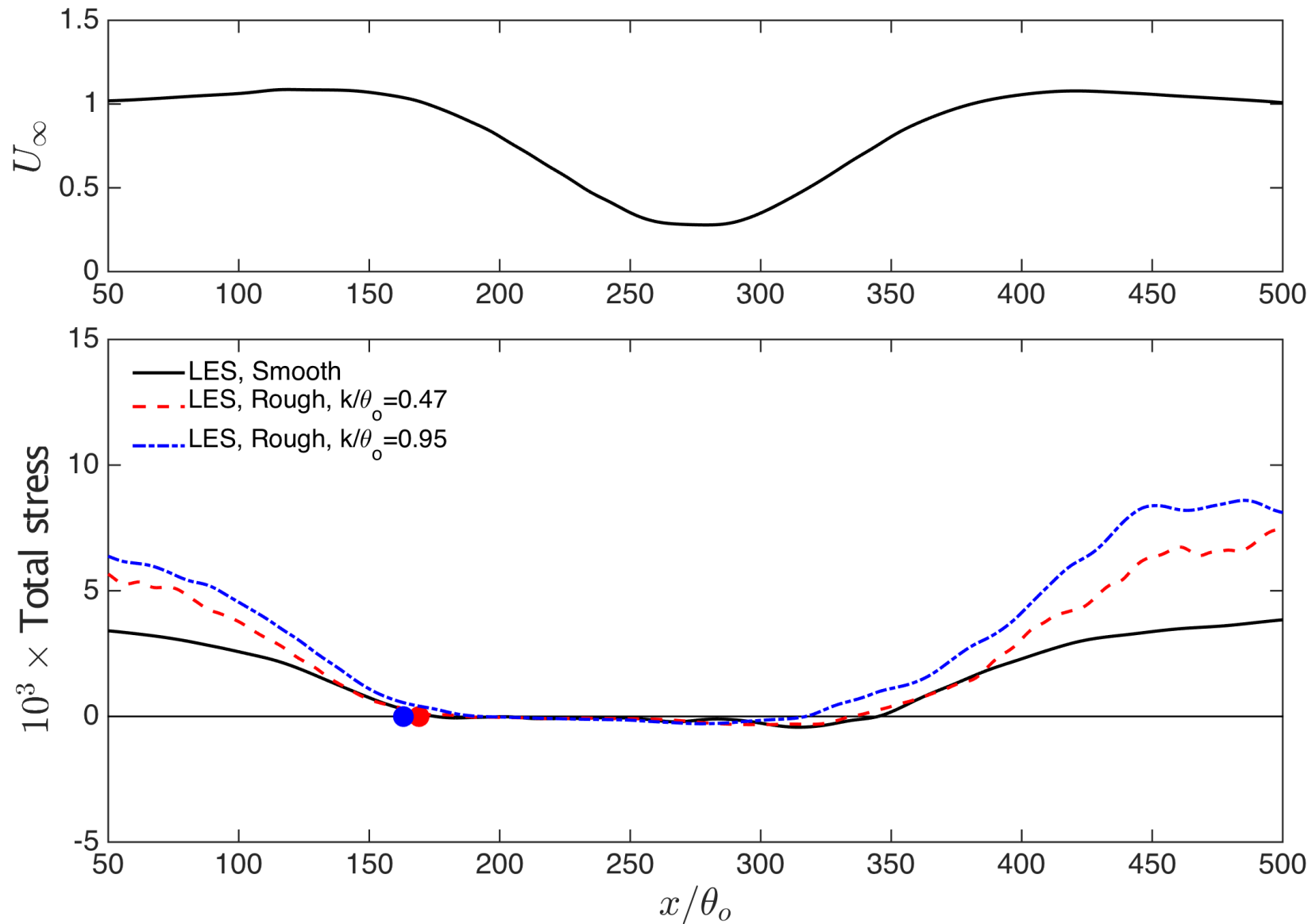




- Standard definition: $\tau_w = 0, \frac{d\tau_w}{dx} < 0$



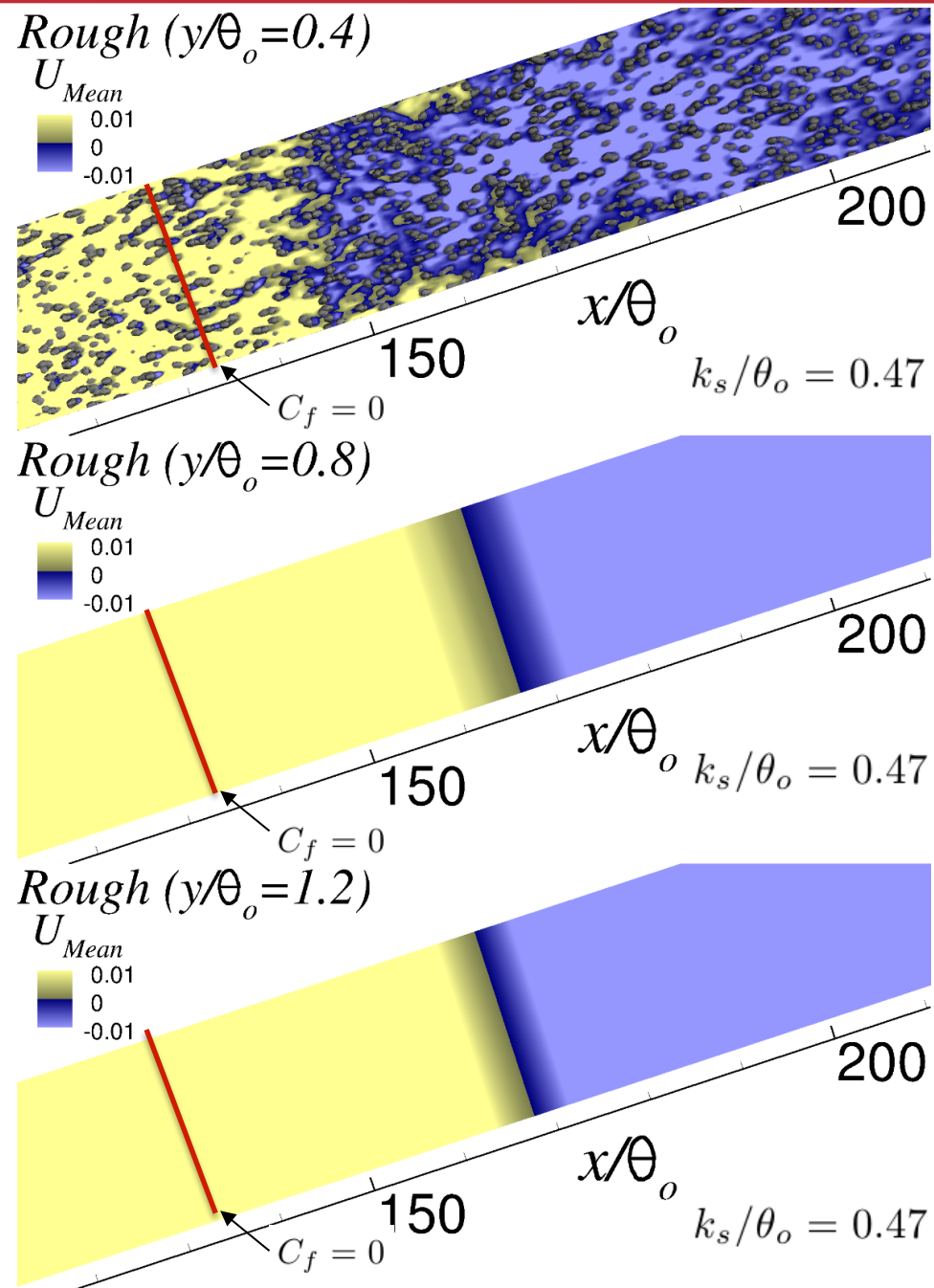
- Total stress above the crest: $\tau = -\langle u'v' \rangle + \frac{1}{Re} \left(\frac{dU}{dx} + \frac{dV}{dy} \right)$





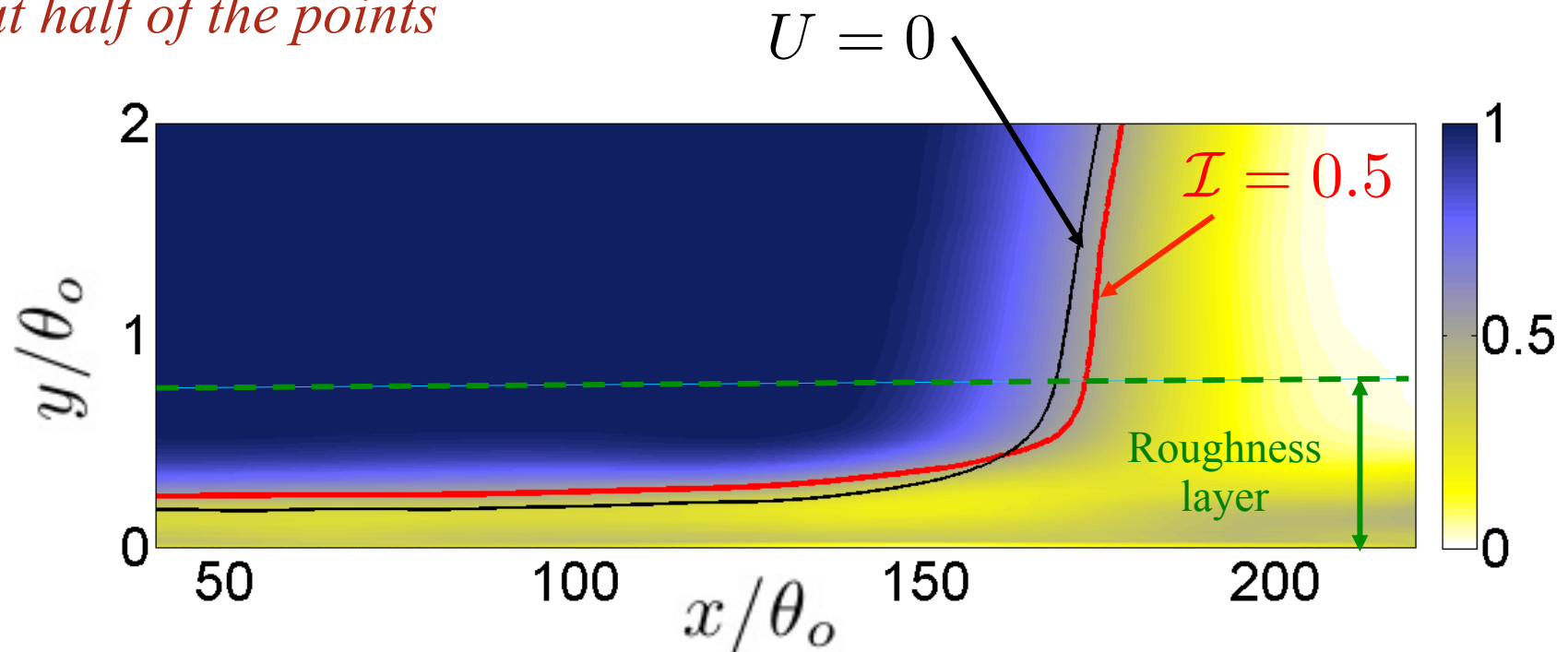
- Time-averaged velocity
 - Flow reversal inside the roughness layer **even in the region where $C_f > 0$**
 - The point where the mean velocity changes sign does not coincide with the point where C_f changes sign

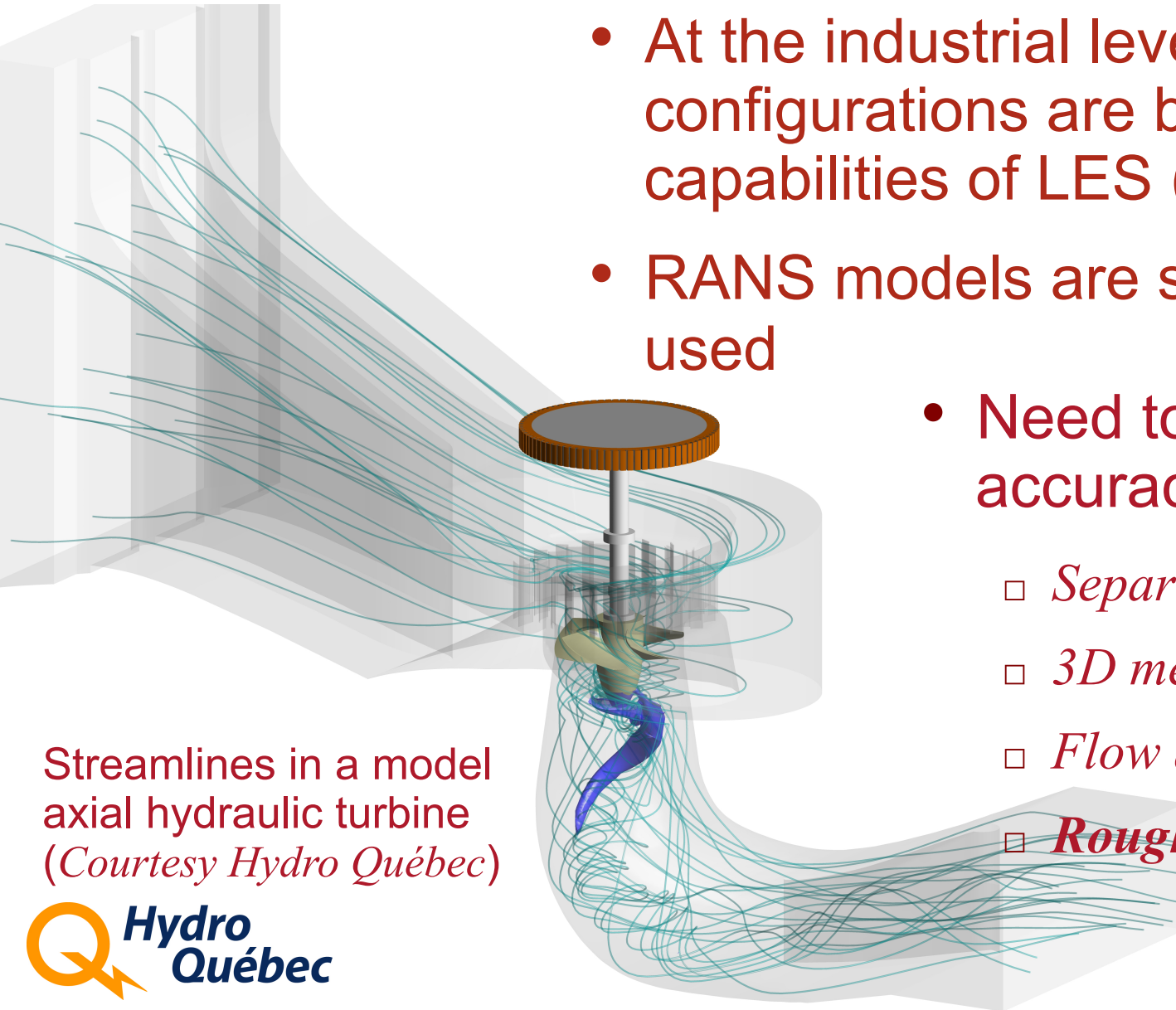
⇒ **Flow reversal without separation**





- Define intermittency function:
 - $\mathcal{I} = 1$ when the time-averaged velocity is in the positive- x direction at all points
 - $\mathcal{I} = 0$ when the time-averaged velocity is in the negative- x direction at all points
 - $\mathcal{I} = 0.5$ when the time-averaged velocity is in the positive- x direction at half of the points





Streamlines in a model
axial hydraulic turbine
(*Courtesy Hydro Québec*)

- At the industrial level, complete configurations are beyond the capabilities of LES (cost)
- RANS models are still extensively used
- Need to evaluate their accuracy in presence of
 - *Separation*
 - *3D mean flow*
 - *Flow acceleration*
 - ***Roughness***

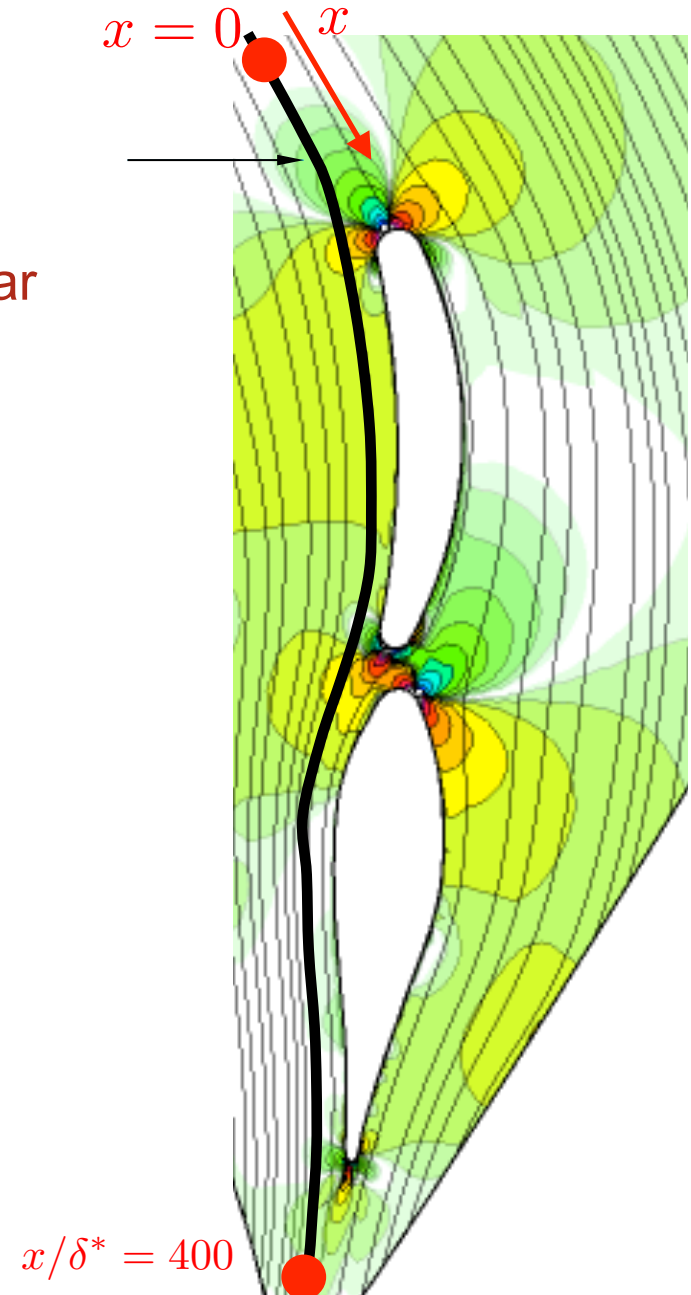
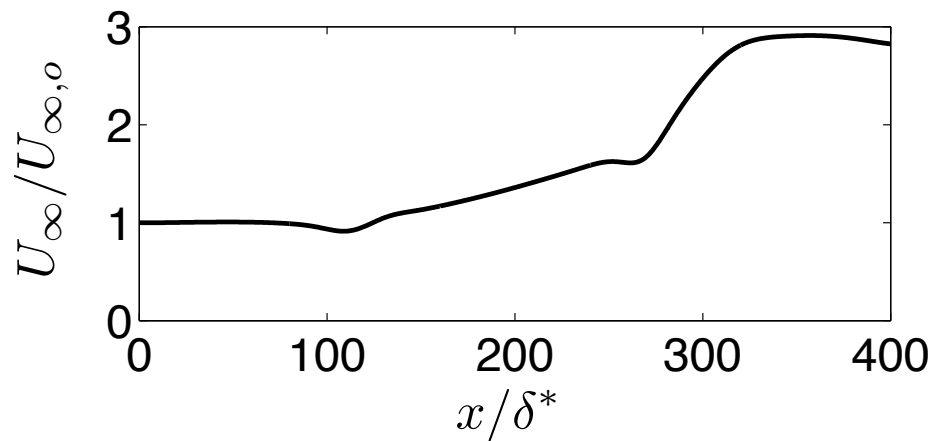
- RANS models for rough-wall boundary layers correct the eddy viscosity ν_T based on the equivalent sand-grain roughness
- The equivalent sand-grain roughness must be prescribed.
 - *Several correlations exist to relate the actual geometric scale of the roughness to k_s (Yuan and Piomelli, JoT 2014).*
- Roughness modifications act by
 - *Shifting the velocity (eddy viscosity, TKE, ...) profiles by an offset to account for the increased momentum near the wall.*
 - *Modifying the boundary conditions for the transported quantities (ν_T , \mathcal{K} , ε , ω ...)*



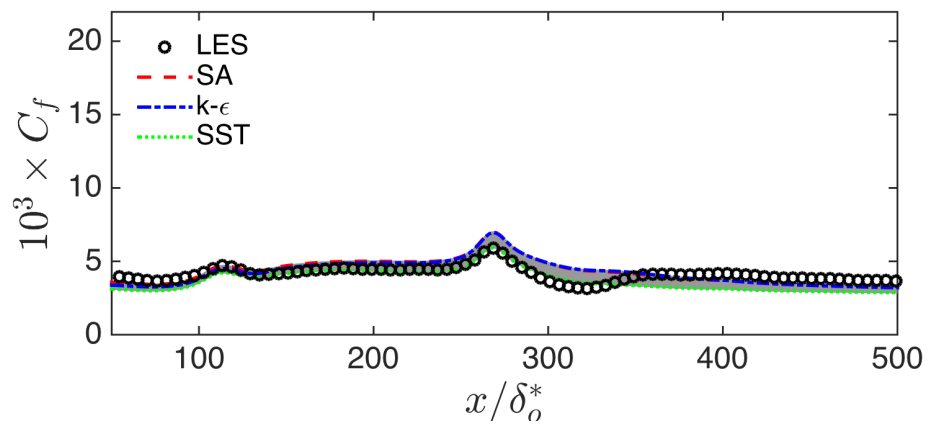
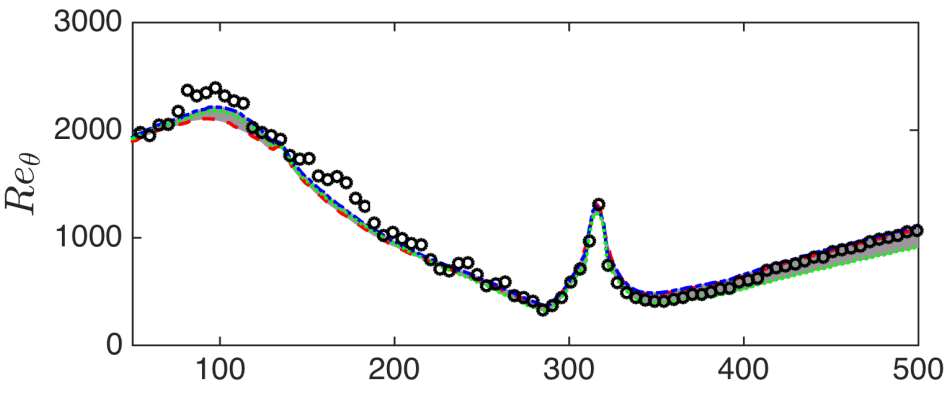
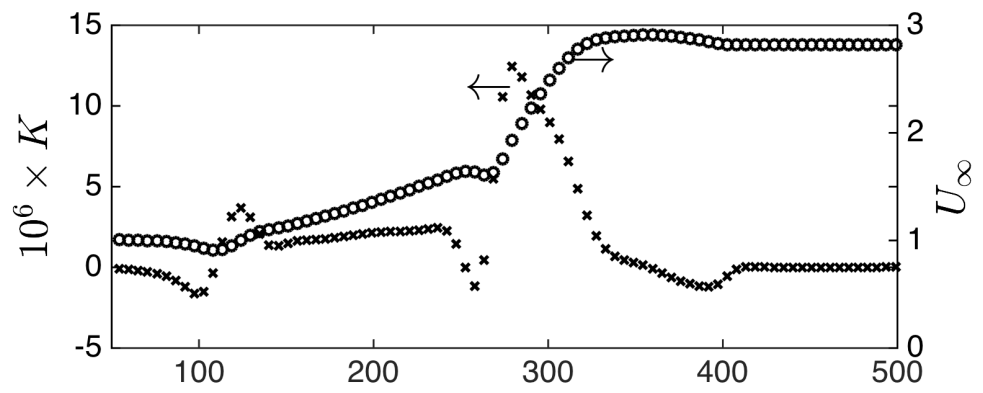
- Flow in a hydraulic turbine

- *Streamline selection:*

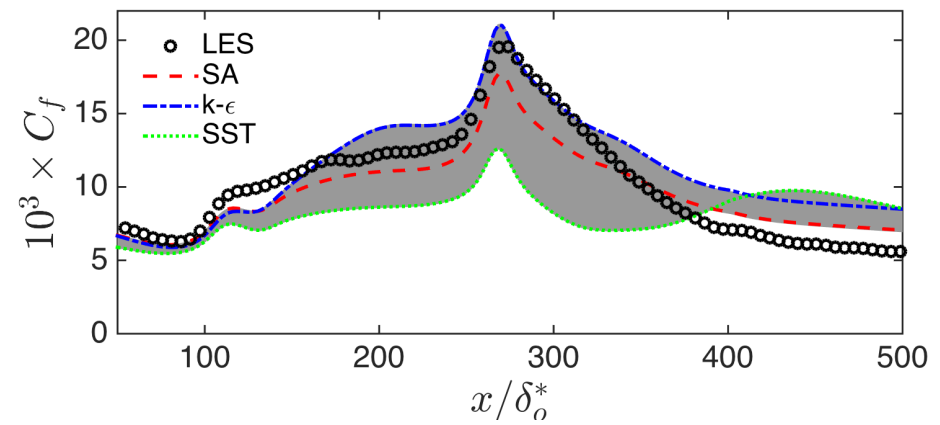
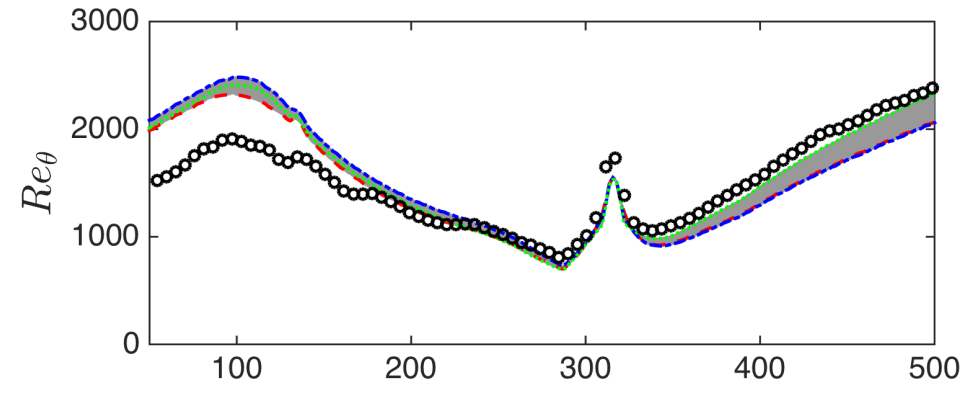
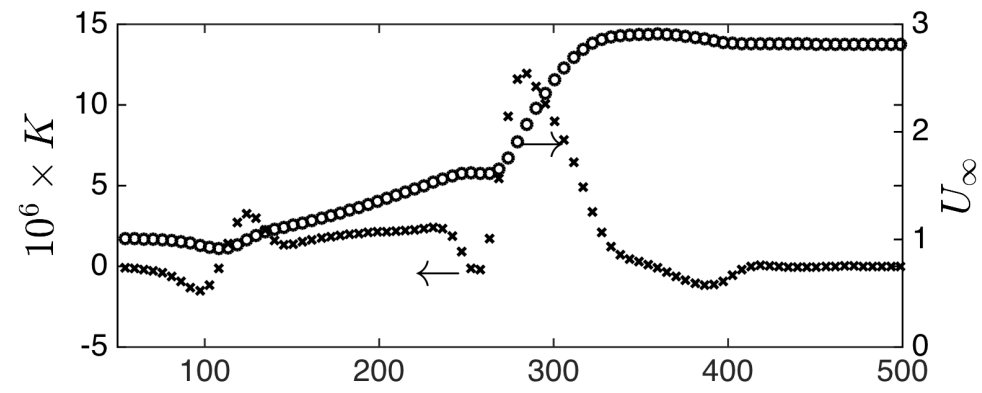
- Outside the boundary layer, but not too far away: $2-3\delta$ away from wall
 - Extensive non-ZPG region



Smooth

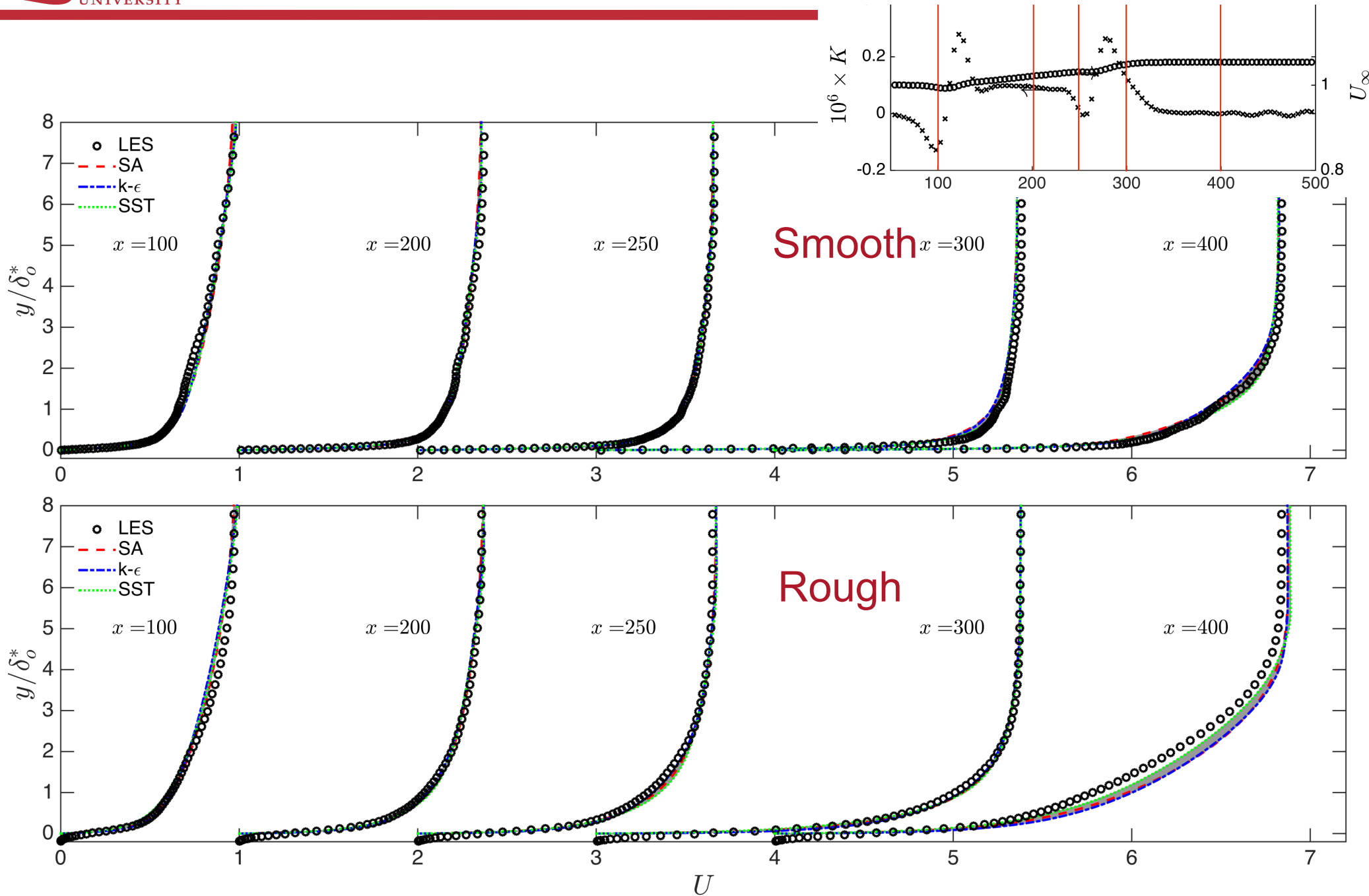


Rough



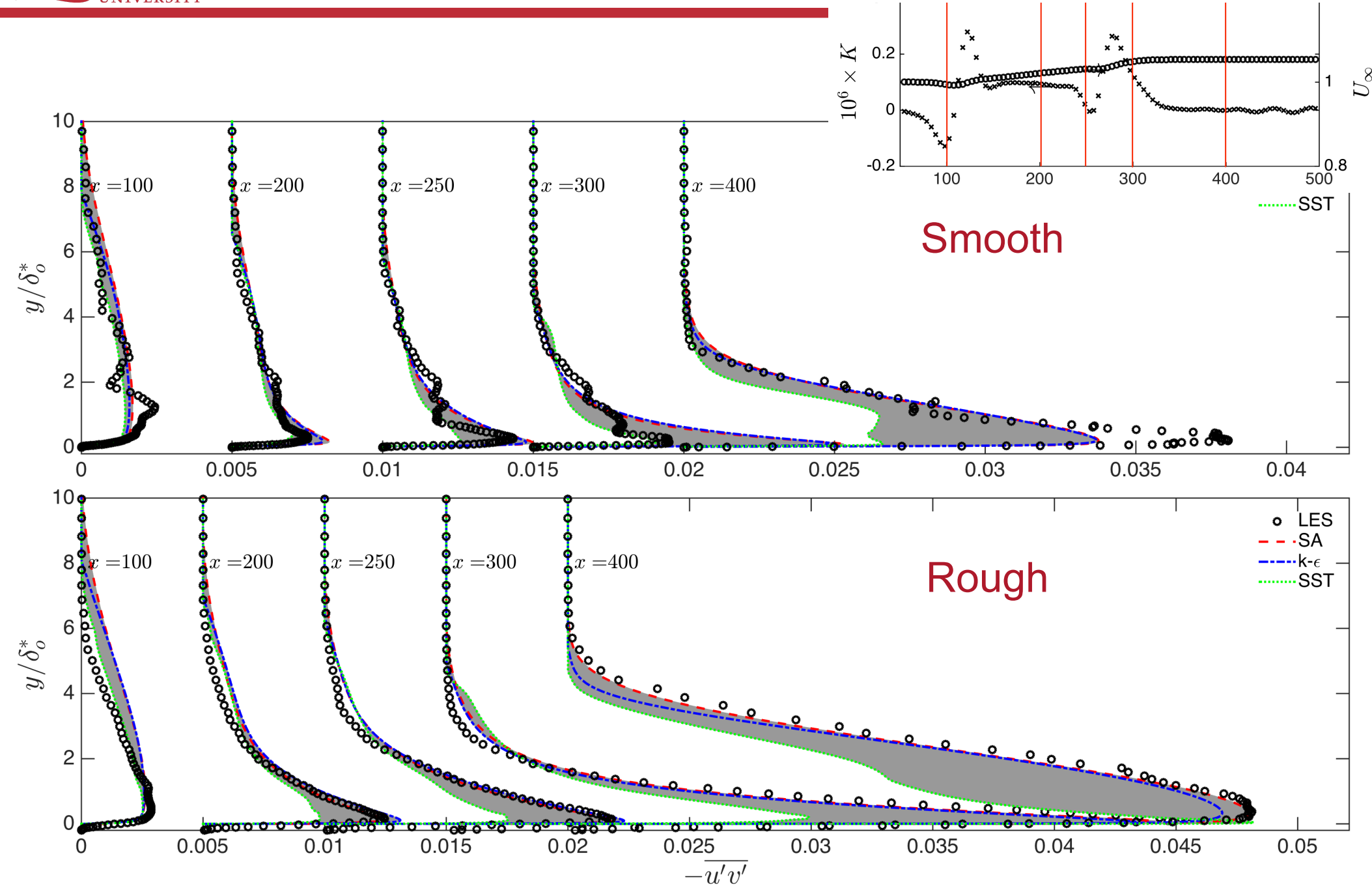


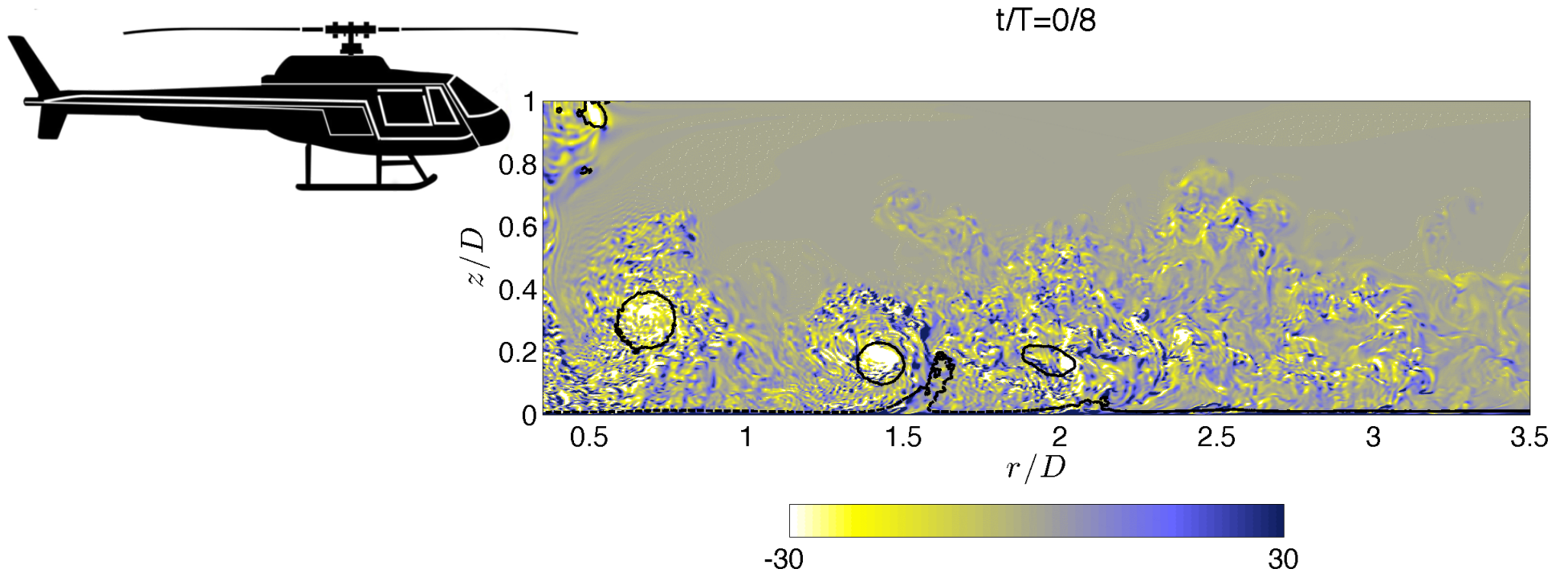
APPLICATIONS: RANS MODELS FOR ROUGH WALL BLS





APPLICATIONS: RANS MODELS FOR ROUGH WALL BLS







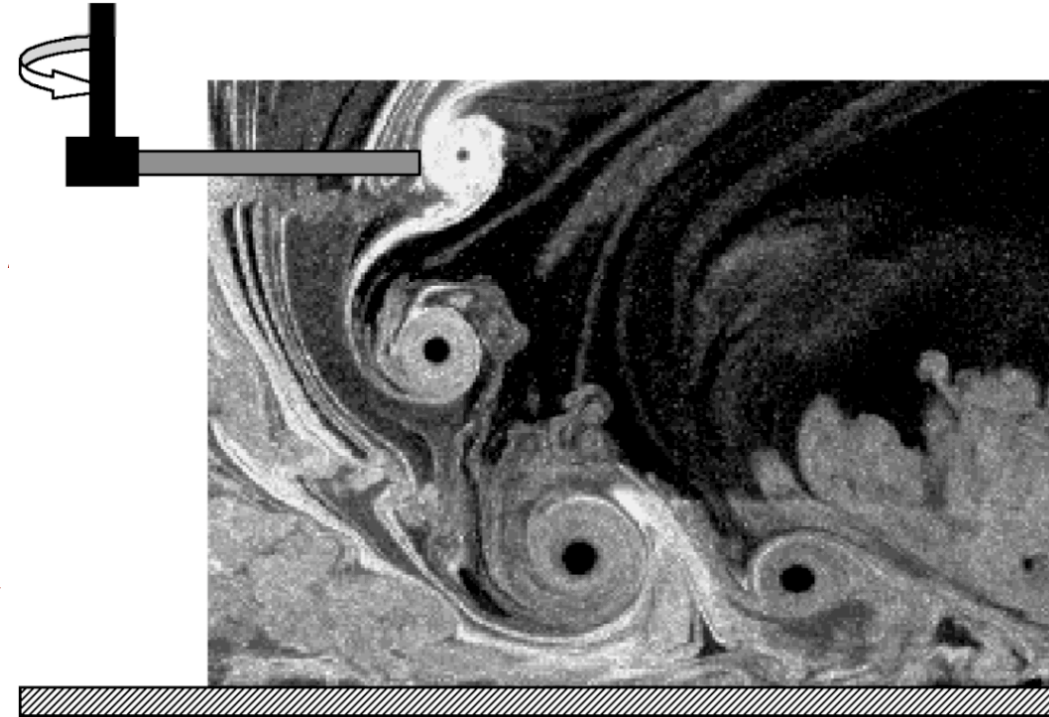
- Impinging jets occur in
 - *Heat transfer applications*
 - *Meteorology (downdrafts)*
 - *Helicopter aerodynamics*





- The interaction of the vortices with the ground

- *Changes the turbulent flow field*
- *Results in the development of secondary vortices, which interact with the primary ones*
- *Changes the vortex development*
- *May result in particle lifting and suspension.*



From T. Lee, J. G. Leishman, and M. Ramasamy, (2008)

- It is important to develop models that relate the impinging jet (i.e., rotor wake) and vortex characteristics to the particle dynamics.

- *Existing models are usually inviscid (vortex line)*



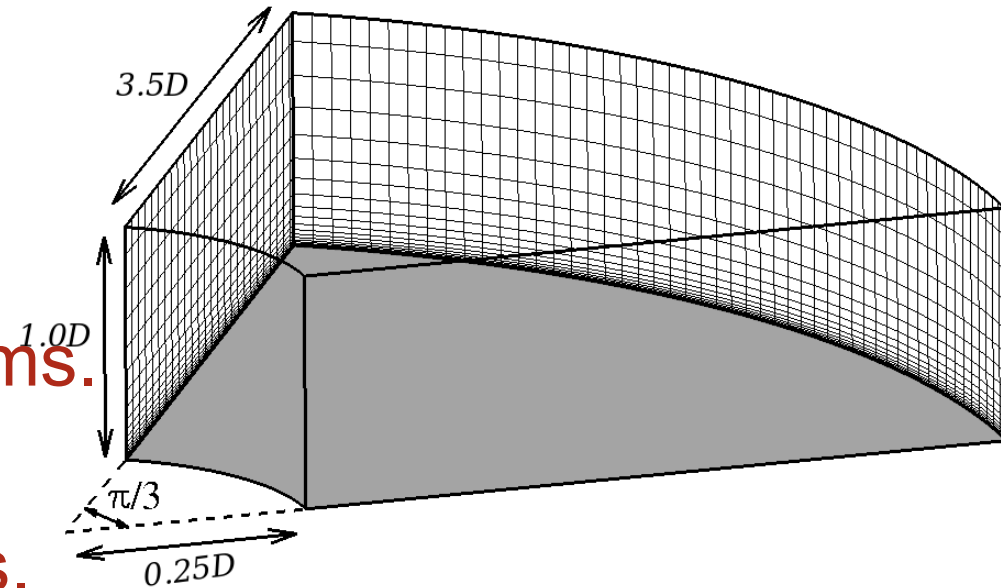
- Study the interaction between the vortices and the near-wall turbulence.
 - *Moderate Reynolds number*
- Quantify the vortex decay in a turbulent wall-bounded flow.
 - *Moderate Reynolds number*
 - *High Reynolds number*
- Understand the physical mechanisms responsible for vortex decay.
- Develop lower level models that account for both viscous and turbulent effects.



- Strategy:
 - *Develop a vortex-generation method that is*
 - Non-intrusive, Controllable
 - *Simulate increasingly realistic configurations*
 - 2D impingement
 - Axisymmetric impingement
 - Axisymmetric wall jet
 - *Perform hierarchical model validation:*
 - LES to validate Hybrid RANS
 - *Extend to high Re*
 - *Study decay laws and develop lower-level models*



- Numerical solution of the filtered Navier-Stokes equations.
- Staggered grid.
- Second-order accurate in space and time.
- Central differences on all terms.
- Axi-symmetric configuration that does not include the axis.



- Inlet condition:

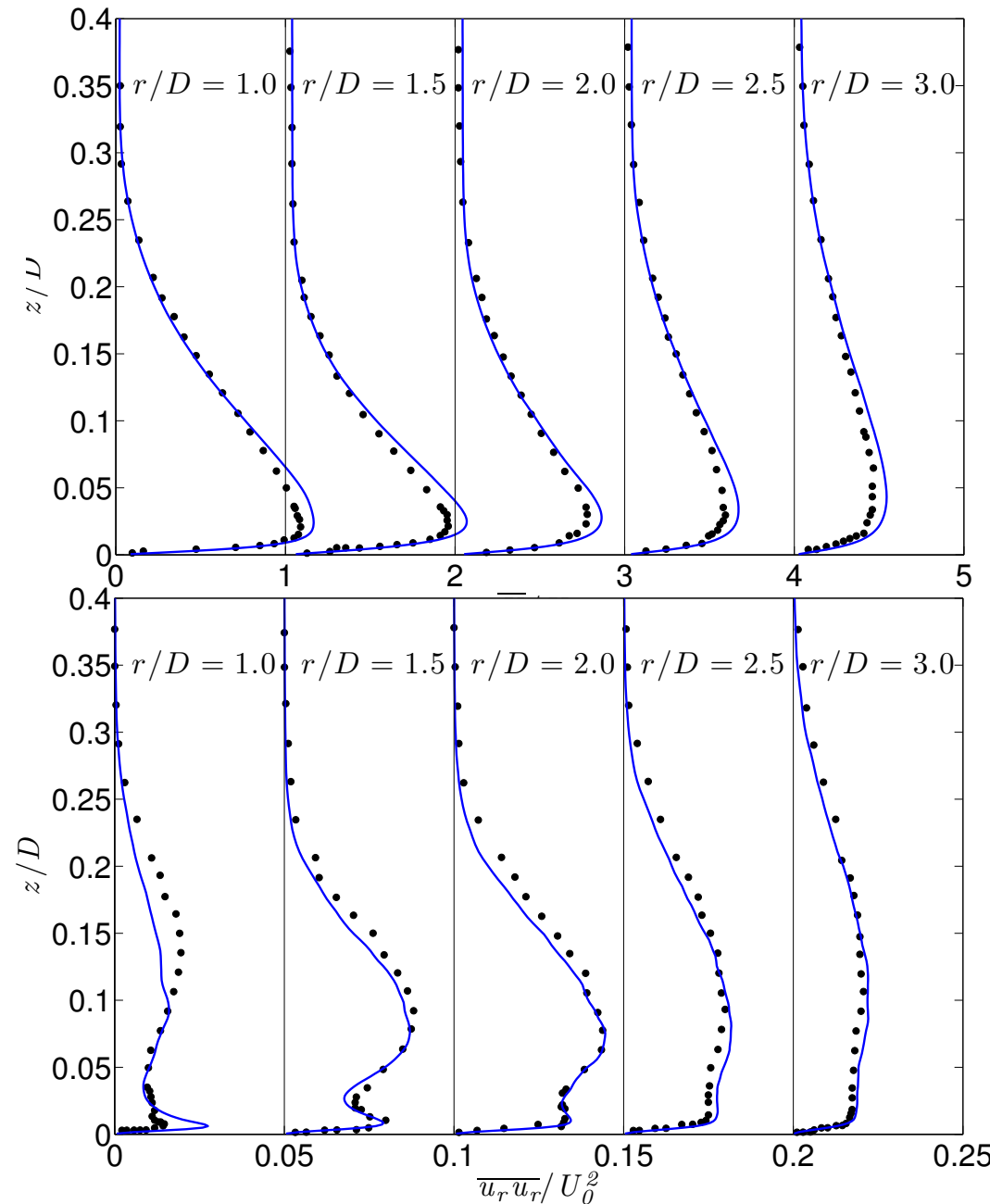
$$\langle U_{jet} \rangle = U_o + A \sin(2\pi t/T)$$

- Synthetic turbulence added at the jet exit and the inner radial boundary.

- $Re = U_{jet} D_{jet} / \nu = 66,000$



- Impinging jet experiment by Cooper, Jackson, Launder & Liao (1993)
- Verified grid requirements
- Verified domain size





$$\langle f(\mathbf{x}, \phi) \rangle = \frac{1}{N} \sum_{n=1}^N f(\mathbf{x}, t_n + T)$$

$$f = \overline{F} + \tilde{f} + f' = \langle f \rangle + f'$$

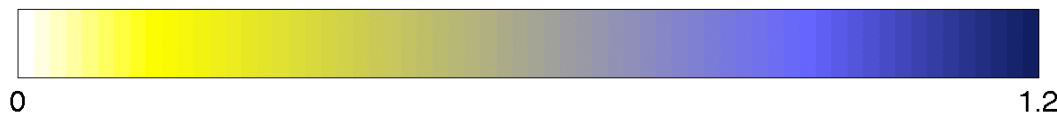
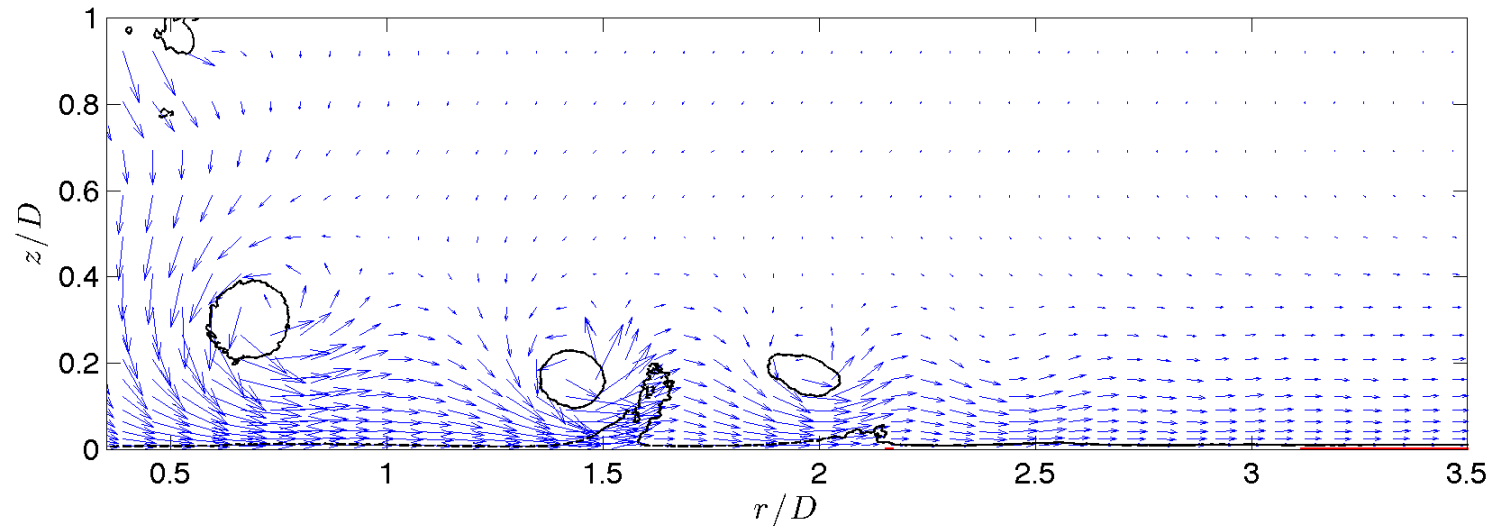
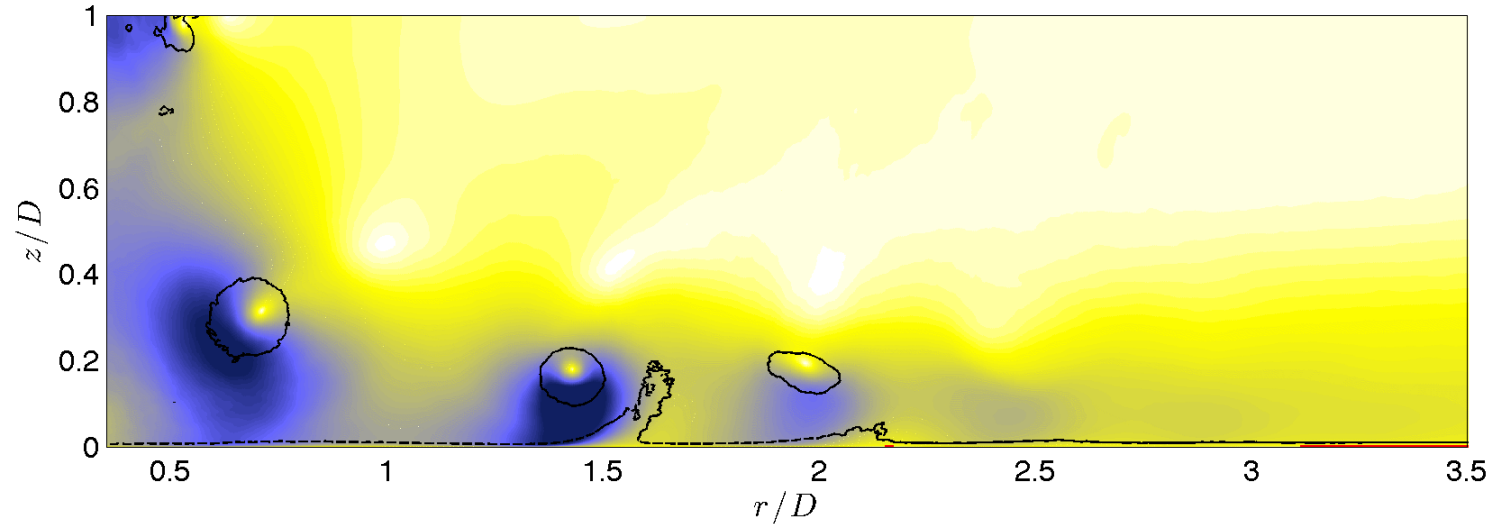
Time average Periodic Stochastic Phase average

$$\langle u_i u_j \rangle - U_i U_j = \langle u_i \rangle \langle u_j \rangle + \langle u'_i u'_j \rangle$$

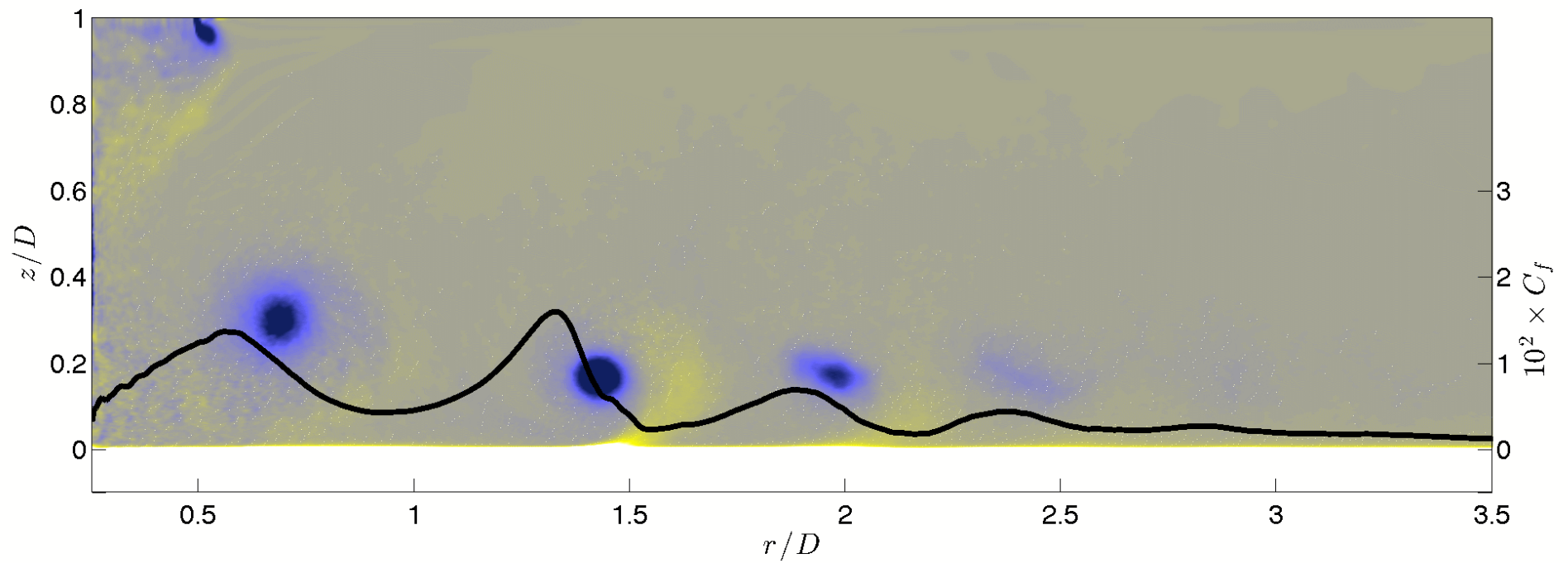


PHASE-AVERAGED VELOCITY

$t/T=0/8$

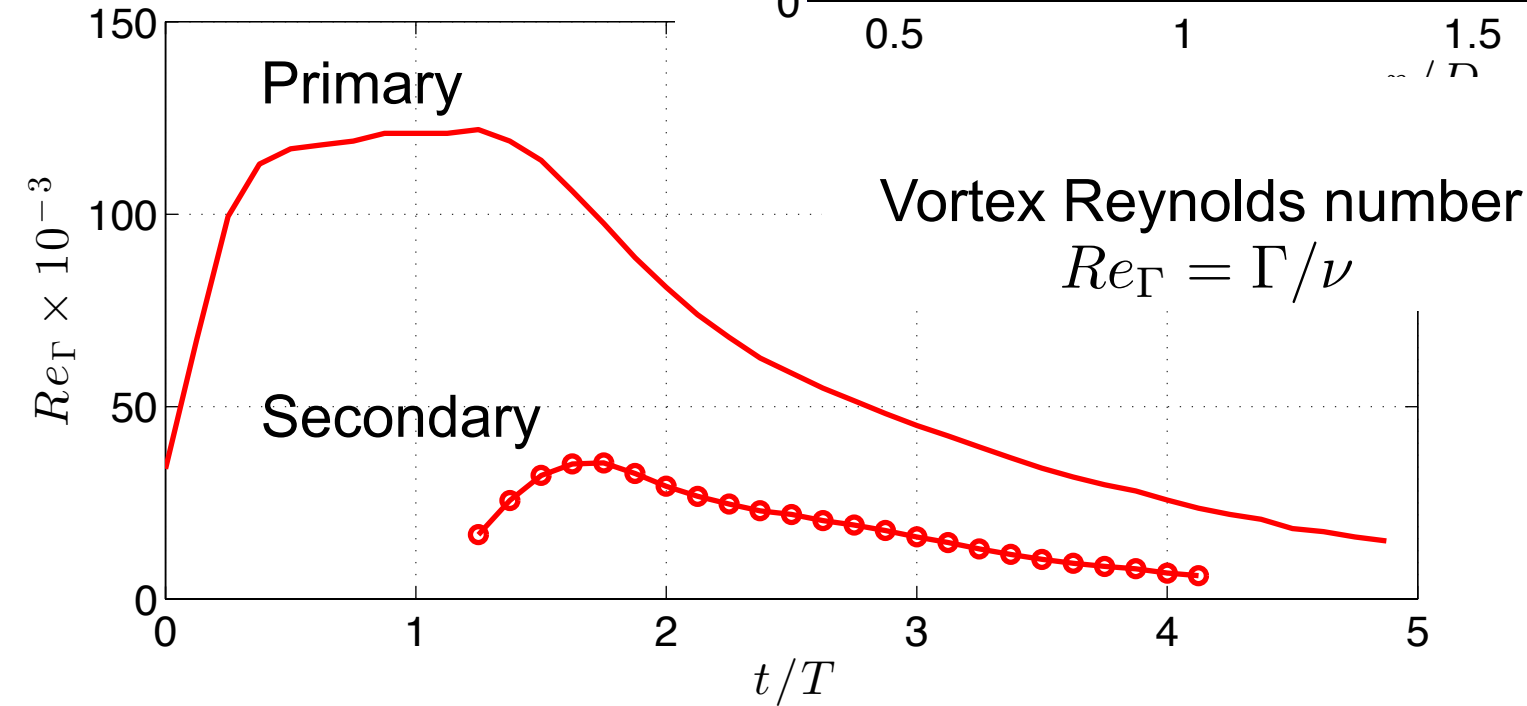
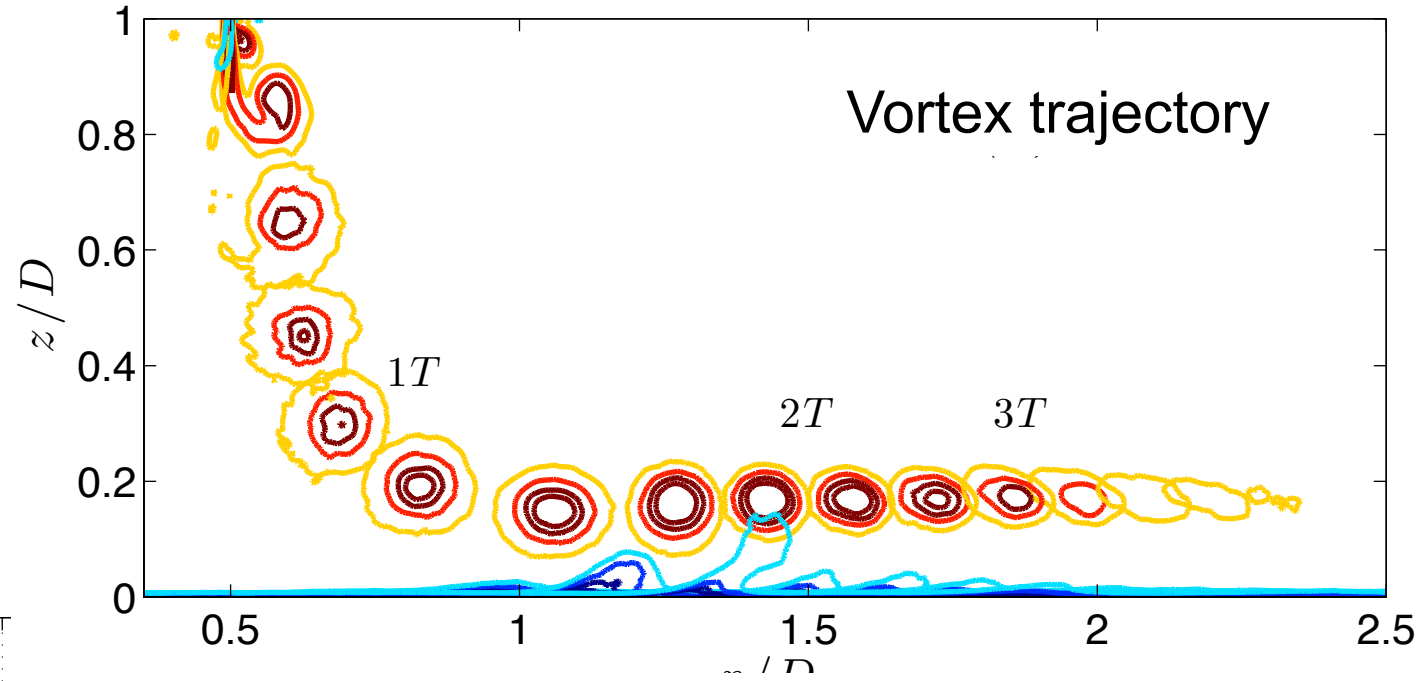


$t/T=0/8$



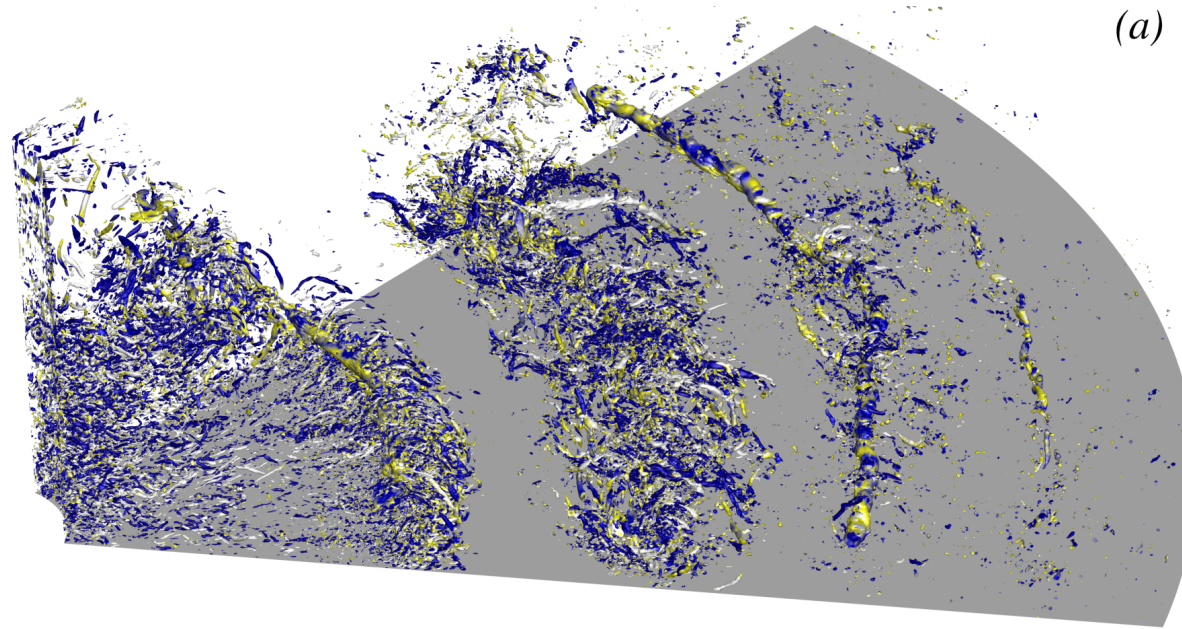


PHASE-AVERAGED VORTICITY AND C_f

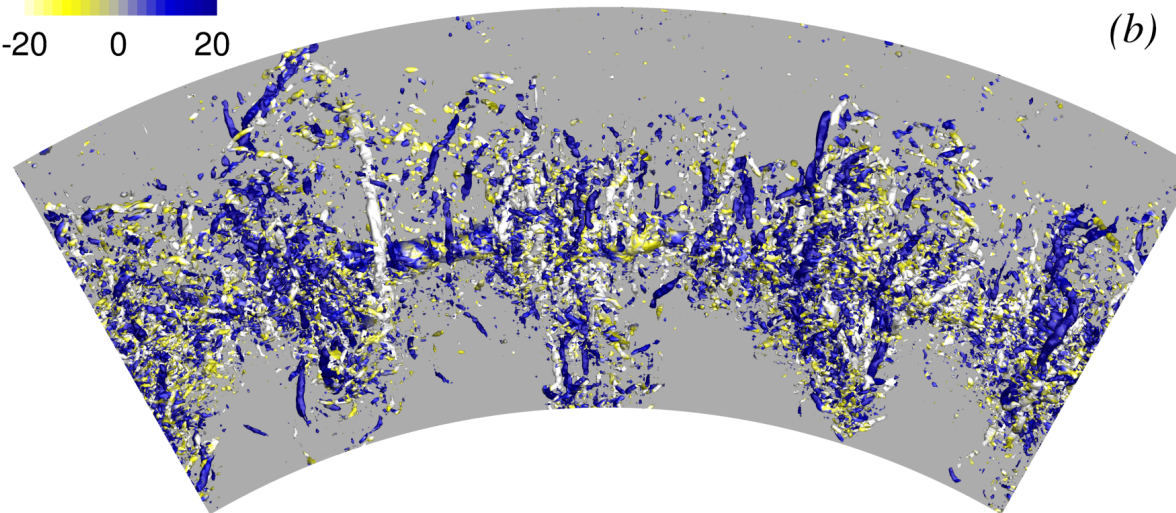
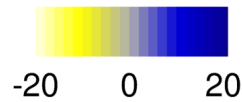




INSTANTANEOUS FIELD



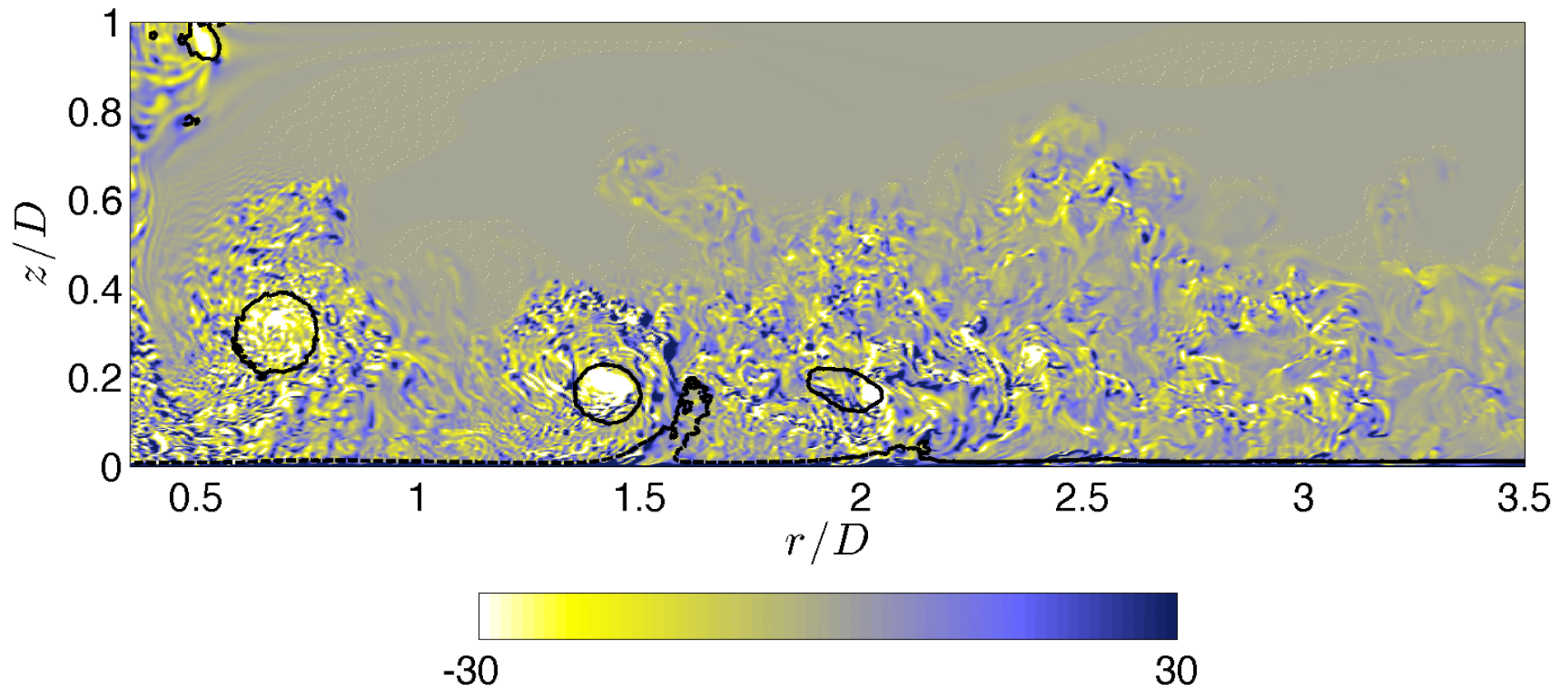
(a)



(b)

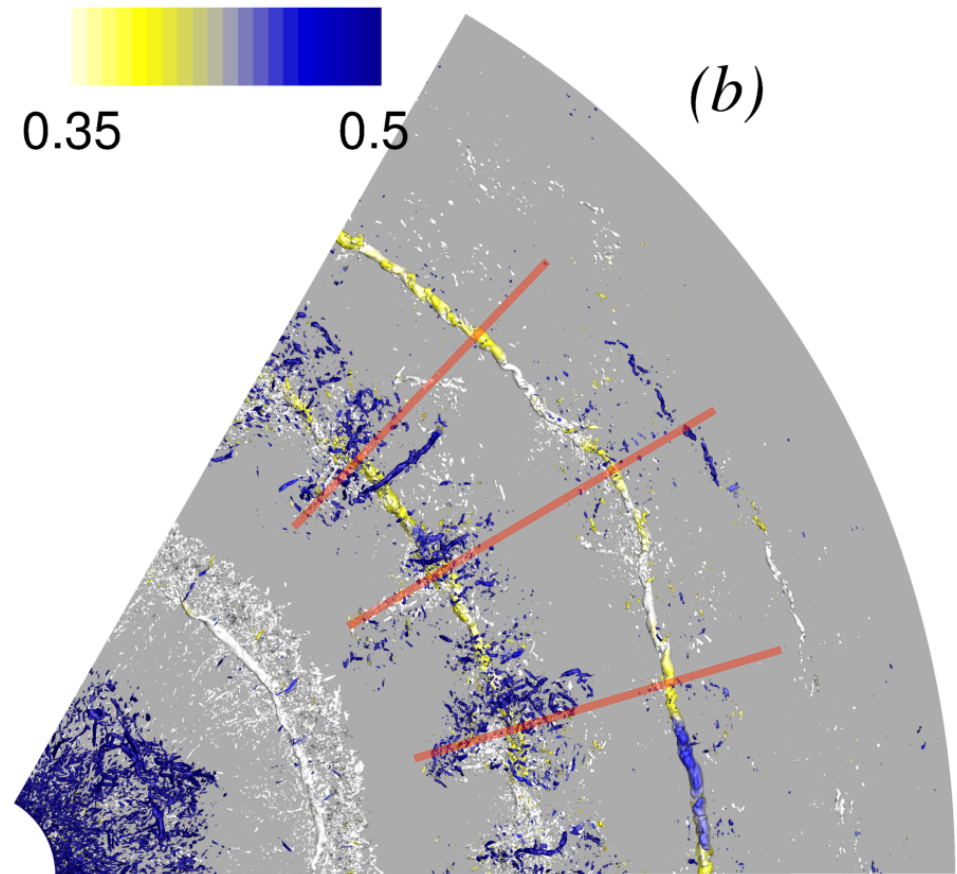
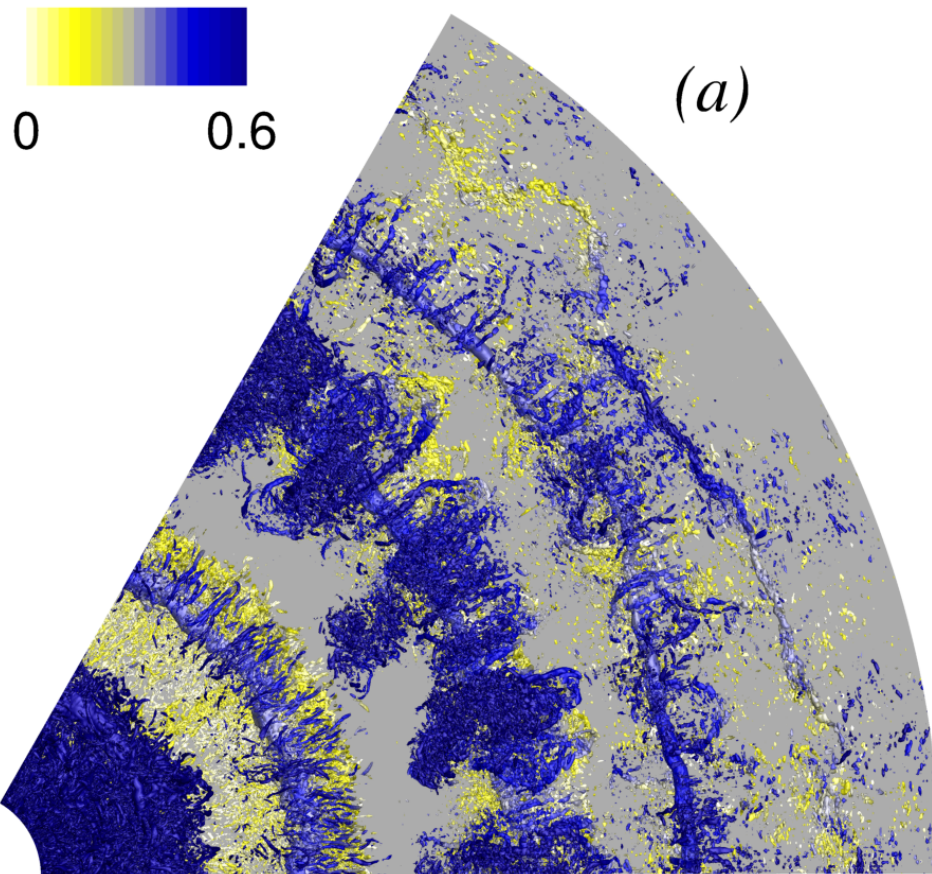
Contours of $Q = -\frac{1}{2} \frac{\partial \bar{u}_j}{\partial x_i} \frac{\partial \bar{u}_i}{\partial x_j} = \frac{1}{2} (\bar{\Omega}_{ij} \bar{\Omega}_{ij} - \bar{S}_{ij} \bar{S}_{ij})$ coloured by ω_r

$t/T=0/8$



- Crow instability.

- *Contributes to development of three-dimensionality.*



Contours of $Q = -\frac{1}{2} \frac{\partial \bar{u}_j}{\partial x_i} \frac{\partial \bar{u}_i}{\partial x_j} = \frac{1}{2} (\bar{\Omega}_{ij} \bar{\Omega}_{ij} - \bar{S}_{ij} \bar{S}_{ij})$ coloured by z



$$\frac{D\langle \omega \rangle}{Dt} = \frac{\partial \langle \omega \rangle}{\partial t} + \langle \mathbf{u} \rangle \cdot \nabla \langle \omega \rangle =$$

$$\langle \omega \rangle \cdot \nabla \langle \mathbf{u} \rangle$$

Vortex stretching by
phase-averaged flow

$$+ \nabla \times (\nabla \cdot \langle \boldsymbol{\tau}_{tot} \rangle)$$

Viscous and SGS
diffusion

$$+ \langle \omega' \cdot \nabla \mathbf{u}' \rangle - \nabla \cdot \langle \mathbf{u}' \omega' \rangle$$

Vortex stretching by
fluctuating field

Turbulent vorticity diffusion

$$- \nabla \times (\nabla \cdot \langle \mathbf{u}' \mathbf{u}' \rangle)$$



BUDGET OF $\langle \omega_\theta \rangle$

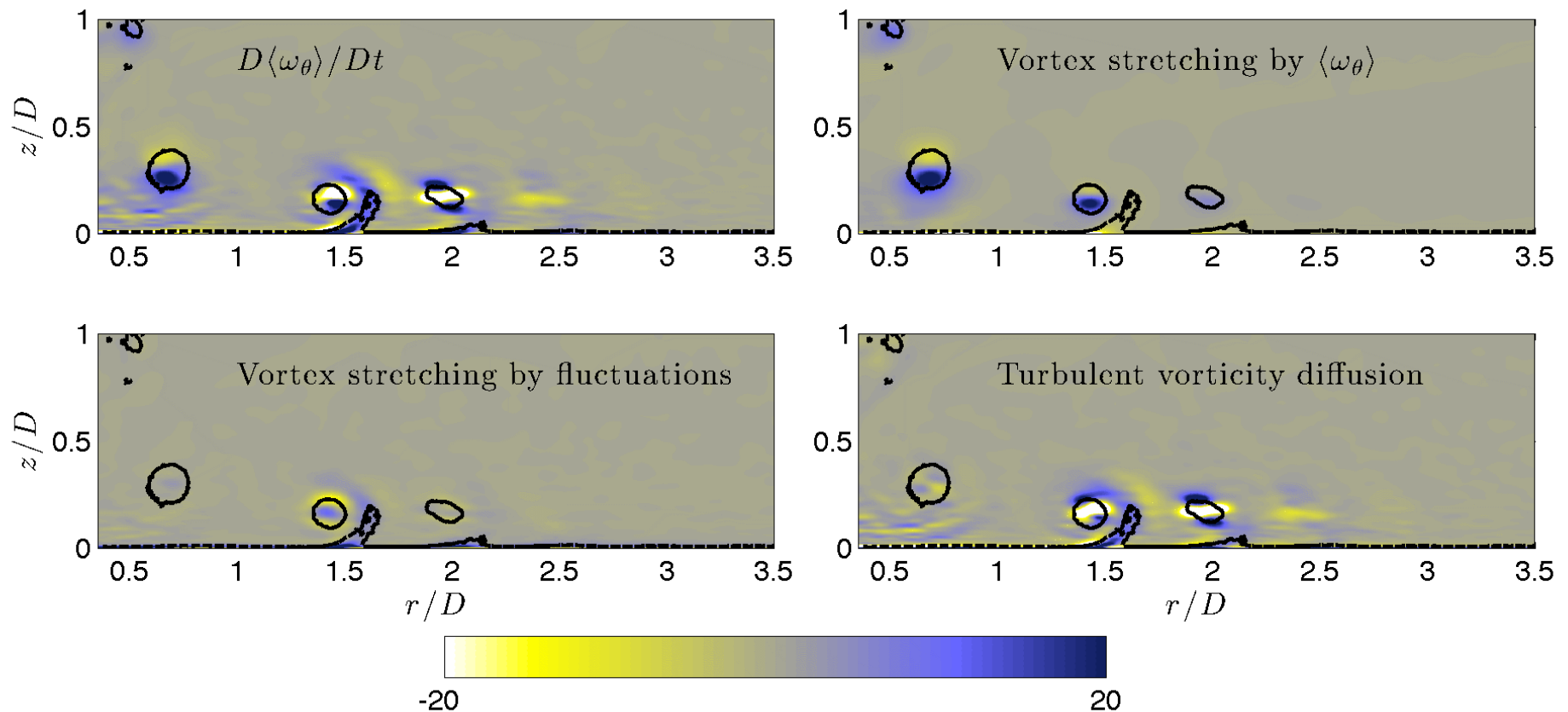
$$\frac{D\langle \omega \rangle}{Dt} =$$

Vortex stretching by phase-averaged flow + ~~Viscous and SGS diffusion~~

+ **Vortex stretching by fluctuating field** + **Turbulent vorticity diffusion**

$$\frac{D\langle \omega \rangle}{Dt} = \boxed{\text{Vortex stretching by phase-averaged flow}} + \boxed{\text{Vortex stretching by fluctuating field}} + \boxed{\text{Turbulent vorticity diffusion}}$$

$t/T=0/8$





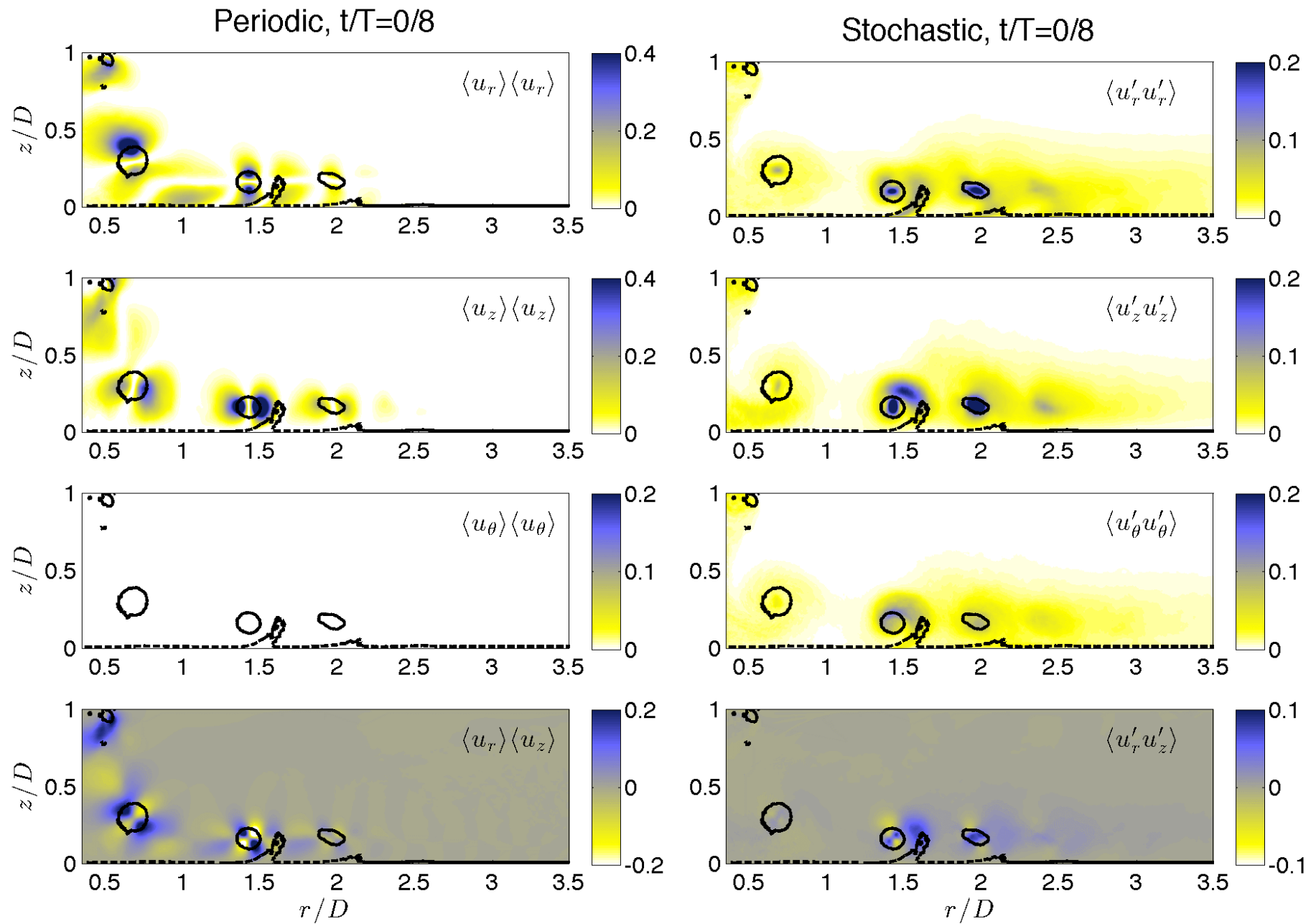
$$\frac{D\langle \omega \rangle}{Dt} = \boxed{\text{Vortex stretching by phase-averaged flow}} +$$

$$+ \boxed{\text{Vortex stretching by fluctuating field}} + \boxed{\text{Turbulent vorticity diffusion}}$$

$$- \nabla \times (\nabla \cdot \mathbf{u}'\mathbf{u}')|_\theta = \frac{\partial}{\partial z \partial r} (\langle u'_r u'_r \rangle - \langle u'_z u'_z \rangle)$$

$$- \frac{1}{r} \frac{\partial}{\partial z} \langle u'_\theta u'_\theta \rangle + \left(\frac{\partial^2}{\partial z^2} - \frac{\partial^2}{\partial r^2} \right) \langle u'_r u'_z \rangle$$

PHASE-AVERAGED REYNOLDS STRESSES





- Motivation
- Governing equations for LES
- Boundary conditions
- Subfilter-scale modelling
- Validation of an LES
- Applications
- **Hybrid RANS/LES methods**
- Challenges
- Conclusions